frontiers | Research Topics

The mechanism of tumor evolution and microenvironmental changes of genitourinary oncology in clinical diagnosis and treatment, volume II

Edited by
Hailiang Zhang, Philippe E. Spiess, Housheng Hansen He and Wen-Hao Xu

Published in
Frontiers in Oncology

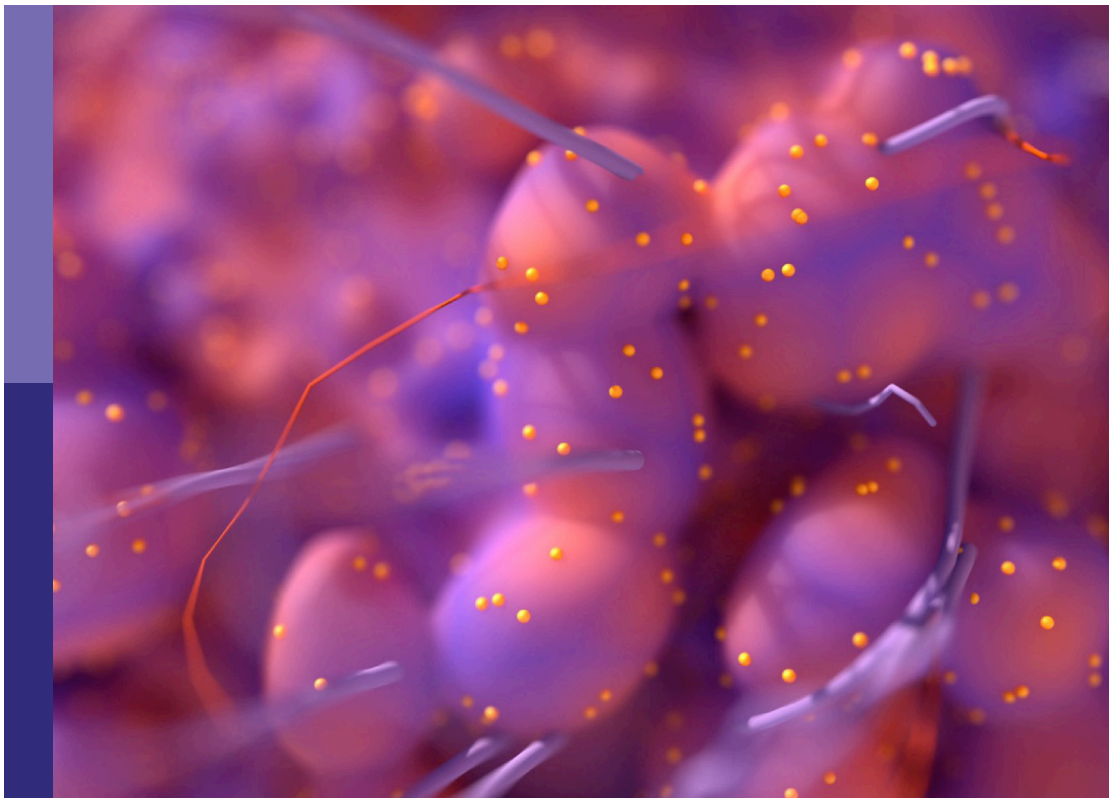

ISSN 1664-8714
ISBN 978-2-8325-5179-0
DOI 10.3389/978-2-8325-5179-0

About Frontiers

Frontiers is more than just an open access publisher of scholarly articles: it is a pioneering approach to the world of academia, radically improving the way scholarly research is managed. The grand vision of Frontiers is a world where all people have an equal opportunity to seek, share and generate knowledge. Frontiers provides immediate and permanent online open access to all its publications, but this alone is not enough to realize our grand goals.

Frontiers journal series

The Frontiers journal series is a multi-tier and interdisciplinary set of open-access, online journals, promising a paradigm shift from the current review, selection and dissemination processes in academic publishing. All Frontiers journals are driven by researchers for researchers; therefore, they constitute a service to the scholarly community. At the same time, the *Frontiers journal series* operates on a revolutionary invention, the tiered publishing system, initially addressing specific communities of scholars, and gradually climbing up to broader public understanding, thus serving the interests of the lay society, too.

Dedication to quality

Each Frontiers article is a landmark of the highest quality, thanks to genuinely collaborative interactions between authors and review editors, who include some of the world's best academicians. Research must be certified by peers before entering a stream of knowledge that may eventually reach the public - and shape society; therefore, Frontiers only applies the most rigorous and unbiased reviews. Frontiers revolutionizes research publishing by freely delivering the most outstanding research, evaluated with no bias from both the academic and social point of view. By applying the most advanced information technologies, Frontiers is catapulting scholarly publishing into a new generation.

What are Frontiers Research Topics?

Frontiers Research Topics are very popular trademarks of the *Frontiers journals series*: they are collections of at least ten articles, all centered on a particular subject. With their unique mix of varied contributions from Original Research to Review Articles, Frontiers Research Topics unify the most influential researchers, the latest key findings and historical advances in a hot research area.

Find out more on how to host your own Frontiers Research Topic or contribute to one as an author by contacting the Frontiers editorial office: frontiersin.org/about/contact

The mechanism of tumor evolution and microenvironmental changes of genitourinary oncology in clinical diagnosis and treatment, volume II

Topic editors

Hailiang Zhang — Fudan University, China

Philippe E. Spiess — Moffitt Cancer Center, United States

Housheng Hansen He — University Health Network (UHN), Canada

Wen-Hao Xu — Fudan University, China

Citation

Zhang, H., Spiess, P. E., He, H. H., Xu, W.-H., eds. (2024). *The mechanism of tumor evolution and microenvironmental changes of genitourinary oncology in clinical diagnosis and treatment, volume II*. Lausanne: Frontiers Media SA.

doi: 10.3389/978-2-8325-5179-0

Table of contents

frontiers | Frontiers in Oncology

TYPE Case Report
PUBLISHED 26 June 2023
DOI 10.3389/fonc.2023.1213631

OPEN ACCESS

EDITED BY
Wen-Hao Xu,
Fudan University, China

REVIEWED BY
Yajun Chen,
Beijing Children's Hospital, China
Sameera Rashid,
The Christie National Health Service Foundation Trust, United Kingdom

*CORRESPONDENCE
Quanliang Liu
liuquanliang2008@163.com

†These authors share first authorship

RECEIVED 28 April 2023
ACCEPTED 09 June 2023
PUBLISHED 26 June 2023

CITATION
Zou Y, Xie X, Wang Q, Zhong C and Liu Q (2023) Case report: A rare case of synchronous mucinous neoplasms of the renal pelvis and the appendix.
Front. Oncol. 13:1213631.
doi: 10.3389/fonc.2023.1213631

Case report: A rare case of synchronous mucinous neoplasms of the renal pelvis and the appendix

Yuhua Zou[1†], Xiaojuan Xie[2†], Qinlin Wang[3], Cunzhi Zhong[3] and Quanliang Liu[1*]

[1]Department of Urology, The First Affiliated Hospital of Gannan Medical University, Ganzhou, China, [2]Department of Cardiology, The First Affiliated Hospital of Gannan Medical University, Ganzhou, China, [3]Department of Anesthesiology, Operation Rom, The First Affiliated Hospital of Gannan Medical University, Ganzhou, China

Background: Mucinous neoplasms are tumors arising in the epithelial tissue, characterized by excessive mucin secretion. They mainly emerge in the digestive system and rarely in the urinary system. They also seldom develop in the renal pelvis and the appendix asynchronously or simultaneously. The concurrence of this disease in these two regions has not yet been reported. In this case report, we discuss the diagnosis and treatment of synchronous mucinous neoplasms of the right renal pelvis and the appendix. The mucinous neoplasm of the renal pelvis was preoperatively misdiagnosed as pyonephrosis caused by renal stones, and the patient underwent laparoscopic nephrectomy. Herein, we summarize our experience with this rare case in combination with related literature.

Case presentation: In this case, A 64-year-old female was admitted to our hospital with persistent pain in the right lower back for over a year. Computer tomography urography (CTU) showed that the patient was confirmed as right kidney stone with large hydronephrosis or pyonephrosis, and appendiceal mucinous neoplasm (AMN). Subsequently, the patient was transferred to the gastrointestinal surgery department. Simultaneously, electronic colonoscopy with biopsy suggested AMN. Open appendectomy plus abdominal exploration was performed after obtaining informed consent. Postoperative pathology indicated low-grade AMN (LAMN) and the incisal margin of the appendix was negative. The patient was re-admitted to the urology department, and underwent laparoscopic right nephrectomy because she was misdiagnosed with calculi and pyonephrosis of the right kidney according to the indistinctive clinical symptoms, standard examination of the gelatinous material, and imaging findings. Postoperative pathology suggested a high-grade mucinous neoplasm of the renal pelvis and mucin residing partly in the interstitium of the cyst walls. Good follow-up results were obtained for 14 months.

Conclusion: Synchronous mucinous neoplasms of the renal pelvis and the appendix are indeed uncommon and have not yet been reported. Primary renal mucinous adenocarcinoma is very rare, metastasis from other organs should be first considered, especially in patients with long-term chronic

inflammation, hydronephrosis, pyonephrosis, and renal stones, otherwise, misdiagnosis and treatment delay may occur. Hence, for patients with rare diseases, strict adherence to treatment principles and close follow-up are necessary to achieve favorable outcomes.

KEYWORDS

mucinous neoplasm, appendiceal mucinous neoplasm, kidney, renal pelvis, pyonephrosis, laparoscopic nephrectomy, case report

1 Introduction

Mucinous neoplasms are tumors that mostly originate in the epithelial tissue and secrete mucin excessively. They commonly emerge in the gastrointestinal tract, as well as in the ovaries and breasts, and they rarely develop in the urinary system (1). Appendiceal mucinous neoplasm (AMN) is a rare type of neoplasm affecting the digestive system, accounting for merely 0.2%–0.3% of all appendectomy specimens and causing atypical clinical symptoms during its early onset (2). Tumors of the renal pelvis mostly originate in the transitional epithelium, and 90% of the cases are urothelial carcinoma. Mucinous neoplasms of the renal pelvis represent only 1% of all malignant cases, thereby rarely reported (3); consequently, making a preoperative diagnosis is rather challenging, and the risk of misdiagnosis is high because of the lack of typical clinical, laboratory, and imaging findings (4, 5). Seeing as a research gap, we report a distinctly rare case of synchronous mucinous neoplasms of the renal pelvis and the appendix. In this case, the mucinous neoplasm of the renal pelvis was preoperatively misdiagnosed as pyonephrosis induced by renal stones. This case report aims to broaden the understanding of the disease and develop standard diagnosis and treatment approaches.

2 Case presentation

The reporting of this study conforms to CARE guidelines (6). A 64-year-old female with a body mass index (BMI) of 20.64 kg/m^2 was admitted to the urology department on June 22, 2021, complaining of persistent pain in the right lower back for over a year. The patient described the pain as intermittent, dull, and sore, occasionally accompanied by chills, low-grade fever (highest temperature: 37.8° C), abdominal distension, nausea, and vomiting. Abdominal pain, migratory pain in the right lower abdomen, urinary frequency, urgency, dysuria, gross hematuria, rectal bleeding, and purulent bloody stool were not reported. The patient also had no history of smoking, abdominal or lumbar surgery, or extracorporeal shockwave lithotripsy (ESWL). Physical examination revealed mild bulging in the right abdomen and tenderness on percussion over the right kidney. Preoperatively, urinalysis was negative for red blood cells and protein but positive for white blood cells (2+); hemanalysis and comprehensive metabolic panel showed no significant abnormalities; tumor marker tests revealed 25.7 ng/ml for carcinoembryonic antigen (CEA) and 33 U/ml for carbohydrate antigen 19-9 (CA-199). Computed tomography urography (CTU) suggested right kidney enlargement, multiple hyperdense nodules measuring approximately 23 × 10 mm in the right renal calyces, and right ureteral wall thickening. In addition, the contrast-enhanced urogram showed significant enlargement and dilatation of the right kidney and the upper segment of the right ureter. The appendix also thickened with mild enhancement, measuring approximately 14 mm in diameter, with a hypodense lumen without enhancement. Working diagnoses were i) right ureteral wall thickening, suggestive of inflammatory changes, multiple stones in the right kidney, and severe hydronephrosis of the right kidney; and ii) abnormal appendiceal density, suggestive of a mucinous tumor (Figures 1A–F). Intravenous urography (IVU) showed no development of the right kidney, right kidney stones, normal excretion of the left kidney, and scoliosis (Figure 1G). Computed tomography (CT) of the chest showed no mass lesions. The estimated glomerular filtration rates (eGFR) were 62.08 and 15.48 mL/min for the left and right kidneys, respectively. On the same day, the patient underwent ultrasound-guided percutaneous right nephrostomy under local anesthesia; consequently, a large amount of gelatinous material was drained. Furthermore, the standard analysis showed that the gelatinous material was negative for red blood cells and bacterial culture but positive for white blood cells (2+). Cystoscopy showed purulent deposits in the bladder. Although the diagnosis of a neoplastic lesion in the appendix was confirmed, we could not establish a definite diagnosis of the right kidney with suspected pyonephrosis preoperatively. The patient's family was informed of her condition and requested to prioritize the treatment for this neoplasm. Therefore, the patient was transferred to the gastrointestinal surgery department for further evaluation. Electronic colonoscopy with biopsy suggested AMN. Exfoliative cytology revealed numerous degenerated cells without apparent atypia in three consecutive tests, the results were negative, and on July 2, open appendectomy plus abdominal exploration was performed under general anesthesia. The appendix was completely removed, and upon specimen collection, a great amount of mucus was seen in the appendix cavity (Figure 2A). Postoperative pathology indicated low-grade AMN (LAMN) and the incisal margin of the appendix was negative (Figures 2B, C). As the patient decided to defer further treatment for the right kidney, she was discharged for rest and recovery.

On October 13, 2021, the patient was re-admitted to the urology department for right kidney treatment. Follow-up abdominal CT scans with contrast enhancement showed multiple stones, severe

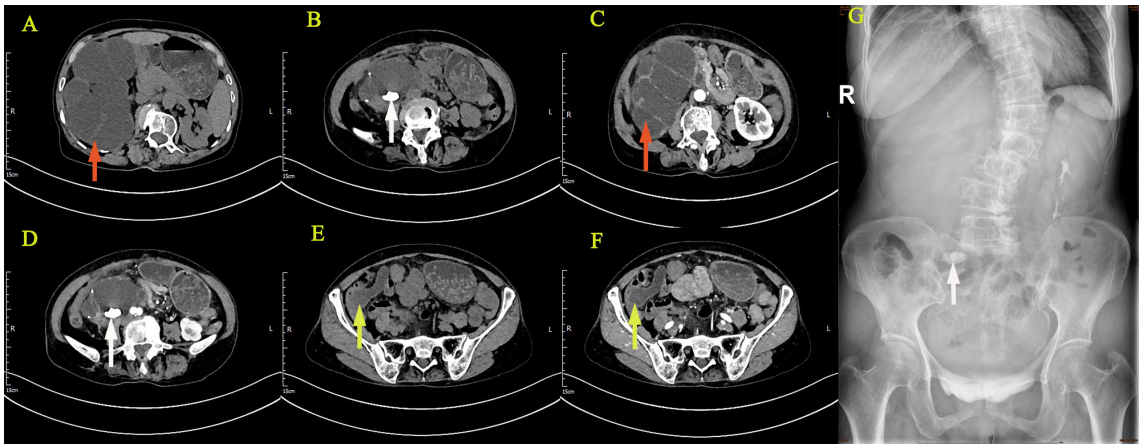

FIGURE 1
Imaging examination: CTU suggested right kidney enlargement **(A–D)**, multiple hyperdense nodules **(B, D)**, the contrast-enhanced urogram showed significant enlargement and dilatation of the right kidney and the upper segment of the right ureter **(C)**. The appendix also thickened with mild enhancement **(E, F)**, with a hypodense lumen without enhancement **(F)**. IVU showed no development of the right kidney, right kidney stone, and normal excretion of the left kidney **(G)**. (The giant right kidney was showed by red arrows, the kidney stone was showed by white arrows, and the appendix was showed by yellow arrows.).

hydronephrosis, and thickening of both the renal pelvis and the ureteral wall of the right kidney. Infectious lesions were considered. The appendix was not shown. Other abdominal parts were unremarkable. At the same time, the patient and her family agreed to laparoscopic right nephrectomy under general anesthesia. The right kidney was severely attached to the lateral peritoneum and surrounding tissues, making it difficult to be removed. Although the surgery went smoothly without conversion to open surgery or causing any incidental injuries, the operation lasted for approximately 230 min, with a blood loss of 200 ml. Postoperatively, 0.4 g of 5-fluorouracil and 500 ml of normal saline were infused once intraperitoneally for 2 h. The affected kidney and upper ureter remained intact after being removed from the body. When the kidney was sliced open, the following were found: dilated renal pelvis, thin renal parenchyma, multilocular and dilated renal calyces with abundant gelatinous mucus, multiple stones measuring approximately 20 × 15 × 9 mm and three cauliflower-like masses measuring approximately 20 × 18 × 8 mm in the renal pelvis, and calyces (Figure 2D). Postoperative pathology suggested a high-grade mucinous neoplasm of the renal pelvis and mucin residing partly in the interstitium of the cyst walls, without the involvement of the ureter, blood vessels, perirenal lymph nodes, or perirenal fat (Figures 2E, F). Immunohistochemistrical results showed that CDX2 (+), Villin (+), GATA3(−), P63 (−), CK7 (−) and Ki-67 (about 60%+), indicated features of appendiceal mucinous neoplasm metastasis to the renal pelvis (Figures 3A–F). The

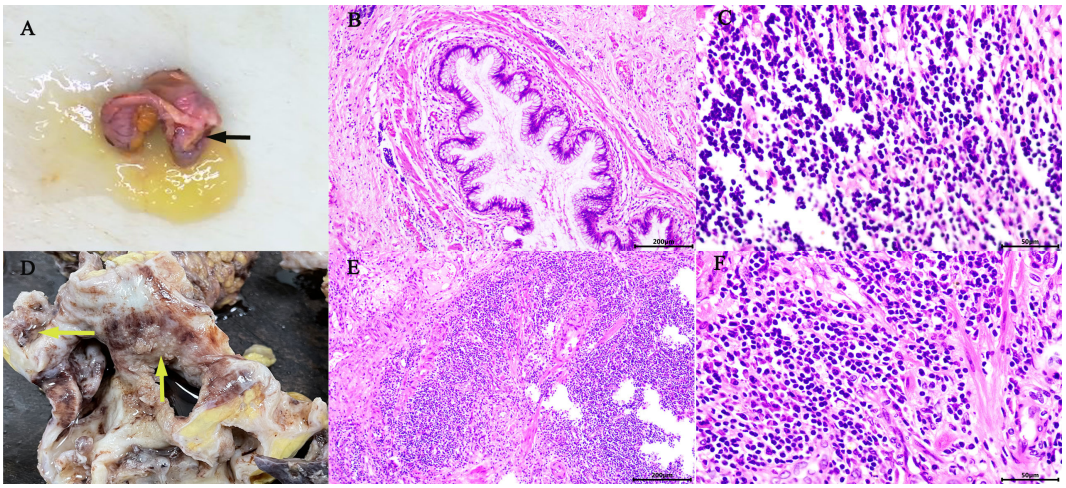

FIGURE 2
Gross appearance: The appendix was swollen and thickened, filled with mucus (black arrow) **(A)**. The right kidney was found: dilated renal pelvis, thin renal parenchyma, multilocular and dilated renal cysts with abundant gelatinous mucus and cauliflower-like masses in the renal pelvis and calyces (yellow arrow) **(D)**. Microscopic overview of the appendix **(B, C)** and the right kidney **(E, F)**. [Hematoxylin-eosin staining, ×100 **(B, E)**, ×400 **(C, F)**].

postoperative pathological stage was pT1N0M0. In the subsequent multidisciplinary consultation, salvage residual ureterectomy with a bladder cuff and chemotherapy were proposed, but both were refused by the patient. Perioperatively, no intestinal injury or any other complications occurred. The patient was satisfied with the treatment. The patient was discharged 7 days postoperatively and was closely followed up for 14 months. During the follow-up period, no secondary infection, intestinal obstruction, metastasis, or recurrence was observed, while the serum levels of CEA and CA-199 returned to normal.

3 Discussion

AMN is a rare type of gastrointestinal tumor with a low incidence, accounting for less than 1% of all cancers and 0.2%–0.3% of appendectomy specimens (2, 7). The incidence is similar between sexes, with a peak age of onset between 50 and 60 years, but the pathogenesis remains unclear. Mucinous cystic lesions of the appendix were first described by Rokitansky in 1842 as "mucoceles of the appendix" and were characterized as a swollen appendix filled with mucus (8). Malignant tumors of the appendix include neuroendocrine tumors, mucoepithelial tumors, lymphoma, goblet/pregoblet cell or complex carcinoid, adenocarcinoma, lymphoid or stromal sarcoma. In particular, neuroendocrine tumors and adenocarcinoma (mucinous, signet ring cell, or nonmucinous) represent approximately 65% and 20% of these malignant tumors of the appendix, respectively (2, 8, 9). Considering the rarity of these diseases and the lack of uniform clinical classification, the pathological characteristics and biological behavior of intraperitoneal dissemination are very difficult to describe. In 2016, the Peritoneal Surface Oncology Group International (PSOGI) classified appendiceal mucinous epithelial tumors of non-neuroendocrine origin into five categories: i) LAMN, ii) high-grade AMN (HAMN), iii) mucinous adenocarcinoma (MAC), iv) poorly differentiated signet ring cell adenocarcinoma (signet ring cells ≤ 50%), and v) signet ring cell carcinoma (signet ring cells > 50%). Among them, LAMN is the most common, accounting for approximately 60%–70% of all cases (10).

Achieving early diagnosis and accurate differentiation of the AMN pathological type is necessary for patient survival. LAMNs lack specific clinical manifestations; hence, most cases appear to be benign tumors at the early onset and need to be differentiated from other diseases, such as appendicitis, appendiceal perforation, and right lower abdominal masses. In advanced stages, LAMNs are manifested by intraperitoneal mucinous ascites or gastrointestinal adhesion-induced symptoms, such as chronic abdominal pain, abdominal distension, anemia, malnutrition, and intestinal obstruction (7, 11). Regardless of the specific classification, when the thin muscle layer of the appendiceal mucosa ruptures and mucin infiltrates through the appendiceal wall, AMNs can progress and induce peritoneal metastasis. An intraoperatively ruptured or residual mucinous tumor may be implanted in the peritoneum and eventually lead to peritoneal pseudomyxoma (PMP) (12, 13). Currently, surgery is the optimal treatment option for AMN (8), ensuring a complete abdominal exploration and tumor integrity preservation. Nevertheless, given the challenge of making an accurate preoperative diagnosis of a malignant AMN and identifying the typical characteristics of implantation metastasis, clinicians should be scrupulously careful when imaging findings suggest the presence of AMN or PMP. Moreover, considering that appendiceal tumors share the same origin as colorectal tumors, AMN may cooccur with colorectal cancer (CRC) (14). Therefore, preoperative colonoscopy is required to closely observe the appendiceal orifice, provide accurate pathology on biopsy, and rule out the possibility of concurrent CRC, facilitating the surgeons in selecting appropriate surgical strategies and determining the extent of surgical resection. Simple appendectomy can produce favorable clinical outcomes for LAMN without any extra-appendiceal disease. In addition, changes in the survival rates of patients with positive surgical margins after extended colectomy have been demonstrated to be

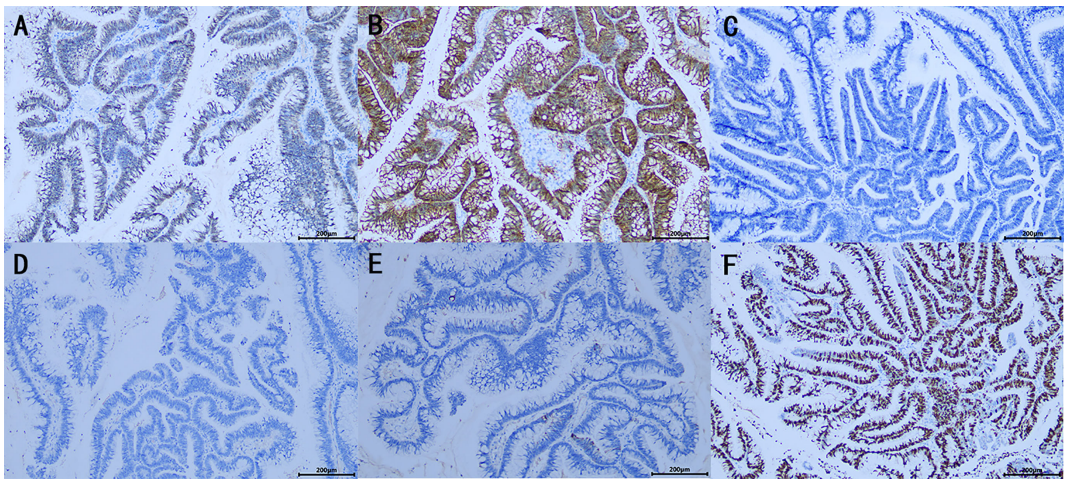

FIGURE 3
Immunohistochemistrical (IHC) analysis **(A–F)**: **(A)** CDX2 (+), **(B)** Villin (+), **(C)** GATA3(–), **(D)** P63 (–), **(E)** CK7 (–), **(F)** Ki-67 (about 60%+), indicated features of appendiceal mucinous neoplasm metastasis to the renal pelvis. (x100).

insignificant (15). AMN with local peritoneal metastasis is managed using the internationally accepted standard treatment regimen of cytoreductive surgery (CRS) with or without early postoperative intraperitoneal chemotherapy (EPIC) and hyperthermic intraperitoneal chemotherapy (HIPEC) to achieve longer survival (16, 17). In the present case, AMN was suspected when the CTU examination revealed appendiceal thickening, intraluminal hypodensities, and increased appendiceal wall thickness. Subsequently, colonoscopy and biopsy were ordered according to the treatment principles. Given that the pathology on biopsy met the diagnostic criteria for LAMN, standard appendectomy, abdominal exploration, and intraoperative freezing microtomy of resection margins were performed to ensure nontumorous tissue resection around the tumor. Moreover, with the postoperative pathology being consistent with the preoperative diagnosis, the treatment outcomes were favorable.

Most of the malignant tumors of the renal pelvis emerge from the transitional epithelium, as observed in approximately 90% of urothelial carcinomas, 10% of squamous cell carcinomas, and less than 1% of adenocarcinomas (18), among them, mucinous neoplasms of the renal pelvis are exceptionally rare, and was first reported by Ackerman in 1946 (19). However, its pathogenesis is still unclear, but it is generally believed that chronic infectious diseases, hydronephrosis, horseshoe kidney or kidney stones lead to obstruction and urothelial injury, which stimulate urothelial regeneration and repair, and then lead to glandular metaplasia of transitional epithelium, which gradually transforms into intestinal epithelium containing goblet cells, columnar cells and Pan's cells. On this basis, the cells further dysplasia and development of cancer, resulting in adenocarcinoma or MAC (20–23). These tumors may exhibit symptoms similar to those of renal stone-induced pyonephrosis; such symptoms include lower back pain, low-grade fever, hematuria, and pyuria. Imaging findings typically show an enlargement of the affected kidney, with renal sinus and pelvis dilation, renal cortex thinning, and concomitant renal stones but without distinctive space-occupying lesions. Given the lack of characteristic clinical manifestations, these conditions can be easily misdiagnosed as renal hydronephrosis or pyonephrosis with renal stones.

Primary mucinous neoplasms generally arise in the gastrointestinal tract or ovaries and are less likely to develop in the urinary system. Cases of AMNs with gynecological tumors of the ovaries, breasts, or endometrium have been reported (24). Unlike MAC of the appendix, LAMN is an indolent disease characterized by noninvasive growth and extremely limited distant metastasis (7, 25). Synchronous mucinous neoplasms of the renal pelvis and the appendix have not yet been reported. Hence, we cannot determine whether these neoplasms are both primary or if one has metastasized to the other. MAC of the renal pelvis may be diagnosed as primary only after ruling out the possibility of metastasis from the appendix, pancreas, colon, rectum, or ovary (26–29). Our patient first underwent appendectomy, and postoperative pathology suggested LAMN. The pathological findings and elevated serum levels of CEA and CA-199 indicated a strong possibility of AMN with secondary mucinous neoplasm of the renal pelvis. Despite all these important findings, the mechanism of LAMN metastasizing to the renal pelvis remains poorly understood. Further research is needed to confirm the potential association of metastasis with persistent obstruction and infection caused by renal stones.

Patients with primary renal pelvis MAC generally have a poor prognosis, with a survival rate of 2-5 years within the follow-up period (30, 31). Similar to transitional cell carcinoma, this primary MAC is managed by radical nephroureterectomy with a bladder cuff (4, 5, 28). Intraoperative renal rupture-induced cancer cell dissemination and inadequate surgical resection usually lead to recurrence and metastasis. Our patient underwent preoperative nephrostomy, which led to the drainage of a substantial amount of gelatinous material. This substance was collected for exfoliative cytology, which confirmed the absence of malignant cells in triplicate sample analyses. However, the patient underwent laparoscopic right nephrectomy because she was misdiagnosed with calculi and pyonephrosis of the right kidney according to the indistinctive clinical symptoms, standard examination of the gelatinous material, and imaging findings. Postoperative pathology suggested that the patient had high-grade mucinous neoplasm of the right renal pelvis, with free surgical margins in the ureter. With the pathology report, residual ureterectomy with a bladder cuff and chemotherapy were recommended to minimize the risk of local recurrence and metastasis caused by residual tumor cells in the ureter. Unfortunately, the patient refused both options. Although the patient's mucus exfoliative cytology was negative for 3 times before surgery, we still considered the possibility of malignant tumor cells in the mucus before surgery, so we performed more careful and removed the tumor as completely as possible during the operation. Considering the large volume of mucin in the opened specimen postoperatively, intraperitoneal chemotherapy using 0.4 g of 5-fluorouracil and 500 ml of normal saline was administered for 2 h immediately after surgery to prevent peritoneal implantation metastasis caused by possible intraoperative mucin spillage. Thus, the physicians need to follow up with the patient and observe the benefits of EPIC in preventing PMP formation induced by the renal pelvis mucinous neoplasm and prolonging survival (32). Fortunately, during the 14-month close postoperative follow-up, the patient showed no evidence of recurrence or metastasis, with the serum CEA and CA-199 levels returning to normal.

4 Conclusions

Currently, the accurate diagnosis of neoplastic lesions in the renal pelvis is still challenging, and undoubtedly needs to rely on pathological diagnosis. We need to rule out not only the common urothelial carcinoma in the pelvis, but also the rare renal cell carcinoma or metastatic tumor in the renal pelvis (33, 34). In this case, synchronous mucinous neoplasms of the renal pelvis and the appendix are indeed uncommon and have not yet been reported. Thus, developing an effective diagnosis and treatment plan is challenging. Limited by a lack of treatment experience, an insufficient understanding of mucinous neoplasms, and inadequate divergent thinking, renal pelvis mucinous neoplasm might be treated inappropriately. To ensure the right choice of surgical approach and achieve a favorable prognosis, clinicians need to confirm the origin and nature of the neoplasm through rapid freezing microtomy when

they detect mucin in the renal lesion intraoperatively. Although it is important to careful resection of the neoplasm with absolute discretion during the operation and ensure the principle of tumor free, long-term close follow-up and monitoring after surgery is also an essential part of improving the prognosis.

Data availability statement

The original contributions presented in the study are included in the article/supplementary material. Further inquiries can be directed to the corresponding author.

Ethics statement

The studies involving human participants were reviewed andapproved by Ethics Committee of the First Affiliated Hospital ofGannan Medical College. The patients/participants provided theirwritten informed consent for the publication of this case report.

Author contributions

YZ and XX prepared and wrote the article. YZ was directly involved in the management of the patients. QW and CZ were responsible for the collection and organization of the literature. QL revised the manuscript and acted as corresponding authors. All authors contributed to the article and approved the submitted version.

Funding

This work was supported by the science and technology plan project of Ganzhou (GZ2020ZSF042).

Acknowledgments

We would like to thank QL for his guidance on this paper and for editing and proofreading this manuscript in English.

Conflict of interest

The authors declare that the research was conducted in the absence of any commercial or financial relationships that could be construed as a potential conflict of interest.

Publisher's note

References

1. Benesch MGK, Mathieson A. Epidemiology of mucinous adenocarcinomas. *Cancers* (2020) 12(11):3193. doi: 10.3390/cancers12113193

2. Smeenk RM, van Velthuysen ML, Verwaal VJ, Zoetmulder FA. Appendiceal neoplasms and pseudomyxoma peritonei: a population based study. *Eur J Surg Oncol* (2008) 34(2):196–201. doi: 10.1016/j.ejso.2007.04.002

3. Tepeler A, Erdem MR, Kurt O, Topaktas R, Kilicaslan I, Armağan A, et al. A rare renal epithelial tumor: mucinous cystadenocarcinoma case report and review of the literature. *Case Rep Med* (2011) 2011:686283. doi: 10.1155/2011/686283

4. Li H, Xie F, Zhao C, Yi Z, Chen J, Zu X. Primary mucinous adenocarcinoma of the renal pelvis misdiagnosed as calculous pyonephrosis: a case report and literature review. *Transl Androl Urol* (2020) 9(2):781–8. doi: 10.21037/tau.2019.12.38

5. Han DS, Yuk SM, Youn CS, Park G, Sul HJ, Jang H. Primary mucinous cystadenocarcinoma of the renal pelvis misdiagnosed as ureteropelvic junction stenosis with renal pelvis stone: a case report and literature review. *World J Surg Oncol* (2015) 13:324. doi: 10.1186/s12957-015-0739-7

6. Agha RA, Franchi T, Sohrabi C, Mathew G, Kerwan ASCARE Group. The SCARE 2020 guideline: updating consensus surgical CAse REport (SCARE) guidelines. *Int J Surg* (2020) 84:226–30. doi: 10.1016/j.ijsu.2020.10.034

7. Shaib WL, Assi R, Shamseddine A, Alese OB, Staley C3rd, Memis B, et al. Appendiceal mucinous neoplasms: diagnosis and management. *Oncologist* (2017) 22 (9):1107–16. doi: 10.1634/theoncologist.2017-0081

8. Hatch QM, Gilbert EW. Appendiceal neoplasms. *Clin Colon Rectal Surg* (2018) 31(5):278–87. doi: 10.1055/s-0038-1642051

9. McCusker ME, Coté TR, Clegg LX, Sobin LH. Primary malignant neoplasms of the appendix: a population-based study from the surveillance, epidemiology and end-results program, 1973-1998. *Cancer* (2002) 94(12):3307–12. doi: 10.1002/cncr.10589

10. Carr NJ, Cecil TD, Mohamed F, Sobin LH, Sugarbaker PH, González-Moreno S, et al. A consensus for classification and pathologic reporting of pseudomyxoma peritonei and associated appendiceal neoplasia: the results of the peritoneal surface oncology group international (PSOGI) modified Delphi process. *Am J Surg Pathol* (2016) 40(1):14–26. doi: 10.1097/PAS.0000000000000535

11. Houlzé-Laroye C, Eveno C. Low-grade appendiceal mucinous neoplasms with bowel obstruction. *Pleura Peritoneum* (2019) 4(3):20190020. doi: 10.1515/pp-2019-0020

12. Carr NJ, Bibeau F, Bradley RF, Dartigues P, Feakins RM, Geisinger KR, et al. The histopathological classification, diagnosis and differential diagnosis of mucinous appendiceal neoplasms, appendiceal adenocarcinomas and pseudomyxoma peritonei. *Histopathology* (2017) 71(6):847–58. doi: 10.1111/his.13324

13. Hissong E, Yantiss RK. The frontiers of appendiceal controversies: mucinous neoplasms and pseudomyxoma peritonei. *Am J Surg Pathol* (2022) 46(1):e27–42. doi: 10.1097/PAS.0000000000001662

14. Ning S, Yang Y, Wang C, Luo F. Pseudomyxoma peritonei induced by low-grade appendiceal mucinous neoplasm accompanied by rectal cancer: a case report and literature review. *BMC Surg* (2019) 19(1):42. doi: 10.1186/s12893-019-0508-6

15. Elias H, Galata C, Warschkow R, Schmied BM, Steffen T, Post S, et al. Survival after resection of appendiceal carcinoma by hemicolectomy and less radical than hemicolectomy: a population-based propensity score matched analysis. *Colorectal Dis* (2017) 19(10):895–906. doi: 10.1111/codi.13746

16. Kusamura S, Barretta F, Yonemura Y, Sugarbaker PH, Moran BJ, Levine EA, et al. The role of hyperthermic intraperitoneal chemotherapy in pseudomyxoma peritonei after cytoreductive surgery. *JAMA Surg* (2021) 156(3):e206363. doi: 10.1001/jamasurg.2020.6363

17. Chua TC, Moran BJ, Sugarbaker PH, Levine EA, Glehen O, Gilly FN, et al. Early- and long-term outcome data of patients with pseudomyxoma peritonei from appendiceal origin treated by a strategy of cytoreductive surgery and hyperthermic intraperitoneal chemotherapy. *J Clin Oncol* (2012) 30(20):2449–56. doi: 10.1200/JCO.2011.39.7166

18. Rouprêt M, Babjuk M, Burger M, Capoun O, Cohen D, Compérat EM, et al. European Association of urology guidelines on upper urinary tract urothelial carcinoma: 2020 update. *Eur Urol* (2021) 79:62–79. doi: 10.1016/j.eururo.2020.05.042

19. Ackerman LV. Mucinous adenocarcinoma of the pelvis of the kidney. *J Urol* (1946) 55:36–45. doi: 10.1016/S0022-5347(17)69875-6

20. Mitome T, Yao M, Udaka N, Fusayasu S, Izumi K, Osaka K, et al. Mucinous cystadenoma of a horseshoe kidney: a case report and literature review. *Can Urol Assoc J* (2015) 9(1-2):E30–2. doi: 10.5489/cuaj.2211

21. Rao P, Pinheiro NJr, Franco M, Ra S, Costa H, Manzano J, et al. Pseudomyxoma peritonei associated with primary mucinous borderline tumor of the renal pelvicalyceal system. *Arch Pathol Lab Med* (2009) 133(9):1472–6. doi: 10.5858/133.9.1472

22. Sagnotta A, Dente M, Socciarelli F, Cacchi C, Stoppacciaro A, Balducci G, et al. Primary adenocarcinoma of the renal pelvis: histologic features of a stepwise process from intestinal hyperplasia to dysplasia in a patient with chronic renal abscess. *Int J Surg Pathol* (2014) 22(2):182–5. doi: 10.1177/1066896913502225

23. Terris MK, Anderson RU. Mucinous adenocarcinoma of the renal pelvis in natives of India. *Urol Int* (1997) 58(2):121–3. doi: 10.1159/000282966

24. Klingbeil KD, Azab B, Moller MG. Low-grade appendiceal mucinous neoplasm and endometriosis of the appendix. *World J Surg Oncol* (2017) 15(1):226. doi: 10.1186/s12957-017-1294-1

25. Zhao XY, Li CQ, Zhang SY, Liu G. Case report: an unusual case of pulmonary metastatic adenocarcinoma from low-grade appendiceal mucinous neoplasms. *Front Oncol* (2022) 12:906344. doi: 10.3389/fonc.2022.906344

26. Tamsin A, Schillebeeckx C, Van Langenhove C, Vander Eeckt K, Ost D, Wetzels K. Mucinous cystadenocarcinoma in the renal pelvis: primary or secondary? case report and literature review. *Acta Chir Belg* (2020) 120(6):417–24. doi: 10.1080/00015458.2019.1617515

27. Park S, Meng MV, Greenberg MS, Deng DY, Stoller ML. Muconephrosis. *Urology* (2002) 60(2):344. doi: 10.1016/s0090-4295(02)01707-7

28. Han B, Xie Q, Tang M, Zhao H, Xu X. Primary mucinous adenocarcinoma of the left renal pelvis with ectopic inferior vena cava and invasion of the left renal vein and the adjacent inferior vena cava: a case report. *Transl Cancer Res* (2021) 10(9):4243–49. doi: 10.21037/tcr-21-719

29. Ho CH, Lin WC, Pu YS, Yu HJ, Huang CY. Primary mucinous adenocarcinoma of renal pelvis with carcinoembryonic antigen production. *Urology* (2008) 71(5):984. doi: 10.1016/j.urology.2007.11.069

30. Ye YL, Bian J, Huang YP, Guo Y, Li ZX, Deng CH, et al. Primary mucinous adenocarcinoma of the renal pelvis with elevated CEA and CA19-9. *Urol Int* (2011) 87(4):484–8. doi: 10.1159/000329767

31. Ning Z, Zhang H, Wang B, Wang Y, Liu Y, Tao B, et al. Case report and literature review: robot-assisted laparoscopic left renal mucinous cystadenocarcinoma radical nephrectomy. *Front Surg* (2023) 9:1053852. doi: 10.3389/fsurg.2022.1053852

32. Shah VB, Amonkar GP, Deshpande JR, Bhalekar H. Mucinous adenocarcinoma of the renal pelvis with pseudomyxoma peritonei. *Indian J Pathol Microbiol* (2008) 51(4):536–7. doi: 10.4103/0377-4929.43753

33. Irama W, Teo JK, Wong KM. Renal cell carcinoma mimicking transitional cell carcinoma: a case report. *Am J Case Rep* (2021) 22:e932098. doi: 10.12659/AJCR.932098

34. Fujita O, Wada K, Yamasaki T, Manabe D, Takeda K, Nakamura S. Renal cell carcinoma with a tumor thrombus in the ureter: a case report. *BMC Urol* (2011) 11:16. doi: 10.1186/1471-2490-11-16

frontiers | Frontiers in Oncology

TYPE Systematic Review
PUBLISHED 19 July 2023
DOI 10.3389/fonc.2023.1210451

OPEN ACCESS

EDITED BY
Wen-Hao Xu,
Fudan University, China

REVIEWED BY
Fahad Quhal,
King Fahad Specialist Hospital Dammam, Saudi Arabia
Jiao Hu,
Central South University, China

*CORRESPONDENCE
Fan Yang
yangyangyang89757@163.com

RECEIVED 22 April 2023
ACCEPTED 03 July 2023
PUBLISHED 19 July 2023

CITATION
Mao H and Yang F (2023) Prognostic significance of albumin-to-globulin ratio in patients with renal cell carcinoma: a meta-analysis.
Front. Oncol. 13:1210451.
doi: 10.3389/fonc.2023.1210451

Prognostic significance of albumin-to-globulin ratio in patients with renal cell carcinoma: a meta-analysis

Huaying Mao[1] and Fan Yang[2]*

[1]Clinical Laboratory, Huzhou Central Hospital, Affiliated Central Hospital of Huzhou University, Huzhou, Zhejiang, China, [2]Clinical Laboratory, Huzhou Maternity and Child Health Care Hospital, Huzhou, Zhejiang, China

Background: Whether the albumin-to-globulin ratio (AGR) predicts the prognosis of renal cell carcinoma (RCC) remains controversial. Herein, we performed a meta-analysis to critically evaluate the relationship between the AGR and RCC prognosis, as well as the association between the AGR and the clinicopathological characteristics of RCC.

Methods: The PubMed, Web of Science, Embase, and Cochrane Library databases were thoroughly and comprehensively searched from their inception until 24 June 2023. To determine the predictive significance of the AGR, hazard ratios (HRs) and corresponding 95% confidence intervals (CIs) were calculated from the pooled data. The relationship between the AGR and the clinicopathological features of RCC was evaluated by estimating odds ratios (ORs) and 95% CIs in subgroup analyses.

Results: The meta-analysis included nine articles involving 5,671 RCC cases. A low AGR significantly correlated with worse overall survival (OS) (HR = 1.82, 95% CI = 1.37–2.41, p <0.001) and progression-free survival (PFS) (HR = 2.44, 95% CI = 1.61–3.70, p <0.001). Analysis of the pooled data also revealed significant associations between a low AGR and the following: female sex (OR = 1.48, 95% CI = 1.31–1.67, p <0.001), pT stage T3–T4 (OR = 4.12, 95% CI = 2.93–5.79, p <0.001), pN stage N1 (OR = 3.99, 95% CI = 2.40–6.64, p <0.001), tumor necrosis (OR = 3.83, 95% CI = 2.23–6.59, p <0.001), and Fuhrman grade 3–4 (OR = 1.82, 95% CI = 1.34–2.42, p <0.001). The AGR was not related to histology (OR = 0.83, 95% CI = 0.60–1.15, p = 0.267).

Conclusion: In patients with RCC, a low AGR strongly predicted poor OS and PFS and significantly correlated with clinicopathological features indicative of disease progression.

KEYWORDS

albumin-to-globulin ratio, renal cell carcinoma, meta-analysis, prognosis, blood test

Introduction

Renal cell carcinoma (RCC) accounts for approximately 2.2% of all cancer cases, and the median age at diagnosis age is 64 years (1, 2). Most (approximately 90%) malignant solid lesions in the kidney are RCCs (3). Globally, there were 431,288 new cases of RCC and 179,368 deaths from RCC in 2020 (1). Since 2012, the number of people developing RCC worldwide has increased by 22% according to the World Cancer Research Fund International (4).

RCC has three major subtypes: clear cell (approximately 80% of cases), papillary (approximately 15%), and chromophobe (approximately 5%) (5, 6). Despite significant advances in therapeutic strategies, RCC still has a poor prognosis. The overall 5-year survival rate is 8–59% (7); for advanced disease, it is <20%, and for metastatic RCC (mRCC), the median overall survival (OS) time is 10 months (8, 9). These poor outcomes may partly reflect the lack of powerful prognostic indicators (10). Consequently, identifying novel and effective biomarkers for prognosis prediction in patients with RCC in clinical settings is imperative.

Current evidence indicates that systemic chronic inflammation and malnutrition contribute to carcinogenesis and tumor progression (11, 12). Albumin (ALB) and globulin (GLB) are two major serum proteins that reflect nutritional and inflammatory status. The ALB-to-GLB ratio (AGR) is an established marker in oncology; it is calculated as follows: AGR = serum ALB/(total serum protein - serum ALB) (13). A low AGR has been widely associated with poor outcomes in various cancers, such as non-small-cell lung cancer (14), esophageal cancer (15), cervical cancer (16), multiple myeloma (17), and pancreatic cancer (18).

Previous studies have explored the prognostic significance of the AGR in patients with RCC (19–27). However, inconsistent results were obtained: in some studies, a low AGR significantly predicted worse survival (23, 26, 27), whereas in others, the AGR was unrelated to prognosis (21, 24, 25). To provide resolution, we performed a meta-analysis that evaluated the relationship between the AGR and RCC prognosis, as well as between the AGR and the clinicopathological characteristics of RCC.

Materials and methods

Study guideline

This meta-analysis was performed in accordance with the Preferred Reporting Items for Systematic Reviews and Meta-Analyses guidelines (28).

Abbreviations: AGR, albumin-to-globulin ratio; RCC, renal cell carcinoma; HR, hazard ratio; CI, confidence interval; OR, odds ratio; OS, overall survival; PFS, progression-free survival; ALB, albumin; GLB, globulin; NSCLC, non-small-cell lung cancer; PRISMA, Preferred Reporting Items for Systematic Reviews and Meta-Analyses; RFS, recurrence-free survival; CSS, cancer-specific survival; NOS, Newcastle-Ottawa Scale; DFS, disease-free survival; DMFS, distant metastasis-free survival.

Ethics statement

This study used data from previous articles, and approval from an ethics committee or institutional review board was therefore waived.

Search strategy

We thoroughly and comprehensively searched the PubMed, Web of Science, Embase, and Cochrane Library databases from their inception until 24 June 2023. Only English publications were selected. The following combinations of Medical Subject Headings and other terms were used: (albumin to globulin ratio, albumin/globulin ratio, AGR, or albumin-globulin ratio) and (renal cancer, kidney neoplasm, kidney cancer, renal cell carcinoma, renal carcinoma, or RCC). The references of the retrieved studies were manually examined to identify additional relevant studies.

Study eligibility criteria

We included English-language articles that reported the following: (1) the association between the AGR and survival outcome [e.g., OS, recurrence-free survival, cancer-specific survival (CSS), and progression-free survival (PFS)]; (2) hazard ratios (HRs) with 95% confidence intervals (CIs) or data that allowed their calculation; and (3) the threshold used to stratify a high/low AGR. Additional inclusion criteria were a pathological diagnosis of RCC and measurement of serum ALB and GLB levels before treatment. Meeting abstracts, reviews, case reports, letters, comments, studies with overlapping patients, and animal studies were excluded.

Data collection and quality evaluation

Two researchers (HM and FY) independently screened the retrieved articles and extracted and crosschecked the data. Disagreements between the two investigators were settled through negotiation until a consensus was reached. The data collected in this study included first author, country, publication year, sample size, study period, patient age and sex, number of study centers (single or multiple), metastatic status, treatment, follow-up period, AGR threshold, survival endpoints, type of survival analysis (univariate or multivariate), and HRs with 95% CIs. We used the Newcastle-Ottawa Scale (NOS) (29) to evaluate the quality of the study in three domains: selection (0–4 points), comparability (0–2 points), and outcome assessment (0–3 points), yielding a total score of 0–9. Articles with NOS scores ≥6 were considered high-quality.

Statistical analysis

HRs with 95% CIs were calculated to determine whether the AGR significantly predicted survival outcome. Inter-study heterogeneity was assessed using Higgin's I^2 statistic (30) and Cochran's Q test (31).

P values <0.10 and I^2 values >50% indicated heterogeneity. Random-effects and fixed-effects models are used for heterogeneous and non-heterogeneous data, respectively.

To further explore the ability of the AGR to predict RCC prognosis, subgroup analyses stratified by country, sample size, study center number, metastatic status, treatment, AGR threshold, and type of survival analysis were performed. Associations between the AGR and the clinicopathological features of RCC were evaluated by determining odds ratios (ORs) with 95% CIs. Begg's test (32) and Egger's test (33) were used to assess publication bias. Statistical analyses were performed using Stata software, version 12.0 (Stata Corporation, College Station, TX, USA). P values <0.05 indicated statistical significance.

Results

The literature selection process

A total of 155 studies were retrieved in the preliminary search; 37 duplicates were eliminated, leaving 118 studies (Figure 1). An additional 97 studies were excluded owing to irrelevance as determined upon title and abstract screening. Among the remaining 21 studies, 12 were discarded following full-text assessment: six did not analyze AGRs, four lacked survival data, one was a meeting abstract, and one had overlapping patients. Finally, nine articles involving 5,671 cases (19–27) were included in the present study.

Study features

Table 1 lists the basic features of the nine included studies. All studies were published between 2017 and 2021; five were performed in China (19, 20, 22, 24, 25), two in Turkey (21, 26), and one each in Korea (23) and Austria (27). All studies were retrospective (19–27), with sample sizes of 95–2,970 (median, 187). Seven studies were single-center (19–22, 24–26) and two were multicenter (23, 27). Four studies examined patients with non-mRCC (19, 21, 23, 24), three examined patients with mRCC (25–27), and two included patients at multiple stages (20, 22). Surgery was performed in eight studies (19–25, 27) and targeted therapy in one study (26). The threshold AGR was 1.11–1.64 (median, 1.43). Eight (19–21, 23–27) and six (19, 21–23, 26, 27) studies assessed the significance of the AGR in predicting OS and PFS, respectively. Multivariate regression analyses with HRs and CIs were performed in seven studies (19–21, 23, 24, 26, 27) and univariate analyses in two (22, 25). The NOS scores for the included articles ranged from 7 to 9, which indicated high quality.

AGR and OS

Eight studies with 5,484 patients provided information regarding the relationship between the pretreatment AGR and OS (19–21, 23–27). Owing to obvious heterogeneity (I^2 = 61.1%, p = 0.012), we used a random-effects model to collectively analyze the data in these studies. We found that a low AGR remarkably predicted worse OS (HR = 1.82, 95% CI = 1.37–2.41, p <0.001; Table 2 and Figure 2). In subgroup analyses, the ability of the AGR to predict OS was

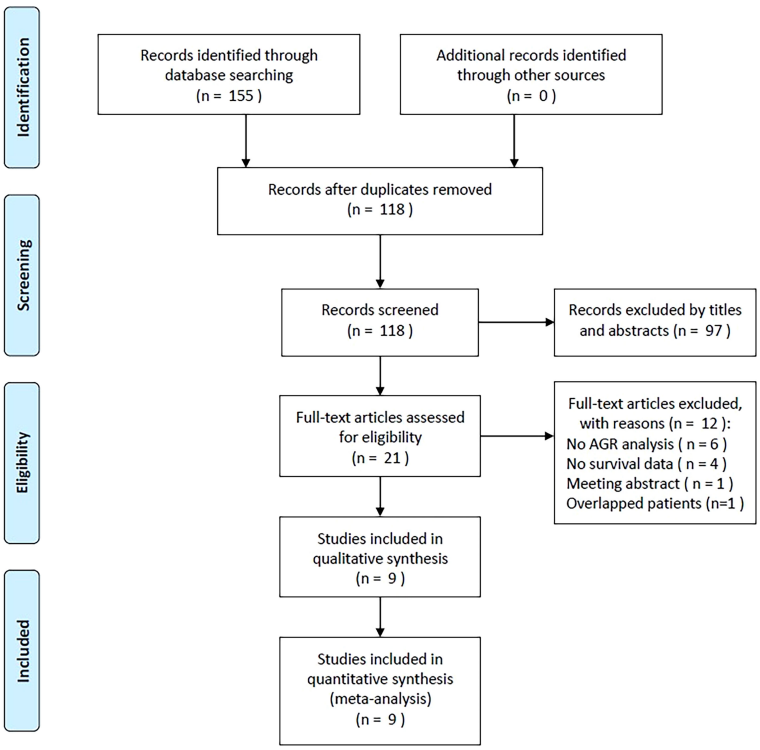

FIGURE 1
PRISMA flowchart of the established screening strategy.

TABLE 1 Baseline characteristics of included studies in this meta-analysis.

Study	Year	Country	Sample size	Study period	Age (year) Median (range)	Study center	Gender (M/F)	Study design	Metastatic status	Treatment	Cut-off value	Follow-up (month) Median (range)	Survival outcomes	Survival analysis	NOS score
Chen, Z.	2017	China	416	2003-2013	56.3 (24-80)	Single center	258/158	Retrospective	Non-metastatic	Surgery	1.22	69.2 (1-151)	OS, PFS	Multivariate	7
He, X.	2017	China	895	2000-2012	51.4	Single center	600/295	Retrospective	Mixed	Surgery	1.47	69.68	OS	Multivariate	7
Koparal, M. Y.	2018	Turkey	162	2010-2016	56.5	Single center	102/60	Retrospective	Non-metastatic	Surgery	1.40	27.5 (6-89)	OS, PFS	Multivariate	8
Bian, Z.	2020	China	187	2011-2017	56.7	Single center	118/69	Retrospective	Mixed	Surgery	1.64	54.6 (1-97.2)	PFS	Univariate	7
Chung, J. W.	2020	Korea	2,970	1999-2015	55.6	Multicenter	2,055/915	Retrospective	Non-metastatic	Surgery	1.47	26.0 (9.0-59.0)	OS, PFS	Multivariate	9
Hu, J.	2020	China	170	2010-2015	52.5	Single center	120/50	Retrospective	Non-metastatic	Surgery	1.35	70	OS	Multivariate	7
Xu, K.	2020	China	95	2005-2016	56 (16-75)	Single center	84/11	Retrospective	Metastatic	Surgery	1.5	51 (6-132)	OS	Univariate	8
Aktepe, O. H.	2021	Turkey	163	2008-2019	60 (53-65)	Single center	120/43	Retrospective	Metastatic	Targeted therapy	1.11	19.05 (1.31-102.6)	OS, PFS	Multivariate	7
Laukhtina, E.	2021	Austria	613	NR	57 (50-64)	Multicenter	428/185	Retrospective	Metastatic	Surgery	1.43	31	OS, PFS	Multivariate	8

M, male; F, female; OS, overall survival; PFS ,progression-free survival; NOS, Newcastle-Ottawa Scale.

10.3389/fonc.2023.1210451

unaffected by sample size, country, study center number, metastatic status, treatment, or AGR threshold (Table 2). Moreover, a low AGR significantly predicted poor OS in a multivariate analysis (HR = 1.98, 95% CI = 1.47–2.66, p <0.001; Table 2).

AGR and PFS

Six articles with 4,511 patients examined the relationship between the pretreatment AGR and PFS (19, 21–23, 26, 27). Owing to obvious heterogeneity (I^2 = 75.9%, p = 0.001), we used a random-effects model to collectively analyze the data in these articles. We found that a low AGR strongly predicted worse PFS (HR = 2.44, 95% CI = 1.61–3.70, p <0.001; Figure 3 and Table 3). In subgroup analyses, a low AGR significantly predicted poor PFS regardless of country, sample size, study center number, metastatic status, treatment, cut-off value, or type of survival analysis (Table 3).

Relationship between the AGR and clinicopathological features

The relationship between the pretreatment AGR and the clinicopathological features of RCC was analyzed using data from six studies with 5,219 patients (19–21, 23, 26, 27). The clinicopathological characteristics examined were as follows: sex (female vs male), pT stage (T3–T4 vs T1–T2), pN stage (N1 vs N0), tumor necrosis (present vs absent), histology (clear cell RCC vs non-clear cell RCC), and Fuhrman grade (3–4 vs 1–2). As shown in Table 4 and Figure 4, a low AGR closely correlated with the female sex (OR = 1.48, 95% CI = 1.31–1.67, p <0.001), pT stage T3–T4 (OR = 4.12, 95% CI = 2.93–5.79, p <0.001), pN stage N1 (OR = 3.99, 95% CI = 2.40–6.64, p <0.001), presence of tumor necrosis (OR = 3.83, 95% CI = 2.23–6.59, p <0.001), and Fuhrman grade 3–4 (OR = 1.82, 95% CI = 1.34–2.42, p <0.001). The AGR was not related to histology (OR = 0.83, 95% CI = 0.60–1.15, p = 0.267).

TABLE 2 Subgroup analysis of prognostic value of AGR for OS in patients with RCC.

Variables	No. of studies	No. of patients	Effects model	HR (95%CI)	p	Heterogeneity I^2(%)	Ph
Total	8	5,484	Random	1.82 (1.37-2.41)	<0.001	61.1	0.012
Country							
China	4	1,576	Random	2.11 (1.10-4.05)	0.025	81.5	0.001
Other than China	4	3,908	Fixed	1.66 (1.37-2.02)	<0.001	0	0.623
Sample size							
<200	4	590	Fixed	1.54 (1.16-2.04)	0.002	37.0	0.190
≥200	4	4,894	Random	2.04 (1.32-3.14)	0.001	76.7	0.005
Study center							
Single center	6	1,901	Random	1.99 (1.27-3.13)	0.003	70.8	0.004
Multicenter	2	3,583	Fixed	1.58 (1.26-1.97)	<0.001	0	0.511
Metastatic status							
Non-metastatic	4	3,718	Random	2.57 (1.28-5.14)	0.008	66.2	0.031
Metastatic	3	871	Random	1.51 (1.12-2.04)	0.007	51.0	0.130
Mixed	1	895	–	1.59 (1.08-2.33)	0.019	–	–
Treatment							
Surgery	7	5,321	Random	1.78 (1.29-2.46)	<0.001	64.3	0.010
Targeted therapy	1	163	–	2.10 (1.34-3.29)	0.001	–	–
Cut-off value							
<1.43	4	911	Random	2.73 (1.45-5.12)	0.002	59.0	0.062
≥1.43	4	4,573	Fixed	1.48 (1.25-1.77)	<0.001	0	0.456
Survival analysis							
Univariate	1	95	–	1.13 (0.75-1.69)	0.567	–	–
Multivariate	7	5,389	Random	1.98 (1.47-2.66)	<0.001	56.7	0.031

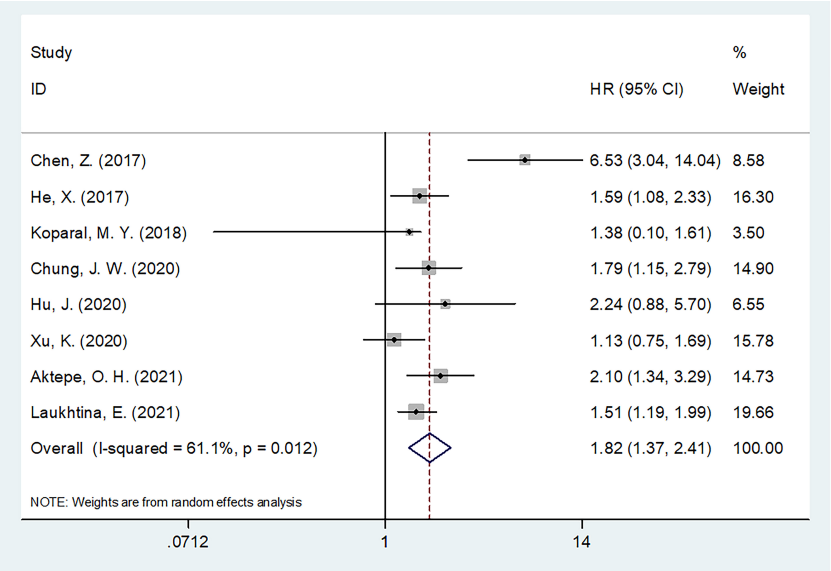

FIGURE 2
Forest plots of the prognostic role of AGR for OS in patients with RCC.

Publication bias

Begg's and Egger's tests were used to assess publication bias. Funnel plots revealed rough symmetry regarding the distribution of many of the included articles, indicating the absence of obvious publication bias for OS (p = 0.266 and 0.236 for Begg's and Egger's tests, respectively) and PFS (p = 0.260 and 0.087, respectively; Figure 5).

Discussion

Whether the AGR predicts RCC prognosis is unclear, with previous reports providing conflicting results (19–27). The present meta-analysis, which synthesized data from nine studies with 5,671 RCC cases, revealed a robust association between a low pretreatment AGR and shorter OS and PFS times. As a reflection of the aggressive nature of RCC, a low AGR also correlated with pT stage T3–T4, pN stage N1, tumor necrosis, and Fuhrman grade 3–4. Hence, it might serve as a stable predictor of the short- and long-term prognosis of patients with RCC; notably, patients with low AGRs tended to experience tumor progression and metastasis. To our knowledge, this is the first reported meta-analysis of the significance of the AGR in predicting the prognosis and clinicopathological features of RCC.

The AGR compares ALB and GLB levels, with a low AGR indicating a low ALB and/or high GLB level. The potential

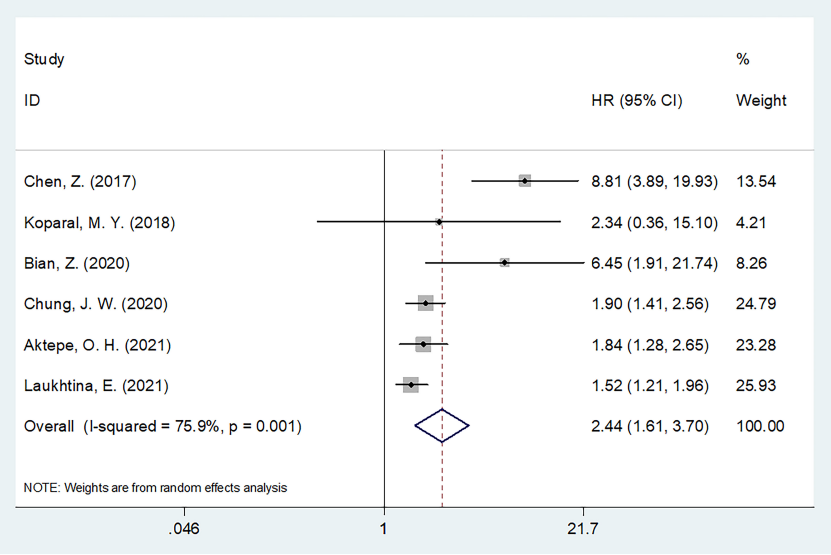

FIGURE 3
Forest plots of the prognostic role of AGR for PFS in patients with RCC.

TABLE 3 Subgroup analysis of prognostic value of AGR for PFS in patients with RCC.

Variables	No. of studies	No. of patients	Effects model	HR (95%CI)	p	Heterogeneity I^2(%) Ph	
Total	6	4,511	Random	2.44 (1.61-3.70)	<0.001	75.9	0.001
Country							
China	2	603	Fixed	8.00 (4.06-15.75)	<0.001	0	0.676
Other than China	4	3,908	Fixed	1.70 (1.44-2.01)	<0.001	0	0.647
Sample size							
<200	3	512	Fixed	2.05 (1.45-2.89)	<0.001	46.9	0.152
≥200	3	3,999	Random	2.51 (1.36-4.65)	0.003	87.9	<0.001
Study center							
Single center	4	928	Random	3.96 (1.48-10.59)	0.006	78.8	0.003
Multicenter	2	3,583	Fixed	1.66 (1.38-2.00)	<0.001	23.6	0.253
Metastatic status							
Non-metastatic	3	3,548	Random	3.46 (1.07-11.26)	0.039	83.3	0.003
Metastatic	2	776	Fixed	1.61 (1.32-1.97)	<0.001	0	0.396
Mixed	1	187	–	6.45 (1.91-21.80)	0.003	–	–
Treatment							
Surgery	5	4,348	Random	2.84 (1.62-4.98)	<0.001	80.7	<0.001
Targeted therapy	1	163	–	1.84 (1.27-2.65)	0.001	–	–
Cut-off value							
<1.43	3	741	Random	3.43 (1.03-11.40)	0.044	83.0	0.003
≥1.43	3	3,770	Random	1.91 (1.28-2.83)	0.001	66.5	0.050
Survival analysis							
Univariate	1	187	–	6.45 (1.91-21.80)	0.003	–	–
Multivariate	5	4,324	Random	2.21 (1.47-3.30)	<0.001	75.9	0.002

mechanisms underlying the correspondence between a low AGR and poor RCC prognosis reflect the anti-oncogenic and pro-oncogenic actions of ALB and GLB, respectively. Serum ALB, a liver-generated soluble protein, maintains capillary osmotic pressure, removes free radicals from the blood (13), inhibits systemic inflammatory reactions, and serves as a marker of nutritional status (34). Malnutrition and inflammation impede its synthesis, as does interleukin-6 during the acute phase of inflammation in hepatocytes (35). ALB levels have been useful for predicting the outcomes of various cancers (36). The GLB component of the AGR includes diverse proinflammatory proteins, such as immunoglobulins, C-reactive protein,

TABLE 4 The association between AGR and clinicopathological features in patients with RCC.

Factors	No. of studies	No. of patients	Effects model	OR (95%CI)	p	Heterogeneity I^2(%) Ph	
Gender (female vs male)	6	5,219	Fixed	1.48 (1.31-1.67)	<0.001	0	0.473
pT stage (T3-T4 vs T1-T2)	3	1,473	Fixed	4.12 (2.93-5.79)	<0.001	17.3	0.299
pN stage (N1 vs N0)	2	1,311	Fixed	3.99 (2.40-6.64)	<0.001	0	0.682
Tumor necrosis (present vs absent)	2	578	Fixed	3.83 (2.23-6.59)	<0.001	0	0.660
Histology (ccRCC vs non-ccRCC)	3	1,671	Fixed	0.83 (0.60-1.15)	0.267	0	0.961
Fuhrman grade (G3-G4 vs G1-G2)	4	1,636	Fixed	1.82 (1.38-2.42)	<0.001	0	0.419

ccRCC, clear cell renal cell carcinoma.

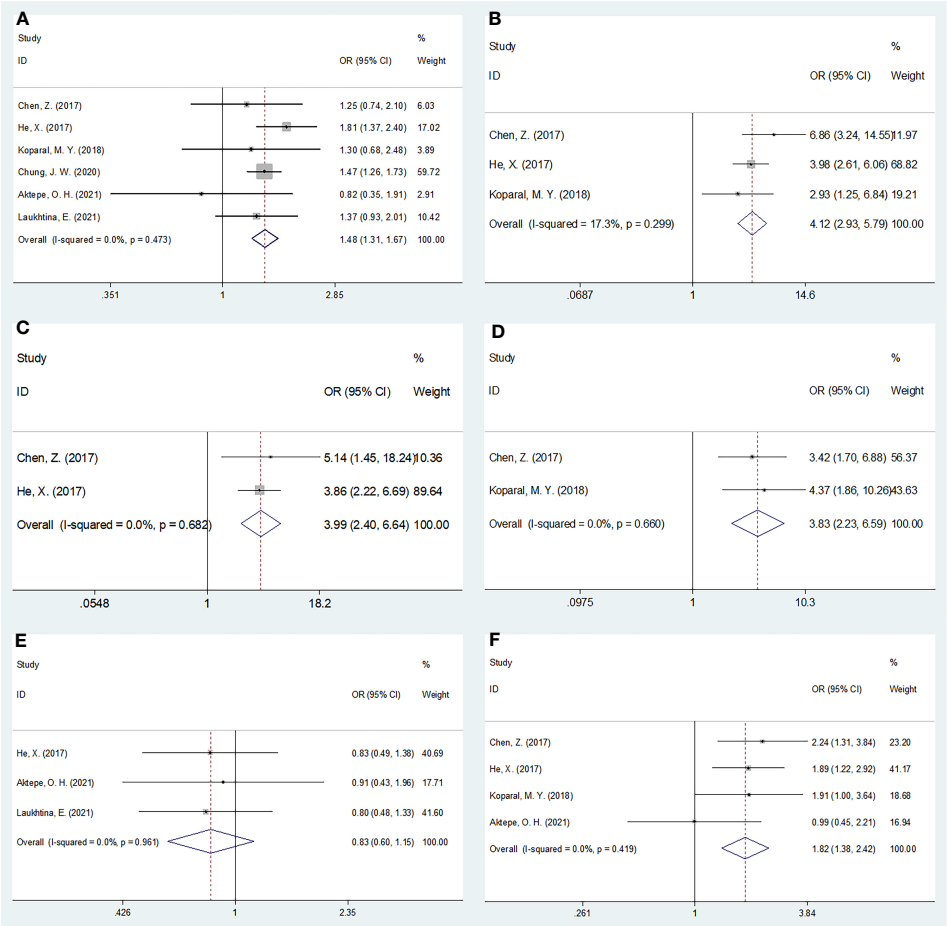

FIGURE 4
Forest plots evaluating the association between AGR and clinicopathological features in RCC. **(A)** Gender (female vs male); **(B)** pT stage (T3-T4 vs T1-T2); **(C)** pN stage (N1 vs N0); **(D)** Tumor necrosis (present vs absent); **(E)** Histology (ccRCC vs non-ccRCC); and **(F)** Fuhrman grade (G3-G4 vs G1-G2).

complement components (37), α-2 macroglobulin, fibrinogen, prothrombin, and serum amyloid A (38, 39). Because immunoglobulins are primarily metabolized in the liver, their clearance is impaired in patients with severe hepatic dysfunction, resulting in hyperglobulinemia (40, 41). In support of a potential role of GLB in apoptosis and carcinogenesis, a previous study associated increases in immunoglobulin levels with variations in the gene encoding tumor necrosis factor receptor 13B (42). Therefore, the AGR, which considers both ALB and GLB levels, is a reasonable and reliable prognostic marker.

Notably, a recent large-scale multicenter real-world retrospective study used pretreatment clinical characteristics to identify patients with muscle-invasive bladder cancer (MIBC) who could benefit from neoadjuvant combination therapy (43). Based on the combined prognostic efficiency of four hematological indexes [platelet-to-lymphocyte ratio (PLR) and hemoglobin, globulin, and platelet levels], a new indicator, the PLR.GHR (PLR*Globulin/Hemoglobin), was developed for MIBC (43). This finding has important implications in terms of the findings of our meta-analysis on RCC

Previous studies have evaluated various hematological parameters as predictors of RCC outcomes. In the report by De Giorgi et al., the systemic immune inflammation index and body mass index independently predicted OS in RCC patients treated with nivolumab (44). In studies of mRCC, a low pretreatment prognostic nutritional index was a potential risk factor after first-line therapy with tyrosine kinase inhibitors (45), and the PLR was an independent indicator of survival in a large cohort (n = 921) (46). Additionally, a recent meta-analysis associated a high pretreatment neutrophil-to-lymphocyte ratio and PLR with progression and mortality in mRCC patients treated with immune checkpoint inhibitors. Collectively, these studies implicate multiple hematological parameters in RCC prognosis (44–47).

Both units of the AGR (ALB and GLB) are important components of the tumor microenvironment. Therefore, the prognostic capability of the AGR can be influenced by tumor immune markers, such as branched chain aminotransferase 2 (BCAT2) (48), 5 methylcytosine (5mC) (49), and Siglec15 (50), all of which have been shown to shape the tumor microenvironment (48–50). The relationship between the AGR and these markers should be investigated in future studies.

Several meta-analyses suggest that a low pretreatment AGR can predict the prognosis of various cancers (51–55). In a meta-analysis of 3,211 patients with head and neck cancer, a low AGR

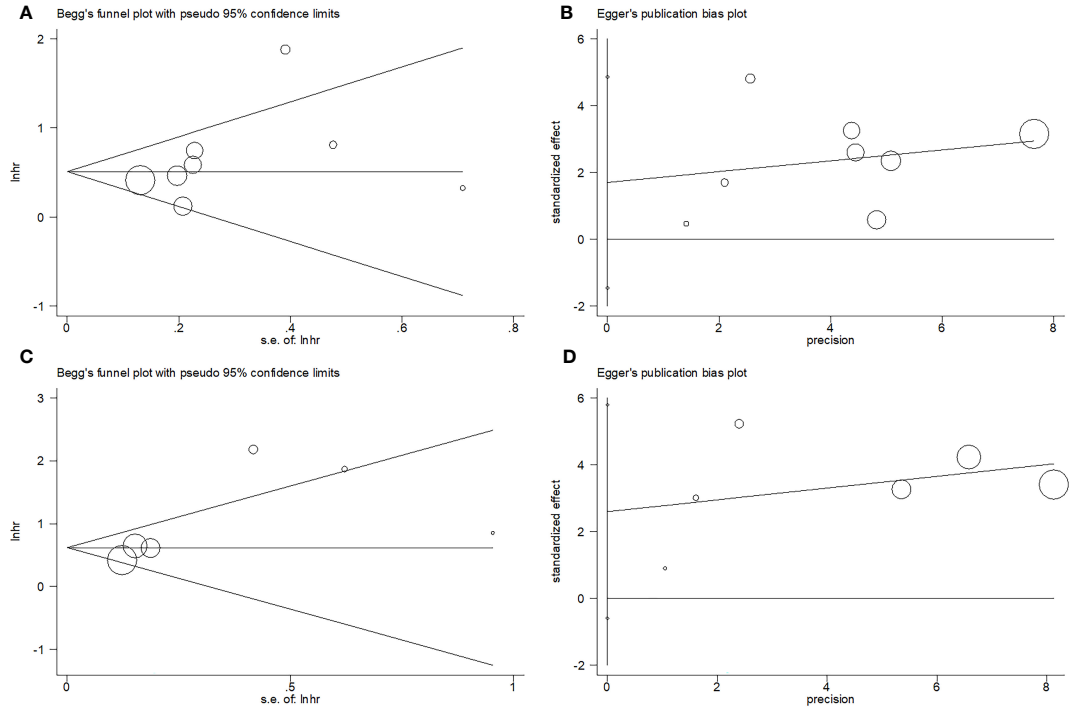

FIGURE 5
Publication test by Begg' test and Egger's test. **(A)** Begg's test for OS, p=0.266; **(B)** Egger's test for OS, p=0.236; **(C)** Begg's test for PFS, p=0.260; and **(D)** Egger's test for PFS, p=0.087.

significantly correlated with poor disease-free survival (DFS), distant metastasis-free survival, OS, T3–T4 status, lymph node metastasis, and stage III–IV disease (51). In a meta-analysis of 7,211 patients with metastatic prostate cancer, the AGR independently predicted PFS and CSS (52). Furthermore, in a meta-analysis of 8,397 patients with colorectal cancer, a low AGR robustly predicted poor OS and DFS/PFS (53). In additional meta-analyses, a low AGR remarkably predicted poor OS and DFS in patients (n = 3,496) with lung cancer (54) and was closely associated with poor OS and DFS/PFS in patients with gastric cancer (12 articles) (55).

The present study had some limitations. First, because all included articles were retrospective, inherent heterogeneity existed. However, the appropriate model for analysis of heterogeneous data (the random-effects model) was used. Second, the sample size was relatively small. Although we searched several databases, only nine relevant studies were retrieved. Third, most of the eligible studies were conducted in Asia. Consequently, our findings might be more applicable to Asian vs non-Asian patients with RCC. Owing to these limitations, larger, multi-arm prospective studies are needed to validate the prognostic significance of the pretreatment AGR in patients with RCC.

In conclusion, a low AGR markedly predicted poor OS and PFS in patients with RCC and significantly correlated with clinicopathological features indicative of disease progression. Use of the AGR will aid the identification of high-risk individuals and expedite the development of effective therapeutic strategies for RCC.

Data availability statement

The data that support the findings of this study are available from the corresponding author upon reasonable request.

Author contributions

HM and FY contributed to conception and design of the study. HM and FY were in charge of data collection. HM and FY performed the statistical analysis. HM wrote the first draft of the manuscript. FY edited the manuscript. All authors contributed to the article and approved the submitted version.

Acknowledgments

We would like to thank Editage (www.editage.com) for English language editing.

Conflict of interest

The authors declare that the research was conducted in the absence of any commercial or financial relationships that could be construed as a potential conflict of interest.

Publisher's note

References

1. Sung H, Ferlay J, Siegel RL, Laversanne M, Soerjomataram I, Jemal A, et al. Global cancer statistics 2020: GLOBOCAN estimates of incidence and mortality worldwide for 36 cancers in 185 countries. *CA: Cancer J Clin* (2021) 71(3):209–49. doi: 10.3322/caac.21660

2. Scelo G, Larose TL. Epidemiology and risk factors for kidney cancer. *J Clin Oncol* (2018) 36(36):Jco2018791905. doi: 10.1200/jco.2018.79.1905

3. Ljungberg B, Albiges L, Abu-Ghanem Y, Bedke J, Capitanio U, Dabestani S, et al. European association of urology guidelines on renal cell carcinoma: the 2022 update. *Eur Urol* (2022) 82(4):399–410. doi: 10.1016/j.eururo.2022.03.006

4. International WCRF. *Kidney cancer statistics* (2020). Available at: https://wwwwcrforg/cancer-trends/kidney-cancer-statistics/.

5. Hsieh JJ, Purdue MP, Signoretti S, Swanton C, Albiges L, Schmidinger M, et al. Renal cell carcinoma. *Nat Rev Dis Primers* (2017) 3:17009. doi: 10.1038/nrdp.2017.9

6. Singh D. Current updates and future perspectives on the management of renal cell carcinoma. *Life Sci* (2021) 264:118632. doi: 10.1016/j.lfs.2020.118632

7. Park JY, Tae BS, Jeong CW, Song C, Seo SI, Hong SK, et al. Development of the clinical calculator for mortality of patients with metastatic clear cell type renal cell carcinoma: An analysis of patients from Korean Renal Cancer Study Group database. *Invest Clin Urol* (2020) 61(3):260–8. doi: 10.4111/icu.2020.61.3.260

8. Culp SH, Karam JA, Wood CG. Population-based analysis of factors associated with survival in patients undergoing cytoreductive nephrectomy in the targeted therapy era. *Urologic Oncol* (2014) 32(5):561–8. doi: 10.1016/j.urolonc.2013.12.003

9. Internò V, De Santis P, Stucci LS, Rudà R, Tucci M, Soffietti R, et al. Prognostic factors and current treatment strategies for renal cell carcinoma metastatic to the brain: an overview. *Cancers (Basel)* (2021) 13(9):2114. doi: 10.3390/cancers13092114

10. Gulati S, Vogelzang NJ. Biomarkers in renal cell carcinoma: Are we there yet? *Asian J Urol* (2021) 8(4):362–75. doi: 10.1016/j.ajur.2021.05.013

11. Bromberg J, Wang TC. Inflammation and cancer: IL-6 and STAT3 complete the link. *Cancer Cell* (2009) 15(2):79–80. doi: 10.1016/j.ccr.2009.01.009

12. McMillan DC, Watson WS, O'Gorman P, Preston T, Scott HR, McArdle CS. Albumin concentrations are primarily determined by the body cell mass and the systemic inflammatory response in cancer patients with weight loss. *Nutr Cancer* (2001) 39(2):210–3. doi: 10.1207/S15327914nc392_8

13. Song WJ, Li NC, Gao J, Xu ZP, Liu JY, Long Z, et al. The predictive significance of prognostic nutritional index and serum albumin/globulin ratio on the overall survival of penile cancer patients undergoing penectomy. *Curr Oncol (Toronto Ont)* (2022) 29(10):7569–78. doi: 10.3390/curroncol29100596

14. Lu P, Ma Y, Wei S, Liang X. A low albumin-to-globulin ratio predicts a poor prognosis in patients with metastatic non-small-cell lung cancer. *Front Med* (2021) 8:621592. doi: 10.3389/fmed.2021.621592

15. Atsumi Y, Kawahara S, Kakuta S, Onodera A, Hara K, Kazama K, et al. Low preoperative albumin-to-globulin ratio is a marker of poor prognosis in patients with esophageal cancer. *In Vivo* (2021) 35(6):3555–61. doi: 10.21873/invivo.12658

16. Kawata A, Taguchi A, Baba S, Miyamoto Y, Tanikawa M, Sone K, et al. A low preoperative albumin-to-globulin ratio is a negative prognostic factor in patients with surgically treated cervical cancer. *Int J Clin Oncol* (2021) 26(5):980–5. doi: 10.1007/s10147-021-01861-8

17. Cai Y, Zhao Y, Dai Q, Xu M, Xu X, Xia W. Prognostic value of the albumin-globulin ratio and albumin-globulin score in patients with multiple myeloma. *J Int Med Res* (2021) 49(3):300060521997736. doi: 10.1177/0300060521997736

18. Hayashi M, Kobayashi D, Takami H, Inokawa Y, Tanaka N, Kurimoto K, et al. Albumin-globulin ratio indicates the survival outcome of pancreatic cancer cases who underwent preoperative treatment and curative surgical resection. *Nutr Cancer* (2023) 75(5):1330–39. doi: 10.1080/01635581.2023.2191384

19. Chen Z, Shao Y, Yao H, Zhuang Q, Wang K, Xing Z, et al. Preoperative albumin to globulin ratio predicts survival in clear cell renal cell carcinoma patients. *Oncotarget* (2017) 8(29):48291–302. doi: 10.18632/oncotarget.15162

20. He X, Guo S, Chen D, Yang G, Chen X, Zhang Y, et al. Preoperative albumin to globulin ratio (AGR) as prognostic factor in renal cell carcinoma. *J Cancer* (2017) 8(2):258–65. doi: 10.7150/jca.16525

21. Koparal MY, Polat F, Çetin S, Bulut EC, Sözen TS. Prognostic role of preoperative albumin to globulin ratio in predicting survival of clear cell renal cell carcinoma. *Int Braz J urol* (2018) 44(5):933–46. doi: 10.1590/s1677-5538.Ibju.2018.0012

22. Bian Z, Meng J, Niu Q, Jin X, Wang J, Feng X, et al. Prognostic role of prothrombin time activity, prothrombin time, albumin/globulin ratio, platelets, sex, and fibrinogen in predicting recurrence-free survival time of renal cancer. *Cancer Manag Res* (2020) 12:8481–90. doi: 10.2147/cmar.S264856

23. Chung JW, Park DJ, Chun SY, Choi SH, Lee JN, Kim BS, et al. The prognostic role of preoperative serum albumin/globulin ratio in patients with non-metastatic renal cell carcinoma undergoing partial or radical nephrectomy. *Sci Rep* (2020) 10(1):11999. doi: 10.1038/s41598-020-68975-3

24. Hu J, Chen J, Li H, He T, Deng H, Gong G, et al. A preoperative nomogram predicting the pseudocapsule status in localized renal cell carcinoma. *Transl Androl Urol* (2020) 9(2):462–72. doi: 10.21037/tau.2020.01.26

25. Xu K, Li J, Hu M, Zhang H, Yang J, Gong H, et al. Prognostic significance of preoperative inflammatory biomarkers and traditional clinical parameters in patients with spinal metastasis from clear cell renal cell carcinoma: A retrospective study of 95 patients in a single center. *Cancer Manag Res* (2020) 12:59–70. doi: 10.2147/cmar.S228570

26. Aktepe OH, Güner G, Güven DC, Taban H, Yıldırım H, Şahin TK, et al. Impact of albumin to globulin ratio on survival outcomes of patients with metastatic renal cell carcinoma. *Turkish J Urol* (2021) 47(2):113–9. doi: 10.5152/tud.2021.20377

27. Laukhtina E, Pradere B, D'Andrea D, Rosiello G, Luzzago S, Pecoraro A, et al. Prognostic effect of preoperative serum albumin to globulin ratio in patients treated with cytoreductive nephrectomy for metastatic renal cell carcinoma. *Transl Androl Urol* (2021) 10(2):609–19. doi: 10.21037/tau-20-1101

28. Moher D, Liberati A, Tetzlaff J, Altman DG, Grp P. Preferred reporting items for systematic reviews and meta-analyses: the PRISMA statement. *J Clin Epidemiol* (2009) 62(10):1006–12. doi: 10.1016/j.jclinepi.2009.06.005

29. Stang A. Critical evaluation of the Newcastle-Ottawa scale for the assessment of the quality of nonrandomized studies in meta-analyses. *Eur J Epidemiol* (2010) 25(9):603–5. doi: 10.1007/s10654-010-9491-z

30. Higgins JPT, Thompson SG. Quantifying heterogeneity in a meta-analysis. *Stat Med* (2002) 21(11):1539–58. doi: 10.1002/sim.1186

31. Cochran W. The combination of estimates from different experiments. *Biometrics* (1954) 10:101–29.

32. Begg CB, Mazumdar M. Operating characteristics of a rank correlation test for publication bias. *Biometrics* (1994) 50(4):1088–101. doi: 10.2307/2533446

33. Egger M, Smith GD, Schneider M, Minder C. Bias in meta-analysis detected by a simple, graphical test. *Bmj-British Med J* (1997) 315(7109):629–34. doi: 10.1136/bmj.315.7109.629

34. Doweiko JP, Nompleggi DJ. The role of albumin in human physiology and pathophysiology, Part III: Albumin and disease states. *JPEN J parenteral enteral Nutr* (1991) 15(4):476–83. doi: 10.1177/0148607191015004476

35. Xu C, Wu X, Hack BK, Bao L, Cunningham PN. TNF causes changes in glomerular endothelial permeability and morphology through a Rho and myosin light chain kinase-dependent mechanism. *Physiol Rep* (2015) 3(12):e12636. doi: 10.14814/phy2.12636

36. Tang LQ, Li CF, Chen QY, Zhang L, Lai XP, He Y, et al. High-sensitivity C-reactive protein complements plasma Epstein-Barr virus deoxyribonucleic acid prognostication in nasopharyngeal carcinoma: a large-scale retrospective and prospective cohort study. *Int J Radiat oncology biology Phys* (2015) 91(2):325–36. doi: 10.1016/j.ijrobp.2014.10.005

37. Afshar-Kharghan V. The role of the complement system in cancer. *J Clin Invest* (2017) 127(3):780–9. doi: 10.1172/jci90962

38. Deng Y, Pang Q, Miao RC, Chen W, Zhou YY, Bi JB, et al. Prognostic significance of pretreatment albumin/globulin ratio in patients with hepatocellular carcinoma. *Onco Targets Ther* (2016) 9:5317–28. doi: 10.2147/ott.S109736

39. Xing Y, Guo ZN, Yan S, Jin H, Wang S, Yang Y. Increased globulin and its association with hemorrhagic transformation in patients receiving intra-arterial thrombolysis therapy. *Neurosci Bull* (2014) 30(3):469–76. doi: 10.1007/s12264-013-1440-x

40. Doi H, Hayashi E, Arai J, Tojo M, Morikawa K, Eguchi J, et al. Enhanced B-cell differentiation driven by advanced cirrhosis resulting in hyperglobulinemia. *J Gastroenterol Hepatol* (2018). doi: 10.1111/jgh.14123

41. Tanaka S, Okamoto Y, Yamazaki M, Mitani N, Nakqjima Y, Fukui H. Significance of hyperglobulinemia in severe chronic liver diseases–with special reference to the correlation between serum globulin/IgG level and ICG clearance. *Hepato-gastroenterology* (2007) 54(80):2301–5.

42. Osman W, Okada Y, Kamatani Y, Kubo M, Matsuda K, Nakamura Y. Association of common variants in TNFRSF13B, TNFSF13, and ANXA3 with serum levels of non-albumin protein and immunoglobulin isotypes in Japanese. *PloS One* (2012) 7(4):e32683. doi: 10.1371/journal.pone.0032683

43. Hu J, Chen J, Ou Z, Chen H, Liu Z, Chen M, et al. Neoadjuvant immunotherapy, chemotherapy, and combination therapy in muscle-invasive bladder cancer: A multi-center real-world retrospective study. *Cell Rep Med* (2022) 3(11):100785. doi: 10.1016/j.xcrm.2022.100785

44. De Giorgi U, Procopio G, Giannarelli D, Sabbatini R, Bearz A, Buti S, et al. Association of systemic inflammation index and body mass index with survival in patients with renal cell cancer treated with nivolumab. *Clin Cancer Res* (2019) 25 (13):3839–46. doi: 10.1158/1078-0432.Ccr-18-3661

45. Cai W, Zhong H, Kong W, Dong B, Chen Y, Zhou L, et al. Significance of preoperative prognostic nutrition index as prognostic predictors in patients with metastatic renal cell carcinoma with tyrosine kinase inhibitors as first-line target therapy. *Int Urol Nephrol* (2017) 49(11):1955–63. doi: 10.1007/s11255-017-1693-9

46. Yuk HD, Kang M, Hwang EC, Park JY, Jeong CW, Song C, et al. The platelet-to-lymphocyte ratio as a significant prognostic factor to predict survival outcomes in patients with synchronous metastatic renal cell carcinoma. *Invest Clin Urol* (2020) 61 (5):475–81. doi: 10.4111/icu.20200002

47. Yanagisawa T, Mori K, Katayama S, Mostafaei H, Quhal F, Laukhtina E, et al. Hematological prognosticators in metastatic renal cell cancer treated with immune checkpoint inhibitors: a meta-analysis. *Immunotherapy* (2022) 14(9):709–25. doi: 10.2217/imt-2021-0207

48. Cai Z, Chen J, Yu Z, Li H, Liu Z, Deng D, et al. BCAT2 shapes a noninflamed tumor microenvironment and induces resistance to anti-PD-1/PD-L1 immunotherapy by negatively regulating proinflammatory chemokines and anticancer immunity. *Adv Sci (Weinh)* (2023) 10(8):e2207155. doi: 10.1002/advs.202207155

49. Hu J, Othmane B, Yu A, Li H, Cai Z, Chen X, et al. 5mC regulator-mediated molecular subtypes depict the hallmarks of the tumor microenvironment and guide precision medicine in bladder cancer. *BMC Med* (2021) 19(1):289. doi: 10.1186/s12916-021-02163-6

50. Hu J, Yu A, Othmane B, Qiu D, Li H, Li C, et al. Siglec15 shapes a non-inflamed tumor microenvironment and predicts the molecular subtype in bladder cancer. *Theranostics* (2021) 11(7):3089–108. doi: 10.7150/thno.53649

51. Wang YT, Kuo LT, Lai CH, Tsai YH, Lee YC, Hsu CM, et al. Low pretreatment albumin-to-globulin ratios predict poor survival outcomes in patients with head and neck cancer: A systematic review and meta-analysis. *J Cancer* (2023) 14(2):281–9. doi: 10.7150/jca.80955

52. Salciccia S, Frisenda M, Bevilacqua G, Viscuso P, Casale P, De Berardinis E, et al. Prognostic value of albumin to globulin ratio in non-metastatic and metastatic prostate cancer patients: A meta-analysis and systematic review. *Int J Mol Sci* (2022) 23 (19):11501. doi: 10.3390/ijms231911501

53. Quan L, Jiang X, Jia X, Cheng F. Prognostic value of the albumin-to-globulin ratio in patients with colorectal cancer: A meta-analysis. *Nutr Cancer* (2022) 74 (9):3329–39. doi: 10.1080/01635581.2022.2076890

54. Li J, Wang Y, Wu Y, Li J, Che G. Prognostic value of pretreatment albumin to globulin ratio in lung cancer: A meta-analysis. *Nutr Cancer* (2021) 73(1):75–82. doi: 10.1080/01635581.2020.1737155

55. Wei C, Yu Z, Wang G, Zhou Y, Tian L. Low pretreatment albumin-to-globulin ratio predicts poor prognosis in gastric cancer: insight from a meta-analysis. *Front Oncol* (2020) 10:623046. doi: 10.3389/fonc.2020.623046

frontiers | Frontiers in Oncology

TYPE Case Report
PUBLISHED 22 August 2023
DOI 10.3389/fonc.2023.1207536

OPEN ACCESS

EDITED BY
Wen-Hao Xu,
Fudan University, China

REVIEWED BY
Murat Akand,
University Hospitals Leuven, Belgium
Xi Tian,
Fudan University, China

*CORRESPONDENCE
Yan Qi
qiyanyan-1998@163.com

†These authors have contributed equally to this work

RECEIVED 17 April 2023
ACCEPTED 28 July 2023
PUBLISHED 22 August 2023

CITATION
Zhang J, Wang W-J, Chen L-H, Wang N, Wang M-W, Liu H, Pang L-J, Jiang H-G and Qi Y (2023) Primary renal malignant epithelioid angiomyolipoma with distant metastasis: a case report and literature review.
Front. Oncol. 13:1207536.
doi: 10.3389/fonc.2023.1207536

Primary renal malignant epithelioid angiomyolipoma with distant metastasis: a case report and literature review

Jun Zhang[1†], Wen-Juan Wang[1†], Li-Hong Chen[1], Ning Wang[2], Ming-Wen Wang[2], Hao Liu[2], Li-Juan Pang[1], Han-Guo Jiang[1] and Yan Qi[1*]

[1]Department of Pathology, Zhanjiang Central Hospital, Guangdong Medical University, Guangdong, China, [2]Department of Pathology, Shihezi University School of Medicine & the First Affiliated Hospital to Shihezi University School of Medicine, Xinjiang, China

Epithelioid angiomyolipoma (EAML) is a rare type of mesenchymal angiomyolipoma with potential malignancy in the kidney that can cause lymph node metastases, local recurrence, and distant metastases. Herein, we describe a case of EAML in the right kidney of a 51-year-old man who was admitted to the hospital with a right abdominal mass. Computed tomography revealed a heterogeneously enhanced mass with blurred margins, which was considered a malignant tumor. A radical nephrectomy was then performed. Two years later, the patient developed liver metastases from EAML and was administered sintilimab combined with bevacizumab. The patient survived after 6 months of follow-up. Histologically, the tumors showed clear boundaries and no obvious capsules. The tumor tissue mainly consisted of epithelioid tumor cells, thick-walled blood vessels, and a small amount of adipose tissue. Tumor cells with lipid vacuoles and acinar areas were large, round, polygonal, eosinophilic, or transparent in the cytoplasm. The enlarged and hyperchromatic nuclei were accompanied by distinct nucleoli and pathological mitosis. These histopathological findings resembled those of renal cell carcinoma, and immunohistochemical analysis was performed. The tumor cells were diffusely positive for HMB45, Melan-A, CK20, vimentin antibodies, and TFE3, suggesting that the tumor originated from perivascular epithelioid cells, excluding renal cell carcinoma. The Ki-67 index was 10%. These histopathological features were observed in liver mass puncture tissues. We also summarized 46 cases of EAML with distant metastasis and explored the clinicopathological features of EAML to improve the treatment of the disease. EAML is often ignored in the clinical setting, leading to metastasis and recurrence. Therefore, EAMLs require long-term follow-up, and timely detection of recurrent disease can improve the prognosis.

KEYWORDS

renal epithelioid angiomyolipoma, liver metastasis, histopathology, immunohistochemistry, differential diagnosis

Introduction

Renal angiomyolipoma (AML) belongs to the perivascular epithelioid tumor (PEComas) family of lesions, which originate in the mesenchymal tissue and are characterized by the coexpression of melanocytes (Melan) and muscle markers by perivascular clear and epithelioid cells (1). Epithelioid angiomyolipoma (EAML) is a rare and special subtype of AML. EAMLs have a major epithelioid component and potentially malignant behavior; they mainly consist of epithelioid cells with diverse morphology and abundant proliferation arranged in sheets, and the proportion of mature adipocytes tends to be <5% (2, 3). It can occur in the kidney, liver, bone, ileum, pelvic retroperitoneum, and most commonly in the kidney, with local invasion or metastasis. About one-third of patients may have lymph nodes, liver, lung, or spinal metastasis (4).

Recently, several cases of malignant EAML have been reported. Edmund et al. first reported a malignant EAML with liver metastasis in 2001 (5). However, only 17 studies have reported malignant EAML with liver metastasis at present (Table 1) (5–8, 11, 12, 16, 20–25, 27, 29, 32, 34). Additionally, there are no established criteria for predicting malignancy. The diagnosis of EAML may be challenging. In particular, the definite diagnosis of malignant EAML is established and confirmed by histological immunohistochemical findings owing to the similarity of its epithelioid morphology with that of renal cell carcinoma (RCC). Therefore, insights into the morphological characteristics and immunophenotype of this disease entity can aid in an accurate diagnosis.

Case report

A 51-year-old man with a history of a painless mass in the right upper abdomen for 20 days presented to the Department of Urology at Zhanjiang Central Hospital, Guangdong Medical University (Guangdong, China). A physical examination revealed a painless mass in the upper right abdomen. A computed tomography (CT) examination revealed a 13 cm × 9.7 cm × 13.8 cm heterogeneously enhanced mass with a blurred boundary in the right renal parenchyma. A high-density calcification shadow is observed. Radical right nephrectomy was performed for renal malignancy. Subsequent histological examination showed that the right kidney was 11 cm × 7 cm × 4 cm in size, with a fat capsule on the surface; the cut surface was gray-red and dark-red. No definite mass was observed in the renal parenchyma. A 14 cm × 13 cm × 8 cm mass with no capsule was linked to the kidney capsule. The tumor showed expansive growth and did not invade the perirenal fat. The section of the mass was reddish-gray yellow and soft in texture, and most necrotic changes were observed.

TABLE 1 Clinical characteristics of the reported cases of EAML.

Case	Published time	Author		Sex/age	Site/location/size (cm)	Clinical symptoms and imaging features	TSC	Metastasis/time of occurrence (month(s))	Outcome and F-up (month(s))	IHC
1	2001	Edmund et al. (5)		F/49	Both/–/4*3*3	Recurrent urinary tract infections/B-ultrasound: hyperechoic masses	None	Liver/24	Live/28	HMB45, Melan-A
2	2001	Radin et al. (6)		M/21	Both/–/1–3.5	Gross hematuria/CT: irregular enhancing wall and central low attenuation	Yes	Liver, spleen, peritoneum, pleura retroperitoneal lymph nodes/5	–/–	HMB45, vimentin, NSE
3	2002	Takumni et al. (7)		M/47	L/U/20*10*10	Acute upper abdominal pain/CT: enhanced unequally mass	None	Lung, liver/2	Died/5	HMB45, SMA, EMA
4	2004	Warakaulle et al. (8)		F/48	L/I/15*14*11	A left-sided abdominal mass/ultrasound: hypoechoic mass	None	Liver/–	Live/10	HMB45, Melan-A, S100, CD10
5	2007	Huang et al. (9)		F/78	L/I/12.5*7.5*8.5	Fever and left flank pain/CT: a heterogeneous mass	None	Lung, bone, regional lymph node/4	Died/5	HMB45
6	2008	Moudoun et al. (10)		F/31	Both/–/1–10	Abdominal mass and intermittent left flank pain/–	Yes	Retroperitoneal lymph nodes/–	Live/12	HMB45, vimentin, NSE
7	2008	Sato et al. (11)		M/36	Both/–/20	–/–	Yes	Renal arterial wall infiltration, lung,	Died/24	HMB45, Melan-A, vimentin,

(Continued)

TABLE 1 Continued

Case	Published time	Author		Sex/age	Site/location/size (cm)	Clinical symptoms and imaging features	TSC	Metastasis/time of occurrence (month(s))	Outcome and F-up (month(s))	IHC
								liver, diaphragm, mesentery/24		CD68, CD63, CD117
8	2011	Nese et al. (12)	1	F/24	–/–/–	–/–	Yes	Pelvic, liver/–	Died/12	–
			2	M/29	–/–/–	–/–	Yes	Lung, liver/18	Died/18	–
			3	M/14	–/–/11	–/–	Yes	Lymph node/–	Live/240	–
			4	F/49	–/–/34	–/–	Yes	Colon/–	–/–	–
			5	F/25	–/–/8	–/–	Yes	Lymph node, peritoneal, liver, lung/–	Died/12	–
			6	M/36	–/–/28	–/–	Yes	Lung, liver, mesentery, diaphragm/–	Autopsy/–	–
			7	M/67	–/–/15	–/–	None	Lymph node/–	–/–	–
			8	M/69	–/–/13	–/–	None	Liver, lymph node/8	Died/28	–
			9	F/46	–/–/17	–/–	None	Liver, peritoneum/12	Live/16	–
			10	M/36	–/–/29	–/–	Yes	Lung, liver/–	Died/4	–
			11	M/58	–/–/37	–/–	None	Lymph node, liver/–	Died/24	–
			12	M/27	–/–/11	–/–	None	Liver/–	Died/24	–
			13	M/29	–/–/27	–/–	Yes	Liver/–	Died/11	–
			14	F/55	–/–/12.8	–/–	None	Extensive metastatic disease/–	Died/12	–
			15	M/57	–/–/4.5	–/–	–	Lymph node/58	Live/58	–
9	2012	Lee et al. (13)		F/63	L/–/–	Left abdominal pain/–	None	Relapse in situ/3	Died/5	HMB45, Melan-A, SMA, vimentin, desmin
10	2012	Li et al. (14)		F/55	L/–/7.5	Left flank pain/ultrasonography: solid mass	None	Lung/84	Died/180	HMB45, P53
11	2013	Yang et al. (15)		F/42	R/–/–	–/B-ultrasound: substantial occupation	None	Lung/48	Live/55	HMB45, SMA, Melan-A
12	2013	Xi et al. (16)		M/7	R/U/15*12*8	Mild abdominal pain/CT: a heterogeneous mass	None	Lung, liver/6	Died/24	HMB45, Melan-A
13	2014	Shi et al. (17)		M/48	R/–/14*11*8	Abdominal pain and blood in urine/–	None	Lung/60 ileum/72	Live/148	HMB45, Melan-A, SMA, S100
14	2014	Wang et al. (18)		F/63	–/–/–	–/–	None	Lung/48	–/–	HMB45, vimentin, Melan-A, SMA

(Continued)

TABLE 1 Continued

Case	Published time	Author		Sex/age	Site/location/size (cm)	Clinical symptoms and imaging features	TSC	Metastasis/time of occurrence (month(s))	Outcome and F-up (month(s))	IHC
15	2014	Zhao et al. (19)		M/49	R/–/–	–/CT: masses of uniform density	None	Lung/36	Live/50	HMB45, Melan-A, SMA, desmin, S100, CD34
16	2014	Fukaya et al. (20)		F/22	R/–/21	–/–	None	Retroperitoneum, liver/84	Live/120	HMB45, SMA, E-cadherin, β-catenin
17	2015	Guo et al. (21)		F/48	R/I/13*12*11	Flank pain in the right-side/CT: a soft tissue mass of heterogeneous density	None	Lung, liver/16	Died/22	HMB45, Melan-A, desmin
18	2016	Xiao et al. (22)	1	–/–	L/–/–	–/CT: mass of heterogeneous density	None	Lung/–	Died/9	HMB45, Melan-A, CD117, SMA
			2	–/–	R/U/10	–/CT: mass of heterogeneous density	None	Liver/–	Died/21	HMB45, Melan-A, CD117, SMA
19	2016	Shen et al. (23)		M/36	L/–/–	–/–	None	Lung, liver/24	Live/5	HMB45, Melan-A, CD117, S-100, vimentin
20	2016	Park et al. (24)		M/48	–/–/–	–/–	None	Scapula, liver, pelvic bone, peritoneal seeding/12	Live/32	HMB45, Melan-A
21	2016	Cho et al. (25)		F/47	L/–/10.7*10*7.5	Acute left abdominal pain/CT: a well demarcated, heterogeneously enhancing, necrotic mass with renal vein thrombosis	None	Liver/1	Live/1	HMB45, vimentin, α-SMA, CD10
22	2018	Wang et al. (26)		F/53	L/–/11.9*10.0*10.1	Gross hematuria with presence of lumbago and fatigue/CT: ill-defined, irregular, slightly hyperdense mass	None	Lung/4	Died/10	HMB45, Melan-A, TFE3
23	2018	Zhan et al. (27)		F/48	R/–/7.5*6*4	–/CT: a well-defined solid tissue mass	None	Liver/13	Live/13	HMB45, Melan-A, SMA
24	2018	Park et al. (28)		F/36	L/–/10*13	Abdominal pain/–	None	Rectus abdominis muscle/60	Live/72	HMB45, Melan-A, CD117
25	2019	Bree et al. (29)		M/60	L/–/14*12*13	–/–	None	Spleen, liver, pelvis/84	Live/192	HMB45, Melan-A, SMA
26	2019	Erickson et al. (30)		F/–	–/–/–	Abdominal discomfort/–	None	Paraortic lymph node/–	–/–	HMB45, Melan-A
27	2020	Umair et al. (31)		F/31	Both/–/–	–/MRI: high signal intensity	None	Lung/–	Live/6	–

(Continued)

TABLE 1 Continued

Case	Published time	Author		Sex/age	Site/location/size (cm)	Clinical symptoms and imaging features	TSC	Metastasis/time of occurrence (month(s))	Outcome and F-up (month(s))	IHC
28	2020	Gupta et al. (32)		F/40	R/–/10.5*11.9*16	Abdominal pain/CT: heterogeneously enhancing mass	None	Liver/–	Died/2.5	Melan-A, SMA
29	2020	Fujiwara et al. (33)		M/37	R/–/11	Abdominal pain/–	None	Right-sided transverse colon/72	Live/198	HMB45, Melan-A
30	2022	Isaac et al. (34)		M/57	L/–/–	Headache and sinus congestion/–	Yes	Lung, liver/2	Died/9	HMB45, Melan-A, SMA, CK
31	2022	Present case		M/51	R/U/13*9	A palpable mass/ultrasound: solid mass; CT: heterogeneously enhancing mass	None	Liver/24	Live/26	HMB45, Melan-A, SMA, vimentin, CK20, TFE3

F, female; M, male; L, left; R, right; Up, upper pole; In, inferior pole; TSC, tuberous sclerosis complex; F-up, follow-up time; IHC, immunohistochemistry; HMB45, human melanoma black 45; Melan-A, melanoma antigen; SMA, smooth muscle actin; CK, cytokeratin; EMA, epithelial membrane antigen; CD, cluster of differentiation; NSE, neuron-specific enolase; TFE3, transcription factor enhancer 3; "–" not known.

Resected tumor specimens were fixed in 10% neutral-buffered formalin and processed for immunohistochemistry using a standard protocol. Paraffin-embedded blocks were sectioned at a thickness of 5 μm and stained with hematoxylin–eosin and various antibodies. The antibody clones, working dilutions, and commercial sources are listed in Supplementary Table S1.

Microscopically, there was no fibrous membrane around the tumor tissue, which was clearly demarcated from the surrounding normal renal tissue at low power. The tumor tissue consisted of numerous epithelioid cells, smooth muscle cells, twisted thick-walled blood vessels (hyalinized vascular walls), and small amounts of adipose tissue. The staining of tumor cells was shallower than that of normal renal cells. They were unevenly distributed. Thick-walled blood vessels, adipose tissue, and fiberglass lesions were observed in the cell-sparse areas. A large number of epithelioid cells were observed in the cell-rich areas. The epithelioid tumor cells were arranged in tight sheets (Figures 1A–C). They were large, round, or polygonal with some adipose vacuolar and acinar areas and had abundant cytoplasm, which was stained eosinophilic or transparent (Figure 1D). The enlarged nuclei were deeply stained with distinct nucleoli. Necrotic and pathological mitosis were also observed (Figure 1E). Vacuolated and weird-type nuclei were also observed (Figure 1F). These morphologies were easily confused with the histological features of RCC. Therefore, we performed an immunohistochemical examination.

Immunohistochemical staining revealed that the tumor cells were diffusively positive for human melanoma black 45 (HMB45), melan antigen (Melan-A), cytokeratin (CK) 20, and transcription factor enhancer 3 (TFE3), and partly positive for smooth muscle actin (SMA) (Figures 2A–E), which indicated that the tumor originated from peripheral vascular epithelioid cells, ruling out RCC. The tumor cells were diffusely vimentin-positive, and a Ki-67 index (Figure 2F) of 10% suggested that the tumor was malignant. The negative response of tumor cells to epithelial membrane antigen (EMA), PAX-8, CK, and CK7 excludes tumors of epithelial origin. The absence of melanocytes in the tumor tissue and the negative response of tumor cells to S100 and cluster of differentiation (CD) 117 precluded melanoma. Based on these pathological findings, the mass was confirmed as an EAML (Supplementary Table S1).

The patient was not treated or followed up after surgery. Two years later, the patient was admitted to the hospital with right lumbago pain, chills, and a fever for more than 1 week. A physical examination revealed tenderness in the right lumbar region without pain. CT examination showed multiple nodules with unequal density in the right nephrectomy area and a mass of 13.9 cm × 12 cm × 12.6 cm mixed with a slightly low-density shadow in the right lobe of the liver with unclear boundary and heterogeneous enhancement, which was considered a metastatic tumor. A biopsy of a liver mass was carried out for a pathological examination. Microscopically, only a small number of tumor cells were observed in the liver biopsy samples. Significant atypical epithelioid tumor cells with hyperchromatic nuclei were observed. The morphological characteristics were similar to those of the primary lesion (Figures 3A–C). Combined with the history of malignant EAML and imaging findings, we suspected that the patient had developed liver metastases. To confirm this hypothesis, we performed an immunohistochemical examination, which suggested diffuse positivity of liver tumor cells for Melan-A (Figure 3D) and SMA (Figure 3E). Its proliferation index hit 5% (Figure 3F). These findings confirmed the diagnosis of EAML metastasis. The patient or his family members had no history of tuberous sclerosis (TSC) or other renal tumors. The patient received sintilimab combined with bevacizumab. The patient survived after 6 months of follow-up.

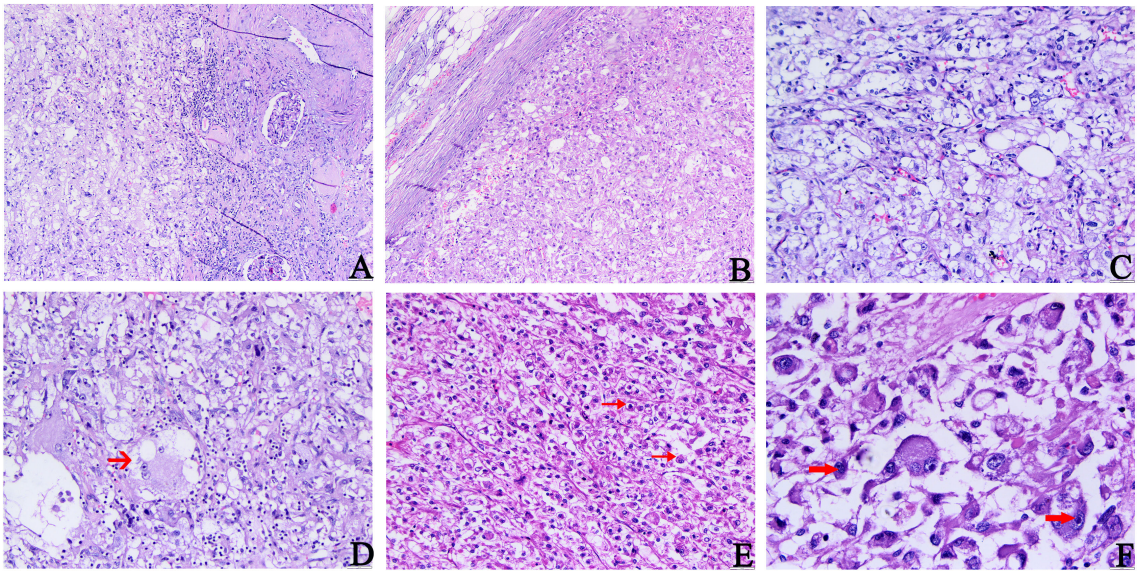

FIGURE 1
Histopathology features of primary tumors. **(A)** The boundary between tumor tissue and surrounding normal kidney tissue is not clear. **(B)** Epithelioid tumor cells were arranged in tight sheets. **(C)** Abundant epithelioid cells, a small amount of adipose tissue, and thick-walled blood vessels were seen in the tumor. **(D–F)** Epithelioid tumor cells are large and diverse, with some adipose vacuolar and acinar areas (indicated by the arrow in **(D)**), which are rich in eosinophilic or translucent cytoplasm. The nuclei were enlarged and deeply stained, partially vacuolated, and accompanied by obvious nucleoli (indicated by the arrow in **(F)**). The scattered megakaryocytes and occasionally pathological mitosis (indicated by the arrow in **(E)**) and necrosis could be observed (**A, B** H&E, ×100; **C–E** H&E, ×200; **F**, H&E, ×400).

Discussion

AML is a renal tumor that accounts for 2%–6.4% of all renal tumors (2, 3). Renal EAML, a subtype of AML, is a rare renal mesenchymal tumor with malignant potential that was first reported by Mai et al. (35). The development of renal AMLs may be associated with TSC. It is a systemic autosomal-dominant disease characterized by hamartomas of the lungs, skin, heart, brain, and kidney (36). It is usually caused by reduced or missing expression of the TSC1 (hamartin) or TSC2 (tuberin) genes (37). Renal AMLs are

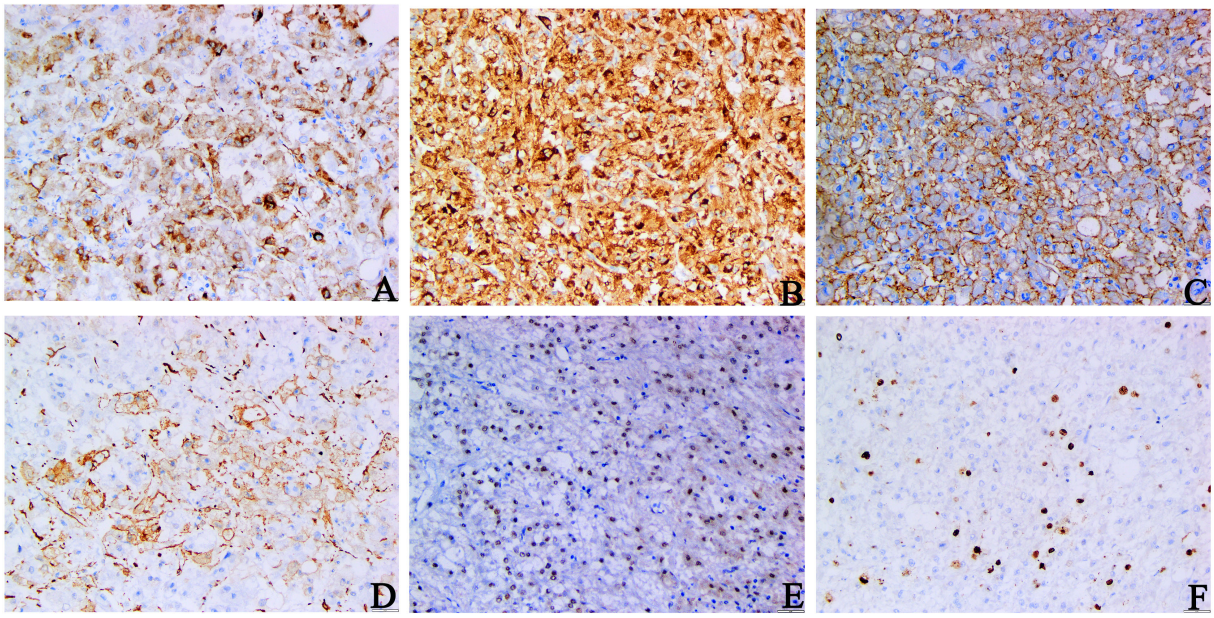

FIGURE 2
Immunohistochemical staining of primary tumors. **(A–C)** HMB45, Melan-A, CK20 staining: diffuse and strong positive cytoplasm of tumor cells. **(D)** SMA staining: tumor cells were positive. **(E)** TFE3 staining: tumor cell nuclear was positive. **(F)** Ki-67 staining: The Ki-67 index hit 10% (**A–D, F** original magnification is ×200; **E** original magnification is ×100).

10.3389/fonc.2023.1207536

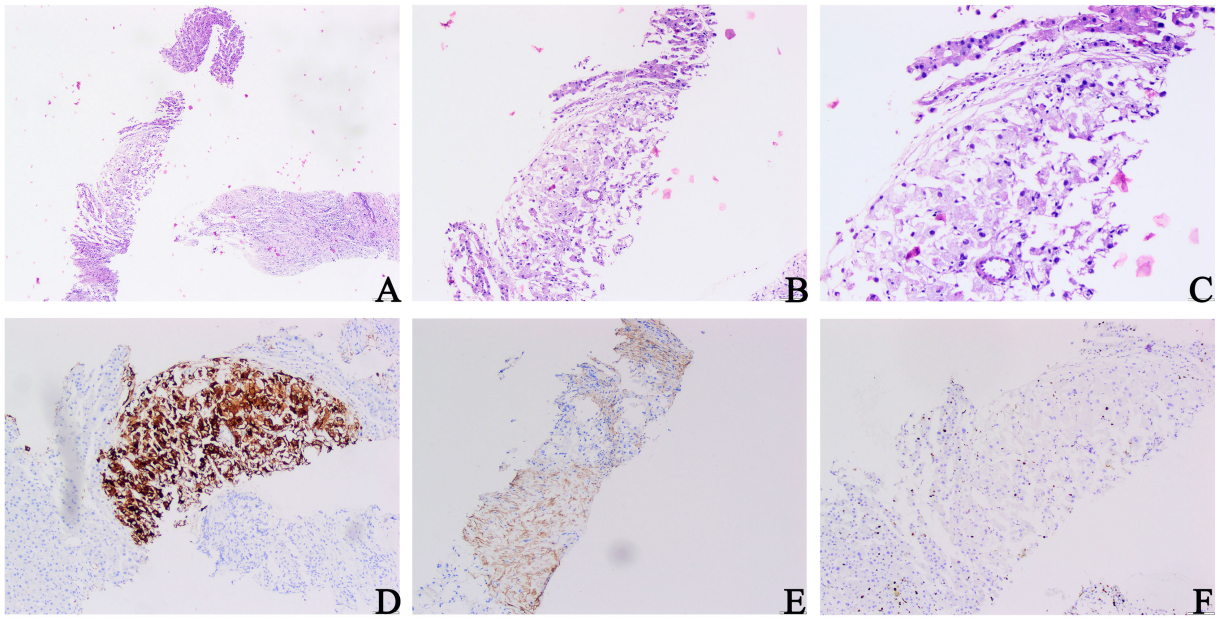

FIGURE 3
Microscopic architectural features of a liver mass biopsy. **(A–C)** Proliferating fibrous tissue, eosinophilic cytoplasm, and significantly hyperchromatic and enlarged nuclei of epithelioid tumor cells could be observed (H&E, **A** ×40; **B** ×100; **C** ×200). **(D)** Melan-A staining: diffuse and strong positive cytoplasm of tumor cells. **(E)** SMA staining: tumor cells were positive. **(F)** Ki-67 staining: the Ki-67 index hit 5% (**D, F** original magnification is ×200; **E** original magnification is ×100).

found in 80% of patients with TSC (38). Similarly, analysis of sporadic AMLs and EAMLs showed an association with TSC2 (9, 38, 39).

To date, only 46 cases of EAML with distant metastasis have been reported in the literature (Table 1) (5–34). Through a review of the literature, we found that these tumors occurred in people over 40 years of age (26/43, 60%, ranging from 7 to 78 years old; median, 49 years; mean, 44 years), and there was no significant difference in sex. The patients were mainly affected by unilateral kidney disease (21/28, 75%), with the left side being the most affected (12/19, 63%). The size of the EAML tumors excised from the kidneys ranged from 1 cm to 37 cm, with an average size of 14.89 cm. A total of 12 patients (12/46, 26%) had TSC. The most distant metastatic sites were the liver (28/46, 60%), lungs (19/46, 41%), and lymph nodes (10/46, 21%). Metastases to other sites, such as the pelvis, peritoneum, and rectus abdominis, are less common (Table 2). Some patients had signs of distant metastasis before the primary tumor was found, and the time range of distant metastasis ranged from 1 month to 12 years after primary tumor resection in most patients, with an average of 2.7 years. The longest postoperative survival time was 20 years (12), and the shortest was 2.5 months (32). We found that the efficacy of surgery or chemotherapy after EAML metastasis was unsatisfactory, with a poor prognosis and a low 5-year survival rate.

Most patients present with abdominal pain, hematuria, palpable masses, or clinical symptoms of EAML that metastasize to the lungs and cause fever, cough, and chest pain. A CT examination is of great significance in planning surgery and predicting patient prognosis, as it may help discover the location of tumors and determine whether they have metastasized. EAML tumors were large (usually >7 cm), and CT showed irregular mixed-density solid or multilocular mass shadows (usually >45 HU) with uneven enhancement and "fast in and slow out." This phenomenon may

TABLE 2 Sites of EAML distant metastasis with their percentages in the literature.

Metastasis sites	Case number (total: 46)	Percentage
Liver (5–8, 11, 12, 16, 20–25, 27, 29, 32, 34)	28	60%
Lung (7, 9, 11, 12, 14–19, 21–23, 26, 31, 34)	19	41%
Lymph node (6, 9, 10, 12, 30)	10	21%
Pelvic (12, 24, 29)	3	7%
Peritoneum (6, 12, 20)	3	7%
Spleen (6, 29)	2	4%
Retroperitoneal cavity (6, 10)	2	4%
Mesentery (11, 12)	2	4%
Relapse *in situ* (13)	1	2%
Rectus abdominis muscle (28)	1	2%
Ileum (17)	1	2%
Scapula (24)	1	2%
Colon (12)	1	2%
Bone (9)	1	2%
Extensive metastatic (12)	1	2%

be associated with higher cell density, reduced tumor stroma, abnormal hyperangiogenesis, the presence of intact tumor capsules, and the absence of tissue structures with reflux vessels (3). The imaging findings of the mass in our case showed an inhomogeneously enhanced mass, which was considered to be a malignant renal tumor, consistent with the above summary of imaging findings. However, the above results may be misdiagnosed as RCC or retroperitoneal sarcoma (40, 41). Therefore, further pathological examinations are required to confirm the diagnosis.

In addition to mature adipocytes, smooth muscle-like spindle cells, and clear, thick-walled blood vessels, EAML contains a variety of clear-to-eosinophilic and cytoplasmic epithelioid cells. There is no uniform standard for determining the number of epithelioid cells required for a final diagnosis of EAML. Current inclusion criteria range from 10% to 95%, whereas the new edition of the World Health Organization in 2016 recommends greater than 80% epithelioid cells as the diagnostic criteria for EAML (42). A precise diagnostic criterion is beneficial for identifying the characteristics of EAML as it can be used as a guide for clinical treatment. Additionally, the diagnosis of malignant renal EAML is controversial, and there are no unified malignant diagnostic criteria. With the accumulation of clinical cases in recent years, researchers have found that recurrence and metastasis rates of the disease are as high as 17% and 49%, respectively, and the mortality rate can reach 33% (43). Therefore, highly invasive biological behaviors and histological features should initially be considered malignant.

Lei (44) concluded that three or more of the following characteristics predicted an increased likelihood of malignancy: (1) necrosis, (2) tumor size >9 cm, (3) tumor thrombus formation in the vein, and (4) epithelioid cells >70% or atypical cells >60%. These criteria greatly aid in the accurate diagnosis of malignant EAML. The proportion of tumor epithelioid cells in our case was 80%, which was consistent with the diagnosis of EAML. The tumor cells showed obvious atypia and hyperchromatic nuclei, accompanied by evident nucleoli, pathological mitosis, and necrosis, consistent with the diagnosis of malignant EAML. Two years later, the patient developed EAML liver metastases, which further confirmed the diagnosis of a malignant tumor. However, when tumor nuclear atypia is evident and the adipose tissue content is significantly reduced, these tumors are most likely to be misdiagnosed as RCC or sarcoma. Therefore, the final diagnosis depends on immunohistochemical staining of the tumor. EAMLs exhibit specific immunohistochemical characteristics. The tumor cells are positive for melanoma-related markers such as HMB45, HMB50, Melan-A, SOX10, and myogenic markers such as SMA but negative for epithelial markers such as AE1/AE3 and EMA (45, 46). Compared with EAML, epithelial markers for RCC were positive, and melanocyte markers were negative. While EAML epithelial cell marker staining was negative, HMB45 and Melan-A staining were generally positive. These cells also expressed SMA. Staining for S-100 protein is usually negative. In this case, the tumor cells were diffuse, strongly positive for HMB45 and Melan-A, and negative for EMA, CK, CK7, and PAX-8, excluding the diagnosis of RCC (Supplementary Table S2) (47–50). Moreover, melanocytes in the tumor tissue and their negative responses to S100 and CD117 excluded the diagnosis of melanoma. To our surprise, our case was strongly positive for CK20 staining, which had not been seen in previous case reports. We reviewed relevant reports on the expression of CK20 in epithelioid tumors and found that epithelioid malignant mesothelioma (51) and malignant hepatic epithelioid hemangioendothelioma (52) could abnormally express CK20. Perhaps our case could serve as the first report of an anomalous EAML expression of CK20. Interestingly, the positive expression of TFE3 in our case can help clinicians adjust the follow-up visit treatment strategy.

Currently, the treatment options for EAML include surgery, chemotherapy, targeted therapy, endocrine therapy, and immunotherapy. Surgical excision is the primary treatment of choice for renal EAML (53). However, some patients experience recurrence or even distant metastasis after surgery. Malignant EAML is prone to tumor thrombus formation, which may cause distant metastasis. A study found that mutations in TSC1/TSC2 and translocations in TFE3 lead to overactivation of the mTOR complex (54). MTOR inhibitors inhibit mTOR activity to control tumors. However, there have been cases of limited efficacy of mTOR inhibitors in TFE3-rearranged malignant PEComas, and targeting VEGF/VEGFR signaling is probably a new effective treatment strategy for TFE3-associated malignant PEComas (54, 55). Therefore, it is important to determine whether TFE3 is positive to guide subsequent treatments. Lattanzi et al. first reported a case of malignant EAML with a TSC mutation and resistance to mTOR inhibitor therapy. After switching to PD-1 antibody therapy, the patient's disease was effectively controlled, suggesting that PD-1 antibody therapy is a breakthrough in the treatment of anti-malignant EAML. Therefore, the standard treatment for EAML with distant metastases is mTOR inhibitor-targeted therapy (everolimus) combined with PD1 immunotherapy (bevacizumab), which is the most effective treatment strategy in the current study (56). However, its therapeutic effects on EAML relapse and distant metastasis remain unsatisfactory. As in our case, the clinicians and patients did not pay attention to long-term return visits and active treatment, which resulted in liver metastases. Therefore, long-term follow-up visits and active treatment are of great significance for detecting recurrence or metastasis as early as possible in EAML. Since there was no mTOR inhibitor available in our hospital, our patient was treated with bevacizumab (200 mg dL^{-1}) combined with sintilimab (200 mg dL^{-1}), and the patient and his family agreed to this treatment strategy. The treatment was effective, and the patient was stable.

Conclusion

EAML is a tumor of interstitial origin that expresses both myogenic and melanin markers. There is increasing evidence that it has malignant potential. Therefore, it is necessary to consider EAML other than RCC when dealing with intravascular thrombosis in renal tumors. The diagnosis is usually made based on

histopathological examination; however, it is easily confused with other tumors, especially RCC. Immunohistochemical markers can be used for efficient differentiation to obtain an accurate diagnosis. Because of the risk of disease recurrence, which may occur very late, renal EAMLs require long-term follow-up to detect recurrence and metastasis as early as possible. In such cases, more efficient active treatment can be performed.

Data availability statement

The original contributions presented in the study are included in the article/Supplementary Material. Further inquiries can be directed to the corresponding author.

Ethics statement

The studies involving human participants were reviewed and approved by Zhanjiang Central Hospital, Guangdong Medical University. The patients/participants provided their written informed consent to participate in this study. Written informed consent was obtained from the individual(s) for the publication of any potentially identifiable images or data included in this article.

Author contributions

JZ, M-WW and HL performed the experiments and analyzed the data; YQ designed and supervised the study. L-JP, H-GJ, NW and L-HC provided crucial input for the project; JZ, W-JW and YQ wrote the manuscript. All authors read and approved the final version of the manuscript.

Acknowledgments

This work was supported by grants from the National Natural Science Foundation of China (Grant No. 81860471), the Zhanjiang Science and Technology Development Special Fund Competitive Allocation Project—key projects of disease prevention and control (2021A05145), and the Provincial Science and Technology Special Fund ("college items + task list") project—special topic of basic and applied research (2021A05236).

Conflict of interest

The authors declare that the research was conducted in the absence of any commercial or financial relationships that could be construed as a potential conflict of interest.

Publisher's note

Supplementary material

The Supplementary Material for this article can be found online at: https://www.frontiersin.org/articles/10.3389/fonc.2023.1207536/full#supplementary-material

References

1. Humphrey P, Moch H, Cubilla A, Ulbright T, Reuter V. The 2016 who classification of tumours of the urinary system and male genital organs-part B: prostate and bladder tumours. *Eur Urol* (2016) 70(1):106–19. doi: 10.1016/j.eururo.2016.02.028

2. Roberts S, Ladi-Seyedian S, Daneshmand S. Vena cava tumor thrombus associated with renal angiomyolipoma in a Jehovah's witness patient. *Uro* (2021) 156:e86–7. doi: 10.1016/j.urology.2021.08.005

3. Yang J, Liang C, Yang L. Advancements in the diagnosis and treatment of renal epithelioid angiomyolipoma: A narrative review. *Kaohsiung J Med Sci* (2022) 38 (10):925–32. doi: 10.1002/kjm2.12586

4. Lee S, Lee J, Kim J, Ko S, Lee K, Hwang I, et al. Renal epithelioid angiomyolipoma with epithelial cysts mimicking cystic renal cell carcinoma: A case report of combination of two rare entities. *J Korean Soc Radiol* (2022) 83(5):1109–15. doi: 10.3348/jksr.2021.0172

5. Cibas E, Goss G, Kulke M, Demetri G. Fletcher CJTAjosp. Malignant epithelioid angiomyolipoma ('Sarcoma ex angiomyolipoma') of the kidney: A case report and review of the literature. *Am J Surg Pathol* (2001) 25(1):121–6. doi: 10.1097/00000478-200101000-00014

6. Radin R, Ma Y. Malignant epithelioid renal angiomyolipoma in a patient with tuberous sclerosis. %J journal of computer assisted tomography. *J Comput Assist Tomogr* (2001) 25(6). doi: 10.1159/000111739

7. Yamamoto T, Ito K, Suzuki K, Yamanaka H, Ebihara K, Sasaki A. Rapidly progressive Malignant epithelioid angiomyolipoma of the kidney. *J Urol* (2002) 168 (1):190–1. doi: 10.1097/00005392-200207000-00046

8. Warakaulle D, Phillips R, Turner G, Davies D, Protheroe A. Malignant monotypic epithelioid angiomyolipoma of the kidney. *J Clin Radiol* (2004) 59 (9):849–52. doi: 10.1016/j.crad.2004.02.009

9. Chuang C, Lin H, Tasi H, Lee K, Kao Y, Chuang F, et al. Clinical presentations and molecular studies of invasive renal epithelioid angiomyolipoma. *Int Urol Nephrol* (2017) 49(9):1527–36. doi: 10.1007/s11255-017-1629-4

10. Huang K, Huang C, Chung S, Pu Y, Shun C, Chen J. Malignant epithelioid angiomyolipoma of the kidney. *J Formos Med Assoc* (2007) 106:S51–4. doi: 10.1016/s0929-6646(09)60353-3

11. Sato K, Ueda Y, Tachibana H, Miyazawa K, Chikazawa I, Kaji S, et al. Malignant epithelioid angiomyolipoma of the kidney in a patient with tuberous sclerosis: an autopsy case report with P53 gene mutation analysis %J pathology - research and practice. *PATHOL RES PRACT* (2008) 204(10). doi: 10.1016/j.prp.2008.04.008

12. Nese N, Martignoni G, Fletcher C, Gupta R, Pan C, Kim H, et al. Pure epithelioid pecomas (So-called epithelioid angiomyolipoma) of the kidney: A clinicopathologic study of 41 cases: detailed assessment of morphology and risk stratification. *Am J Surg Pathol* (2011) 35(2):161–76. doi: 10.1097/PAS.0b013e318206f2a9

13. Moudouni S, Tligui M, Sibony M, Doublet J, Haab F, Gattegno B, et al. Malignant epithelioid renal angiomyolipoma involving the inferior vena cava in a patient with tuberous sclerosis. *J Uro Int* (2008) 80(1):102–4. doi: 10.1159/000111739

14. Lee H-Y, Huang C-W, Li C-C, Wu W-C, Liu T-C, Wu C-C, et al. Malignant renal epithelioid angiomyolipoma with an inferior vena cava and right atrium thrombus %J urological science. *Urol Sci* (2012) 23(4). doi: 10.1016/j.urols.2012.10.009

15. Li J, Zhu M, Wang Y. Malignant epithelioid angiomyolipoma of the kidney with pulmonary metastases and P53 gene mutation. *World J Surg Oncol* (2012) 10:213. doi: 10.1186/1477-7819-10-213

16. Xi S, Chen H, Wu X, Jiang H, Liu J, Wu Q, et al. Malignant renal angiomyolipoma with metastases in a child. *Int J Surg Pathol* (2014) 22(2):160–6. doi: 10.1177/1066896913497395

17. Yang S-L, Zhao J-L, Yan Z-J, liu J. Pulmonary metastatic renal epithelioid angiomyolipoma: A case report %J journal of practical cancer. *J Pract Cancer* (2013) 28 (01):94.

18. Shi H, Cao Q, Li H, Zhen T, Lai Y, AJIjoc H, et al. Malignant perivascular epithelioid cell tumor of the kidney with rare pulmonary and ileum metastases. *Int J Clin Exp Pathol* (2014) 7(9):6357–63.

19. Wang M-H, Ling Y, Gao Q-Q, Huang Z-S, Wan M-Z, Chen Y-F, et al. Lung metastasis of renal epithelioid angiomyolipoma: A case report and literature review %J journal of clinical and pathological studies. *J Clin Pathological Stud* (2014) 34(03):326–9.

20. Konosu-Fukaya S, Nakamura Y, Fujishima F, Kasajima A, McNamara K, Takahashi Y, et al. Renal epithelioid angiomyolipoma with Malignant features: histological evaluation and novel immunohistochemical findings. *Pathol Int* (2014) 64(3):133–41. doi: 10.1111/pin.12142

21. Guo B, Song H, Yue J, Li G. Malignant renal epithelioid angiomyolipoma: A case report and review of the literature. *Oncol Lett* (2016) 11(1):95–8. doi: 10.3892/ol.2015.3846

22. Xiao Y-M, Liao H, Tan Z, Mao D, Wu Y, Li C. Clinical features and prognosis of renal epithelioid angiomyolipoma %J journal of oncology. *J Oncol* (2016) 22(07):579–82.

23. Shen B-H, Cheng G, Xie L-P eds. Malignant Epithelioid Renal Angiomyolipoma: A Case Report and Literature Review. In: *2009 Zhejiang Andrology and Urology Annual Conference*. Jinyun, Zhejiang, China.

24. Park J, Lee C, Suh J, Kim G, Song B, Moon K. Renal epithelioid angiomyolipoma: histopathologic review, immunohistochemical evaluation and prognostic significance. *Pathol Int* (2016) 66(10):571–7. doi: 10.1111/pin.12458

25. Cho S, Choi H, Lee S. Rapidly progressing Malignant epithelioid renal angiomyolipoma: A case report. *J Urol* (2016) 13(2):2653–5.

26. Zhao R-R, Su Y-J. Lung metastasis of renal epithelioid angiomyolipoma: case report %J journal of clinical pulmonary science. *J Clin Pulmonary Sci* (2014) 19 (07):1357–8.

27. Zhan R, Li Y, Chen C, Hu H, Zhang CJM. Primary kidney Malignant epithelioid angiomyolipoma: two cases report and review of literature. *Med (Baltim)* (2018) 97(32): e11805. doi: 10.1097/md.0000000000011805

28. Wang H, Zhan H, Yao Z, Liu Q. Malignant renal epithelioid angiomyolipoma with tfe3 gene amplification mimicking renal carcinoma. *J Clin Nephrol Case Stud* (2018) 6:11–5. doi: 10.5414/cncs109443

29. De Bree E, Stamatiou D, Chryssou E, Michelakis D, Tzardi MJM. Late local, peritoneal and systemic recurrence of renal angiomyolipoma: A case report. *Mol Clin Oncol* (2019) 10(1):43–8. doi: 10.3892/mco.2018.1755

30. PE J, Arden P, Ryan P, Patricia V, Sarah P. Epithelioid angiomyolipoma metastasis to the rectus abdominis. *Can J Uro* (2018) 25(5).

31. Erickson L. Malignant epithelioid angiomyolipoma of the kidney (Malignant perivascular epithelioid cell neoplasm). *Mayo Clin Proc* (2020) 95(1):205–6. doi: 10.1016/j.mayocp.2019.11.015

32. Gupta C, Malani A, Gupta V, Singh J, Ammar H. Metastatic retroperitoneal epithelioid angiomyolipoma. *Autops Case Rep* (2007) 60(4):428–31. doi: 10.1136/jcp.2006.039503

33. Al Umairi R, Al Shamsi R, Kamona A, Al Lawati F, Baqi S, Kurian G, et al. Renal epithelioid angiomyolipoma: A case report and review of literature. *Oman Med J* (2020) 35(5):e178. doi: 10.5001/omj.2020

34. Tessone I, Lichtbroun B, Srivastava A, Tabakin A, Polotti C, Groisberg R, et al. Massive Malignant epithelioid angiomyolipoma of the kidney. *J Kidney Cancer VHL* (2022) 9(2):13–8. doi: 10.15586/jkcvhl.v9i2.210

35. Martignoni G, Pea M, Rigaud G, Manfrin E, Colato C, Zamboni G, et al. Renal angiomyolipoma with epithelioid sarcomatous transformation and metastases: demonstration of the same genetic defects in the primary and metastatic lesions. *Am J Surg Pathol* (2000) 24(6):889–94. doi: 10.1097/00000478-200006000-00017

36. Lam H, Siroky B, Henske E. Renal disease in tuberous sclerosis complex: pathogenesis and therapy. *Nat Rev Nephrol* (2018) 14(11):704–16. doi: 10.1038/s41581-018-0059-6

37. Cai Y, Guo H, Wang W, Li H, Sun H, Shi B, et al. Assessing the outcomes of everolimus on renal angiomyolipoma associated with tuberous sclerosis complex in China: A two years trial. *Orphanet J Rare Dis* (2018) 13(1):43. doi: 10.1186/s13023-018-0781-y

38. Sauter M, Belousova E, Benedik M, Carter T, Cottin V, Curatolo P, et al. Rare manifestations and Malignancies in tuberous sclerosis complex: findings from the tuberous sclerosis registry to increase disease awareness (Tosca). *Orphanet J Rare Dis* (2021) 16(1):301. doi: 10.1186/s13023-021-01917-y

39. Henske E, Neumann H, Scheithauer B, Herbst E, Short M, Kwiatkowski D. Loss of heterozygosity in the tuberous sclerosis (Tsc2) region of chromosome band 16p13 occurs in sporadic as well as tsc-associated renal angiomyolipomas. *Genes Chromosomes Cancer* (1995) 13(4):295–8. doi: 10.1002/gcc.2870130411

40. Luo C, Liu Z, Gao M, Hu Q, He X, Xi Y, et al. Renal epithelioid angiomyolipoma: computed tomography manifestation and radiologic-pathologic correlation depending on different epithelioid component percentages. *Abdom Radiol (NY)* (2022) 47(1):310–9. doi: 10.1007/s00261-021-03313-3

41. Caliò A, Brunelli M, Segala D, Pedron S, Tardanico R, Remo A, et al. T(6;11) renal cell carcinoma: A study of seven cases including two with aggressive behavior, and utility of cd68 (Pg-M1) in the differential diagnosis with pure epithelioid pecoma/epithelioid angiomyolipoma. *Mod Pathol* (2018) 31(3):474–87. doi: 10.1038/modpathol.2017.144

42. Bansal A, Goyal S, Goyal A, Jana M. Who classification of soft tissue tumours 2020: an update and simplified approach for radiologists. *Eur J Radiol* (2021) 143:109937. doi: 10.1016/j.ejrad.2021.109937

43. Stock K, Slotta-Huspenina J, Kübler H, Autenrieth M. [Innovative ultrasound-based diagnosis of renal tumors]. *Der Urologe Ausg A* (2019) 58(12):1418–28. doi: 10.1007/s00120-019-01066-y

44. Lei J, Liu L, Wei Q, Song T, Yang L, Yuan H, et al. A four-year follow-up study of renal epithelioid angiomyolipoma: A multi-center experience and literature review. *Sci Rep* (2015) 5:10030. doi: 10.1038/srep10030

45. Kobayashi Y, Shimizu S, Arai H, Yoshida K, Honda M. Fat-poor leiomyomatous angiomyolipoma arising from renal parenchyma negative for hmb-45: A case report. *Clin Case Rep* (2022) 10(12):e6771. doi: 10.1002/ccr3.6771

46. Stone C, Lee M, Amin M, Yaziji H, Gown A, Ro J, et al. Renal angiomyolipoma: further immunophenotypic characterization of an expanding morphologic spectrum. *Arch Pathol Lab Med* (2001) 125(6):751–8. doi: 10.5858/2001-125-0751-ra

47. Zheng S, Bi X, Song Q, Yuan Z, Guo L, Zhang H, et al. A suggestion for pathological grossing and reporting based on prognostic indicators of Malignancies from a pooled analysis of renal epithelioid angiomyolipoma. *Int Urol Nephrol* (2015) 47 (10):1643–51. doi: 10.1007/s11255-015-1079-9

48. Liu L, Feng Y, Guo C, Weng S, Xu H, Xing Z, et al. Multi-center validation of an immune-related lncrna signature for predicting survival and immune status of patients with renal cell carcinoma: an integrating machine learning-derived study. *J Cancer Res Clin Oncol* (2023). doi: 10.1007/s00432-023-05107-0

49. Liu C, Sunday H, Jing Z. Imaging diagnosis of renal epithelioid angiomyolipoma. *J Med Imaging (Chinese)* (2017) 27(09):1800–2. doi: 10.1007/s00432-023-05107-0

50. Jia Z, Tang L, Liu K, Guo A, Huang Q, Peng C, et al. Venous tumor thrombus consistency: is it a prognostic factor of survival for patients with renal cell carcinoma? *Updates Surg* (2023). doi: 10.1007/s13304-023-01544-1

51. Manur R, Lamzabi I. Aberrant cytokeratin 20 reactivity in epithelioid Malignant mesothelioma: A case report. *Appl immunohistochem Mol morphology AIMM* (2019) 27(10):e93–e6. doi: 10.1097/pai.0000000000000504

52. Boukhris I, Azzabi S, Kéchaou I, Chérif E, Kooli C, Romdhane K, et al. [Hypercalcemia related to pth-rp revealing Malignant hepatic epithelioid hemangioendothelioma]. *Annales biologie clinique* (2016) 74(1):98–102. doi: 10.1684/abc.2015.1118

53. De la Sancha C, Khan S, Alruwaii F, Cramer H, Saxena R. Hepatic angiomyolipoma with predominant epithelioid component: diagnostic clues on aspiration and core needle biopsies. *Diagn Cytopathol* (2021) 49(7):E238–E41. doi: 10.1002/dc.24688

54. Sanfilippo R, Jones R, Blay J, Le Cesne A, Provenzano S, Antoniou G, et al. Role of chemotherapy, vegfr inhibitors, and mtor inhibitors in advanced perivascular epithelioid cell tumors (Pecomas). *Clin Cancer Res* (2019) 25(17):5295–300. doi: 10.1158/1078-0432.Ccr-19-0288

55. Liapi A, Mathevet P, Herrera F, Hastir D, Sarivalasis A. Vegfr inhibitors for uterine metastatic perivascular epithelioid tumors (Pecoma) resistant to mtor inhibitors. A case report and review of literature. *Front Oncol* (2021) 11:641376. doi: 10.3389/fonc.2021.641376

56. Lattanzi M, Deng F, Chiriboga L, Femia A, Meehan S, Iyer G, et al. Durable response to anti-pd-1 immunotherapy in epithelioid angiomyolipoma: A report on the successful treatment of a rare Malignancy. *J Immunother Cancer* (2018) 6(1):97. doi: 10.1186/s40425-018-0415-x

frontiers | Frontiers in Oncology

TYPE Review
PUBLISHED 08 September 2023
DOI 10.3389/fonc.2023.1224913

OPEN ACCESS

EDITED BY
Philippe E. Spiess,
Moffitt Cancer Center, United States

REVIEWED BY
Eswar Shankar,
The Ohio State University, United States
Kenichi Takayama,
Tokyo Metropolitan Institute of Gerontology, Japan

*CORRESPONDENCE
Zhiqun Shang
zhiqun_shang@tmu.edu.cn
Jing Tian
jing_tian@tmu.edu.cn

RECEIVED 18 May 2023
ACCEPTED 15 August 2023
PUBLISHED 08 September 2023

CITATION
Yu W, Wang C, Shang Z and Tian J (2023) Unveiling novel insights in prostate cancer through single-cell RNA sequencing. *Front. Oncol.* 13:1224913. doi: 10.3389/fonc.2023.1224913

Unveiling novel insights in prostate cancer through single-cell RNA sequencing

Wenyue Yu, Chun Wang, Zhiqun Shang* and Jing Tian*

Tianjin Institute of Urology, Second Hospital of Tianjin Medical University, Tianjin, China

Single-cell RNA sequencing (scRNA-seq) is a cutting-edge technology that provides insights at the individual cell level. In contrast to traditional bulk RNA-seq, which captures gene expression at an average level and may overlook important details, scRNA-seq examines each individual cell as a fundamental unit and is particularly well-suited for identifying rare cell populations. Analogous to a microscope that distinguishes various cell types within a tissue sample, scRNA-seq unravels the heterogeneity and diversity within a single cell species, offering great potential as a leading sequencing method in the future. In the context of prostate cancer (PCa), a disease characterized by significant heterogeneity and multiple stages of progression, scRNA-seq emerges as a powerful tool for uncovering its intricate secrets.

KEYWORDS

prostate cancer, ScRNA-seq, tumor microenvironment, tumor heterogeneity, cell interactions

Introduction

Prostate cancer is currently the most prevalent cancer diagnosed in men within the United States, accounting for 29% of all diagnoses in 2023 and ranking as the second leading cause of cancer-related deaths in men of all ages in 2020 (1). Globally, there are approximately 1.3 million new cases of prostate cancer reported each year (2). It is widely recognized that prostate cancer exhibits significant heterogeneity, both clinically and at the molecular and morphological levels (3). Consequently, comprehensive assessment of this disease often proves challenging when relying solely on molecular analyses of tissue samples as a whole. Thankfully, the advancement of technology has allowed for substantial progress in the field of cancer research, enabling us to explore the genomic landscape and developmental processes of prostate cancer in greater detail.

Among the rapidly evolving technologies, scRNA-seq has emerged as a prominent tool. Leveraging specialized technological expertise and sophisticated bioinformatic analysis, scRNA-seq enables us to investigate gene expression at the individual cell level. By employing mature analytical approaches such as clustering, trajectory inference,

cell-typeannotation, and dataset integration (4), scRNA-seq provides us with novel dimensions to comprehend prostate cancer in terms of its plasticity, metastatic potential, and tumor microenvironment (TME).

This review aims to highlight the latest findings in the field of prostate cancer uncovered through scRNA-seq (Figure 1). By examining each stage of prostate cancer progression from a single-cell perspective, and drawing insights from a selection of recently published representative articles, we will explore the impact of this emerging technology on reinterpreting earlier research and shaping the future landscape of prostate cancer study.

Single-cell RNA sequencing on normal prostate

Traditional fluorescence-activated cell sorting (FACS) has been widely used for cell type identification in tissues. However, it has limitations in detailed cell sorting and discovering new subtypes due to gating strategies and limited antibody availability. In a pioneering study, Henry et al. employed single-cell RNA sequencing to comprehensively profile the transcriptome of the normal adult human prostate. By combining their findings with immunofluorescence and flow cytometry, they achieved the first cellular anatomy of the normal human prostate, establishing a baseline for future prostate disease studies (5).

The anatomical composition of the prostate was originally defined into four main regions: peripheral zone, central zone, preprostatic zone, and anterior fibromuscular stroma by McNeal in 1968 (6). Based on gene expression, cellular location, and surface antigens, three types of epithelial cells have been described in the prostate: basal, luminal, and neuroendocrine (NE) (7–11). Henry et al.'s findings were consistent with previous knowledge, with the addition of two epithelial cell subtypes expressing low levels of both basal and luminal markers (luminal KLK3+ and basal KRT14+). These subtypes were labeled as "other epithelia" (OE), further divided into "OE1" and "OE2". OE1 was characterized by high expression of SCGB1A1, PIGR, MMP7, CP, and LCN2, while OE2 expressed KRT13, SERPINB1, and CLDN4 (5). By comparing these subtypes with epithelial cells from the mouse lung, they found that OE1 exhibited similarities to lung Scgb1a1+ clara (club) cells and Krt13+ hillock cells, whereas OE2 showed similarities to lung Krt5+ basal and Krt13+ hillock cells (5, 12, 13).

The localization of different cell types was further examined using *in situ* triple immunofluorescence. OE1 cells (SCGB1A1+) were predominantly found in the prostatic urethra and collecting ducts, but were rare in the prostate itself. On the other hand, OE2 cells (KRT13+) were abundant in the prostatic urethra, collecting ducts, and the central zone surrounding the ejaculatory ducts, but were scarce in the peripheral zone (5).

Previous studies have indicated low expression of KRT family genes in the adult prostate, with enrichment observed in fetal

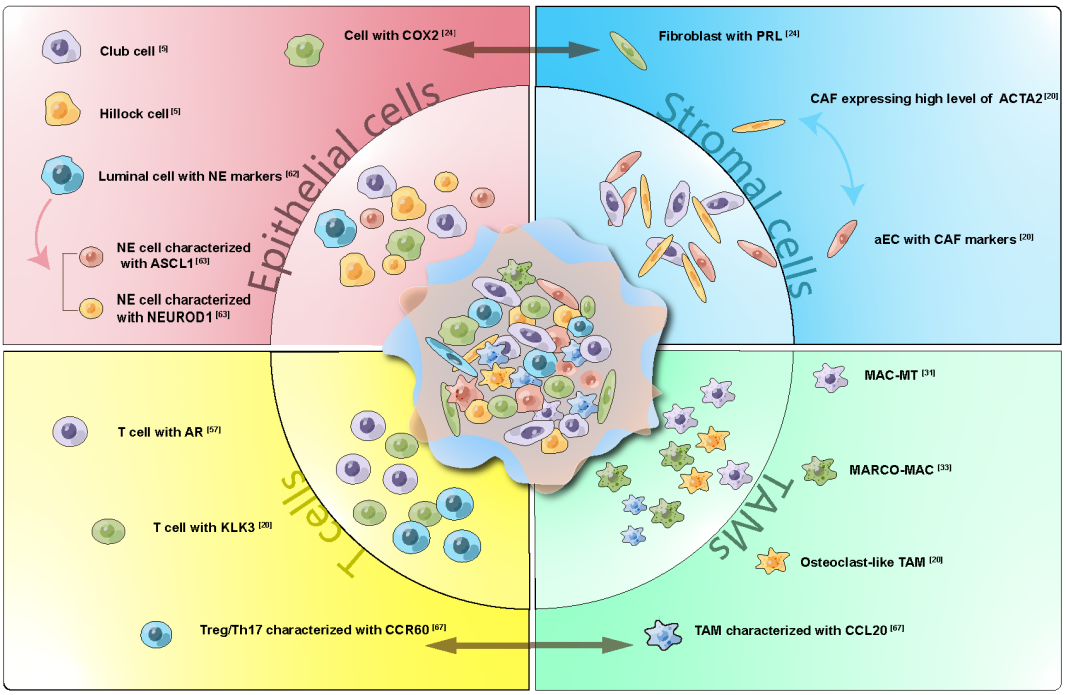

FIGURE 1
Cell Subtypes, Interactions, and Development Trajectory Revealed by ScRNA-seq in Prostate Cancer. Representative subgroups within Epithelial cells, Stromal cells, T cells, and Tumor Associated Macrophages (TAMs) were delineated. Cellular trajectories were depicted through one-way arrays, while interactions were visualized using two-way arrays. scRNA-seq has proven instrumental in identifying less prevalent cell subtypes and enhancing our understanding of cellular communication and lineage connections within prostate cancer.

prostate and localized prostate tumors (14). Thus, the KRT13+ OE2 cell type was suggested to be associated with tumorigenesis (5). The specific function of OE1 cells is yet to be elucidated.

The study also identified stromal components of the prostate, including smooth muscle cells, fibroblasts, and leukocytes. This application of scRNA-seq on human prostate represents a significant milestone in prostate research, as it demonstrated the technology's impressive ability to identify previously unrecognized subtypes. Although the study did not explicitly identify neuroendocrine cells, possibly due to their scarcity, subsequent research has addressed these limitations and further explored the biological functions of the newly discovered subgroups.

Primary prostate tumors

Building upon the discoveries made by Henry et al., Song et al. aimed to investigate the representation of epithelial diversity within primary prostate tumors (15).

Using scRNA-seq, they examined the profiles of four pairs of tumors and their corresponding benign-appearing tissue. The analysis revealed the presence of basal and luminal cells, consistent with epithelial populations. Additionally, they identified a subset of cells exhibiting lower scores for basal epithelial (BE) and luminal epithelial (LE) signatures, but displaying elevated expression of PIGR, MMP7, and CP. These cells closely resembled the previously reported OE1 cells, as indicated by their expression of SCGB1A1, PIGR, MMP7, CP, and LCN2, as documented by Henry et al. (5). Notably, the identified markers expressed by these OE1 cells have been linked to the generation and progression of tumors (16–18). Consequently, it was inferred that these OE1-like cells may be associated with the process of carcinogenesis.

Due to the observed similarities between OE1 cells in the prostate and club cells in the lung (5), the analogous cells discovered by Song et al. were designated as "club cells" in their study. To further investigate the role of club cells in PCa, the researchers categorized both tumor and normal samples' club cells into six distinct cell states labeled as club 0 to club 5. Among these clusters, club 0 was found to be significantly enriched in the tumor group. This cluster exhibited upregulation of LTF, luminal markers, and a range of downstream genes related to the androgen receptor (AR) pathway. Enrichment analysis also revealed a substantial enrichment in the Hallmark Androgen Response pathway. Another cluster, club 6, which was also enriched in the tumor group, displayed similar characteristics. Collectively, these findings suggested a luminal-like and androgen-responsive state of PCa epithelial cells (15).

Further investigation led to the identification of LE and BE subclusters characterized by the expression of club cell markers (initially proposed for normal prostate cancer by Henry et al., as mentioned above, encompassing SCGB1A1, PIGR, MMP7, CP, and LCN2 (5)). These subclusters were referred to as "club cell states." Supported by additional scRNA-seq datasets (19, 20), a set of PCa-club cell signatures was established, including PIGR, LTF, and NKX3-1 (15).

It is noteworthy that in their investigation, Song et al. did not observe the presence of OE2-like cells (also referred to as "hillock cells" due to their similarity to hillock cells in the lung) within their PCa samples (5). However, these cells were identified in PCa organoids. This disparity suggests that hillock cells may experience depletion during the progression of prostate cancer. Despite this intriguing observation, further research is required to unravel the underlying mechanisms responsible for this phenomenon and provide a more comprehensive explanation (15).

Song et al.'s study elucidated the heterogeneity of epithelial cells in prostate cancer, specifically investigating the functional characteristics of club and hillock cells within PCa. Their research significantly expanded upon the previous findings of Henry et al.

Additionally, Song et al. conducted a study aiming to elucidate the distinctions attributed to TMPRSS2-ERG fusion, a prevalent oncogenic transcription factor in PCa. Tumor cells exhibiting elevated ERG expression were categorized as ERG+, while cells lacking ERG expression were designated as ERG-. Notably, there was no noteworthy disparity in copy number variations (CNV) between ERG+ and ERG- tumor cells. However, variations were observed in terms of inter-tumor heterogeneity and transcriptomic profiles. Firstly, ERG+ cells exhibited a patient-specific clustering pattern, unlike ERG- cells. Secondly, ERG- cells displayed a greater overlap in gene expression with non-malignant LE cells and occupied a closer proximity to LE on the UMAP map, indicating a higher degree of similarity (15). Moreover, ERG- patients demonstrated increased shared signaling pathways between T-cells and stromal cells, and both CD4 and CD8 cells associated with ERG- tumor cells displayed signs of exhaustion and a cytotoxic phenotype, thereby suggesting a promising potential for immunotherapy in clinical trials (15). In conclusion, these findings suggest that the overexpression of ERG in PCa epithelia contributes to increased intra- and inter-cellular heterogeneity and is associated with unfavorable outcomes.

The study conducted by Chen et al. provides a novel perspective on the heterogeneity of PCa epithelia.

The researchers analyzed epithelial cells obtained from 13 tissue samples of PCa, including 12 primary tumors and 1 lymph node metastasis. Through the utilization of PAM50, a gene expression signature initially discovered in breast cancer, the epithelial cells were classified into three subtypes: luminal A, luminal B, and basal (16). Most of the subclusters exhibited characteristics of both luminal A and luminal B subtypes, with the exception of clusters 10 and 12. Cluster 10 demonstrated a high expression signal for luminal A genes but also expressed gene markers associated with basal/intermediate cells. Therefore, it was designated as "Basal/Intermediate cells" (20). Conversely, cluster 12 displayed a high expression signal for luminal B genes and exhibited an overexpression of genes involved in cell-cycle phases, leading to its designation as "CellCycle" (20). Survival analysis using data from the TCGA database revealed that patients with the CellCycle signature had a worse prognosis, consistent with previous studies (21). On the other hand, patients with Basal/Intermediate signatures exhibited a better outcome, partially aligning with the findings of Song et al. that PCa epithelia display a more luminal-like state (15). Chen et al. also investigated the immune aspect of the

findings. They discovered that basal/intermediate cells showed high expression of antigen processing and presentation genes (20), specifically expressing HLA class II and the chemokine gene CCL2, which could enhance the immune response against tumor cells and potentially contribute to better survival. Additionally, basal/intermediate cells involved in perineural invasion (PNI) were found to have significant communication with neural cells through the CXCL and CCL signaling networks (22). This communication was identified as a critical factor in promoting cancer progression and metastasis in PNI-PCa (22). Furthermore, a separate study involving primary tumor tissues from 14 untreated PCa patients reported that the epithelial subcluster with the highest number of cycling cells exhibited the highest epithelial-to-mesenchymal transition (EMT) score, indicating greater tumor ecosystem diversity, which was associated with a poorer prognosis (23).

The heterogeneity observed among epithelial tumor cells can often be attributed to the diverse interactions occurring within the tumor tissue. Utilizing scRNA-seq, Zheng et al. identified a distinct subtype of tumor cells derived from micro-metastases of prostate cancer in mice. This subtype displayed notable differences compared to tumor cells found at primary sites and exhibited a high expression of prolactin receptor (Prlr) (24). Building upon this discovery, subsequent experiments revealed a significant intercellular interaction pathway: tumor cells exhibited elevated levels of COX-2 (prostaglandin endoperoxide synthase 2), which facilitated the synthesis of PGE2. This, in turn, stimulated the secretion of prolactin by upregulating nuclear receptor 4A (NR4A) in stromal cells. The increased concentration of prolactin subsequently induced the expression of PRLR in neighboring tumor cells, thereby promoting early metastasis in prostate cancer (24). The identification of this new tumor cell subtype unveiled the important role played by COX-2 in the progression of prostate cancer. Furthermore, when combined with the findings of Peng et al., which highlighted the various immunosuppressive effects derived from EP4, a high-affinity receptor of PGE2 (25), it can be inferred that COX-2 inhibitors could serve as meaningful additions to clinical therapies.

The heterogeneity observed in PCa extends beyond epithelial cells and also encompasses the stromal compartment.

Fibroblast and endothelial cells (ECs) are recognized as vital components of the TME. The interactions between cancer-associated fibroblasts (CAFs) and tumor cells, as well as tumor-infiltrating immune cells, have been identified as key factors in promoting tumor progression (26). In the study conducted by Chen et al., it was observed that ACTA2, a gene encoding actin proteins, which was reported to be decreased in CAFs of PCa due to changes in stromal composition (27), exhibited abundant expression in CAFs. Through correlation analysis, researchers suggested its association with EMT (20). Transcription factor (TF) analysis revealed a subset of CAFs enriched in genes involved in the extracellular matrix (ECM), leading to their characterization as "activated CAFs". Genes related to activated CAFs were also expressed in certain subsets of ECs, which were labeled as "aECs." These particular aECs were found to be enriched in castration-resistant prostate cancer (CRPC) and exhibited the ability to modify the ECM and downregulate immune activation through cell-cell interactions (20).

CAFs that are enriched in invasive prostate cribriform carcinoma (ICC) and intraductal carcinoma (IDC) were found to exhibit elevated expression levels of CTHRC1, ASPN, FAP, and ENG. This upregulation of genes in CAFs was hypothesized to be associated with dysfunctional T cells (28).

The roles of immune cells in tumor progression have garnered increasing attention in recent years. The use of scRNA-seq to characterize the diverse population of infiltrating immune cells in PCa provides valuable insights for a better understanding of this phenomenon.

Tumor-associated macrophages (TAMs) play significant roles in regulating tumorigenesis (29). While macrophages have traditionally been viewed as anti-tumor cells involved in immune defense, numerous studies have highlighted the dual nature of TAMs. Specifically, TAMs have been shown to stimulate angiogenesis, enhance tumor cell migration and invasion, and suppress antitumor immunity, thereby contributing to the progression of tumors towards malignancy (29, 30).

In a scRNA-seq study involving 10 pairs of human cancer and adjacent normal tissue, a distinct subset of TAMs characterized by high expression of metallothionein family genes, particularly zinc transporter genes SLC30A1 (ZNT-1) and SLC39A8 (ZIP-8), was identified. These TAMs were labeled as "MAC-MT" (31). Since zinc is a crucial component of prostatic fluid, the MAC-MT subset was considered a prostate-specific macrophage subtype that plays a role in maintaining zinc metabolism homeostasis (32). Importantly, the MAC-MT subset exhibited increased expression of IFNγ-, THF-, as well as CXCL9 and CXCL10, indicating its association with anti-cancer immune response and potentially contributing to better patient outcomes (31).

In addition to TAMs associated with zinc metabolism, TAMs linked to lipid metabolism have also been discovered. Through clustering analysis of macrophages from three treatment-naïve patients, two distinct macrophage subtypes, Mac1 and Mac2, were identified. Comparison of tumor and adjacent nontumor tissues revealed that both Mac1 and Mac2 subtypes increased in tumor tissues and were associated with pathways related to lipid metabolism, with Mac2 showing a more pronounced association (33). Further investigation focused on Mac2 revealed that TAMs characterized by the high expression of MARCO exhibited a significant correlation with lipid metabolism and could serve as a prognostic signature (33).

TAMs can also serve as a predictive factor for metastasis. Chen et al. identified a specific subset of macrophages characterized by a high expression level of osteoclast (OC)-related pathways, including mineral absorption and lysosome functions (20). This finding is particularly significant considering that prostate cancer commonly metastasizes to bone, where osteoclasts play crucial roles, and inhibiting osteoclast activity has been shown to delay bone metastasis in prostate cancer (34). The discovery of this subset of TAMs suggests that the potential for metastasis may already be present in the early stages of the tumor (20).

Tumor-associated macrophages (TAMs) characterized by the M2 markers CD163 and MSR1 in ICC and ICD were found to exhibit upregulated expression of C1QB, TREM2, and APOE. Importantly, the presence of these TAMs was associated with worse progression survival outcomes (28).

T cells play a crucial role in TME and serve as indicators of immune activity. In PCa, the TME is generally considered to be immunosuppressive, as evidenced by the proportion of regulatory T cells (Tregs) and the expression of cytotoxic genes in CD4+ and CD8+ T cells (31, 33). However, subsets of T cells within PCa tissue samples have been found to express high levels of KLK3, the gene encoding prostate-specific antigen (PSA) (20). These KLK3-high T-cell clusters exhibit specific modules associated with extracellular vesicles (EVs) and exosomes, suggesting that the abundance of KLK3 might be attributed to EVs derived from tumor cells. This hypothesis was confirmed through subsequent experiments, which demonstrated that T cells expressing KLK3 contribute to the establishment of a pre-metastatic niche for tumor cells (20). Furthermore, single-cell proteomics analysis involving 58 prostate cancer patients with different International Society of Urological Pathology (ISUP) grades revealed that T cells were enriched in the high-grade sub-cohort and exhibited a highly proliferative phenotype (35).

Oncogenesis

The process of tumor formation, known as oncogenesis, has been a subject of extensive discussion. One theory proposes that tumors originate from a specific group of stem cells (36), while another suggests that a majority of cells can contribute to tumorigenesis. To gain insights into the underlying mechanisms of oncogenesis in PCa, researchers have employed scRNA-seq technology.

Karthaus et al. conducted an experiment to investigate the stemness potential of mouse prostate epithelia during androgen deprivation and restoration, focusing on the regeneration of the prostate. The epithelial cells were classified into seminal vesicle subsets, basal subsets, and three luminal subsets referred to as luminal 1, 2, and 3 cells (L1, L2, L3). Among these luminal subpopulations, L1 cells constituted the largest proportion. L1 cells exhibited high expression of canonical androgen receptor target genes (such as Pbsn, Nkx3.1) and genes associated with mature secretory cells (CD26/Dpp4+, DC59a, and CD133/Prom 1). L2 cells were characterized by the expression of Scal/Ly6a, Tacstd2/Trop2, and Psca, which have been reported to be involved in stem cell-like activity. L3 cells expressed the transcription factor Foxil, a master regulator of subunits of the vacuolar ATPase proton pump, suggesting a potential association between the L3 subset and epididymal fluid acidification (19). Furthermore, regarding their spatial distribution, L1 cells were primarily located in the distal prostate ducts, L2 cells were predominantly found in the proximal prostate region, and L3 cells were interspersed in both proximal and distal locations (19).

In order to identify potential stem cells during the regeneration process following androgen deprivation, scRNA-seq data from mouse prostate across a castration/regeneration (C/R) cycle was collected and analyzed. Interestingly, despite L1 cells remaining the majority population, they exhibited striking similarities to L2 cells after castration. However, during the regeneration phase, the expression pattern of L1 cells reverted back to their baseline state, indicating the loss of androgen receptor-regulated transcription. Notably, all three subsets (L1, L2, and L3) displayed an increase in proliferation markers during the regeneration process. The stem-like potential of both L1 and L2 cells was further confirmed through organoid culture, where organoids derived from these subsets gave rise to Krt5+ basal cells, indicating their bi-lineage potential (19).

Furthermore, during the process of regeneration, stromal cells exhibited increased expression of growth factor ligands, such as Nrg2, Igf1, Fgf10, and Rspo3. Simultaneously, the expression of corresponding receptors, including Fgfr2 and Lgr4, was enhanced in L1 cells. This reciprocal interaction between stromal cells and luminal cells indicated the influence of the microenvironment on luminal proliferation and highlighted the importance of cell-cell circuits in this process (19).

These findings suggest that the potential for self-renewal is present in the majority of luminal cells, including the well-differentiated secretory cells of the L1 subset, during the castration/regeneration cycle. This challenges the conventional belief that self-renewal ability is limited to rare stem cells and indicates that almost all luminal cells have the capacity for redifferentiation (19).

In a separate research study focused on identifying a potential population with luminal stem/progenitor properties during prostate homeostasis and regeneration, researchers proposed an alternative theory.

Cells derived from freshly dissociated whole prostate tissue of healthy adult male mice were classified into 11 distinct cell clusters, including three clusters of luminal cells denoted as Luminal-A/B/C (37). Among these subclusters, Luminal-A/B was characterized by the expression of genes associated with iron homeostasis and fluid secretion, suggesting their functional maturation and differentiation (37). Meanwhile, the Luminal-C cluster exhibited high expression levels of Tacst2, Psca, and Ck4. The protein product of Tacstd2 has been identified as a stem cell marker (38), while Psca is known as a tumor antigen associated with prostate cancer (39). Pathway enrichment analysis revealed a significant enrichment in tissue development and epithelial cell differentiation within the Luminal-C clusters (37). Moreover, cell trajectory analysis demonstrated a trajectory from Luminal-C to Luminal-A and Luminal-B, indicating the potential progenitor role of Luminal-C cells (37). This conclusion was supported by co-immunofluorescence experiments. Notably, a subset of Luminal-C cells located at the distal prostate glandular invagination tips, referred to as Dist-Luminal-C, showed high expression levels of Tastd2 and played a crucial role in prostate generation and potential tumorigenesis (37).

It should be noted that the study conducted by Guo et al. exhibited notable similarities to the research conducted by Karthaus et al. Both studies focused on the mouse prostate, conducted castration/regeneration assays, and identified a cluster of cells (Luminal-C in Guo's study and L2 in Karthaus' study) with high expression levels of Tastd2 and Psca. However, despite these similarities, different conclusions were drawn between the two studies. The underlying mechanism behind these divergent findings remains to be further explored.

In addition to androgen, vitamin D is a well-known factor associated with prostate cancer. The active form of vitamin D, 1,25

(OH)2D3, interacts with its receptor, the vitamin D receptor (VDR), to exert pleiotropic effects in mammals, including proliferation, differentiation, and apoptosis (40–42). Studies have reported that vitamin D deficiency increases the risk of prostate cancer (43), while men with higher plasma 25(OH)D levels in the highest quartile have been found to have less than half the risk of lethal prostate cancer compared to those with lower levels in the lowest quartile (44). The mechanisms underlying the preventive effect of vitamin D on prostate cancer are currently being investigated (45).

McCray et al. conducted a study using organoids derived from the benign region of the human prostate. ScRNA-seq was performed on organoids cultured with sufficient 1,25D (active form of vitamin D) and control organoids at day 8 and day 14, respectively. At day 8, the organoids cultured with sufficient 1,25D exhibited an increase in dividing cells compared to the control group. However, at day 14, the 1,25D-treated organoids showed an increase in polarized and basal cells, as well as a decrease in progenitor and intermediate cells, in comparison to the control group (46). Additionally, the organoids cultured with 1,25D at day 14 showed a higher percentage of cells expressing high levels of Integrin. These findings suggested that 1,25D could promote both growth and differentiation in the prostate. Transcriptome analysis revealed that the promotion of growth and differentiation by 1,25D was primarily achieved by inhibiting the Wnt pathway through upregulation of the dickoff family number 3 (DKK3) gene (46).

In another study, mice with Pten-deficient PIN were utilized to investigate the effects of the vitamin D analog Gemini-72 on prostatic precancerous lesions. ScRNA-seq analysis revealed that the down-regulated genes in response to Gemini-72 treatment were primarily involved in the encoding of collagen proteins, extracellular matrix (ECM) proteins, and ECM remodeling enzymes, suggesting that the main impact of Gemini-72 was on ECM remodeling (47). Epithelial cells were also influenced by Gemini-72 treatment. Among the subclusters of epithelial cells, the luminal-C subcluster characterized by Tacstd2, Krt4, and Ly6a exhibited a significant reduction in proportion after one week of treatment with Gemini-72. However, the proportion of luminal-A/B cells remained similar between the treatment and control conditions. Further subcluster analysis of the Luminal-C cells identified a particularly sensitive cell group characterized by high transcript levels of SASP components, which accumulate in cells undergoing cellular senescence (47). Additionally, persistent subsets of luminal-C cells exhibited upregulated NF-γB pathway activity, which is associated with antiapoptotic processes. These findings suggest that vitamin D analogs such as Gemini-72 may have potential benefits in the prevention and treatment of prostate cancer, as they eliminate precancerous cells through apoptotic cell death (47).

Castration resistance

Prostate cancer is commonly treated with castration, either through surgical or medical means, as the first-line treatment (48, 49). Initially, castration therapy demonstrates an efficiency rate of 80-90% (50, 51). However, a significant challenge arises as nearly all patients treated with castration therapy eventually develop castration-resistant prostate cancer (52). Therefore, it is crucial to explore the mechanisms underlying castration resistance in order to better understand the progression of prostate cancer.

The utilization of scRNA-seq has proven effective in constructing a longitudinal landscape of prostate cancer progression. Bolis et al. conducted a study using patient-derived xenografts (PDX), providing valuable insights into the trajectory of tumor cell progression during castration. The tumor model exhibiting rapid castration resistance displayed significant differences in single-cell transcriptional profiles before and after castration. A consistent shift was observed across all subsets, characterized by a suppression of canonical AR signaling and an upregulation of pro-proliferation genes associated with MYC (53). This shift across all cell subpopulations supports Karthaus et al.'s conclusion that plasticity potential exists in all prostate cells (19). However, it is worth noting that the PDX cells used in this study were derived from patients with castration-resistant prostate cancer (CRPC). The selection of stem-cell-like subsets may have already occurred due to prior therapy targeting the androgen receptor. Consequently, the conclusion may lack sufficient convincing power.

Another study associated with castration induced tumor cells is the study conducted using $Pten^{fl/fl}$ mice (54). Researchers identified a specific group of cells characterized by the expression of Krt4, Tacstd2, and Ppp1r1b, which were named as intermediate cells (54). These intermediate cells demonstrated a propensity for survival and diversification under castration conditions. Genes that were upregulated in castrated intermediate cells, such as ATP1B1, BST2, CP, IGFBP3, and PTTG1, have been shown to be associated with resistance to ADT in human tumors (54).

In addition, castration was found to induce perturbations in the tumor microenvironment (TME). Following castration, there was an increase in the abundance of tumor-associated macrophages with M2-like characteristics. This was accompanied by a reduction in M1-like features, including TNFα signaling and inflammatory signatures (53).

After profiling the trajectory of PCa at the single-cell level, the study took a further step. By analyzing high-throughput transcriptional datasets from 13 studies, the researchers identified EZH2, a member of the polycomb-repressive complex-2, as the most regulated gene during tumor progression (53). To unravel how EZH2 inhibition restores transcriptional output in CRPC progression, they utilized the EZH2 protein inhibitor GSK126 in LNCaP cells cultured in charcoal-stripped serum (CSS) to investigate the role of EZH2 in PCa progression under castration conditions. Remarkably, the introduction of co-targeting AR and EZH2 resulted in the formation of a completely new subgroup marked by heightened AR signaling and diminished expression of E2F-related cell cycle genes. This underscores that the inhibition of EZH2 within an androgen-depleted context resulted in a near-complete rewiring of transcriptional patterns. Additionally, in xenograft tumors on mice, inhibition of EZH2 delayed the regrowth of LNCaP xenografts. ScRNA-seq profiles demonstrated that GSK126 treatment led to an augmentation in the least progressed subcluster, indicating a reversal of progression along

the trajectory. Furthermore, a decrease in M2-like macrophages was observed in GSK126-pretreated tumors. These findings highlight the crucial role of EZH2 in castration-resistant PCa progression and introduce a novel potential for utilizing EZH2 inhibition in clinical treatment for CRPC progression (53).

To investigate the significance of the androgen receptor (AR) in castration resistance, He et al. conducted a study involving the collection of biopsies from three metastatic sites (bone, lymph node, and liver) before and after enzalutamide therapy. ScRNA-seq was utilized to exclude the influence of cells from the metastatic sites. By comparing the transcription profiles before and after castration therapy, the researchers observed an overall upregulation of AR and its isoforms, which was expected (55).

The study aimed to explore the relationship between specific AR isoforms and castration resistance. However, no individual AR isoform exhibited any relevance, even when examining paired biopsies from the same patient before and after therapy (55). The increased expression of AR isoforms was more likely a consequence of the overall increase in total AR expression, rather than playing an independent role in castration resistance (55).

Nevertheless, there were other differences observed due to castration aside from AR isoforms. Cells subjected to castration displayed a higher enrichment of gene sets associated with epithelial-mesenchymal transition (EMT) and transforming growth factor (TGF)-β signaling. Furthermore, castration therapy also influenced the immune microenvironment (55).

It has long been recognized that the majority of prostate tumors are not responsive to immune checkpoint inhibitors (56). Further investigation of T cells provided additional evidence in this regard. Several markers associated with exhaustion and dysfunction, such as PDCD1, HAVCR2, TOX, TIGIT, ICOS, FASLG, and LAG3, were observed, aligning with expectations (55). Additionally, clonotype groups of T cells detected in metastases exhibited genes related to co-inhibitory receptors and CXCR4, which may contribute to the unresponsiveness to immune checkpoint inhibitors (ICI/ICB) (55).

Another study focused on the association between checkpoint blockade and the efficacy of T cells. Guan et al. conducted research involving eight patients with metastatic castration-resistant prostate cancer (mCRPC), among whom three patients responded to pembrolizumab (defined as a prostate-specific antigen (PSA) decline of >25% upon immune checkpoint blockade), while five did not respond (57). ScRNA-seq was conducted on metastatic tumor lesions obtained from patients. The CD8+ T cells from these patients formed two clusters referred to as CD8 k1 and CD8 k2. Remarkably, these two clusters closely overlapped with CD8 T cell clusters divided by responders (CD8 R) and non-responders (CD8 NR). Analysis of differentially expressed genes between CD8 R and CD8 NR revealed a deactivation of AR in CD8 R (57). Inspired by the findings from scRNA-seq, a series of experiments were conducted, unveiling that AR could bind to open chromatin regions associated with Ifng and Gzmb, thereby causing immune suppression. These bindings could be suppressed by enzalutamide. The combination of androgen deprivation therapy (ADT) and enzalutamide enhanced the effect of PD-1/PD-L1 blockade in mice (57).

In the context of longitudinally exploring cancer progression, scRNA-seq provides a novel perspective for investigating the lineage and evolution of tumor cells. By employing cell trajectory analysis, it becomes possible to uncover hidden subtypes that may play a dominant role in tumor progression. This approach allows for a deeper understanding of the cellular dynamics and heterogeneity within the tumor, contributing to a more comprehensive characterization of cancer progression.

Taavitsainen et al. conducted a study utilizing PCa cell lines to investigate the mechanism underlying drug castration resistance. They performed both scRNA-seq and single-cell transposase-accessible chromatin sequencing (scATAC-seq) on LNCaP parental cell lines and LNCaP-derived enzalutamide (ENZ) cell lines. The scRNA-seq profiles were largely consistent with the scATAC-seq data, characterized by high expression of genes associated with AR and MYC, indicating that the transcriptional changes induced by drug castration were primarily driven by chromatin reprogramming (58). The cells were classified into different clusters, and certain clusters, referred to as "persist clusters," showed no significant change in their percentage before and after castration. The persist clusters exhibited high proliferative activity, and some of them demonstrated relatively high expression of genes associated with stemness (58). Trajectory analysis revealed that these cells possessed high developmental potential and could give rise to other clusters. They were characterized by a gene signature named "Persist". Genes associated with regenerative mouse prostate luminal 2 cells, as reported by Karthaus et al., were extracted (19). Among these, 78 genes with human homologs were designated as the "PROSGenesis signature". When assessing clusters using the PROSGenesis signature, cluster 10 in the parental cell line before treatment displayed the highest score. Subsequent trajectory analysis demonstrated that this cluster served as a precursor to castration-induced clusters (58). Scores of xenografts from AR+/NE−, AR−/NE+, or AR−/NE− CRPC and NEPC tumors resistant to ENZ revealed that the PROSGenesis signature exhibited notably high scores in AR+ tumors. Among primary treatment-naive patients, a high PROSGenesis score was linked to an extended response to ADT, potentially attributed to the heightened influence of AR activity within these tumors. Moreover, clinical data revealed that the PROSGenesis signature was associated with longer progression-free survival (PFS), and cells with a high PROSGenesis signature score predominantly belonged to the basal/intermediate subtype (58). This finding further supports the results from Chen et al., who reported that basal/intermediate cells were indicative of longer recurrence-free survival (20).

Cheng et al. conducted a study using clinical samples to define pre-existing castration-resistant subpopulations in primary prostate cancer, specifically in castration-resistant prostate cancer classified as adenocarcinoma (CRPC-adeno) and small cell neuroendocrine carcinoma (SCNC or CRPC-NE or NEPC). They performed scRNA-seq on specimens from three cases of primary adenocarcinoma and three castration-resistant PCa (including two CRPC-adeno and one NEPC). Based on the trajectory analysis generated by Monocle, non-basal cells followed two main directions: AR-dependent CRPC-adeno trajectory and an AR-

independent NEPC trajectory. Surprisingly, in addition to cells derived from CRPC/NEPC samples, a small number of primary PCa cells were also classified into CRPC/NEPC clusters (59). These cells were identified as either NE or CRPC-like cells based on their gene expression profiles. The trajectory analysis of NEPC progression revealed that NE cells from primary PCa were distributed along the trajectory, indicating their self-renewal capability and ability to evolve under the pressure of castration. On the other hand, CRPC-like cells were primarily located at the terminal state of the CRPC trajectory, indicating their advanced progression (59). These newly identified CRPC-like cells were found to exist in multiple databases, and the gene signature derived from them was shown to be meaningful in predicting clinical outcomes (59).

As mentioned earlier, NEPC represents a distinct stage in castration-resistant prostate cancer, characterized by the loss of AR expression and acquisition of neuroendocrine features (16, 60–62). The study conducted by Brady et al. delved into the development and composition of NEPC. Using gene-edited mice, the initial part of the research aimed to confirm that $Pten^{f/f}$; $RB1^{f/f}$; MYCN+ (PRN) mice had a higher propensity to develop NEPC compared to $Pten^{f/f}$; MYCN+ (PN) mice and $Pten^{f/f}$; $RB1^{f/f}$ (PR) mice. This suggested that the presence of MYCN amplification and Rb1 deletion could expedite the progression to castration resistance and NEPC tumors (62). Subsequently, scRNA-seq was performed on both PRN mice and age-matched PR mice. As anticipated, cells derived from PRN mice exhibited a higher proportion of neuroendocrine (NE) cells, with 75% originating from PRN tumors and 25% from PR tumors. Furthermore, these NEPC cells displayed an increased adult stem cell (ASC) signature score (62).

Remarkably, the trajectory analysis conducted in the study unveiled the existence of a distinctive subtype of luminal epithelial cells. Despite being classified as luminal cells, this particular cluster exhibited low expression levels of neuroendocrine markers and was positioned adjacent to the neuroendocrine (NE) cells along the cell trajectories. These luminal cells emerged more frequently and at an earlier stage in pseudotime in PRN tumors compared to PR tumors. Additionally, they shared an expression module with NE cells, suggesting their role as precursors to NE cells (62).

Furthermore, the study identified two distinct subclusters within the neuroendocrine (NE) cells, distinguished by the expression of Ascl1 and Pou2f3, respectively (62). This finding is somewhat consistent with the research conducted by Cejas et al., which focused on treatment-emergent neuroendocrine prostate cancer (NEPC) using patient-derived xenograft (PDX) models. Cejas et al. classified NEPC into two subtypes, but based on the expression of ASCL1 and NEUROD1 rather than ASCL1 and POU2F3 (63). Moreover, another study involving seven patients with prostate cancer identified two NEPC gene expression signatures: NE1 characterized by ASCL1, and NE2 marked by GHGA, GHGB, and ENO2 (64). These discrepancies in subtype classification may be attributed to differences in the sample species (gene-edited mice vs. PDX models) and potential batch effects. Ultimately, further research is needed to precisely define the subtypes of NEPC.

Additionally, the study highlighted two axes of NEPC evolution from androgen-dependent prostate cancer (ADPC). One axis was driven by genetic events, which involved gains in 12q, losses in 15q, amplification of MYC, and losses in RB1. The other axis was influenced by transcription factors. Specifically, NKX2-2 was identified as a key transcription factor at the early stage of NEPC development, while POU3F2 and SOX2 played crucial roles at the late stage (64). These findings provide insights into the molecular mechanisms underlying the transition from ADPC to NEPC, with both genetic alterations and transcriptional regulation contributing to the evolution of NEPC.

Migration

Bone metastases, a severe complication of cancer, have the potential to be life-threatening. In the context of prostate tumors, bone metastases are often regarded as an advanced stage and are observed in approximately 90% of men who experience treatment-resistant disease (65–67). Typically associated with castration resistance and immunosuppression (68), PCa with bone metastasis is commonly considered incurable. The underlying mechanisms behind this phenomenon have been extensively examined and debated.

Intercellular communication within the tumor microenvironment (TME) plays a crucial role in regulating immunity and has significant implications in bone metastasis. In a study conducted by Owen et al., scRNA-seq techniques were employed to investigate the dormancy and proliferation of PCa cells residing in bone metastases. Differential gene expression analysis revealed an enrichment of interferon-regulated genes (IRGs) in dormant cells, with type I interferons (IFN-α/β) being the most prominent (67). Notably, the clusters of dormant cells exhibited significant upregulation of genes associated with positive regulation of immune cells, including lymphocyte activation, as well as antigen processing and presentation. These findings suggest that immune-activating mechanisms in the bone microenvironment contribute to maintaining the dormant state of tumor cells. Conversely, the loss of intrinsic type I interferon signaling was found to promote the proliferation of metastatic tumor cells. Follow-up experiments provided further support for this hypothesis. It was also demonstrated that the suppression of tumor-intrinsic type I interferon signaling is induced by the bone marrow environment, and its reversion enhances the effectiveness of immunotherapy (67). These findings indicate a potential novel therapeutic approach targeting bone metastases.

Further investigation into the relationship between the immune microenvironment and bone migration was carried out. Kfoury et al. conducted a study that elucidated how immunocytes collaborate to establish an immunosuppressive TME. The study utilized scRNA-seq data from patients with spinal metastasis, including samples obtained from the solid tumor, involved

vertebral area, and distant vertebral regions, as well as benign controls. This comprehensive analysis provided insights into the immune compartment at both the tumor and liquid bone marrow levels. Differences in cell composition and gene expression profiles were observed between the benign and malignant samples, with the most significant disparities found in myeloid and T cells (69).

Regarding myeloid cells, the malignant fractions exhibited notable enrichment in tumor inflammatory monocytes (TIMs) and TAMs. TIMs demonstrated high expression of genes associated with activation and proliferation, while TAMs displayed characteristics consistent with the M2 phenotype (69). It has been reported that both TIMs and TAMs contribute to tumor progression and inflammation suppression by secreting factors such as epiregulin, EGF, NFKBIA, and TNFAIP3. The presence of these cells is often associated with a poor outcome (70, 71).

In terms of T cells, the tumor fractions demonstrated a significant decrease in the proportions of T cells compared to those found in healthy individuals. Among the cytotoxic T lymphocytes (CTLs), two distinct groups were identified. CTL-1 exhibited gene expression patterns associated with effector T cells, such as KLRG1, GZMK, and other cytotoxic mediators. On the other hand, CTL-2 displayed a transcriptional profile characteristic of effector/memory-like T cells, including genes like IL7R and KLRB1 (69). CTL-2 displayed an overall dysfunctional and exhausted phenotype, while increased activity signatures were observed in regulatory T cells (Tregs) at the metastatic site. These findings collectively indicate an immunosuppressive environment within TME.

Subsequent analysis suggested a correlation between the proportion of TAMs and the exhaustion of CTL-2. This finding implies a communication between the myeloid and lymphoid compartments within the tumor microenvironment. To further validate this observation, the researchers investigated the ligands and cognate receptors involved in the interaction between TIMs/TAMs and T cells. The results revealed that CCL20, expressed by TIMs/TAMs, could recruit Tregs and T_H17 cells through its cognate receptor CCR6. This recruitment mechanism contributes to an overall immunosuppressive environment in bone metastases (69).

Discussion

The concept of implementing RNA sequencing at the single-cell level was first demonstrated using neuronal cells in 1992 (72). Through a 15-year evolution, the high-throughput sequencing approach known as 10x Genomics was introduced in 2016, marking a pivotal advancement. This development laid the essential groundwork for the subsequent widespread adoption of single-cell RNA sequencing. The first application of scRNA-seq to prostate research was published in December 2018 (5), which is within a span of less than five years. As with any nascent technique, there are challenges to be faced. A primary hurdle involves sample acquisition and preparation. Given scRNA-seq's stringent demand for fresh tumor specimens, it has brought difficulties to postoperative pathological examination or disease recurrence observation. This constraint is partially alleviated through nuclear sequencing, viable for frozen or fixed samples. Another challenge pertains to noise. The modest sample size and shallow sequencing depth inherent to scRNA-seq yield extensive sparse and noisy data. Effective processing strategies, encompassing QC (quality control), normalization, imputation, feature selection, and dimensionality reduction, offer partial mitigation (73).

ScRNA-seq has significantly advanced prostate cancer research and clinical assessment by identifying subtypes and gene sets with prognostic implications. Notably, MAC-MT signifies a favorable prognosis (31), while T cells expressing KLK3 serve as metastasis predictors (20), and the PROSGenesis signature correlates with extended PFS (58). Moreover, this technology has unveiled new potential candidates for clinical intervention, such as COX-2 inhibitors (24, 25), Gemini-72 (47), and GSK126 (53). As a promising platform, scRNA-seq offers a higher-resolution landscape, empowering researchers to delve into rare subtypes, unravel tumor cell lineages, and investigate cellular interactions.

Beyond scRNA-seq, the rapid evolution of single-cell multi-omics, encompassing scATAC-seq (single-cell Assay for Transposase-Accessible Chromatin sequencing), single-cell proteomics, single-cell spatial transcriptomics, and single-cell metabolomics, is evident. The dawn of the single-cell omics era for human cancer is imminent, promising a comprehensive grasp of prostate cancer and laying the groundwork for personalized medicine.

The utilization of scRNA-seq, either alone or in combination with other experimental approaches, has significantly contributed to reinforcing and reinterpreting our understanding of prostate cancer within a relatively short timeframe. This rapidly advancing technology has enabled us to explore the heterogeneity of both tumor cells and the TME from a novel perspective. The application of scRNA-seq in prostate cancer research provides us with a precise anatomical understanding of different cell types and reveals the lineage relationships within subpopulations of the same cell type. Furthermore, it allows for the characterization of intercellular communication between different cell types. By subjecting the transcriptome of prostate cancer cells to the scrutiny of scRNA-seq, we can visualize the transcriptomic landscape at the level of individual cells, while at the same time understand tumor as a dynamic and communicative ensemble.

Author contributions

WY wrote the first draft of the manuscript. ZS, JT, and CW did revision and editing of the manuscript. All authors contributed to the article and approved the submitted version.

Funding

Tianjin Science and Technology Program Grant number: 21ZXJBY00090.

Conflict of interest

The authors declare that the research was conducted in the absence of any commercial or financial relationships that could be construed as a potential conflict of interest.

Publisher's note

All claims expressed in this article are solely those of the authors and do not necessarily represent those of their affiliated organizations, or those of the publisher, the editors and the reviewers. Any product that may be evaluated in this article, or claim that may be made by its manufacturer, is not guaranteed or endorsed by the publisher.

Supplementary material

The Supplementary Material for this article can be found online at: https://www.frontiersin.org/articles/10.3389/fonc.2023.1224913/full#supplementary-material

References

1. Siegel RL, Miller KD, Wagle NS, Jemal A. Cancer statistics, 2023. *CA Cancer J Clin* (2023) 73:17–48. doi: 10.3322/caac.21763

2. Sandhu S, Moore CM, Chiong E, Beltran H, Bristow RG, Williams SG, et al. Prostate cancer. *Lancet* (2021) 398:1075–90. doi: 10.1016/S0140-6736(21)00950-8

3. Haffner MC, Zwart W, Roudier MP, True LD, Nelson WG, Epstein JI, et al. Genomic and phenotypic heterogeneity in prostate cancer. *Nat Rev Urol* (2021) 18:79–92. doi: 10.1038/s41585-020-00400-w

4. Zhang Z, Cui F, Lin C, Zhao L, Wang C, Zou Q, et al. Critical downstream analysis steps for single-cell RNA sequencing data. *Brief Bioinform* (2021) 22(5):bbab105. doi: 10.1093/bib/bbab105

5. Henry GH, Malewska A, Joseph DB, Malladi VS, Lee J, Torrealba J, et al. A cellular anatomy of the normal adult human prostate and prostatic urethra. *Cell Rep* (2018) 25:3530–42. doi: 10.1016/j.celrep.2018.11.086

6. McNeal JE. The zonal anatomy of the prostate. *Prostate* (1981) 2:35–49. doi: 10.1002/pros.2990020105

7. Shen MM, Abate-Shen C. Molecular genetics of prostate cancer: new prospects for old challenges. *Genes Dev* (2010) 24:1967–2000. doi: 10.1101/gad.1965810

8. Foster CS, Dodson A, Karavana V, Smith PH, Ke Y. Prostatic stem cells. *J Pathol* (2002) 197:551–65. doi: 10.1002/path.1194

9. van Leenders GJ, Schalken JA. Epithelial cell differentiation in the human prostate epithelium: implications for the pathogenesis and therapy of prostate cancer. *Crit Rev Oncol Hematol* (2003) 46 Suppl:S3–10. doi: 10.1016/S1040-8428(03)00059-3

10. Hudson DL. Epithelial stem cells in human prostate growth and disease. *Prostate Cancer Prostatic Dis* (2004) 7:188–94. doi: 10.1038/sj.pcan.4500745

11. Shappell SB, Thomas GV, Roberts RL, Herbert R, Ittmann MM, Rubin MA, et al. Prostate pathology of genetically engineered mice: definitions and classification. The consensus report from the Bar Harbor meeting of the Mouse Models of Human Cancer Consortium Prostate Pathology Committee. *Cancer Res* (2004) 64:2270–305. doi: 10.1158/0008-5472.CAN-03-0946

12. Hong KU, Reynolds SD, Giangreco A, Hurley CM, Stripp BR. Clara cell secretory protein-expressing cells of the airway neuroepithelial body microenvironment include a label-retaining subset and are critical for epithelial renewal after progenitor cell depletion. *Am J Respir Cell Mol Biol* (2001) 24:671–81. doi: 10.1165/ajrcmb.24.6.4498

13. Montoro DT, Haber AL, Biton M, Vinarsky V, Lin B, Birket SE, et al. A revised airway epithelial hierarchy includes CFTR-expressing ionocytes. *Nature* (2018) 560:319–24. doi: 10.1038/s41586-018-0393-7

14. Liu S, Cadaneanu RM, Zhang B, Huo L, Lai K, Li X, et al. Keratin 13 is enriched in prostate tubule-initiating cells and may identify primary prostate tumors that metastasize to the bone. *PLoS One* (2016) 11:e0163232. doi: 10.1371/journal.pone.0163232

15. Song HA-O, Weinstein HNW, Allegakoen P, Wadsworth MH 2nd, Xie J, Yang H, et al. Single-cell analysis of human primary prostate cancer reveals the heterogeneity of tumor-associated epithelial cell states. *Nat Commun* (2022) 13(1):141. doi: 10.1038/s41467-021-27322-4

16. Wang JJ, Mao JH. The etiology of congenital nephrotic syndrome: current status and challenges. *World J Pediatr* (2016) 12:149–58. doi: 10.1007/s12519-016-0009-y

17. Zhang Q, Liu S, Parajuli KR, Zhang W, Zhang K, Mo Z, et al. Interleukin-17 promotes prostate cancer via MMP7-induced epithelial-to-mesenchymal transition. *Oncogene* (2017) 36:687–99. doi: 10.1038/onc.2016.240

18. Fotiou K, Vaiopoulos G, Lilakos K, Giannopoulos A, Mandalenaki K, Marinos G, et al. Serum ceruloplasmin as a marker in prostate cancer. *Minerva Urol Nefrol* (2007) 59:407–11.

19. Karthaus WA-O, Hofree M, Choi D, Linton EL, Turkekul M, Bejnood A, et al. Regenerative potential of prostate luminal cells revealed by single-cell analysis. *Science* (2020) 368(6490):497–505. doi: 10.1126/science.aay0267

20. Chen S, Zhu G, Yang Y, Wang F, Xiao Y-T, Zhang N, et al. Single-cell analysis reveals transcriptomic remodellings in distinct cell types that contribute to human prostate cancer progression. *Nat Cell Biol* (2021) 23(1):87–98. doi: 10.1038/s41556-020-00613-6

21. Cuzick J, Swanson GP, Fisher G, Brothman AR, Berney DM, Reid JE, et al. Prognostic value of an RNA expression signature derived from cell cycle proliferation genes in patients with prostate cancer: a retrospective study. *Lancet Oncol* (2011) 12:245–55. doi: 10.1016/S1470-2045(10)70295-3

22. Zhang B, Wang S, Fu Z, Gao Q, Yang L, Lei Z, et al. Single-cell RNA sequencing reveals intratumoral heterogeneity and potential mechanisms of Malignant progression in prostate cancer with perineural invasion. *Front Genet* (2022) 13:1073232. doi: 10.3389/fgene.2022.1073232

23. Ge G, Han Y, Zhang J, Li X, Liu X, Gong Y, et al. Single-cell RNA-seq reveals a developmental hierarchy super-imposed over subclonal evolution in the cellular ecosystem of prostate cancer. *Adv Sci (Weinh)* (2022) 9:e2105530. doi: 10.1002/advs.202105530

24. Zheng Y, Comaills V, Burr R, Boulay G, Miyamoto DT, Wittner BS, et al. COX-2 mediates tumor-stromal prolactin signaling to initiate tumorigenesis. *Proc Natl Acad Sci U.S.A.* (2019) 116(12):5223–32. doi: 10.1073/pnas.1819303116

25. Peng S, Hu P, Xiao Y-T, Lu W, Guo D, Hu S, et al. Single-cell analysis reveals EP4 as a target for restoring T-cell infiltration and sensitizing prostate cancer to immunotherapy. *Cli Cancer Res* (2022) 28(3):552–67. doi: 10.1158/1078-0432.CCR-21-0299

26. Mao X, Xu J, Wang W, Liang C, Hua J, Liu J, et al. Crosstalk between cancer-associated fibroblasts and immune cells in the tumor microenvironment: new findings and future perspectives. *Mol Cancer* (2021) 20:131. doi: 10.1186/s12943-021-01428-1

27. Ayala G, Tuxhorn JA, Wheeler TM, Frolov A, Scardino PT, Ohor M, et al. Reactive stroma as a predictor of biochemical-free recurrence in prostate cancer. *Clin Cancer Res* (2003) 9:4792–801.

28. Wong HY, Sheng Q, Hesterberg AB, Croessmann S, Rios BL, Giri K, et al. Single cell analysis of cribriform prostate cancer reveals cell intrinsic and tumor microenvironmental pathways of aggressive disease. *Nat Commun* (2022) 13:6036. doi: 10.1038/s41467-022-33780-1

29. Quail DF, Joyce JA. Microenvironmental regulation of tumor progression and metastasis. *Nat Med* (2013) 19:1423–37. doi: 10.1038/nm.3394

30. Qian BZ, Pollard JW. Macrophage diversity enhances tumor progression and metastasis. *Cell* (2010) 141:39–51. doi: 10.1016/j.cell.2010.03.014

31. Tuong ZK, Loudon KW, Berry B, Richoz N, Jones J, Tan X, et al. Resolving the immune landscape of human prostate at a single-cell level in health and cancer. *Cell Rep* (2021) 37(12):110132. doi: 10.1016/j.celrep.2021.110132

32. Costello LC, Franklin RB. A comprehensive review of the role of zinc in normal prostate function and metabolism; and its implications in prostate cancer. *Arch Biochem Biophys* (2016) 611:100–12. doi: 10.1016/j.abb.2016.04.014

33. Masetti M, Carriero R, Portale F, Marelli G, Morina N, Pandini M, et al. Lipid-loaded tumor-associated macrophages sustain tumor growth and invasiveness in prostate cancer. *J Exp Med* (2021) 219(2):e20210564. doi: 10.1084/jem.20210564

34. Hayes AR, Brungs D, Pavlakis N. Osteoclast inhibitors to prevent bone metastases in men with high-risk, non-metastatic prostate cancer: A systematic review and meta-analysis. *PLoS One* (2018) 13:e0191455. doi: 10.1371/journal.pone.0191455

35. De Vargas Roditi L, Jacobs A, Rueschoff JH, Bankhead P, Chevrier S, Jackson HW, et al. Single-cell proteomics defines the cellular heterogeneity of localized prostate cancer. *Cell Rep Med* (2022) 3:100604. doi: 10.1016/j.xcrm.2022.100604

36. Clevers H, Watt FM. Defining adult stem cells by function, not by phenotype. *Annu Rev Biochem* (2018) 87:1015–27. doi: 10.1146/annurev-biochem-062917-012341

37. Guo WA-O, Li L, He J, Liu Z, Han M, Li F, et al. Single-cell transcriptomics identifies a distinct luminal progenitor cell type in distal prostate invagination tips. *Nat Genet* (2020) 52(9):908–18. doi: 10.1038/s41588-020-0642-1

38. Goldstein AS, Huang J, Guo C, Garraway IP, Witte ON. Identification of a cell of origin for human prostate cancer. *Science* (2010) 329:568–71. doi: 10.1126/science.1189992

39. Reiter RE, Gu Z, Watabe T, Thomas G, Szigeti K, Davis E, et al. Prostate stem cell antigen: a cell surface marker overexpressed in prostate cancer. *Proc Natl Acad Sci U.S.A.* (1998) 95:1735–40. doi: 10.1073/pnas.95.4.1735

40. Holick MF. Vitamin D deficiency. *N Engl J Med* (2007) 357:266–81. doi: 10.1056/NEJMra070553

41. Feldman D, Krishnan AV, Swami S, Giovannucci E, Feldman BJ. The role of vitamin D in reducing cancer risk and progression. *Nat Rev Cancer* (2014) 14:342–57. doi: 10.1038/nrc3691

42. Bikle D, Christakos S. New aspects of vitamin D metabolism and action - addressing the skin as source and target. *Nat Rev Endocrinol* (2020) 16:234–52. doi: 10.1038/s41574-019-0312-5

43. Murphy AB, Nyame Y, Martin IK, Catalona WJ, Hollowell CMP, Nadler RB, et al. Vitamin D deficiency predicts prostate biopsy outcomes. *Clin Cancer Res* (2014) 20:2289–99. doi: 10.1158/1078-0432.CCR-13-3085

44. Shui IM, Mucci LA, Kraft P, Tamimi RM, Lindstrom S, Penney KL, et al. Vitamin D-related genetic variation, plasma vitamin D, and risk of lethal prostate cancer: a prospective nested case-control study. *J Natl Cancer Inst* (2012) 104:690–9. doi: 10.1093/jnci/djs189

45. Fleet JC, Kovalenko PL, Li Y, Smolinski J, Spees C, Yu J-G, et al. Vitamin D signaling suppresses early prostate carcinogenesis in tgAPT(121) mice. *Cancer Prev Res (Phila)* (2019) 12:343–56. doi: 10.1158/1940-6207.CAPR-18-0401

46. McCray T, Pacheco JV, Loitz CC, Garcia J, Baumann B, Schlicht MJ, et al. Vitamin D sufficiency enhances differentiation of patient-derived prostate epithelial organoids. *iScience* (2021) 24(1):101974. doi: 10.1016/j.isci.2020.101974

47. Abu El Maaty MA-O, Grelet E, Keime C, Rerra A-I, Gantzer J, Emprou C, et al. Single-cell analyses unravel cell type-specific responses to a vitamin D analog in prostatic precancerous lesions. *Sci Adv* (2021) 7(31). doi: 10.1126/sciadv.abg5982

48. Schmidt KT, Huitema ADR, Chau CH, Figg WD. Resistance to second-generation androgen receptor antagonists in prostate cancer. *Nat Rev Urol* (2021) 18:209–26. doi: 10.1038/s41585-021-00438-4

49. Hou Z, Huang S, Li Z. Androgens in prostate cancer: A tale that never ends. *Cancer Lett* (2021) 516:1–12. doi: 10.1016/j.canlet.2021.04.010

50. Trewartha D, Carter K. Advances in prostate cancer treatment. *Nat Rev Drug Discovery* (2013) 12:823–4. doi: 10.1038/nrd4068

51. Wang Y, Chen J, Wu Z, Ding W, Gao S, Gao Y, et al. Mechanisms of enzalutamide resistance in castration-resistant prostate cancer and therapeutic strategies to overcome it. *Br J Pharmacol* (2021) 178:239–61. doi: 10.1111/bph.15300

52. Davies A, Conteduca V, Zoubeidi A, Beltran H. Biological evolution of castration-resistant prostate cancer. *Eur Urol Focus* (2019) 5:147–54. doi: 10.1016/j.euf.2019.01.016

53. Bolis MA-O, Bossi D, Vallerga A, Ceserani V, Cavalli M, Impellizzieri D, et al. Dynamic prostate cancer transcriptome analysis delineates the trajectory to disease progression. *Nat Commun* (2021) 12(1):7033. doi: 10.1038/s41467-021-26840-5

54. Germanos AA, Arora S, Zheng Y, Goddard ET, Coleman IM, Ku AT, et al. Defining cellular population dynamics at single-cell resolution during prostate cancer progression. *Elife* (2022) 11.:e79076 doi: 10.7554/eLife.79076.sa2

55. He MX, Cuoco MS, Crowdis J, Bosma-Moody A, Zhang Z, Bi K, et al. Transcriptional mediators of treatment resistance in lethal prostate cancer. *Nat Med* (2021) 27(3):426–33. doi: 10.1038/s41591-021-01244-6

56. Teo MY, Rathkopf DE, Kantoff P. Treatment of advanced prostate cancer. *Annu Rev Med* (2019) 70:479–99. doi: 10.1146/annurev-med-051517-011947

57. Guan X, Polesso F, Wang C, Sehrawat A, Hawkins RM, Murray SE, et al. Androgen receptor activity in T cells limits checkpoint blockade efficacy. *Nature* (2022) 606(7915):791–6. doi: 10.1038/s41586-022-04522-6

58. Taavitsainen SA-O, Engedal N, Cao S, Handle F, Erickson A, Prekovic S, et al. Single-cell ATAC and RNA sequencing reveal pre-existing and persistent cells associated with prostate cancer relapse. *Nat Commun* (2021) 12(1):5307. doi: 10.1038/s41467-021-25624-1

59. Cheng Q, Butler W, Zhou Y, Zhang H, Tang L, Perkinson K, et al. Pre-existing castration-resistant prostate cancer-like cells in primary prostate cancer promote resistance to hormonal therapy. *Eur Urol* (2022) 81(5):446–55. doi: 10.1016/j.eururo.2021.12.039

60. Aparicio A, Tzelepi V, Araujo JC, Guo CC, Liang S, Troncoso P, et al. Neuroendocrine prostate cancer xenografts with large-cell and small-cell features derived from a single patient's tumor: morphological, immunohistochemical, and gene expression profiles. *Prostate* (2011) 71:846–56. doi: 10.1002/pros.21301

61. Beltran H, Prandi D, Mosquera JM, Benelli M, Puca L, Cyrta J, et al. Divergent clonal evolution of castration-resistant neuroendocrine prostate cancer. *Nat Med* (2016) 22:298–305. doi: 10.1038/nm.4045

62. Brady NA-O, Bagadion AM, Singh R, Conteduca V, Emmenis Van L, Arceci E, et al. Temporal evolution of cellular heterogeneity during the progression to advanced AR-negative prostate cancer. *Nat Commun* (2021) 12(1):3372. doi: 10.1038/s41467-021-23780-y

63. Cejas PA-O, Xie Y, Font-Tello A, Lim K, Syamala S, Qiu X, et al. Subtype heterogeneity and epigenetic convergence in neuroendocrine prostate cancer. *Nat Commun* (2021) 12(1):5775. doi: 10.1038/s41467-021-26042-z

64. Wang Z, Wang T, Hong D, Dong B, Wang Y, Huang H, et al. Single-cell transcriptional regulation and genetic evolution of neuroendocrine prostate cancer. *iScience* (2022) 25:104576. doi: 10.1016/j.isci.2022.104576

65. Nørgaard M, Jensen AØ, Jacobsen JB, Cetin K, Fryzek JP, Sørensen HT, et al. Skeletal related events, bone metastasis and survival of prostate cancer: a population based cohort study in Denmark (1999 to 2007). *J Urol* (2010) 184:162–7. doi: 10.1016/j.juro.2010.03.034

66. Perrault L, Fradet V, Lauzon V, LeLorier J, Mitchell D, Habib M. Burden of illness of bone metastases in prostate cancer patients in Québec, Canada: A population-based analysis. *Can Urol Assoc J* (2015) 9:307–14. doi: 10.5489/cuaj.2707

67. Owen KL, Gearing LJ, Zanker DJ, Brockwell NK, Khoo WH, Roden DL, et al. Prostate cancer cell-intrinsic interferon signaling regulates dormancy and metastatic outgrowth in bone. *EMBO Rep* (2020) 21(6):e50162. doi: 10.15252/embr.202050162

68. Xiang L, Gilkes DM. The contribution of the immune system in bone metastasis pathogenesis. *Int J Mol Sci* (2019) 20(4):999. doi: 10.3390/ijms20040999

69. Kfoury Y, Baryawno N, Severe N, Mei S, Gustafsson K, Hirz T, et al. Human prostate cancer bone metastases have an actionable immunosuppressive microenvironment. *Cancer Cell* (2021) 39:1464–1478.e1468. doi: 10.1016/j.ccell.2021.09.005

70. Huynh J, Etemadi N, Hollande F, Ernst M, Buchert M. The JAK/STAT3 axis: A comprehensive drug target for solid Malignancies. *Semin Cancer Biol* (2017) 45:13–22. doi: 10.1016/j.semcancer.2017.06.001

71. Lawrence T. The nuclear factor NF-kappaB pathway in inflammation. *Cold Spring Harb Perspect Biol* (2009) 1:a001651. doi: 10.1101/cshperspect.a001651

72. Eberwine J, Yeh H, Miyashiro K, Cao Y, Nair S, Finnell R, et al. Analysis of gene expression in single live neurons. *Proc Natl Acad Sci U.S.A.* (1992) 89:3010–4. doi: 10.1073/pnas.89.7.3010

73. Zhang Z, Cui F, Wang C, Zhao L, Zou Q. Goals and approaches for each processing step for single-cell RNA sequencing data. *Brief Bioinform* (2021) 22. doi: 10.1093/bib/bbaa314

frontiers | Frontiers in Oncology

TYPE Review
PUBLISHED 21 September 2023
DOI 10.3389/fonc.2023.1202656

OPEN ACCESS

EDITED BY
Wen-Hao Xu,
Fudan University, China

REVIEWED BY
Jiao Hu,
Central South University, China
Francesco Pezzella,
University of Oxford, United Kingdom

*CORRESPONDENCE
Gengqing Wu
gengqing169@126.com

RECEIVED 09 April 2023
ACCEPTED 06 September 2023
PUBLISHED 21 September 2023

CITATION
Lin X, Long S, Yan C, Zou X, Zhang G, Zou J and Wu G (2023) Therapeutic potential of vasculogenic mimicry in urological tumors.
Front. Oncol. 13:1202656.
doi: 10.3389/fonc.2023.1202656

Therapeutic potential of vasculogenic mimicry in urological tumors

Xinyu Lin[1,2], Sheng Long[1,2], Congcong Yan[1,2], Xiaofeng Zou[1,2], Guoxi Zhang[1,2], Junrong Zou[1,2] and Gengqing Wu[1,2]*

[1]The First Clinical College, Gannan Medical University, Ganzhou, Jiangxi, China, [2]Department of Urology, The First Affiliated hospital of Gannan Medical University, Ganzhou, Jiangxi, China

Angiogenesis is an essential process in the growth and metastasis of cancer cells, which can be hampered by an anti-angiogenesis mechanism, thereby delaying the progression of tumors. However, the benefit of this treatment modality could be restricted, as most patients tend to develop acquired resistance during treatment. Vasculogenic mimicry (VM) is regarded as a critical alternative mechanism of tumor angiogenesis, where studies have demonstrated that patients with tumors supplemented with VM generally have a shorter survival period and a poorer prognosis. Inhibiting VM may be an effective therapeutic strategy to prevent cancer progression, which could prove helpful in impeding the limitations of lone use of anti-angiogenic therapy when performed concurrently with other anti-tumor therapies. This review summarizes the mechanism of VM signaling pathways in urological tumors, i.e., prostate cancer, clear cell renal cell carcinoma, and bladder cancer. Furthermore, it also summarizes the potential of VM as a therapeutic strategy for urological tumors.

KEYWORDS

vasculogenic mimicry, urological, tumors, therapeutic potential, angiogenesis

1 Introduction

Urological cancers include cancers of the urinary system, including kidneys, urinary tract epithelium (including bladder, ureter, and urethra), prostate, testes, and penis. The American Cancer Society predicted in 2022 that there would be 1,918,030 new cases of cancer diagnosed with estimated 31,990 death from urological cancers in the United States. Prostate cancer is the most common malignancy and the third leading cause of cancer-related deaths in men, while kidney and bladder cancer are regarded among the top ten most common malignancies in the United States (1). The growth, invasion, and metastasis of malignant tumors are closely related to angiogenesis, which has become one of the hot topics in cancer research (2). Over the past few decades, it has been thought that the growth of tumors is dependent on angiogenesis. Tumors larger than 2mm in diameter cannot rely solely on diffusion for oxygen supply, and without the intervention of neovascularization,

tumors cannot continue to grow (3). Based on this hypothesis, it has been proposed that antiangiogenic drugs should be able to inhibit the growth of all solid tumors (4). However, anti-angiogenic therapy has so far shown only limited efficacy in patients. As early as before, researchers have proposed the idea of non-angiogenic tumors. But only recently has the special biological status of non-angiogenic tumors been formally described (5). Non-angiogenic tumors grow through two main mechanisms in the absence of angiogenesis. One way is to utilize pre-existing blood vessels by infiltrating cancer cells and occupying normal tissue, this is called vessel co-option. The second is through the formation of channels that provide blood flow through the cancer cells themselves, known as vasculogenic mimicry (6). To ensure sufficient nutrient supply, tumors release angiogenic factors that promote neovascularization. The coexistence of angiogenesis and VM is common in invasive tumors, and anti-angiogenic agents have been found to have little to no effect on VM (7). The VM can replace the angiogenesis role, providing tumors with oxygen and nutrients. Further, Qu et al. reported that anti-angiogenic therapy might even facilitate the formation of VM (8). As research progresses, more and more scientists are paying attention to the potential of vasculogenic mimicry (VM) in cancer treatment, and it has been found that a treatment plan using a combination of anti-angiogenic and anti-VM drugs is imperative. Currently, VM is of particular interest in the three types of cancers mentioned above. This review will focus on the research progress made regarding VM in prostate, kidney, and bladder tumors.

2 Forms of tumor angiogenesis

2.1 Angiogenesis and vasculogenesis

Angiogenesis is the process of forming new blood vessels from pre-existing ones through sprouting, which is stimulated by endothelial growth factors promoting paracrine signaling, leading to the proliferation and migration of endothelial cells, in addition to recruitment of other cell types such as smooth muscle cells (9). Angiogenesis occurs under physiological conditions, such as during embryonic development or adult wound healing. However, half a century ago, Dr. Judah Folkman proposed that pathological angiogenesis is mandatory for the growth of solid tumors (10). Cancer is characterized by the dysregulated function of angiogenesis, where the newly formed blood vessels no longer regulated by the body will promote tumor growth, metastasis, and invasion (11). The classical angiogenesis theory believes that there are two modes of tumor angiogenesis: angiogenesis based on the original blood vessel (12). The other is vasculogenesis (13). At present, more research is angiogenesis, that is, host mature vascular endothelial cells are exposed to pro-angiogenic factors in the tumor microenvironment, such as vascular endothelial growth factor (VEGF), basic fibroblast growth factor (bFGF), platelet-derived growth factor (PDGF). Under the action of these angiogenic factors and chemokines, a new collateral blood vessel of the tumor tissue is formed to provide nutrients to the tumor tissue (14). Another form of tumor angiogenesis is vasculogenesis, which refers to endothelial precursors derived from bone marrow and hematopoietic cells, called endothelial progenitor cells (EPCs) (15). And through growth factors, cytokines and hypoxia-related signaling pathways recruited to the tumor site, where they differentiate into mature endothelial cells, and under the stimulation of angiogrowth factor, division, proliferation, endothelial cells clump together to form a vascular channel to supply nutrients to tumor cells (16, 17). Targeting tumor angiogenesis has become an important target in cancer treatment, as angiogenesis plays a significant role in tumor progression. Targeted drugs such as bevacizumab, Sorafenib, and Sunitinib have been successfully used in clinical practice, advocating the success of anti-angiogenic therapy in cancer treatment (18). However, some studies have reported that these drugs have poor therapeutic effects on certain patients and could even promote tumor progression (19, 20). Therefore, some researchers speculated that new microcirculation patterns might exist for tumor blood nutrition supply.

2.2 Vessel co-option

Vessel co-option(VCO) is a phenomenon associated with tumor growth and progression, which differs from the traditional tumor angiogenic process. In tumor co-selection, tumor cells do not induce new angiogenesis, but choose to "borrow" existing blood vessels from surrounding normal tissues to supply their own nutritional and oxygen needs (6). In some cases, cells from malignant tumors move along existing vascular pathways, invading and occupying the blood vessels of normal tissue, thereby obtaining nutrients and oxygen from the blood (21). VCO causes less prominent vascular structures in morphology, making tumors more difficult to detect (22). VCO has been observed in a variety of cancers, such as liver, brain, skin, lymph node, and many others (23–25). Several studies have shown that many solid tumors can progress through vascular co-selection, and blocking co-selection and anti-angiogenic therapy can more effectively inhibit tumor growth (26–28). And the effect of inhibiting VCO can be achieved by targeting the signaling pathways related to VCO, such as targeting the Ang-2 pathway, VEGF pathway and YAP-TAZ pathway (29). Therefore, understanding tumor co-selection is essential to develop more precise treatment strategies and predict tumor growth patterns (Figure 1).

2.3 Vasculogenic mimicry

In 1999, Maniotis et al. discovered the formation of tumor blood vessels lacking endothelial cells in highly invasive melanoma tissue samples. These vessels were positive for PAS staining, but staining of endothelial cell markers (Factor VIII-related antigen and CD31) failed to stain the luminal contents of the vessels (30). Similarly, culturing highly invasive cell lines in a 3D extracellular matrix (ECM) demonstrated that tumor cells cultured *in vitro* produce patterned vascular channels and are PAS-positive, indicating its functionality as a blood vessel. This phenomenon

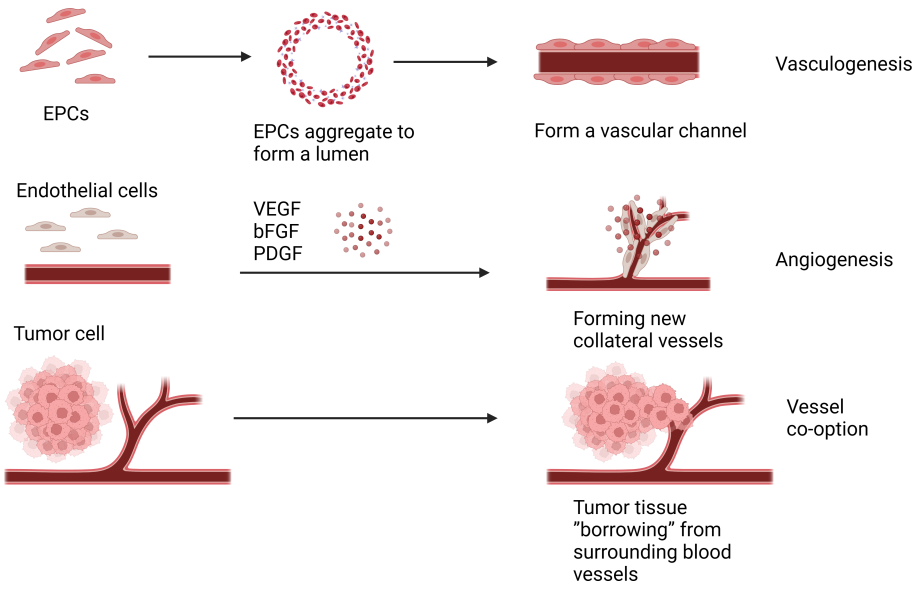

FIGURE 1
Molecular mechanisms related to VM in urological tumors. This figure summarizes the signal pathways involved in VM regulation in urological tumors. Red represents VM related signaling pathway in prostate cancer, yellow represents VM related signaling pathway in renal cell carcinoma, and the green represents VM related signaling pathway in bladder cancer.

was named VM (30). With further research, VM was also reported in other invasive tumors such as breast, ovarian and liver cancer and some urological tumors (31–35). VM is closely related to tumor growth, invasion, metastasis, and patient prognosis, and patients with VM generally had a shorter survival time and poorer prognosis (36).

Current research suggests that VM formation may be primarily related to cancer stem cells (CSCs) and epithelial-mesenchymal transition (EMT). CSCs are a subset of tumor cells with self-renewal and differentiation capabilities and are considered the main drivers of tumor growth, metastasis, and recurrence (37). Among them, the VEGF (vascular endothelial growth factor) pathway is considered the most important, promoting the generation of new blood vessels through signal transduction mediated by VEGFR. Mirshahi et al. found that CD133+/CD34+ stem cells derived from acute leukemia (AL) patients could secrete more IGF-1 and SDF-1, leading to the formation of VM in Matrigel (38). In melanoma, Lai et al. found that a population of cells with stem cell-like characteristics, marked by CD133, drove tumor growth by promoting VM formation and the morphogenesis of a specialized perivascular niche (39).

EMT is the process by which epithelial cells transform into mesenchymal cells and plays a vital role in embryonic development, inflammation, fibrosis, and cancer progression (40). It has been reported that EMT activation triggers cancer cell invasion and metastasis and contributes to VM (41). During EMT, epithelial cells lose polarity and epithelial characteristics and acquire mesenchymal cell features (13). These cells can attract endothelial cells by releasing various cytokines and signaling molecules, promoting endothelial cell migration and invasion, thereby promoting angiogenesis and expansion of the vascular network. In addition, EMT also releases some matrix-degrading enzymes, such as MMPs, which can degrade the matrix and provide more space for new blood vessels (42). On the other hand, tumor vasculature can also inversely affect the process of EMT. Newly formed tumor vessels can release various factors such as VEGF and TGF-β (transforming growth factor-β), promoting EMT of tumor cells, thereby enhancing their invasive and metastatic ability (43–45). In addition, the lack of tumor vasculature can lead to tumor cell hypoxia, thereby promoting the occurrence and progression of EMT (Figure 2).

Moreover, some studies have suggested an interaction between tumor angiogenesis and immune evasion. Vasculogenic mimicry can weaken the body's immune system's attack on tumors by forming immune escape areas on the vascular wall (46). Therefore, simultaneously inhibiting tumor vasculogenic mimicry and enhancing the immune system's ability to attack tumors may be an important therapeutic strategy in treating tumors.

3 Factors involved in urological tumor vasculogenic mimicry

3.1 Vasculogenic mimicry in prostate cancer

Prostate cancer (PCa) is one of the most common solid malignancies in the male urogenital system, second only to lung cancer in incidence, and ranked second among male malignant tumors (47). The treatment for localized PCa includes radical surgery and radiation therapy, while androgen deprivation therapy (ADT) is used for metastatic PCa. However, after 18 months, most metastatic PCa eventually progresses to ADT-resistant PCa (48). In patients with PCa, the incidence of VM is higher in those with higher Gleason scores, TNM staging, more lymph nodes, and distant metastases (32).

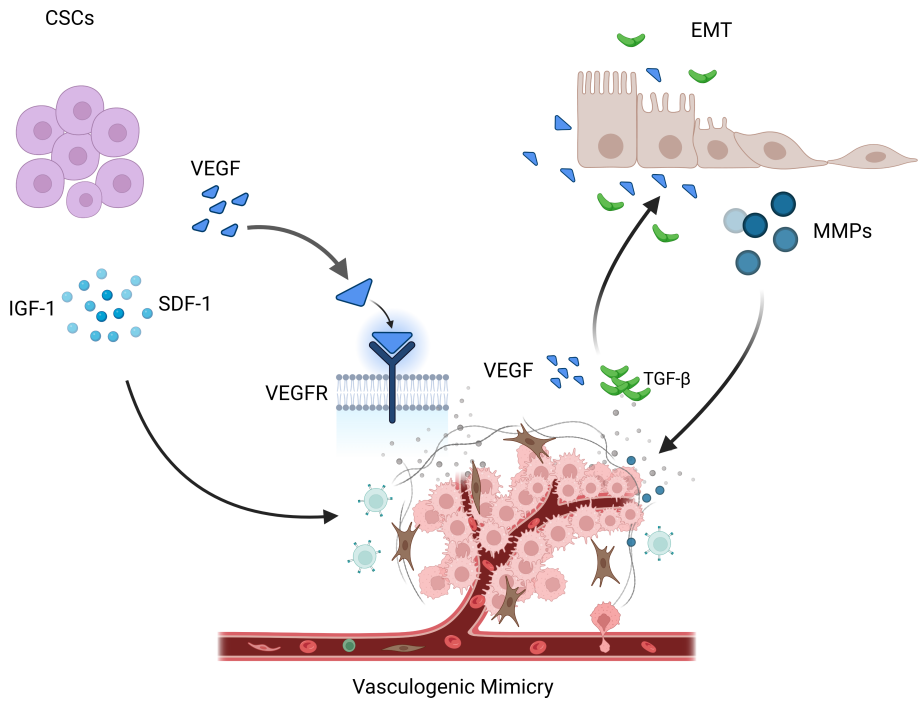

FIGURE 2
Angiogenesis is under the action of these angiogenic factors and chemokines, a new collateral blood vessel of the tumor tissue is formed to provide nutrients to the tumor tissue. Vasculogenesis is endothelial cells clump together to form a vascular channel to supply nutrients to tumor cells. Vessel co-option(VCO) is the tumor cell choose to "borrow" existing blood vessels from surrounding normal tissues to supply their own nutritional and oxygen needs.

The presence of VM in prostate cancer is associated with higher expression of certain related factors, like HIF1α, EphA2, ZEB1, and Sp1. Luo et al. found that MCT1 can stabilize HIF1α through lactylation by introducing MCT1 into PCa cells, thereby promoting the transcriptional activity of KIAA1199 (49). KIAA1199 further reduces the expression of Sema3A, increases the expression of VE-cadherin and phosphorylated EphA2, and enhances angiogenesis and vasculogenic mimicry in prostate cancer by enhancing hyaluronic acid-mediated VEGFA signaling (49). EphA2 is a receptor tyrosine kinase expressed in most epithelial cells (50). In gastric cancer cells, cancer-associated fibroblasts overexpressing EphA2 promote VM formation by activating the EphA2-PI3K pathway (51). While PI3K is a heterodimeric protein composed of a catalytic subunit (p110α/β/γ/δ) and a regulatory subunit (p85α/β) (52). Wang et al. demonstrated that higher levels of EphA2 expression and PI3K activity were associated with VM in more invasive prostate cancer cell lines PC3 and DU-145, but with no significant correlation between EphA2 and PI3K expression levels (53), Luo et al. suggested that PI3K is necessary for VM in PCa and may function by regulating the phosphorylation of EphA2 (53).

ZEB1 is a critical activator of EMT, which upregulates tumor cell plasticity and EMT to acquire cancer stem cell properties (54). In a previous study, Peng et al. found that *ZEB1* promotes EMT in lung cancer cells by activating Fak/Src signaling (55). Wang et al. found that *ZEB1* is required for VM formation *in vitro*, mediating the expression of EMT-related and CSC-related proteins in PCa cells.The study data showed that ZEB1 knockdown reduced the inhibition of Src phosphorylation at the p-Src527 site in PCa cells while reducing the formation of VMs. They further confirmed that treating PCa cells with the Src inhibitor PP2 resulted in a decrease in VM formation, while Src overexpression in stable ZEB1 knockdown cells restored VM formation (56). Where similar results were also observed in *in vivo* studies, indicating depletion of *ZEB1* protein in PC3 cells inhibited the growth of xenograft tumors in mice (56).

The transcription factor Sp1 is overexpressed in many types of cancer cells, including PCa, and is associated with various fundamental biological processes. It has been shown to play an important role in cell growth, differentiation, apoptosis, and carcinogenesis (57). Han et al. found that Sp1 controls the nuclear expression of the transcription factor twist to regulate the expression of VE-cadherin in PC3 cells. Sp1 induces the upregulation of twist/VE-cadherin, activating the AKT pathway, activated AKT enhances the expression of matrix metalloproteinases (MMPs) such as MMP-2 and -14, leading to VM formation by remodeling the extracellular matrix including LAMC2, leading to VM occurrence and development (58). Sp1, Twist, VE-cadherin, and AKT form a loop, and targeting Sp1 expression may provide a new therapeutic strategy for PCa patients with VM.

As mentioned earlier, VM formation involves proliferation, migration, and invasive changes. Therefore, the treatment for inhibiting VM can target any of these processes. Kaempferol is a natural flavonol found in many fruits and vegetables, which was reported to significantly inhibit the proliferation of AR-positive prostate cancer cell line LNCaP and promote apoptosis (59). Resveratrol (3,5,4'-trihydroxy-trans-stilbene, RES) is one of the

most well-known phytochemicals found in red wine, grapes, berries, and peanuts with potent antioxidant and anticancerous properties (60). Han et al. found that RES inhibited the VM structure formation at non-cytotoxic concentrations by inactivating EphA2 and reducing twist-mediated VE-cadherin expression when co-cultured with prostate cancer cell line PC-3 cells (61). Chrysin, also known as 5,7-dihydroxyflavone, is another natural compound with anti-tumor properties, chrysin inhibits the growth and VM formation of prostate cancer cell line PC-3 by inhibiting HIF-1α, SPHK-1, and phosphorylation of the AKT/GSK-3β signaling pathway (62).

3.2 Vasculogenic mimicry in renal cell carcinoma

Renal cell carcinoma (RCC) accounts for 3.8% of all cancers and 2.5% of all cancer deaths worldwide (63). Early-stage RCC is commonly treated with partial or radical nephrectomy, with a 5-year survival rate of 92.6%. However, about 25% of RCC patients are diagnosed at the metastatic stage and one-third of patients undergoing local tumor resection experience recurrence (64). Angiogenesis is a key aspect of pathogenesis, and anti-angiogenic drugs such as Sunitinib have been shown to significantly reduce tumor blood flow. However, most Sunitinib-treated patients eventually experience tumor progression after several months of treatment (65). More than a decade ago, Amalia A Vartanian et al. found through retrospective studies that RCC patients who tested positive for VM had a significantly lower disease-free survival rate and a significantly increased risk of recurrence (66). Therefore, VM as a novel neovascularization pathway cannot be ignored in treating RCC.

The MMP family plays a role in promoting VM progression in various cancers. Lin et al. found that MMP9 was overexpressed in RCC patient tissues, which was positively correlated with clinical stage, pathological grade, RCC metastasis, and VM formation (67). Targeted inhibition of MMP9 prevented the formation of VM in RCC cell lines 786-O and 769-P that were originally able to form VM (67). *Vimentin* (*VIM*) is a major component of the intermediate filament (IF) protein family and a hallmark of EMT (68). In RCC, *VIM* overexpression is one of the independent predictors of poor clinical outcomes (69). Many studies have also shown that *VIM* plays an important role in the formation of VM (67, 69–71). Bai et al. found that TR4 downregulates the expression of miR490-3p, which upregulates *VIM* expression, thereby promoting RCC VM formation and metastasis (72). Lin et al. further validated the role of *VIM* in promoting VM in RCC by inducing EMT through hypoxia, upregulating *VIM* and *AXL*, and downregulating E-cadherin expression to promote RCC cell VM formation (71). He et al. found Sunitinib regulates ERβ signaling to increase cancer stem cell and angiogenic mimicry formation (73), However, first-line anti-angiogenesis drugs such as Sunitinib or Bevacizumab cannot inhibit VM and may even induce VM, Ding et al. found that targeting ERβ/circDGKD by downregulating VE-cadherin reduced RCC growth and proliferation and significantly weakened the VM formation, which is envisaged to enhance the efficacy of Sunitinib providing a new combinational therapy strategy to prevent RCC progression (74).

Paired-related homeobox 1 (PRRX1) is a novel inducer of EMT, and its expression is associated with metastasis and prognosis in multiple tumors (75, 76). Protein phosphatase 2A (PP2A) is an effective tumor suppressor that acts on various oncogenic transcription factors (77). CIP2A is an important oncogene that inhibits the activity of PP2A, thereby maintaining the malignant phenotype of tumor cells and playing an important role in the occurrence, development, and biological behavior of tumor cells (78). Both PRRX1 and CIP2A are major inducers of EMT. Wang et al. investigated the roles of PRRX1, CIP2A, and VM in RCC and found that PRRX1 expression was negatively correlated with VM and CIP2A, whereas CIP2A expression was positively correlated with VM development. Low PRRX1 expression combined with high VM and CIP2A was associated with poor prognosis and metastasis in RCC (79). However, Wang et al. only observed this correlation in RCC patient specimens and did not perform animal or cell line investigations to explore the underlying mechanisms. Further research is needed to clarify the mechanisms involved.

Androgen receptor (AR) has an oncogenic function in RCC, promoting progression and hematogenous metastasis (80). You et al. showed that a long non-coding RNA, lncRNA-TANAR, regulated by AR transcription, increased the stability of TWIST1 mRNA by directly binding to its 5′UTR, disrupting UPF1-mediated nonsense-mediated TWIST1 mRNA decay, thereby leading to a decrease in VM formation (81).

Tumor-associated macrophages (TAMs) play a crucial role in reshaping the tumor microenvironment (TME) to promote tumor development (82). Numerous studies have shown that TAMs can promote tumor cell proliferation, invasion, and migration (83, 84). Polarized macrophages commonly exist as either M1 or M2 macrophages. Unlike M1 macrophages, which have pro-inflammatory and immune-stimulatory effects, M2 polarized macrophages are similar to TAMs and have pro-tumor functions (85). It has been found that macrophages can affect cancer progression through miRNAs carried by extracellular vesicles (86). Liu et al. evaluated ten VM-related genes in RCC cells co-cultured with or without TAMs using protein imprinting and found that TIMP2, which was restrained by TAMs, might be a key VM regulatory factor in RCC (87). Subsequently, through bioinformatics analysis and experimental validation, Liu et al. found that miR-193a-5p derived from macrophage-derived extracellular vesicles targeted TIMP2 in RCC cells, enhancing VM and cell invasion capability (87).

Metabolic reprogramming is a hallmark of cancer and is critical in tumor progression. Accumulation of the tumor metabolite L-2-hydroxyglutarate (L-2HG) occurs in cancer due to hypoxia (88), which is also an important factor in VM formation. Wang et al. found that tumors with high levels of L-2HG exhibited more VM structures than tumors with low levels of L-2HG. They also compared RNA sequencing analysis of RCC cell lines with and without L-2HG treatment and found that PHLDB2 was downregulated by L-2H (89). PHLDB2 (also known as LL5β) is a protein containing a PH domain that plays an important role in mediating cell migration by forming complexes with partners such

as CLASPs and Prickle 1 (90). Wang et al. found that inhibiting PHLDB2 reduced VM formation while restoring PHLDB2 expression levels reversed this phenomenon. They also found that decreasing PHLDB2 expression increased ERK1/2 phosphorylation, but there was no statistically significant difference in ERK1/2 phosphorylation due to limited replicates. However, the trend of changes in ERK1/2 phosphorylation was consistent in each group (89). Therefore, the L-2HG/PHLDB2 pathway may be a potential signaling pathway for treating VM in RCC.

3.3 Vasculogenic mimicry in bladder cancer

It is estimated that there are reported 500,000 new cases and 200,000 deaths from bladder cancer (BCa) globally. Over 80,000 new cases are reported in the United States alone, with 17,000 deaths from BCa annually (91). Despite various treatments such as surgery, bladder infusion, and immunotherapy being used in clinical practice, the rate of tumor progression within 5 years is still very high (92). In particular, the treatment options for advanced BCa are minimal (93). Early on, Fujimoto et al. found that ECV304, derived initially from BCa epithelial cells and now known as the T24/83 BCa epithelial cell line, can connect with blood vessels around the normal endothelial source, forming tumor tissues with vascular characteristics and is typically found in highly invasive tumors with poor prognosis (94).

A protein TG2, which has been demonstrated to be associated with endothelial cell-derived angiogenesis (95), can be overexpressed under pathological and stress conditions, leading to increased cell surface externalization and deposition into the extracellular matrix (ECM), thereby exerting crosslinking effects with various ECM proteins such as fibronectin and laminin, etc. (96). Moreover, previous studies have suggested that exogenous TG2 added to a rat dorsal skin flap wound healing model can enhance angiogenesis (97). Jones et al. found that TG2 was not detected in normal human fibroblast C378, while there was an abundant expression of TG2 in ECV304 cells. Targeted inhibition of TG2 expression in ECV304 cells could block cell migration, thereby preventing the formation of the actin cytoskeleton and focal adhesion (98).

MicroRNAs (miRNAs) are evolutionarily conserved small non-coding RNAs that function as endogenous regulators of gene expression (99). Dysregulation of certain miRNAs has been associated with numerous tumorigenic changes, including growth, apoptosis, metastasis, and tumor angiogenesis (100). It has been reported that miR-124 inhibits the malignant potential, proliferation, and invasiveness of malignant tumor cells by targeting multiple proteins (101–103). Studies have shown that *UHRF1* is an oncogene promoting cancer cell development (104). In different types of cancers, the expression of *UHRF1* incurs many changes getting out of control. The expression or activity of this protein is often modified, leading to transformation and increased proliferation, motility, and invasiveness, as well as providing tumor cells with resistance to chemotherapy (105). Wang et al. found that miR-124 and *UHRF1* are negatively correlated in BCa tissue, where miR-124 inhibited BCa invasiveness by reducing *UHRF1* expression (106).

Many studies have proposed that EMT is crucial for VM formation and tumor progression, with *ZEB1* as an essential EMT inducer that is elevated in colorectal cancer specimens showing EMT features both *in vivo* and *in vitro* (107). Li et al. found that *ZEB1* is also highly expressed in BCa, and to further elucidate the relationship between VM and *ZEB1* in BCa, they performed 3D culture assays after transfection with specific siRNA to reduce *ZEB1* expression in bladder transitional cell carcinoma cell lines. Moreover, after *ZEB1* restoration, VM formation was inhibited in UM-UC-3 and J82 cell lines (35). However, Li et al. did not observe changes in EMT markers after suppressing *ZEB1* expression in BCa, suggesting that *ZEB1* is an intermediate step in BCa VM formation, regulated or influenced by some unknown upstream molecules and downstream genes, and it may not have a direct relationship with epithelial phenotype (35).

It is well known that the tumor microenvironment exists in a hypoxic state (108). In the hypoxic microenvironment, tumor cells form new blood vessels to obtain the oxygen and nutrients they need to support their continued proliferation. Numerous studies have shown that hypoxia is closely related to the development of VM. For example, in the melanoma mouse model, mice in the ischemic model group were found to exhibit higher VMs compared to the control group, which was positively correlated with HIF-1α and HIF-2α expression, indicating that hypoxia promoted VM (109). Liu et al. developed and validated a novel hypoxia risk score that can predict clinical outcomes and TME characteristics of BLCA, and for patients in the high-risk score group, they may benefit from immunotherapy, chemotherapy, and radiotherapy, and patients in the low-risk score group may benefit from targeted therapy with VM-associated signaling pathways (WNT-β-catenin network, PPARG network, and FGFR3 network), contributing to the development of BCa precision medicine (108).

In recent years, there has been increasing evidence that the status and formation of angiogenic mimetics (VMs) in the tumor microenvironment is regulated by various factors, especially the immune factors present in the tumor microenvironment (110). BCATRANSFERASE 2 (BCAT2) is a core enzyme in sulfur amino acid metabolism (111). Cai et al. found that BCAT2 has the effect of modulating TME immune status, and patients with high BCAT2 expression may have better efficacy in anti-VM therapy (112). Siglec15, a member of the sialic acid-bound immunoglobulin-like lectin family, is an emerging broad-spectrum target for normalizing cancer immunotherapy (113). Jiao et al. found that BCa patients in the high Siglec15 group were more sensitive to targeting vascular mimicry-related signaling pathways (β-catenin, PPAR-γ, and FGFR3 pathways) (114, 115). Therefore, Siglec15 may be used as an indicator of targeted therapy for VM.

In BCa, DNA methylation plays a key role in early diagnosis, predicting prognosis, predicting therapeutic opportunities, and serving as a potential therapeutic target (116), 5-Methylcytosine (5mC) in DNA is the most important epigenetic modification that shapes TME by influencing genomic stability, determining cancer cell differentiation status, and selecting cell identity (117, 118). Jiao et al. found that the high 5 mC score group may not be

sensitive to neoadjuvant chemotherapy, but there are several immunosuppressive oncogenic pathways significantly enriched in the heterogeneous high 5 mC score group associated with VM, including WNT-β-catenin network, FGFR3 network, and VEGFA (114, 119–121). These VM pathways may provide promising therapeutic opportunities for BLCA patients in the high 5mC scoring group.

The utilization of glucose in tumor cells significantly increases, producing a large number of intermediate metabolites through glycolysis to meet the needs of tumor cell proliferation. Increasing evidence indicated that accumulated lactate, as the final product of glycolysis, is a key regulatory factor in tumor development, immune escape, metastasis, and angiogenesis (122, 123). Hepatitis B X-interacting protein (HBXIP), also known as LAMTOR5, is a conserved protein that is often expressed in various tissues in mammals (124). HBXIP is highly expressed in several types of cancers and is associated with a series of clinical pathological features and poor prognosis (125). Overexpression of HBXIP in BCa tissues is related to clinical staging, lymph node metastasis, tumor recurrence, and patient survival. In addition, silencing HBXIP reduces the proliferation, migration, and invasion of BCa cells *in vitro* and tumor formation *in vivo* (126). Moreover, the high expression of HBXIP in high-grade tissues suggests that HBXIP may be an important indicator for judging the prognosis of BCa patients. Some studies have shown that the PI3K/AKT/mTOR pathway is a central signaling pathway that coordinates aerobic glycolysis and cell biosynthesis in malignant tumor cells (127). Liu et al. provided evidence that HBXIP as an oncogene regulates glycolysis of BC cells through the AKT/mTOR pathway, thereby promoting VM in BCa cells (128). They found that reducing HBXIP in BCa cells affected the migration and angiogenesis of HUVECs and decreased the expression of VEGF and EPO. Both glucose and lactate stimulation reversed the cell viability, migration, and tubular formation of HUVECs co-cultured with HBXIP-silenced BCa cells. Glucose stimulation demonstrated that HBXIP further promotes glycolysis by regulating glucose uptake by tumor cells, while lactate stimulation demonstrated that glycolysis further promotes VM, suggesting HBXIP plays a key role in VM (Figure 3) (128) (Table 1).

4 Potential targeted drugs for vasculogenic mimicry

4.1 Targeting VEGF and VEGFR

It is now widely believed that VM plays a crucial role in tumor growth, proliferation, and metastasis formation. VEGF is one of the important promoting factors for VM, and the VEGF and its receptor are one of the main inducers of tumor angiogenesis (129). Inhibitors targeting the VEGF/VEGFR system have been used clinically. Clinical trials using VEGF molecules can induce moderate improvement in overall survival, measured in weeks to just a few months, and tumors respond differently to these drugs (130). Antibodies targeting VEGF, such as Bevacizumab, can effectively inhibit tumor angiogenesis and growth and have been widely used to treat various cancers (130). In addition to directly inhibiting VEGF, tumor angiogenesis can also be inhibited by hindering the activity of VEGF receptors. Sorafenib and Sunitinib are tyrosine kinase inhibitors that block VEGFR-2, which are currently approved for treating cancers such as hepatocellular

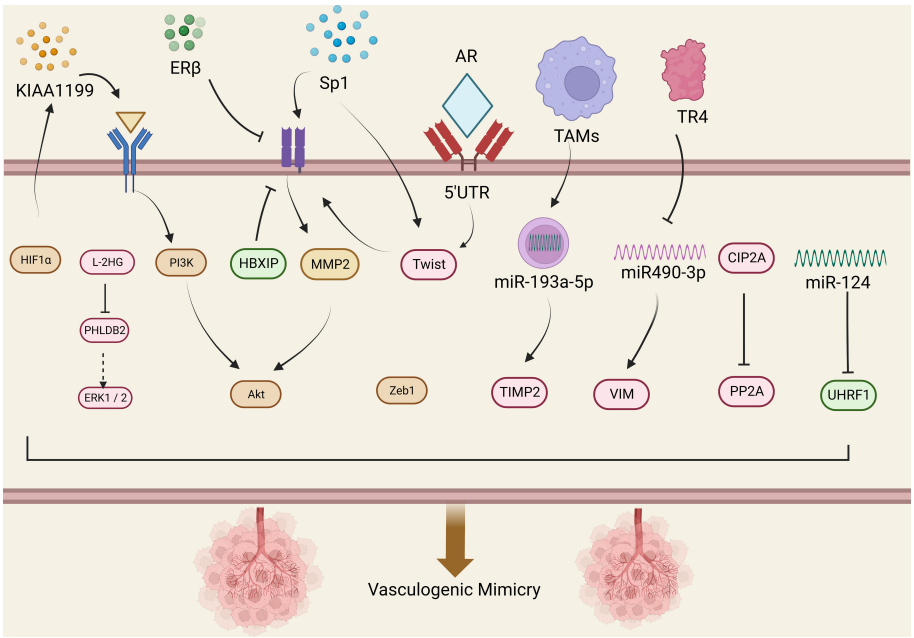

FIGURE 3
VM is regulated by various mechanisms. CSCs promote the occurrence of VM phenomenon by releasing IGF-1, SDF-1, and VEGF. During EMT, some matrix degrading enzymes are released, such as MMPs, which can promote the occurrence of the VM phenomenon. At the same time, new tumor blood vessels release various factors, such as VEGF and TGF- β, thereby promoting the occurrence and progress of EMT.

TABLE 1 Genes and their functions related to vascular mimicry in urological tumors.

Cancer Type	Factors	Signaling pathway	Function	Ref.
Prostate cancer	KIAA1199	EphA2-PI3K pathway	reduces the expression of Sema3A, increases the expression of VE-cadherin and phosphorylated EphA2	(49)
	ZEB1	Fak-Src pathway	a critical activator of EMT, upregulates tumor cell plasticity and EMT to acquire cancer stem cell properties	(55, 56)
	Sp1	Twist-VE-cadherin pathway	induces the upregulation of twist/VE-cadherin	(58)
Renal cell carcinoma	TR4	miR490-3p/vimentin signals pathway	downregulates the expression of miR490-3p	(72)
	VE-cadherin	ERβ/circDGKD pathway	reduced RCC growth and proliferation and significantly weakened the VM formation	(74)
	PRRX1		a novel inducer of EMT	(76)
	PP2A		an effective tumor suppressor that acts on various oncogenic transcription factors	(77)
	CIP2A		inhibits the activity of PP2A	(78)
	AR		increased the stability of TWIST1 mRNA by directly binding to its 5′UTR	(81)
	L-2HG	L-2HG/PHLDB2 pathway	downregulated PHLDB2	(89)
	PHLDB2	L-2HG/PHLDB2 pathway	mediating cell migration	(89)
Bladder cancer	TG2		increased cell surface externalization and deposition into the extracellular matrix (ECM)	(96)
	miR-124		miR-124 inhibited BCa invasiveness by reducing *UHRF1* expression	(106)
	BCAT2		the effect of modulating TME immune status	(112)
	Siglec15	β-catenin, PPAR-γ, FGFR3 pathways	an emerging broad-spectrum target for normalizing cancer	(113)
	HBXIP	PI3K/AKT/mTOR pathway	promotes glycolysis by regulating glucose uptake by tumor cells	(128)

carcinoma, neuroendocrine pancreatic tumors, and metastatic renal cell carcinoma (130, 131). However, tumor cells are prone to develop resistance to these drugs, resulting in poor clinical efficacy (132).

Studies have shown that when VEGF is blocked, other angiogenic factors modulate sensitivity against VEGF therapy and allow regeneration of the tumor-associated vasculature (133). A phase III trial by Rini et al. on bevacizumab plus interferon α in patients with metastatic renal cell carcinoma showed that bevacizumab blocked the VEGF pathway and that patients with bevacizumab plus IFN-α had significantly improved PFS and OS compared with IFN-α alone (134). Although the data emphasize the importance of VEGF signaling, there are many intracellular pathways in tumorigenesis VM, and inhibitors targeting individual signaling pathways have limited inhibitory effect on VMs because other signaling pathways immediately compensate and eventually resume the process of switching to the VM phenotype (135). Therefore, exploring multi-target combination therapies to limit VM-mediated tumor resistance is expected to maximize anti-tumor efficacy in the future.

4.2 Targeting extracellular matrix

An extracellular matrix (ECM) is a complex extracellular biological macromolecular network involved in angiogenesis. Drugs targeting ECM can inhibit angiogenesis by interfering with the biological functions of ECM. MMPs is particularly important in ECM degradation. Under hypoxic conditions, high expression of MMP-9 molecules increases tumor invasiveness and promotes VM (136). Therefore, MMP inhibitors can inhibit MMP activity, thus blocking ECM degradation and remodeling and reducing VM. In addition, ECM is an important structure for cell adhesion, and inhibiting the binding of ECM to cells can inhibit the proliferation and migration of endothelial cells. For example, using RGD peptide sequences can block the binding of ECM to cells, thereby inhibiting VM (137).

4.3 Targeting PI3K/Akt/mTOR

The PI3K/Akt/mTOR signaling pathway is a crucial pathway in regulating cell proliferation, survival, and metabolism and is considered an important regulatory mechanism for tumor angiogenesis and development (138). Drugs targeting this pathway, such as Rapamycin, have been extensively studied to inhibit tumor angiogenesis and growth, thereby suppressing tumor progression and metastasis (139). Huang et al. found that under normal oxygen or hypoxic conditions, with the increase of rapamycin concentration, the duct-forming structure of glioma cell line U87-MG in stromal gum decreased, demonstrating that inhibition of mTOR can eliminate glioma VM formation (139).

Therefore, Huang et al. deduced that the mTOR signaling pathway is related to VM formation and that mTOR is an upstream molecule of HIF-1α. In the final stage of the VM signaling pathway, express and activate MMP-14 to activate MMP-2. MMP-2 combined with MMP-14 cuts Ln-5-γ2 chains into migration fragments. The release of fragments of these into the tumor microenvironment can increase the migration of tumor cells, invasion, and eventually lead to VM (139). It is worth mentioning that since PI3K/Akt/mTOR signaling pathway also plays an important physiological role in normal cells, these drugs lack selective activity on cancerous cells and thus may adversely affect the normal cells (140). The results of a recent study have shown a delicate balance between the growth-promoting activity of AKT and the growth-promoting activity of p53, which is essential for preventing cellular aging and cancer (141). PI3K/AKT/mTOR inhibition also has associated clinical adverse effects, including hyperglycemia, hyperlipidemia, myelosuppression, and severe hepatotoxicity (142). Further research and optimization of targeted therapy for the PI3K/Akt/mTOR signaling pathway are imperative to improve treatment efficacy and reduce the incidence of adverse reactions.

4.4 Targeting perivascular cells

The tumor microenvironment contains a series of non-cancer cells around the tumor, such as fibroblasts, macrophages, and endothelial cells, as well as some ECM and molecular signaling substances. These non-cancerous cells and molecules play an important role in tumorigenesis, growth, invasion, metastasis, and tumor angiogenesis (143). In tumor angiogenesis, tumor cells release some promoting factors, such as VEGF, PDGF, etc., to stimulate tumor cells to generate VM. At the same time, tumor cells induce surrounding fibroblasts and macrophages to transform into tumor-related cell types, releasing various factors that promote tumor growth and invasion (144). Therefore, targeting non-cancer cells and molecules in the tumor microenvironment has become a strategy for treating tumor angiogenesis. Among them, drugs targeting fibroblasts and macrophages, such as Imatinib and Dasatinib.Studies have shown that dasatinib can effectively inhibit the growth of fibroblasts by inhibiting PDGF receptor signaling at biologically relevant concentrations (145, 146). PDGF is normally expressed in a variety of cell types, including fibroblasts, neuronal cells, macrophages, smooth muscle cells, platelets, and preosteoclastic cells. They typically use autocrine or paracrine mechanisms to perform their biological functions, and Imatinib can target inhibition of PDGFR (147), can inhibit the proliferation and function of these cells, thereby reducing their promotion of VM (148). In addition, drugs targeting endothelial cells, such as Bevacizumab and Ramucirumab, can inhibit the migration and proliferation of endothelial cells(EC), thereby reducing tumor vascular density and tumor growth rate (149). Bevacizumab is the first humanized anti-VEGF neutralizing antibody approved by the FDA for the treatment of metastatic colon cancer (150), Bevacizumab treatment blocked extracellular VEGF-induced apoptosis, inhibiting EC proliferation (149). In short, targeting non-cancer cells and molecules in the tumor microenvironment can effectively inhibit tumor angiogenesis and growth, a potential tumor treatment strategy (Table 2).

5 Conclusion and future directions

The review on VM in urinary tumors provides in-depth new ideas and solutions for treating urinary tumors. Tumor growth and metastasis can be slowed down by targeted inhibition of tumor VM, and VM inhibitors can also be used in combination with other therapeutic methods to increase anti-cancer effects.

However, the current study faces some challenges. First, different VM targeted inhibitors may have different efficacy for different urinary tumors. Secondly, the dose and timing of VM inhibitors in clinical application and the combination regimen and sequence of combination therapy strategies require further research.

With the in-depth study of tumor VM, the efficacy and safety of treatments targeting to inhibit VM will continue to improve.

TABLE 2 Potential drugs that inhibit vascular mimicry and their targets inhibition.

Agents	Target	Tumor type	Cell/animal	Ref.
Kaempferol	AR	Prostate cancer	HEK293/PC3/LNCaP	(59)
RES	EphA2/VE-cadherin	Prostate cancer	PC3	(61)
Chrysin	SPHK/HIF-1α	Prostate cancer	PC3	(62)
Sorafenib	VEGFR-2	Metastatic RCC	Human	(131)
Sunitinib	VEGFR-2	Metastatic RCC	Human	(151)
Bevacizumab	VEGF	Metastatic RCC	Human	(134, 152)
MMP inhibitor	ECM	Oral squamous cell carcinoma	UMSCC1	(136)
RGD peptide	ECM	–	Mice	(137)
Rapamycin	PI3K/Akt/mTOR	Gliomas	Human	(139)
Imatinib	PDGFR	Ovarian cancer	Human	(147)
Dasatinib	PDGF	ccRCC	Human	(146, 153)

Combinational use of VM targeted inhibitors with other antitumor methods is envisaged to improve the therapeutic effect further and reduce the side effects. Therefore, we can expect targeted therapy for tumor VM to play an increasingly important role in the future.

Author contributions

XL: validation, writing, formal analysis and visualization. SL and CY reviewed the manuscript and polished the grammar. SH, SL, XZ and GZ: searched related publications. GW and JZ: supervision. All authors contributed to the article and approved the submitted version.

Funding

This project was supported by the Graduate Innovation Special Fund Project of Gannan Medical University (YC2022-S955).

Acknowledgments

We thank Home for Researchers editorial team (www.home-for-researchers.com) for language editing service.

Conflict of interest

The authors declare that the research was conducted in the absence of any commercial or financial relationships that could be construed as a potential conflict of interest.

Publisher's note

References

1. Siegel RL, Miller KD, Fuchs HE, Jemal A. Cancer statistics, 2022. *CA: Cancer J Clin* (2022) 72:7–33. doi: 10.3322/caac.21708

2. Janic B, Arbab AS. The role and therapeutic potential of endothelial progenitor cells in tumor neovascularization. *TheScientificWorldJournal* (2010) 10:1088–99. doi: 10.1100/tsw.2010.100

3. Hillen F, Griffioen AW. Tumour vascularization: sprouting angiogenesis and beyond. *Cancer metastasis Rev* (2007) 26:489–502. doi: 10.1007/s10555-007-9094-7

4. Folkman J. Tumor angiogenesis: therapeutic implications. *New Engl J Med* (1971) 285:1182–6. doi: 10.1056/nejm197111182852108

5. Pezzella F, Ribatti D. Vascular co-option and vasculogenic mimicry mediate resistance to antiangiogenic strategies. *Cancer Rep (Hoboken N.J.)* (2022) 5:e1318. doi: 10.1002/cnr2.1318

6. Donnem T, Reynolds AR, Kuczynski EA, Gatter K, Vermeulen PB, Kerbel RS, et al. Non-angiogenic tumours and their influence on cancer biology. *Nat Rev Cancer* (2018) 18:323–36. doi: 10.1038/nrc.2018.14

7. van der Schaft DW, Seftor RE, Seftor EA, Hess AR, Gruman LM, Kirschmann DA, et al. Effects of angiogenesis inhibitors on vascular network formation by human endothelial and melanoma cells. *J Natl Cancer Institute* (2004) 96:1473–7. doi: 10.1093/jnci/djh267

8. Qu B, Guo L, Ma J, Lv Y. Antiangiogenesis therapy might have the unintended effect of promoting tumor metastasis by increasing an alternative circulatory system. *Med Hypotheses* (2010) 74:360–1. doi: 10.1016/j.mehy.2009.08.020

9. Aldebasi YH, Rahmani AH, Khan AA, Aly SM. The effect of vascular endothelial growth factor in the progression of bladder cancer and diabetic retinopathy. *Int J Clin Exp Med* (2013) 6:239–51.

10. Folkman J, Merler E, Abernathy C, Williams G. Isolation of a tumor factor responsible for angiogenesis. *J Exp Med* (1971) 133:275–88. doi: 10.1084/jem.133.2.275

11. Bernardini S, Fauconnet S, Chabannes E, Henry PC, Adessi G, Bittard H. Serum levels of vascular endothelial growth factor as a prognostic factor in bladder cancer. *J Urol* (2001) 166:1275–9. doi: 10.1016/S0022-5347(05)65752-7

12. Yang J, Weinberg RA. Epithelial-mesenchymal transition: at the crossroads of development and tumor metastasis. *Dev Cell* (2008) 14:818–29. doi: 10.1016/j.devcel.2008.05.009

13. Hugo H, Ackland ML, Blick T, Lawrence MG, Clements JA, Williams ED, et al. Epithelial–mesenchymal and mesenchymal–epithelial transitions in carcinoma progression. *J Cell Physiol* (2007) 213:374–83. doi: 10.1002/jcp.21223

14. Lugano R, Ramachandran M, Dimberg A. Tumor angiogenesis: causes, consequences, challenges and opportunities. *Cell Mol Life Sci CMLS* (2020) 77:1745–70. doi: 10.1007/s00018-019-03351-7

15. Chopra H, Hung MK, Kwong DL, Zhang CF, Pow EHN. Insights into endothelial progenitor cells: origin, classification, potentials, and prospects. *Stem Cells Int* (2018) 2018:9847015. doi: 10.1155/2018/9847015

16. Asahara T, Murohara T, Sullivan A, Silver M, van der Zee R, Li T, et al. Isolation of putative progenitor endothelial cells for angiogenesis. *Sci (New York N.Y.)* (1997) 275:964–7. doi: 10.1126/science.275.5302.964

17. Reale A, Melaccio A, Lamanuzzi A, Saltarella I, Dammacco F, Vacca A, et al. Functional and biological role of endothelial precursor cells in tumour progression: A new potential therapeutic target in haematological malignancies. *Stem Cells Int* (2016) 2016:7954580. doi: 10.1155/2016/7954580

18. Li T, Kang G, Wang T, Huang H. Tumor angiogenesis and anti-angiogenic gene therapy for cancer. *Oncol Lett* (2018) 16:687–702. doi: 10.3892/ol.2018.8733

19. Carbone C, Moccia T, Zhu C, Paradiso G, Budillon A, Chiao PJ, et al. Anti-VEGF treatment-resistant pancreatic cancers secrete proinflammatory factors that contribute to Malignant progression by inducing an EMT cell phenotype. *Clin Cancer Res* (2011) 17:5822–32. doi: 10.1158/1078-0432.Ccr-11-1185

20. Pàez-Ribes M, Allen E, Hudock J, Takeda T, Okuyama H, Viñals F, et al. Antiangiogenic therapy elicits Malignant progression of tumors to increased local invasion and distant metastasis. *Cancer Cell* (2009) 15:220–31. doi: 10.1016/j.ccr.2009.01.027

21. Kuczynski EA, Vermeulen PB, Pezzella F, Kerbel RS, Reynolds AR. Vessel co-option in cancer. *Nat Rev Clin Oncol* (2019) 16:469–93. doi: 10.1038/s41571-019-0181-9

22. Pezzella F, Pastorino U, Tagliabue E, Andreola S, Sozzi G, Gasparini G, et al. Non-small-cell lung carcinoma tumor growth without morphological evidence of neo-angiogenesis. *Am J Pathol* (1997) 151:1417–23.

23. Valiente M, Obenauf AC, Jin X, Chen Q, Zhang XH, Lee DJ, et al. Serpins promote cancer cell survival and vascular co-option in brain metastasis. *Cell* (2014) 156:1002–16. doi: 10.1016/j.cell.2014.01.040

24. Mandelcorn ED, Palestine AG, Dubovy S, Davis JL. Vascular co-option in lung cancer metastatic to the eye after treatment with bevacizumab. *J ophthalmic Inflammation infection* (2010) 1:35–8. doi: 10.1007/s12348-010-0013-7

25. Kuczynski EA, Yin M, Bar-Zion A, Lee CR, Butz H, Man S, et al. Co-option of liver vessels and not sprouting angiogenesis drives acquired sorafenib resistance in hepatocellular carcinoma. *J Natl Cancer Institute* (2016) 108. doi: 10.1093/jnci/djw030

26. Ribatti D, Pezzella F. Vascular co-option and other alternative modalities of growth of tumor vasculature in glioblastoma. *Front Oncol* (2022) 12:874554. doi: 10.3389/fonc.2022.874554

27. Billaud M, Santoro M. Is Co-option a prevailing mechanism during cancer progression? *Cancer Res* (2011) 71:6572–5. doi: 10.1158/0008-5472.Can-11-2158

28. Frentzas S, Simoneau E, Bridgeman VL, Vermeulen PB, Foo S, Kostaras E, et al. Vessel co-option mediates resistance to anti-angiogenic therapy in liver metastases. *Nat Med* (2016) 22:1294–302. doi: 10.1038/nm.4197

29. Cuypers A, Truong AK, Becker LM, Saavedra-García P, Carmeliet P. Tumor vessel co-option: The past & the future. *Front Oncol* (2022) 12:965277. doi: 10.3389/fonc.2022.965277

30. Maniotis AJ, Folberg R, Hess A, Seftor EA, Gardner LM, Pe'er J, et al. Vascular channel formation by human melanoma cells in *vivo* and in *vitro*: vasculogenic mimicry. *Am J Pathol* (1999) 155:739–52. doi: 10.1016/s0002-9440(10)65173-5

31. Lim D, Do Y, Kwon BS, Chang W, Lee MS, Kim J, et al. Angiogenesis and vasculogenic mimicry as therapeutic targets in ovarian cancer. *BMB Rep* (2020) 53:291–8. doi: 10.5483/BMBRep.2020.53.6.060

32. Liu R, Yang K, Meng C, Zhang Z, Xu Y. Vasculogenic mimicry is a marker of poor prognosis in prostate cancer. *Cancer Biol Ther* (2012) 13:527–33. doi: 10.4161/cbt.19602

33. Morales-Guadarrama G, García-Becerra R, Méndez-Pérez EA, García-Quiroz J, Avila E, Díaz L. Vasculogenic mimicry in breast cancer: clinical relevance and drivers. *Cells* (2021) 10. doi: 10.3390/cells10071758

34. Zheng N, Zhang S, Wu W, Zhang N, Wang J. Regulatory mechanisms and therapeutic targeting of vasculogenic mimicry in hepatocellular carcinoma. *Pharmacol Res* (2021) 166:105507. doi: 10.1016/j.phrs.2021.105507

35. Li B, Mao X, Wang H, Su G, Mo C, Cao K, et al. Vasculogenic mimicry in bladder cancer and its association with the aberrant expression of ZEB1. *Oncol Lett* (2018) 15:5193–200. doi: 10.3892/ol.2018.7975

36. Cao Z, Bao M, Miele L, Sarkar FH, Wang Z, Zhou Q. Tumour vasculogenic mimicry is associated with poor prognosis of human cancer patients: a systemic review and meta-analysis. *Eur J Cancer (Oxford Engl 1990)* (2013) 49:3914–23. doi: 10.1016/j.ejca.2013.07.148

37. Nassar D, Blanpain C. Cancer stem cells: basic concepts and therapeutic implications. *Annu Rev Pathol* (2016) 11:47–76. doi: 10.1146/annurev-pathol-012615-044438

38. Mirshahi P, Rafii A, Vincent L, Berthaut A, Varin R, Kalantar G, et al. Vasculogenic mimicry of acute leukemic bone marrow stromal cells. *Leukemia* (2009) 23:1039–48. doi: 10.1038/leu.2009.10

39. Lai CY, Schwartz BE, Hsu MY. CD133+ melanoma subpopulations contribute to perivascular niche morphogenesis and tumorigenicity through vasculogenic mimicry. *Cancer Res* (2012) 72:5111–8. doi: 10.1158/0008-5472.Can-12-0624

40. Chen T, You Y, Jiang H, Wang ZZ. Epithelial-mesenchymal transition (EMT): A biological process in the development, stem cell differentiation, and tumorigenesis. *J Cell Physiol* (2017) 232:3261–72. doi: 10.1002/jcp.25797

41. Fan YL, Zheng M, Tang YL, Liang XH. A new perspective of vasculogenic mimicry: EMT and cancer stem cells (Review). *Oncol Lett* (2013) 6:1174–80. doi: 10.3892/ol.2013.1555

42. Scheau C, Badarau IA, Costache R, Caruntu C, Mihai GL, Didilescu AC, et al. The role of matrix metalloproteinases in the epithelial-mesenchymal transition of hepatocellular carcinoma. *Analytical Cell Pathol (Amsterdam)* (2019) 2019:9423907. doi: 10.1155/2019/9423907

43. Chen L, Lin G, Chen K, Liang R, Wan F, Zhang C, et al. VEGF promotes migration and invasion by regulating EMT and MMPs in nasopharyngeal carcinoma. *J Cancer* (2020) 11:7291–301. doi: 10.7150/jca.46429

44. Bowman T, Broome MA, Sinibaldi D, Wharton W, Pledger WJ, Sedivy JM, et al. Stat3-mediated Myc expression is required for Src transformation and PDGF-induced mitogenesis. *Proc Natl Acad Sci United States America* (2001) 98:7319–24. doi: 10.1073/pnas.131568898

45. Butler JM, Kobayashi H, Rafii S. Instructive role of the vascular niche in promoting tumour growth and tissue repair by angiocrine factors. *Nat Rev Cancer* (2010) 10:138–46. doi: 10.1038/nrc2791

46. Reiman JM, Knutson KL, Radisky DC. Immune promotion of epithelial-mesenchymal transition and generation of breast cancer stem cells. *Cancer Res* (2010) 70:3005–8. doi: 10.1158/0008-5472.Can-09-4041

47. Wang H, Huang B, Li BM, Cao KY, Mo CQ, Jiang SJ. Erratum: Global cancer statistics 2018: GLOBOCAN estimates of incidence and mortality worldwide for 36 cancers in 185 countries. *CA: Cancer J Clin* (2020) 70:313. doi: 10.3322/caac.21609

48. Chang AJ, Autio KA, Roach M. 3rd; Scher, H.I. High-risk prostate cancer-classification and therapy. *Nat Rev Clin Oncol* (2014) 11:308–23. doi: 10.1038/nrclinonc.2014.68

49. Luo Y, Yang Z, Yu Y, Zhang P. HIF1α lactylation enhances KIAA1199 transcription to promote angiogenesis and vasculogenic mimicry in prostate cancer. *Int J Biol macromolecules* (2022) 222:2225–43. doi: 10.1016/j.ijbiomac.2022.10.014

50. Lindberg RA, Hunter T. cDNA cloning and characterization of eck, an epithelial cell receptor protein-tyrosine kinase in the eph/elk family of protein kinases. *Mol Cell Biol* (1990) 10:6316–24. doi: 10.1128/mcb.10.12.6316-6324.1990

51. Kim HS, Won YJ, Shim JH, Kim HJ, Kim BS, Hong HN. Role of EphA2-PI3K signaling in vasculogenic mimicry induced by cancer-associated fibroblasts in gastric cancer cells. *Oncol Lett* (2019) 18:3031–8. doi: 10.3892/ol.2019.10677

52. Shukla S, Maclennan GT, Hartman DJ, Fu P, Resnick MI, Gupta S. Activation of PI3K-Akt signaling pathway promotes prostate cancer cell invasion. *Int J Cancer* (2007) 121:1424–32. doi: 10.1002/ijc.22862

53. Wang H, Lin H, Pan J, Mo C, Zhang F, Huang B, et al. Vasculogenic mimicry in prostate cancer: the roles of ephA2 and PI3K. *J Cancer* (2016) 7:1114–24. doi: 10.7150/jca.14120

54. Zhang P, Sun Y, Ma L. ZEB1: at the crossroads of epithelial-mesenchymal transition, metastasis and therapy resistance. *Cell Cycle (Georgetown Tex.)* (2015) 14:481–7. doi: 10.1080/15384101.2015.1006048

55. Peng DH, Ungewiss C, Tong P, Byers LA, Wang J, Canales JR, et al. ZEB1 induces LOXL2-mediated collagen stabilization and deposition in the extracellular matrix to drive lung cancer invasion and metastasis. *Oncogene* (2017) 36:1925–38. doi: 10.1038/onc.2016.358

56. Wang H, Huang B, Li BM, Cao KY, Mo CQ, Jiang SJ, et al. ZEB1-mediated vasculogenic mimicry formation associates with epithelial-mesenchymal transition and cancer stem cell phenotypes in prostate cancer. *J Cell Mol Med* (2018) 22:3768–81. doi: 10.1111/jcmm.13637

57. Vizcaíno C, Mansilla S, Portugal J. Sp1 transcription factor: A long-standing target in cancer chemotherapy. *Pharmacol Ther* (2015) 152:111–24. doi: 10.1016/j.pharmthera.2015.05.008

58. Han DS, Lee EO. Sp1 plays a key role in vasculogenic mimicry of human prostate cancer cells. *Int J Mol Sci* (2022) 23. doi: 10.3390/ijms23031321

59. Da J, Xu M, Wang Y, Li W, Lu M, Wang Z. Kaempferol promotes apoptosis while inhibiting cell proliferation *via* androgen-dependent pathway and suppressing vasculogenic mimicry and invasion in prostate cancer. *Analytical Cell Pathol (Amsterdam)* (2019) 2019:1907698. doi: 10.1155/2019/1907698

60. Aggarwal BB, Bhardwaj A, Aggarwal RS, Seeram NP, Shishodia S, Takada Y. Role of resveratrol in prevention and therapy of cancer: preclinical and clinical studies. *Anticancer Res* (2004) 24:2783–840.

61. Han DS, Lee HJ, Lee EO. Resveratrol suppresses serum-induced vasculogenic mimicry through impairing the EphA2/twist-VE-cadherin/AKT pathway in human prostate cancer PC-3 cells. *Sci Rep* (2022) 12:20125. doi: 10.1038/s41598-022-24414-z

62. Han H, Lee SO, Xu Y, Kim JE, Lee HJ. SPHK/HIF-1α Signaling pathway has a critical role in chrysin-induced anticancer activity in hypoxia-induced PC-3 cells. *Cells* (2022) 11. doi: 10.3390/cells11182787

63. Capitanio U, Montorsi F. Renal cancer. *Lancet (London England)* (2016) 387:894–906. doi: 10.1016/s0140-6736(15)00046-x

64. Lam JS, Shvarts O, Pantuck AJ. Changing concepts in the surgical management of renal cell carcinoma. *Eur Urol* (2004) 45:692–705. doi: 10.1016/j.eururo.2004.02.002

65. Nerich V, Hugues M, Paillard MJ, Borowski L, Nai T, Stein U, et al. Clinical impact of targeted therapies in patients with metastatic clear-cell renal cell carcinoma. *OncoTargets Ther* (2014) 7:365–74. doi: 10.2147/ott.S56370

66. Vartanian AA, Stepanova EV, Gutorov SL, Solomko E, Grigorieva IN, Sokolova IN, et al. Prognostic significance of periodic acid-Schiff-positive patterns in clear cell renal cell carcinoma. *Can J Urol* (2009) 16:4726–32.

67. Lin H, Pan JC, Zhang FM, Huang B, Chen X, Zhuang JT, et al. Matrix metalloproteinase-9 is required for vasculogenic mimicry by clear cell renal carcinoma cells. *Urologic Oncol 2015 33* (2015) 168:e169–116. doi: 10.1016/j.urolonc.2014.12.007

68. Thiery JP. Epithelial-mesenchymal transitions in tumour progression. *Nat Rev Cancer* (2002) 2:442–54. doi: 10.1038/nrc822

69. Ingels A, Hew M, Algaba F, de Boer OJ, van Moorselaar RJ, Horenblas S, et al. Vimentin over-expression and carbonic anhydrase IX under-expression are independent predictors of recurrence, specific and overall survival in non-metastatic clear-cell renal carcinoma: a validation study. *World J Urol* (2017) 35:81–7. doi: 10.1007/s00345-016-1854-y

70. Du J, Sun B, Zhao X, Gu Q, Dong X, Mo J, et al. Hypoxia promotes vasculogenic mimicry formation by inducing epithelial-mesenchymal transition in ovarian carcinoma. *Gynecologic Oncol* (2014) 133:575–83. doi: 10.1016/j.ygyno.2014.02.034

71. Lin H, Hong Y, Huang B, Liu X, Zheng J, Qiu S. Vimentin overexpressions induced by cell hypoxia promote vasculogenic mimicry by renal cell carcinoma cells. *BioMed Res Int* (2019) 2019:7259691. doi: 10.1155/2019/7259691

72. Bai J, Yeh S, Qiu X, Hu L, Zeng J, Cai Y, et al. TR4 nuclear receptor promotes clear cell renal cell carcinoma (ccRCC) vasculogenic mimicry (VM) formation and metastasis *via* altering the miR490-3p/vimentin signals. . *Oncogene* (2018) 37:5901–12. doi: 10.1038/s41388-018-0269-1

73. He M, Yang H, Shi H, Hu Y, Chang C, Liu S, et al. Sunitinib increases the cancer stem cells and vasculogenic mimicry formation *via* modulating the lncRNA-ECVSR/ERβ/Hif2-α signaling. *Cancer Lett* (2022) 524:15–28. doi: 10.1016/j.canlet.2021.08.028

74. Ding J, Cui XG, Chen HJ, Sun Y, Yu WW, Luo J, et al. Targeting circDGKD intercepts TKI's effects on up-regulation of estrogen receptor β and vasculogenic mimicry in renal cell carcinoma. *Cancers* (2022) 14. doi: 10.3390/cancers14071639

75. Takahashi Y, Sawada G, Kurashige J, Uchi R, Matsumura T, Ueo H, et al. Paired related homoeobox 1, a new EMT inducer, is involved in metastasis and poor prognosis in colorectal cancer. *Br J Cancer* (2013) 109:307–11. doi: 10.1038/bjc.2013.339

76. Hirata H, Sugimachi K, Takahashi Y, Ueda M, Sakimura S, Uchi R, et al. Downregulation of PRRX1 confers cancer stem cell-like properties and predicts poor prognosis in hepatocellular carcinoma. *Ann Surg Oncol* (2015) 22 Suppl 3:S1402–1409. doi: 10.1245/s10434-014-4242-0

77. Westermarck J, Hahn WC. Multiple pathways regulated by the tumor suppressor PP2A in transformation. *Trends Mol Med* (2008) 14:152–60. doi: 10.1016/j.molmed.2008.02.001

78. Tang Q, Wang Q, Zeng G, Li Q, Jiang T, Zhang Z, et al. Overexpression of CIP2A in clear cell renal cell carcinoma promotes cellular epithelial-mesenchymal transition and is associated with poor prognosis. *Oncol Rep* (2015) 34:2515–22. doi: 10.3892/or.2015.4217

79. Wang X, Yang R, Wang Q, Wang Y, Ci H, Wu S. Aberrant expression of vasculogenic mimicry, PRRX1, and CIP2A in clear cell renal cell carcinoma and its clinicopathological significance. *Medicine* (2019) 98:e17028. doi: 10.1097/md.0000000000017028

80. Zhao H, Leppert JT, Peehl DMA. Protective role for androgen receptor in clear cell renal cell carcinoma based on mining TCGA data. *PloS One* (2016) 11:e0146505. doi: 10.1371/journal.pone.0146505

81. You B, Sun Y, Luo J, Wang K, Liu Q, Fang R, et al. Androgen receptor promotes renal cell carcinoma (RCC) vasculogenic mimicry (VM) *via* altering TWIST1 nonsense-mediated decay through lncRNA-TANAR. *Oncogene* (2021) 40:1674–89. doi: 10.1038/s41388-020-01616-1

82. Pollard JW. Tumour-educated macrophages promote tumour progression and metastasis. *Nat Rev Cancer* (2004) 4:71–8. doi: 10.1038/nrc1256

83. Komohara Y, Hasita H, Ohnishi K, Fujiwara Y, Suzu S, Eto M, et al. Macrophage infiltration and its prognostic relevance in clear cell renal cell carcinoma. *Cancer Sci* (2011) 102:1424–31. doi: 10.1111/j.1349-7006.2011.01945.x

84. Chen XW, Yu TJ, Zhang J, Li Y, Chen HL, Yang GF, et al. CYP4A in tumor-associated macrophages promotes pre-metastatic niche formation and metastasis. *Oncogene* (2017) 36:5045–57. doi: 10.1038/onc.2017.118

85. Sica A, Erreni M, Allavena P, Porta C. Macrophage polarization in pathology. *Cell Mol Life Sci CMLS* (2015) 72:4111–26. doi: 10.1007/s00018-015-1995-y

86. Lan J, Sun L, Xu F, Liu L, Hu F, Song D, et al. M2 macrophage-derived exosomes promote cell migration and invasion in colon cancer. *Cancer Res* (2019) 79:146–58. doi: 10.1158/0008-5472.Can-18-0014

87. Liu Q, Zhao E, Geng B, Gao S, Yu H, He X, et al. Tumor-associated macrophage-derived exosomes transmitting miR-193a-5p promote the progression of renal cell carcinoma *via* TIMP2-dependent vasculogenic mimicry. *Cell Death Dis* (2022) 13:382. doi: 10.1038/s41419-022-04814-9

88. Intlekofer AM, Dematteo RG, Venneti S, Finley LW, Lu C, Judkins AR, et al. Hypoxia induces production of L-2-hydroxyglutarate. *Cell Metab* (2015) 22:304–11. doi: 10.1016/j.cmet.2015.06.023

89. Wang H, Wang L, Zheng Q, Lu Z, Chen Y, Shen D, et al. Oncometabolite L-2-hydroxyglurate directly induces vasculogenic mimicry through PHLDB2 in renal cell carcinoma. *Int J Cancer* (2021) 148:1743–55. doi: 10.1002/ijc.33435

90. Lim BC, Matsumoto S, Yamamoto H, Mizuno H, Kikuta J, Ishii M, et al. Prickle1 promotes focal adhesion disassembly in cooperation with the CLASP-LL5β complex in migrating cells. *J Cell Sci* (2016) 129:3115–29. doi: 10.1242/jcs.185439

91. Richters A, Aben KKH, Kiemeney L. The global burden of urinary bladder cancer: an update. *World J Urol* (2020) 38:1895–904. doi: 10.1007/s00345-019-02984-4

92. Dy GW, Gore JL, Forouzanfar MH, Naghavi M, Fitzmaurice C. Global burden of urologic cancers, 1990-2013. *Eur Urol* (2017) 71:437–46. doi: 10.1016/j.eururo.2016.10.008

93. Mayr R, Fritsche HM, Pycha A, Pycha A. Radical cystectomy and the implications of comorbidity. *Expert Rev Anticancer Ther* (2014) 14:289–95. doi: 10.1586/14737140.2014.868775

94. Fujimoto A, Onodera H, Mori A, Nagayama S, Yonenaga Y, Tachibana T. Tumour plasticity and extravascular circulation in ECV304 human bladder carcinoma cells. *Anticancer Res* (2006) 26:59–69. doi: 10.1586/14737140.6.1.59

95. Griffin M, Casadio R, Bergamini CM. Transglutaminases: nature's biological glues. *Biochem J* (2002) 368:377–96. doi: 10.1042/bj20021234

96. Collighan RJ, Griffin M. Transglutaminase 2 cross-linking of matrix proteins: biological significance and medical applications. *Amino Acids* (2009) 36:659–70. doi: 10.1007/s00726-008-0190-y

97. Haroon ZA, Hettasch JM, Lai TS, Dewhirst MW, Greenberg CS. Tissue transglutaminase is expressed, active, and directly involved in rat dermal wound healing and angiogenesis. *FASEB J* (1999) 13:1787–95. doi: 10.1096/fasebj.13.13.1787

98. Jones RA, Wang Z, Dookie S, Griffin M. The role of TG2 in ECV304-related vasculogenic mimicry. *Amino Acids* (2013) 44:89–101. doi: 10.1007/s00726-011-1214-6

99. Yang L, Zou X, Zou J, Zhang G. Functions of circular RNAs in bladder, prostate and renal cell cancer (Review). *Mol Med Rep* (2021) 23. doi: 10.3892/mmr.2021.11946

100. Sato F, Tsuchiya S, Meltzer SJ, Shimizu K. MicroRNAs and epigenetics. *FEBS J* (2011) 278:1598–609. doi: 10.1111/j.1742-4658.2011.08089.x

101. Zhang T, Wang J, Zhai X, Li H, Li C, Chang J. MiR-124 retards bladder cancer growth by directly targeting CDK4. *Acta Biochim Biophys Sin* (2014) 46:1072–9. doi: 10.1093/abbs/gmu105

102. Qian C, Wang Y, Ji Y, Chen D, Wang C, Zhang G, et al. Neural stem cell –derived exosomes transfer miR–124–3p into cells to inhibit glioma growth by targeting FLOT2. *Int J Oncol* (2022) 61. doi: 10.3892/ijo.2022.5405

103. Ren X, Fan Y, Shi D, Xu E, Liu Y. MicroRNA-124 inhibits canine mammary carcinoma cell proliferation, migration and invasion by targeting CDH2. *Res veterinary Sci* (2022) 146:5–14. doi: 10.1016/j.rvsc.2022.03.004

104. Reardon ES, Shukla V, Xi S, Gara SK, Liu Y, Straughan D, et al. UHRF1 is a novel druggable epigenetic target in Malignant pleural mesothelioma. *J Thorac Oncol* (2021) 16:89–103. doi: 10.1016/j.jtho.2020.08.024

105. Bronner C, Krifa M, Mousli M. Increasing role of UHRF1 in the reading and inheritance of the epigenetic code as well as in tumorogenesis. *Biochem Pharmacol* (2013) 86:1643–9. doi: 10.1016/j.bcp.2013.10.002

106. Wang X, Wu Q, Xu B, Wang P, Fan W, Cai Y, et al. MiR-124 exerts tumor suppressive functions on the cell proliferation, motility and angiogenesis of bladder cancer by fine-tuning UHRF1. *FEBS J* (2015) 282:4376–88. doi: 10.1111/febs.13502

107. Liu Z, Sun B, Qi L, Li H, Gao J, Leng X. Zinc finger E-box binding homeobox 1 promotes vasculogenic mimicry in colorectal cancer through induction of epithelial-to-mesenchymal transition. *Cancer Sci* (2012) 103:813–20. doi: 10.1111/j.1349-7006.2011.02199.x

108. Liu Z, Tang Q, Qi T, Othmane B, Yang Z, Chen J, et al. Robust hypoxia risk score predicts the clinical outcomes and tumor microenvironment immune characters in bladder cancer. *Front Immunol* (2021) 12:725223. doi: 10.3389/fimmu.2021.725223

109. Sun B, Zhang D, Zhang S, Zhang W, Guo H, Zhao X. Hypoxia influences vasculogenic mimicry channel formation and tumor invasion-related protein expression in melanoma. *Cancer Lett* (2007) 249:188–97. doi: 10.1016/j.canlet.2006.08.016

110. Wei X, Chen Y, Jiang X, Peng M, Liu Y, Mo Y, et al. Mechanisms of vasculogenic mimicry in hypoxic tumor microenvironments. *Mol Cancer* (2021) 20:7. doi: 10.1186/s12943-020-01288-1

111. Mayers JR, Torrence ME, Danai LV, Papagiannakopoulos T, Davidson SM, Bauer MR, et al. Tissue of origin dictates branched-chain amino acid metabolism in mutant Kras-driven cancers. *Sci (New York N.Y.)* (2016) 353:1161–5. doi: 10.1126/science.aaf5171

112. Cai Z, Chen J, Yu Z, Li H, Liu Z, Deng D, et al. BCAT2 shapes a noninflamed tumor microenvironment and induces resistance to anti-PD-1/PD-L1 immunotherapy by negatively regulating proinflammatory chemokines and anticancer immunity. *Advanced Sci (Weinheim Baden-Wurttemberg Germany)* (2023) 10:e2207155. doi: 10.1002/advs.202207155

113. Wang J, Sun J, Liu LN, Flies DB, Nie X, Toki M, et al. Siglec-15 as an immune suppressor and potential target for normalization cancer immunotherapy. *Nat Med* (2019) 25:656–66. doi: 10.1038/s41591-019-0374-x

114. Zhang C, Xiao J, Yuan T, He Y, Deng D, Xiao Z, et al. Molecular vasculogenic mimicry-Related signatures predict clinical outcomes and therapeutic responses in bladder cancer: Results from real-world cohorts. *Front Pharmacol* (2023) 14:1163115. doi: 10.3389/fphar.2023.1163115

115. Hu J, Yu A, Othmane B, Qiu D, Li H, Li C, et al. Siglec15 shapes a non-inflamed tumor microenvironment and predicts the molecular subtype in bladder cancer. *Theranostics* (2021) 11:3089–108. doi: 10.7150/thno.53649

116. Nunes SP, Henrique R, Jerónimo C, Paramio JM. DNA methylation as a therapeutic target for bladder cancer. *Cells* (2020) 9. doi: 10.3390/cells9081850

117. Kelly AD, Issa JJ. The promise of epigenetic therapy: reprogramming the cancer epigenome. *Curr Opin Genet Dev* (2017) 42:68–77. doi: 10.1016/j.gde.2017.03.015

118. Biswas S, Rao CM. Epigenetic tools (The Writers, The Readers and The Erasers) and their implications in cancer therapy. *Eur J Pharmacol* (2018) 837:8–24. doi: 10.1016/j.ejphar.2018.08.021

119. Hu J, Othmane B, Yu A, Li H, Cai Z, Chen X, et al. 5mC regulator-mediated molecular subtypes depict the hallmarks of the tumor microenvironment and guide precision medicine in bladder cancer. *BMC Med* (2021) 19:289. doi: 10.1186/s12916-021-02163-6

120. Qi L, Song W, Liu Z, Zhao X, Cao W, Sun B. Wnt3a promotes the vasculogenic mimicry formation of colon cancer *via* Wnt/β-catenin signaling. *Int J Mol Sci* (2015) 16:18564–79. doi: 10.3390/ijms160818564

121. Liu X, He H, Zhang F, Hu X, Bi F, Li K, et al. m6A methylated EphA2 and VEGFA through IGF2BP2/3 regulation promotes vasculogenic mimicry in colorectal cancer *via* PI3K/AKT and ERK1/2 signaling. *Cell Death Dis* (2022) 13:483. doi: 10.1038/s41419-022-04950-2

122. Deng F, Zhou R, Lin C, Yang S, Wang H, Li W, et al. Tumor-secreted dickkopf2 accelerates aerobic glycolysis and promotes angiogenesis in colorectal cancer. *Theranostics* (2019) 9:1001–14. doi: 10.7150/thno.30056

123. Mashreghi M, Azarpara H, Bazaz MR, Jafari A, Masoudifar A, Mirzaei H, et al. Angiogenesis biomarkers and their targeting ligands as potential targets for tumor angiogenesis. *J Cell Physiol* (2018) 233:2949–65. doi: 10.1002/jcp.26049

124. Liu B, Wang T, Wang H, Zhang L, Xu F, Fang R, et al. Oncoprotein HBXIP enhances HOXB13 acetylation and co-activates HOXB13 to confer tamoxifen resistance in breast cancer. *J Hematol Oncol* (2018) 11:26. doi: 10.1186/s13045-018-0577-5

125. Xiu M, Zeng X, Shan R, Wen W, Li J, Wan R. The oncogenic role of HBXIP. *Biomedicine pharmacotherapy = Biomedecine pharmacotherapie* (2021) 133:111045. doi: 10.1016/j.biopha.2020.111045

126. Li X, Liu S. Suppression of HBXIP reduces cell proliferation, migration and invasion *in vitro*, and tumorigenesis *in vivo* in human urothelial carcinoma of the bladder. *Cancer biotherapy radiopharmaceuticals* (2016) 31:311–6. doi: 10.1089/cbr.2016.2038

127. Zheng YL, Li L, Jia YX, Zhang BZ, Li JC, Zhu YH, et al. LINC01554-mediated glucose metabolism reprogramming suppresses tumorigenicity in hepatocellular carcinoma *via* downregulating PKM2 expression and inhibiting AKT/mTOR signaling pathway. *Theranostics* (2019) 9:796–810. doi: 10.7150/thno.28992

128. Liu X, Li H, Che N, Zheng Y, Fan W, Li M, et al. HBXIP accelerates glycolysis and promotes cancer angiogenesis *via* AKT/mTOR pathway in bladder cancer. *Exp Mol Pathol* (2021) 121:104665. doi: 10.1016/j.yexmp.2021.104665

129. Prager GW, Poettler M, Unseld M, Zielinski CC. Angiogenesis in cancer: Anti-VEGF escape mechanisms. *Trans Lung Cancer Res* (2012) 1:14–25. doi: 10.3978/j.issn.2218-6751.2011.11.02

130. Aguilar-Cazares D, Chavez-Dominguez R, Carlos-Reyes A, Lopez-Camarillo C, Hernadez de la Cruz ON, Lopez-Gonzalez JS. Contribution of angiogenesis to inflammation and cancer. *Front Oncol* (2019) 9:1399. doi: 10.3389/fonc.2019.01399

131. Escudier B, Eisen T, Stadler WM, Szczylik C, Oudard S, Siebels M, et al. Sorafenib in advanced clear-cell renal-cell carcinoma. *New Engl J Med* (2007) 356:125–34. doi: 10.1056/NEJMoa060655

132. Lacal PM, Graziani G. Therapeutic implication of vascular endothelial growth factor receptor-1 (VEGFR-1) targeting in cancer cells and tumor microenvironment by competitive and non-competitive inhibitors. *Pharmacol Res* (2018) 136:97–107. doi: 10.1016/j.phrs.2018.08.023

133. Ellis LM, Hicklin DJ. Pathways mediating resistance to vascular endothelial growth factor-targeted therapy. *Clin Cancer Res* (2008) 14:6371–5. doi: 10.1158/1078-0432.Ccr-07-5287

134. Rini BI, Halabi S, Rosenberg JE, Stadler WM, Vaena DA, Archer L, et al. Phase III trial of bevacizumab plus interferon alfa versus interferon alfa monotherapy in patients with metastatic renal cell carcinoma: final results of CALGB 90206. *J Clin Oncol* (2010) 28:2137–43. doi: 10.1200/jco.2009.26.5561

135. Hori A, Shimoda M, Naoi Y, Kagara N, Tanei T, Miyake T, et al. Vasculogenic mimicry is associated with trastuzumab resistance of HER2-positive breast cancer. *Breast Cancer Res BCR* (2019) 21:88. doi: 10.1186/s13058-019-1167-3

136. Sun L, Diamond ME, Ottaviano AJ, Joseph MJ, Ananthanarayan V, Munshi HG. Transforming growth factor-beta 1 promotes matrix metalloproteinase-9-mediated oral cancer invasion through snail expression. *Mol Cancer Res MCR* (2008) 6:10–20. doi: 10.1158/1541-7786.Mcr-07-0208

137. Munger JS, Sheppard D. Cross talk among TGF-β signaling pathways, integrins, and the extracellular matrix. *Cold Spring Harbor Perspect Biol* (2011) 3: a005017. doi: 10.1101/cshperspect.a005017

138. Jiang L, Shi S, Li F, Shi Q, Zhong T, Zhang H, et al. miR–519d–3p/HIF–2α axis increases the chemosensitivity of human cervical cancer cells to cisplatin via inactivation of PI3K/AKT signaling. *Mol Med Rep* (2021) 23. doi: 10.3892/mmr.2021.11992

139. Huang M, Ke Y, Sun X, Yu L, Yang Z, Zhang Y, et al. Mammalian target of rapamycin signaling is involved in the vasculogenic mimicry of glioma *via* hypoxia-inducible factor-1α. . *Oncol Rep* (2014) 32:1973–80. doi: 10.3892/or.2014.3454

140. Metcalfe SM, Canman CE, Milner J, Morris RE, Goldman S, Kastan MB. Rapamycin and p53 act on different pathways to induce G1 arrest in mammalian cells. *Oncogene* (1997) 15:1635–42. doi: 10.1038/sj.onc.1201341

141. Jung SH, Hwang HJ, Kang D, Park HA, Lee HC, Jeong D, et al. mTOR kinase leads to PTEN-loss-induced cellular senescence by phosphorylating p53. *Oncogene* (2019) 38:1639–50. doi: 10.1038/s41388-018-0521-8

142. Zhang Y, Yan H, Xu Z, Yang B, Luo P, He Q. Molecular basis for class side effects associated with PI3K/AKT/mTOR pathway inhibitors. *Expert Opin Drug Metab Toxicol* (2019) 15:767–74. doi: 10.1080/17425255.2019.1663169

143. Cannone S, Greco MR, Carvalho TMA, Guizouarn H, Soriani O, Di Molfetta D, et al. Cancer associated fibroblast (CAF) regulation of PDAC parenchymal (CPC) and CSC phenotypes is modulated by ECM composition. *Cancers* (2022) 14. doi: 10.3390/cancers14153737

144. Li F, Xu J, Liu S. Cancer stem cells and neovascularization. *Cells* (2021) 10. doi: 10.3390/cells10051070

145. Akhmetshina A, Dees C, Pileckyte M, Maurer B, Axmann R, Jüngel A, et al. Dual inhibition of c-abl and PDGF receptor signaling by dasatinib and nilotinib for the treatment of dermal fibrosis. *FASEB J* (2008) 22:2214–22. doi: 10.1096/fj.07-105627

146. Ferician AM, Ferician OC, Cumpanas AD, Berzava PL, Nesiu A, Barmayoun A, et al. Heterogeneity of platelet derived growth factor pathway gene expression profile defines three distinct subgroups of renal cell carcinomas. *Cancer Genomics Proteomics* (2022) 19:477–89. doi: 10.21873/cgp.20334

147. Mundhenke C, Weigel MT, Sturner KH, Roesel F, Meinhold-Heerlein I, Bauerschlag DO, et al. Novel treatment of ovarian cancer cell lines with Imatinib mesylate combined with Paclitaxel and Carboplatin leads to receptor-mediated antiproliferative effects. *J Cancer Res Clin Oncol* (2008) 134:1397–405. doi: 10.1007/s00432-008-0408-0

148. Kwon YC, Bose SK, Steele R, Meyer K, Di Bisceglie AM, Ray RB, et al. Promotion of cancer stem-like cell properties in hepatitis C virus-infected hepatocytes. *J Virol* (2015) 89:11549–56. doi: 10.1128/jvi.01946-15

149. Carneiro A, Falcão M, Azevedo I, Falcão Reis F, Soares R. Multiple effects of bevacizumab in angiogenesis: implications for its use in age-related macular degeneration. *Acta ophthalmologica* (2009) 87:517–23. doi: 10.1111/j.1755-3768.2008.01257.x

150. Ferrara N, Hillan KJ, Gerber HP, Novotny W. Discovery and development of bevacizumab, an anti-VEGF antibody for treating cancer. *Nat Rev Drug Discovery* (2004) 3:391–400. doi: 10.1038/nrd1381

151. Motzer RJ, Hutson TE, Tomczak P, Michaelson MD, Bukowski RM, Rixe O, et al. Sunitinib versus interferon alfa in metastatic renal-cell carcinoma. *New Engl J Med* (2007) 356:115–24. doi: 10.1056/NEJMoa065044

152. Kopetz S, Hoff PM, Morris JS, Wolff RA, Eng C, Glover KY, et al. Phase II trial of infusional fluorouracil, irinotecan, and bevacizumab for metastatic colorectal cancer: efficacy and circulating angiogenic biomarkers associated with therapeutic resistance. *J Clin Oncol* (2010) 28:453–9. doi: 10.1200/jco.2009.24.8252

153. Pandey P, Khan F, Upadhyay TK, Seungjoon M, Park MN, Kim B. New insights about the PDGF/PDGFR signaling pathway as a promising target to develop cancer therapeutic strategies. *Biomedicine pharmacotherapy = Biomedecine pharmacotherapie* (2023) 161:114491. doi: 10.1016/j.biopha.2023.114491

frontiers | Frontiers in Oncology

TYPE Systematic Review
PUBLISHED 06 October 2023
DOI 10.3389/fonc.2023.1265276

OPEN ACCESS

EDITED BY
Housheng Hansen He,
University Health Network (UHN), Canada

REVIEWED BY
Wangrui Liu,
Shanghai Jiao Tong University, China
Yantao Cai,
Shanghai Jiaotong University School of Medicine, China

*CORRESPONDENCE
Yunhua Qiu
18917982481@189.cn
Jianfeng Yang
yangjianfeng@shutcm.edu.cn
Youyang Shi
syyshutcm@163.com

†These authors have contributed equally to this work

RECEIVED 22 July 2023
ACCEPTED 18 September 2023
PUBLISHED 06 October 2023

CITATION
Luo Z, Zhu B, Xu H, Chen L, Song X, Wang Y, Wang R, Zheng J, Qiu Y, Yang J and Shi Y (2023) Efficacy and safety of olaparib combined with abiraterone in patients with metastatic castration-resistant prostate cancer: a systematic review and meta-analysis of randomized controlled trials. *Front. Oncol.* 13:1265276. doi: 10.3389/fonc.2023.1265276

Efficacy and safety of olaparib combined with abiraterone in patients with metastatic castration-resistant prostate cancer: a systematic review and meta-analysis of randomized controlled trials

Zhanyang Luo[1†], Bukun Zhu[1†], Hong Xu[2†], Lixin Chen[1], Xiaoyun Song[1], Yu Wang[1], Rui Wang[1], Jinzhou Zheng[1], Yunhua Qiu[1*], Jianfeng Yang[1*] and Youyang Shi[1*]

[1]Longhua Hospital, Shanghai University of Traditional Chinese Medicine, Shanghai, China, [2]Affiliated Hospital of Youjiang Medical University for Nationalities, Baise, China

Background: Olaparib has been proven for the treatment of metastatic castration-resistant prostate cancer (mCRPC). This meta-analysis aims to comprehensively evaluate the efficacy and safety of the combination of olaparib and abiraterone in patients with mCRPC.

Methods: The literature in PubMed, Embase, and Cochrane Library up until April 27, 2023, was systematically searched. In the studies included in this meta-analysis, olaparib combined with abiraterone was compared with abiraterone combined with placebo.

Results: Two randomized controlled trials involving a total of 938 patients were included. Analysis indicated that olaparib combined with abiraterone significantly prolonged radiographic progression-free survival (rPFS: relative risk [RR] 0.66, 95% confidence interval [CI] 0.55–0.79), time to secondary progression or death (PFS2: hazard ratio [HR] 0.72, 95% CI 0.56–0.93), time to first subsequent therapy or death (TFST: HR 0.75, 95% CI 0.63–0.89), time to second subsequent therapy or death (TSST: HR 0.73, 95% CI 0.58–0.93), and confirmed prostate-specific antigen (PSA) response (RR 1.14, 95% CI 1.05–1.24). However, no statistically significant differences were found in the overall survival (OS: HR 0.87 95% CI 0.70–1.09), objective response rate (ORR: RR 0.97, 95% CI 0.70–1.33), and incidence of total adverse events (RR 1.07, 95% CI 0.94–1.22). A notable detail that the combination of olaparib and abiraterone was associated with an increased incidence of high-grade anemia (RR 7.47, 95% CI 1.36–40.88).

Conclusion: Olaparib combined with abiraterone is effective for patients with mCRPC. However, combination therapy has treatment-related adverse events compared with monotherapy, and this could be improved in future treatment management.

Systematic review registration: https://www.crd.york.ac.uk/PROSPERO/, identifier CRD42023432287.

KEYWORDS

olaparib, abiraterone, metastatic castration-resistant prostate cancer (mCRPC), efficacy, safety, meta-analysis

1 Introduction

Prostate cancer is the second most common cancer in men, comprising 14.1% of all cases and accounting for 6.8% of all cancer-related mortality in 2020 worldwide (1). Despite survival and quality of life having greatly improved in patients using next-generation hormonal agents (NHA), chemotherapy or radiotherapy, metastatic castration-resistant prostate cancer (mCRPC) remains lethal and has poor prognosis (2). Approximately 20%–30% (3–5) of patients with mCRPC exhibit alterations in homologous recombination repair (HRR), specifically *BRCA1* and *BRCA2*. Moreover, HRR gene aberrations in patients with mCRPC are correlated with a poor prognosis, which renders them susceptible to poly(ADP-ribose) polymerase inhibitors (PARPis) (6).

Olaparib (Lynparza) was approved by the US Food and Drug Administration for the treatment of mCRPC harboring HRR deficiency after patients used next generation hormonal agents (7). In the phase III PROfound study (NCT02987543), olaparib monotherapy showed clinical improvement in radiographic progression-free survival (rPFS) and overall survival (OS) for patients with mCRPC who had a mutation in BRCA1, BRCA2, or ATM (8). Abiraterone acetate (hereafter abiraterone), as a selective and irreversible inhibitor of CYP17, effectively impedes androgen biosynthesis (9). Preclinical studies suggested that PARPi combined with NHA may be a novel antitumor therapy (10, 11). These studies reported that NHA can result in HRR deficiency by inhibiting transcription in some HRR genes, leading to sensitivity to PARPi of mCRPC.

Previous evidence from meta-analyses focused on assessing the efficacy of NHA and docetaxel (12) or PARPi (13–15). However, the systematic review of evidence supporting the use of combination of olaparib and abiraterone is limited and unclear. Hence, the present study aimed to comprehensively evaluate the efficacy and safety of the combination of olaparib and abiraterone in patients with mCRPC by pooling new data from two randomized controlled trials. Understanding the role of the above combination therapy in patients with mCRPC may enhance clinical decision-making.

Abbreviations: NHA, next-generation hormonal agents; mCRPC, metastatic castration-resistant prostate cancer; HRR, homologous recombination repair; PARPis, poly (ADP-ribose) polymerase inhibitors; rPFS, radiographic progression-free survival; OS, overall survival; TFST, time to first subsequent therapy or death; TSST, time to second subsequent anti-cancer therapy or death; PFS2, time to secondary progression or death, PSA, prostate-specific antigen; ORR, objective response rate; RCT, randomized control trial; ROB, risk of bias; HR, hazard Ratio; CI, confidence intervals; RR, relative risk.

2 Materials and methods

This meta-analysis was carried out on the basis of the guideline of Preferred Reporting Items for Systematic Reviews and Meta-Analyses (PRISMA) (16). The protocol was registered with the International Prospective Register of Systematic Reviews (PROSPERO, CRD42023432287).

2.1 Data sources and search strategy

The literature in PubMed, Embase, and Cochrane Library up until April 27, 2023, was systematically searched using the following term combinations: ("Olaparib or AZD2281 or KU0059436") and ("prostatic neoplasms or prostatic carcinoma or prostate cancer") and ("randomized controlled trial"). The search strategies for the three databases are fully provided in Supplementary Table 1. Besides, potential articles were manually searched in related studies and reviews. The eligibility of titles and abstracts in all articles was independently assessed by two reviewers (ZL and BZ).

2.2 Inclusion and exclusion criteria

On the basis of PICOS criteria, two reviewers independently assessed the studies by the initial literature search, subsequently incorporating the studies that met the eligibility criteria. The studies included in this meta-analysis met the following criteria:

Participants: must be diagnosed with mCRPC and at least 18 years of age.

Intervention: combination of olaparib and abiraterone.

Comparator: placebo or other active drugs.

Outcomes: radiological progression free survival (rPFS), overall survival (OS), time to first subsequent therapy or death (TFST), time to second subsequent anti-cancer therapy or death (TSST), time to secondary progression or death (PFS2), confirmed prostate-specific antigen (PSA) response, objective response rate (ORR), and adverse events.

Study design: the included studies had a phase II or III randomized control trial (RCT) design.

The exclusion criteria were as follows: phase I trials, letters, comments, reviews, or meta-analyses; studies without sufficient data and proper control drugs; and repeat publications.

When disagreements arose, a third reviewer was involved and evaluated all the eligible articles until a consensus was reached.

2.3 Data extraction and risk of bias assessment

In accordance with the Cochrane Handbook guidelines, two investigators (YQ and JY) independently assessed and extracted the proper data including: first author, publication year, NCT number, inclusion criteria, phase of study, intervention and control group, median follow-up, and survival endpoints.

The ROB of the included RCTs was assessed using version 1.0 of the Cochrane Handbook's ROB tool, which involves five domains: random sequence generation, allocation concealment, blinding, incomplete outcome data, and selective reporting. The ROB of each included study was assessed independently by two reviewers (ZL and YS). Each domain was classified as having a high, low, or unclear ROB.

2.4 Definition of outcomes

The primary outcomes were rPFS and OS. The secondary outcomes included TFST, TSST, PFS2, confirmed PSA response, ORR, and adverse events.

rPFS is defined as the time from randomization to radiological progression (assessed by the investigator per the Response Evaluation Criteria in Solid Tumors [RECIST] 1.1 for soft tissue or the Prostate Cancer Working Group-3 [PCWG3] criteria for bone) or death from any cause (17).

OS is defined as the time from randomization to death from any cause (18).

TFST and TSST are defined as the time from randomization to the earlier of the first subsequent or the second subsequent anti-cancer therapy start date following study treatment discontinuation, or death, respectively.

PFS2 is defined as objective radiological progression by RECIST 1.1 for soft tissue, symptomatic progression, a rise in PSA level, or death in the absence of overall progression (19).

Confirmed PSA response is defined as a reduction in PSA level of 50% or more on two consecutive occasions at least 4 weeks apart compared with baseline (20).

ORR is defined as the percentage of patients with a complete response or partial response in soft tissue disease and a bone scan status of non-progressive disease (21).

The adverse events from olaparib combined with abiraterone and the control assessed in this article included total adverse events, grade 3 or worse adverse events, anemia, fatigue or asthenia, nausea, and diarrhea.

2.5 Data synthesis and statistical analysis

Statistical analysis was performed using Stata software version 12.0. For survival outcomes, the hazard Ratios (HRs) and 95% confidence intervals (CIs) for rPFS, OS, TFST, TSST, and PFS2 were extracted from each included article. Pooled HRs were obtained using the generic inverse of variance method with a random-effect model (22). When an HR < 1, it implied that the related endpoints of olaparib combined with abiraterone were associated with a lower risk than the control group. For dichotomous variables (i.e., ORR, confirmed PSA response and adverse events), relative risk (RR) was used to assess the differences between combination therapy and control interventions. The random-effect model was used to analyze all quantitative data. The results were analyzed and presented in forest plot. I^2 statistic and the Cochrane Q statistic were used to assess between-study heterogeneity. A value of I^2 greater than 50% and a p-value < 0.10 were considered indicative of a substantial level of heterogeneity (23). A p-value < 0.05 was considered statistically significant.

3 Results

3.1 Study selection and characteristics

The results of all records identified in the search are shown in a flow diagram (Figure 1). A total of 603 studies were identified through the systematic literature search. Two potential records were also identified from the references of the reviews by hand searching. After 108 duplicate articles and 461 irrelevant articles were excluded on the basis of title or abstract screening, a total of 36 full-text articles and conference abstracts were considered potentially eligible for this review. Subsequently, 34 studies were excluded, including four with phase I trials; 11 with letters, comments, reviews, or meta-analyses; 14 with insufficient data; three with improper control drugs; and two with repeat publications. Finally, only 2 RCTs were included for assessment in this meta-analysis (24, 25).

The characteristics of the included studies in this meta-analysis are summarized in Table 1. Trials involving a total of 938 patients, including one phase II (24) and one phase III (25) trials, were conducted in Europe, America, Asia, and Oceania. All participants had histologically confirmed mCRPC, which included 470 men receiving olaparib combined with abiraterone and 468 men receiving abiraterone combined with placebo. Olaparib was

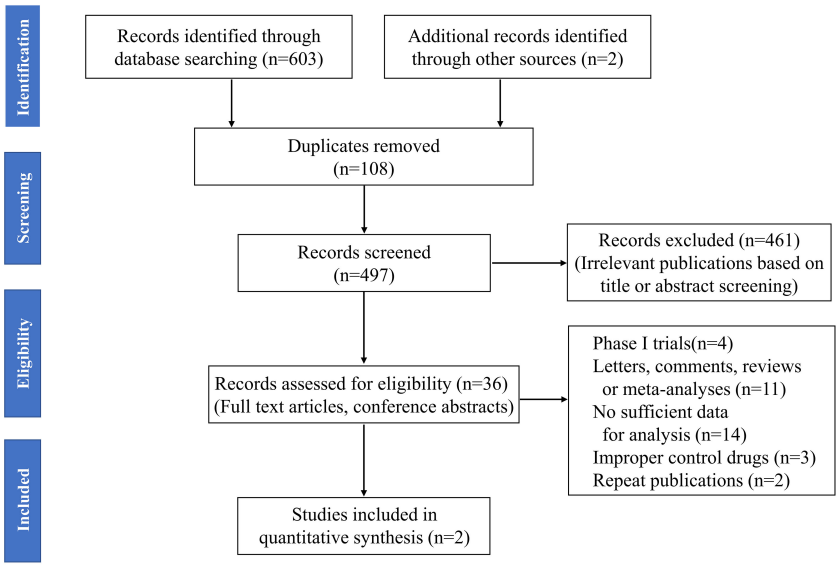

FIGURE 1
Flowchart of study screening in this meta-analysis.

administered orally at a dose of 300 mg two times daily, and abiraterone was administered orally at a dose of 1000 mg per day. More details about the characteristics of patients at baseline are shown in Supplementary Table 2. The ROB graph (Figure 2) indicated that the ROB was low across all domains.

3.2 Results of the meta-analysis

3.2.1 Primary outcomes

3.2.1.1 Radiologic progression-free survival

As shown in Figure 3A, the pooled HR for rPFS in the total patient population comparing olaparib combined with abiraterone versus abiraterone combined with placebo was 0.66 (95% CI 0.55–0.79). The use of olaparib in combination with abiraterone was significantly associated with improved rPFS in patients with mCRPC (n = 938, $p < 0.01$), and no significant heterogeneity was found between the studies ($I^2 = 0\%$, $p = 0.946$). Moreover, the subgroup analysis that considered HRR mutation status to HRR mutation/wild-type showed that the olaparib combination group had favorable rPFS benefits (HRR mutation: n = 247, HR 0.52, 95% CI 0.37–0.75; wild-type HRR: n = 587, HR 0.74, 95% CI 0.58–0.93; $p < 0.01$), as illustrated in Figures 3B, C. No significant heterogeneity existed across the studies in neither the HRR mutation group ($I^2 = 0\%$, $p = 0.491$) nor the wild-type HRR group ($I^2 = 0\%$, $p = 0.364$).

3.2.1.2 Overall survival

Two studies reported the outcome of OS in patients with mCRPC, with a total of 938 individuals. Figure 3D shows that the pooled HR for OS comparing olaparib combined with abiraterone and abiraterone combined placebo was 0.87 (95% CI 0.70–1.09, $p = 0.237$), indicating no significant differences between the olaparib combination group and the control group, and no significant heterogeneity ($I^2 = 0\%$, $p = 0.822$).

TABLE 1 Characteristics of included randomized controlled trials.

First author year	NCT number	Inclusion criteria	Phase	Intervention (N)	Control (N)	Median follow-up (months)	Survival endpoints
Clarke 2018 (24)	NCT01972217	Patients had mCRPC, and had previously received docetaxel and up to one additional line of previous chemotherapy.	II	Olaparib +abiraterone (71)	Abiraterone +placebo (71)	Intervention: 15.9 Control: 24.5	rPFS, OS, PFS2, TFST, TSST, ORR, PSA response, adverse events, *etc.*
Clarke 2022 (25)	NCT03732820	Patients had histologically or cytologically confirmed prostate cancer with at least one documented metastatic lesion.	III	Olaparib +abiraterone (399)	Abiraterone +placebo (397)	Intervention: 19.3 Control: 19.4	rPFS, OS, ORR, PSA, time to PSA progression, adverse events, *etc.*

NCT, ClinicalTrials.gov number; mCRPC, metastatic Castration-resistant prostate cancer; rPFS, radiologic Progression-free survival; OS, overall survival; TFST, time to first subsequent therapy or death; TSST, time to second subsequent anti-cancer therapy or death; ORR, objective response rate; PSA, prostate-specific antigen.

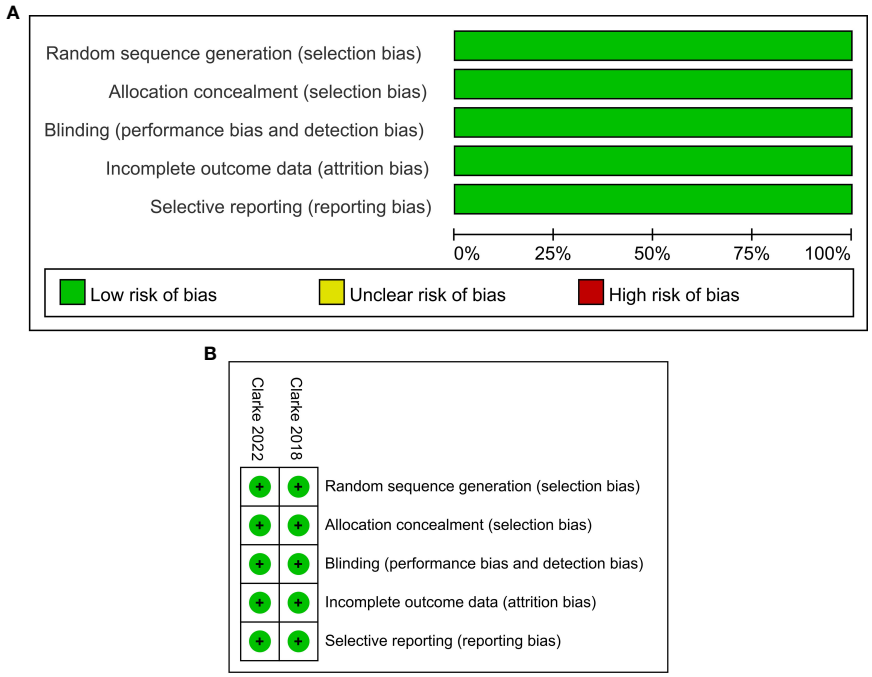

FIGURE 2
Risk of bias graph: reviewers' judgments about each risk of bias item presented as percentages across all included studies **(A)**. Risk of bias summary: reviewers' judgments about each risk of bias item for each included study according to the Cochrane Collaboration's "Risk of Bias" tool, the green circle with "plus" sign representing low risk of bias, the yellow circle with "question mark" sign representing unclear risk of bias and the red circle with "minus" sign represents high risk of bias **(B)**.

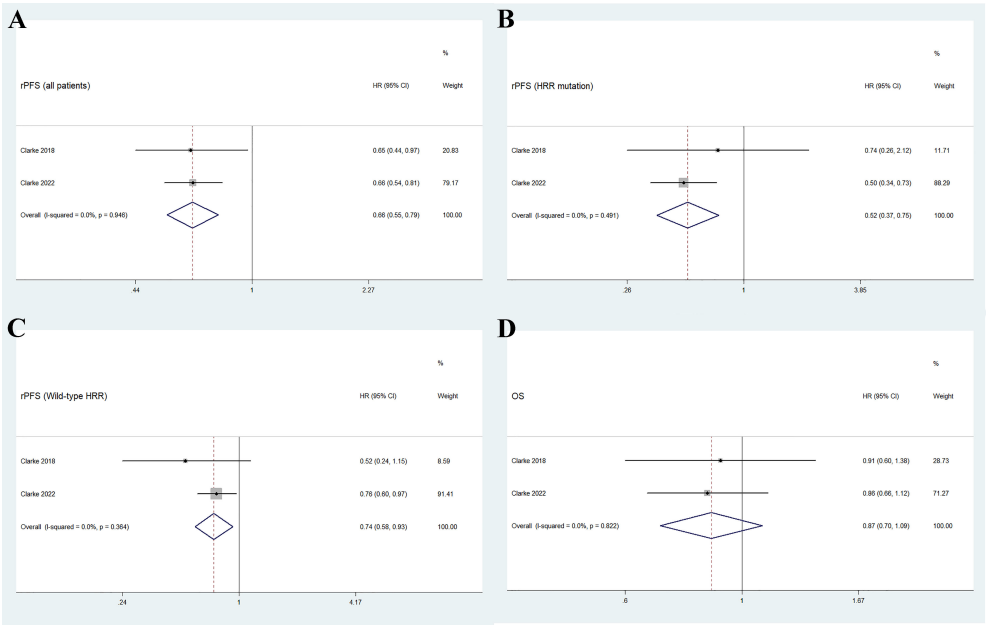

FIGURE 3
Forest plot of randomized controlled trials on olaparib combination therapy for primary outcomes: rPFS **(A)**, rPFS in HRR mutation subgroup **(B)**, rPFS in wild-type HRR subgroup **(C)**, and OS **(D)**.

3.2.2 Secondary outcomes

3.2.2.1 Time to secondary progression or death, first and second subsequent therapy or death

As shown in Figure 4, the pooled results indicate that olaparib combined with abiraterone significantly prolonged PFS2 (HR 0.72, 95% CI 0.56–0.93, p = 0.01), TFST (HR 0.75, 95% CI 0.63-0.89, p = 0.001), and TSST (HR 0.73, 95% CI 0.58–0.93, p = 0.012) compared with abiraterone plus placebo. No significant heterogeneity was observed between the olaparib combination group and the abiraterone group (I^2 = 0%, p > 0.10).

3.2.2.2 Objective response rate and confirmed prostate-specific antigen response

The two RCTs reported the ORR, including a total of 194 individuals in the olaparib combination group and 198 individuals in the control group. The overall results showed no significant difference between the two groups (RR 0.97, 95% CI 0.70–1.33, p = 0.838), and no significant heterogeneity (I^2 = 19.3%, p = 0.294), as shown in Figure 5A. Further subgroup analysis indicated that the two treatment groups had similar effects on complete response (RR 0.57, 95% CI 0.24–1.35, p = 0.203) and partial response (RR 1.06, 95% CI 0.96–1.18, p = 0.257). Furthermore, no significant inter-study heterogeneity was observed (complete response: I^2 = 0%, p = 0.997; partial response: I^2 = 0%, p = 0.671).

As shown in Figure 5B, the findings of the pooled data revealed that the olaparib combination therapy was superior in terms of confirmed PSA response (RR 1.14, 95% CI 1.05–1.24, p = 0.001), but no significant heterogeneity was observed between the two groups (I^2 = 0%, p = 0.96).

3.2.2.3 Adverse events

The most common adverse events in the olaparib and abiraterone groups were anemia, fatigue or asthenia, nausea, and diarrhea. No statistical differences were found in the incidence risk of total adverse events and anemia between the treatment groups and control groups (total adverse events: RR 1.07, 95% CI 0.94–1.22, p = 0.283; anemia: RR 6.26, 95% CI 0.82–48.02, p = 0.078). Fatigue or asthenia, nausea, and diarrhea were more common in the olaparib and abiraterone combination group than in the abiraterone group (fatigue or asthenia: RR 1.36, 95% CI 1.13–1.64, p = 0.001; nausea: RR 2.12, 95% CI 1.63–2.76, p < 0.01; and diarrhea: RR 1.77, 95% CI 1.25–2.49, p = 0.001), Figure 6A.

For grade 3 or more severe adverse events, the occurrence of anemia significantly increased in the olaparib and abiraterone group (RR 7.47, 95% CI 1.36–40.88, p = 0.02). However, no significant differences were observed in the occurrence of other adverse events between the two groups (all adverse events: RR 1.07, 95% CI 0.94–1.22, p = 0.283; fatigue or asthenia: RR 1.62, 95% CI 0.68–3.87, p = 0.28; nausea: RR 0.67, 95% CI 0.11–4.07, p = 0.663; and diarrhea: RR 1.34, 95% CI 0.17–10.63, p = 0.779), as shown in Figure 6B.

4 Discussion

4.1 Findings and interpretations

To the best of our knowledge, this study is the first meta-analysis pooling the data from two RCTs involving a total of 938

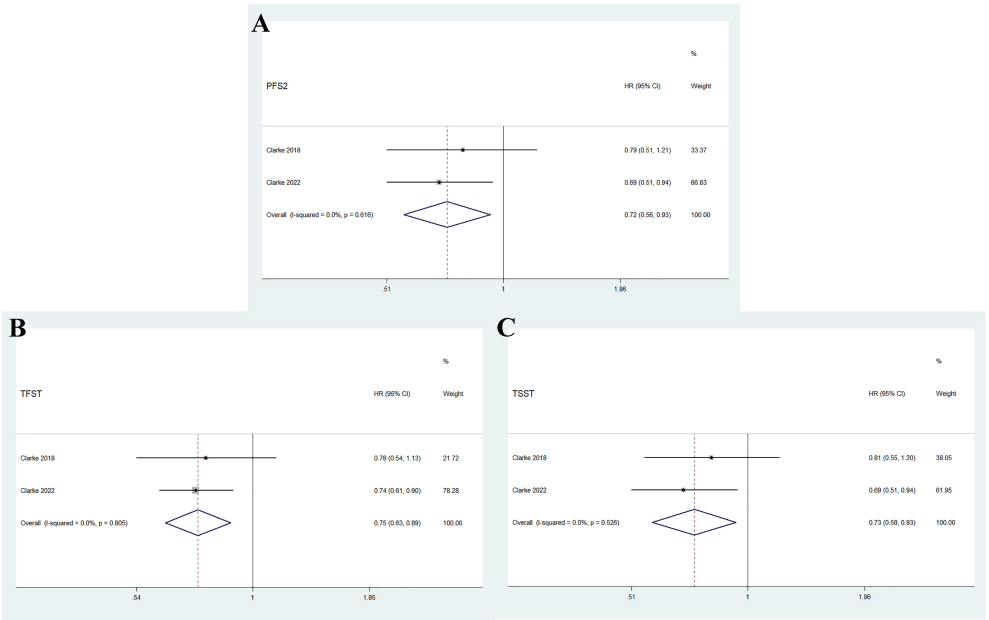

FIGURE 4
Forest plot of randomized controlled trials on olaparib combination therapy for secondary outcomes: PFS2 **(A)**, TFST **(B)**, and TSST **(C)**.

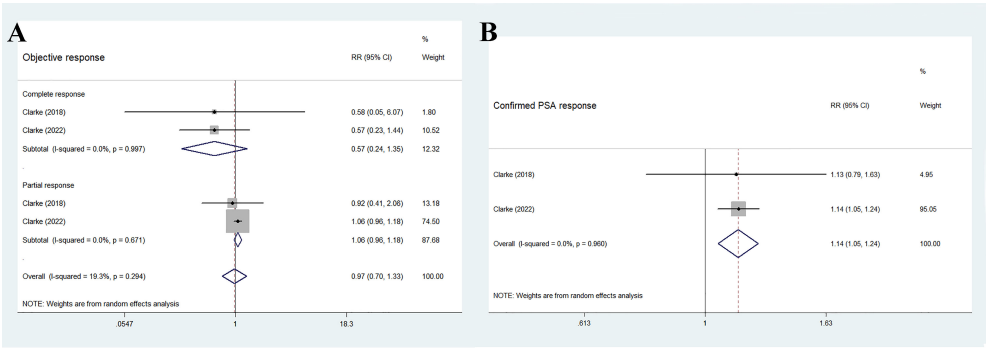

FIGURE 5
Forest plot of randomized controlled trials on olaparib combination therapy for secondary outcomes: ORR **(A)** and confirmed PSA response **(B)**.

patients with mCRPC, and comparing the combination use of olaparib with abiraterone versus abiraterone monotherapy. A key finding of this systematic review is that the olaparib combination therapy offers a considerable rPFS benefit for patients with mCPPC compared with abiraterone monotherapy. Furthermore, patients who received olaparib experienced significant benefits in terms of PFS2, TFST, TSST, and confirmed PSA response compared with those who received abiraterone. Meanwhile, the olaparib combination therapy showed a similar effect on OS, ORR, and several adverse events compared with abiraterone monotherapy.

The primary objective of this review was to evaluate the rPFS of olaparib in combination with abiraterone for patients with mCRPC. The data indicated that this combination offers a substantial rPFS benefit for patients with mCRPC, regardless of HRR mutation status (HR 0.66; 95% CI, 0.55–0.79; $p < 0.01$). Consistent with previous studies (10), the findings of the present study validated the synergistic interaction between PPAR inhibitor (olaparib) and androgen receptor antagonist (abiraterone), regardless of HRR mutation status. Previous studies (26–28) evaluating castration and androgen deprivation in prostate cancer revealed a potential connection between the androgen pathway and the DNA damage response. Inhibition of androgen signaling seems to decrease the expression of HRR genes and impair the ability of cells to repair DNA double-strand breaks, leading to increased sensitivity to RARP inhibition. This evidence could potentially elucidate the rationale behind the enhanced effectiveness of olaparib combination therapy.

The evaluation of the efficacy of anti-tumor drugs in clinical trials often relies on assessing the clinical outcome of OS (18). OS is considered one of the most important measures as it provides unambiguous and unbiased results. Positive outcomes in OS can serve as confirmatory evidence that a particular drug has potential to prolong life. However, in the present study, the combination of olaparib and abiraterone failed to show a statistically prolonged OS in patients with mCRPC. This finding may be attributed to factors such as the limited sample size and baseline prognostic factors (age, ECOG status and PSA concentration). A retrospective analysis of 15 studies demonstrated a robust correlation between PFS2 and OS, suggesting that PFS2 can serve as a reliable measure of long-term clinical benefit in cases where OS assessment is not feasible (29). By contrast, the present study showed a significant benefit in PFS2 (HR 0.72, 95% CI 0.56–0.93, $p < 0.05$). One plausible explanation for the

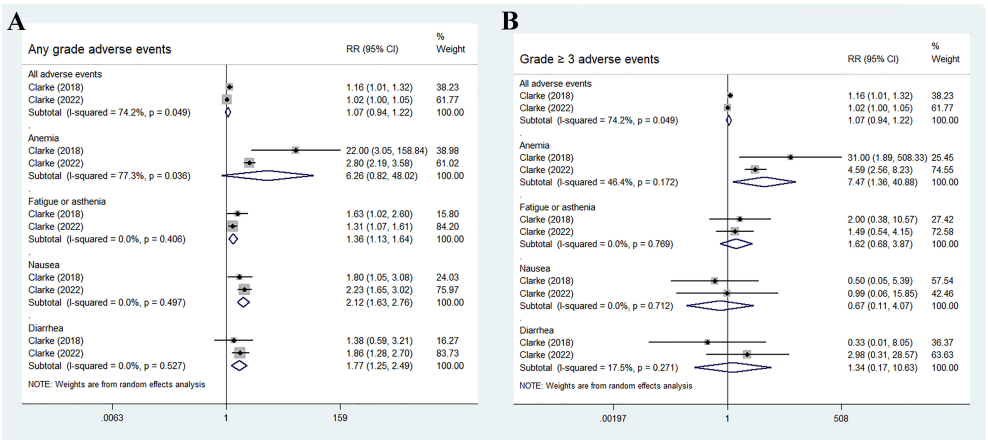

FIGURE 6
Forest plot of randomized controlled trials on olaparib combination therapy for secondary outcomes: any grades adverse events **(A)** and grade 3 or more severe adverse events **(B)**.

disparity observed between rPFS and OS could be the influence of crossover and post-progression therapies (30). In clinical practice, the need for immediate subsequent treatment following disease progression may not always be necessary, because the process of clinical decision-making should involve a comprehensive evaluation of the patient's physical health, tumor status, and clinical symptoms. Consequently, the time to subsequent therapy may be more clinically meaningful than the time to progression alone for patients. The findings of the present study suggested that the combination of olaparib and abiraterone has potential to prolong TFST (HR 0.75, 95% CI 0.63–0.89, $p < 0.01$) and TSST (HR 0.73, 95% CI 0.58–0.93, $p < 0.05$).

In this study, the ORR in the olaparib combination and control groups were 53.1% and 44.9%, respectively, without statistical significance (RR = 1.18, 95% CI 0.97–1.44, $p > 0.05$). The subgroup analysis revealed similar results for complete and partial responses ($p > 0.05$). However, a higher proportion of patients in the combination therapy group achieved a confirmed PSA response rate of at least 50% (349 [74.3%] of 470 patients) compared with the monotherapy group (304 [65.0%] of 468, RR 1.14, 95% CI 1.05–1.24, $p < 0.01$). A phase I clinical trial reported that abiraterone achieved a decline in PSA concentration in 58% of patients with mCRPC (31). In the present study, olaparib and abiraterone demonstrated a good activity in reducing PSA levels.

In this study, the four most commonly reported adverse events were anemia, fatigue or asthenia, nausea, and diarrhea. Olaparib combination therapy resulted in higher incidences of high-grade anemia and any-grade adverse events (fatigue or asthenia, nausea, and diarrhea; $p<0.05$) than abiraterone monotherapy, whereas similar effects were observed in the other adverse events ($p>0.05$). In total, 43.7% of patients in the olaparib combination group experienced any-grade anemia (16.0% had grade 3 or higher), compared with 14.1% of patients in the control group (2.8% had grade 3 or higher). A recent meta-analysis of 29 trials found that anemia is the most frequently reported hematological toxicity associated with PARPi (such as olaparib, rucaparib, veliparib, niraparib and talazoparib) when compared with alternative treatment (32). However, the underlying cause of anemia resulting from PARPi remains poorly understood. Preclinical evidence suggested that PARP-2 plays a crucial role in erythroid differentiation, and its deletion can lead to extravascular hemolytic anemia. This finding revealed that PARPi may influence hematopoiesis, potentially explaining the observed hematological adverse events in these studies (33, 34). Recent evidence revealed that olaparib induced temporary macrocytic anemia. However, the contribution of potential deficiencies in the vitamin B12 or folic acid pathway to the development of this anemia remains uncertain (35). A notable detail that additional toxicities were frequently observed, unrelated to hematological effects. For patients with underlying disorders, conducting a comprehensive evaluation of the risks and benefits, and closely monitoring safety during the initial stages of treatment are crucial. Considering these factors, healthcare professionals should be well-informed about the potential adverse events, including fatigue, nausea, and diarrhea, that may occur in patients receiving PARPi. They should also utilize laboratory tests, physical examinations, and clinical judgment before and during the treatment period to ensure thorough monitoring.

4.2 Strengths and limitations

This meta-analysis possesses several notable strengths, including a comprehensive search across relevant databases and the inclusion of recent high-quality, well-designed, randomized, double-blinded trials. To our knowledge, this review is the first to systematically explore the efficacy and safety of olaparib and abiraterone combination therapy in patients with mCRPC. However, this systematic review had some unavoidable limitations. Firstly, the investigation of the effect of olaparib in combination with abiraterone on patients with different HRR mutation statuses is limited by the current lack of available phase II/III trials. Second, the inclusion of OS as a secondary endpoint in this study does not provide direct evidence of clinical benefit. Lastly, the number of studies (<10) included in the analysis is limited, and funnel plotting or Egger's test was not conducted to assess the potential publication bias.

5 Conclusion

The analysis revealed that combination of olaparib and abiraterone significantly prolonged rPFS, PFS2, TFST, TSST and confirmed PSA response in patients with mCRPC. However, statistically significant differences were found in terms of OS and ORR. Regarding safety, no significant difference was observed in the incidence of adverse events between the olaparib combination group and the control group. The combination of olaparib and abiraterone was associated with increased incidence of high-grade anemia. Clinicians should consider the potential adverse events linked to these interventions in the context of clinical practice to enhance patients' health-related quality of life.

Data availability statement

The original contributions presented in the study are included in the article/Supplementary Material. Further inquiries can be directed to the corresponding authors.

Ethics statement

The studies involving human participants were reviewed and approved by Ethics Committee of the Ethics Committee of Longhua Hospital, Shanghai University of Traditional Chinese Medicine. The patients/participants provided their written informed consent for the publication in this study.

Author contributions

ZL: Writing – original draft, Writing – review & editing. BZ: Data curation, Writing – original draft. HX: Project administration, Writing – original draft, Writing – review & editing. LC: Data curation, Software, Writing – review & editing. XS: Formal Analysis,

Methodology, Writing – review & editing. YW: Formal Analysis, Validation, Writing – review & editing. RW: Writing – review & editing, Formal Analysis. JZ: Writing – review & editing, Methodology, Validation. YQ: Supervision, Formal Analysis, Resources, Writing – original draft, Writing – review & editing. JY: Writing – review & editing, Validation. YS: Writing – review & editing, Funding acquisition, Supervision, Writing – original draft

Funding

The research, authorship, and publication of this article were funded by the Natural Science Foundation of Shanghai, China (grant number: 23ZR1464100), the Science and technology development project of Shanghai University of Traditional Chinese Medicine (grant number: 23KFL070) and the National Natural Science Foundation of China (grant number: 82205114).

Acknowledgments

We would like to thank all the authors of the original studies included in this meta-analysis. The authors also thank Martin J. Booth for proof-reading the entire article to improve the use of English.

Conflict of interest

The authors declare that the research was conducted in the absence of any commercial or financial relationships that could be construed as a potential conflict of interest.

Publisher's note

Supplementary material

The Supplementary Material for this article can be found online at: https://www.frontiersin.org/articles/10.3389/fonc.2023.1265276/full#supplementary-material

References

1. Sung H, Ferlay J, Siegel RL, Laversanne M, Soerjomataram I, Jemal A, et al. Global cancer statistics 2020: GLOBOCAN estimates of incidence and mortality worldwide for 36 cancers in 185 countries. *CA Cancer J Clin* (2021) 71(3):209–49. doi: 10.3322/caac.21660

2. Schaeffer E, Srinivas S, Antonarakis ES, Armstrong AJ, Bekelman JE, Cheng H, et al. NCCN guidelines insights: Prostate cancer, version 1.2021. *J Natl Compr Canc Netw* (2021) 19(2):134–43. doi: 10.6004/jnccn.2021.0008

3. Pritchard CC, Mateo J, Walsh MF, De Sarkar N, Abida W, Beltran H, et al. Inherited DNA-repair gene mutations in men with metastatic prostate cancer. *N Engl J Med* (2016) 375(5):443–53. doi: 10.1056/NEJMoa1603144

4. Robinson D, Van Allen EM, Wu YM, Schultz N, Lonigro RJ, Mosquera JM, et al. Integrative clinical genomics of advanced prostate cancer. *Cell* (2015) 161(5):1215–28. doi: 10.1016/j.cell.2015.05.001

5. Abida W, Armenia J, Gopalan A, Brennan R, Walsh M, Barron D, et al. Prospective genomic profiling of prostate cancer across disease states reveals germline and somatic alterations that may affect clinical decision making. *JCO Precis Oncol* (2017) 2017:PO.17.00029. doi: 10.1200/PO.17.00029

6. Lord CJ, Ashworth A. PARP inhibitors: Synthetic lethality in the clinic. *Science*, (2017) 355(6330):1095–9203. doi: 10.1126/science.aam7344

7. Gonzalez-Padilla DA, Subiela JD. Are PARP inhibitors ready for prime time in metastatic prostate cancer? Maybe not. *Eur Urol* (2023) S0302-2838(23):02824-5. doi: 10.1016/j.eururo.2023.05.017

8. de Bono J, Mateo J, Fizazi K, Saad F, Shore N, Sandhu S, et al. Olaparib for metastatic castration-resistant prostate cancer. *N Engl J Med* (2020) 382(22):2091–102. doi: 10.1056/NEJMoa1911440

9. Attard G, Reid AH, Yap TA, Raynaud F, Dowsett M, Settatree S, et al. Phase I clinical trial of a selective inhibitor of CYP17, abiraterone acetate, confirms that castration-resistant prostate cancer commonly remains hormone driven. *J Clin Oncol* (2008) 26(28):4563–71. doi: 10.1200/JCO.2007.15.9749

10. Asim M, Tarish F, Zecchini HI, Sanjiv K, Gelali E, Massie CE, et al. Synthetic lethality between androgen receptor signalling and the PARP pathway in prostate cancer. *Nat Commun* (2017) 8(1):374. doi: 10.1038/s41467-017-00393-y

11. Li LA-O, Karanika S, Yang G, Wang J, Park S, Broom BA-O, et al. Androgen receptor inhibitor-induced "BRCAness" and PARP inhibition are synthetically lethal for castration-resistant prostate cancer. *Sci Signal* (2017) 10(480):eaam7479. doi: 10.1126/scisignal.aam7479

12. Fazekas T, Szeles AD, Teutsch B, Csizmarik A, Vekony B, Varadi A, et al. Therapeutic sensitivity to standard treatments in BRCA positive metastatic castration-resistant prostate cancer patients-a systematic review and meta-analysis. *Prostate Cancer Prostatic Dis* (2022). doi: 10.1038/s41391-022-00626-2

13. Rizzo A, Mollica V, Merler S, Morelli F, Sorgentoni G, Oderda M, et al. Incidence of grade 3-4 adverse events, dose reduction, and treatment discontinuation in castration-resistant prostate cancer patients receiving PARP inhibitors: A meta-analysis. *Expert Opin Drug Metab Toxicol* (2022) 18(3):235–40. doi: 10.1080/17425255.2022.2072727

14. Niazi M, Jahangir A, Sahra S, Sattar S, Asti D, Bershadskiy A. Efficacy of PARP inhibitors as maintenance therapy for metastatic castration-resistant prostate cancer: A meta-analysis of randomized controlled trials. *Oncol (Williston Park)* (2021) 35 (11):708–15. doi: 10.46883/ONC.2021.3511.0708

15. Wu K, Liang J, Shao Y, Xiong S, Feng S, Li X. Evaluation of the efficacy of PARP inhibitors in metastatic castration-resistant prostate cancer: A systematic review and meta-analysis. *Front Pharmacol* (2021) 12:777663. doi: 10.3389/fphar.2021.777663

16. Moher D, Shamseer L, Clarke M, Ghersi D, Liberati A, Petticrew M, et al. Preferred reporting items for systematic review and meta-analysis protocols (PRISMA-P) 2015 statement. *Systematic Rev* (2015) 4(1):1. doi: 10.1186/2046-4053-4-1

17. Scher HI, Morris MJ, Stadler WM, Higano C, Basch E, Fizazi K, et al. Trial design and objectives for castration-resistant prostate cancer: Updated recommendations from the prostate cancer clinical trials working group 3. *J Clin Oncol* (2016) 34(12):1402–18. doi: 10.1200/JCO.2015.64.2702

18. Driscoll JJ, Rixe O. Overall survival: Still the gold standard: Why overall survival remains the definitive end point in cancer clinical trials. *Cancer J* (2009) 15(5):401–5. doi: 10.1097/PPO.0b013e3181bdc2e0

19. Denmeade S, Wang H, Agarwal N, Smith D, Schweizer M, Stein M, et al. TRANSFORMER: A randomized phase II study comparing bipolar androgen therapy versus enzalutamide in asymptomatic men with castration-resistant metastatic prostate cancer. *J Clin Oncol* (2021) 39(12):1371–82. doi: 10.1200/JCO.20.02759

20. Scher HI, Halabi S, Tannock I, Morris M, Sternberg CN, Carducci MA, et al. Design and end points of clinical trials for patients with progressive prostate cancer and castrate levels of testosterone: Recommendations of the prostate cancer clinical trials working group. *J Clin Oncol* (2008) 26(7):1148–59. doi: 10.1200/JCO.2007.12.4487

21. Arrieta O, Barrón F, Padilla MS, Avilés-Salas A, Ramírez-Tirado LA, Arguelles Jiménez MJ, et al. Effect of metformin plus tyrosine kinase inhibitors compared with tyrosine kinase inhibitors alone in patients with epidermal growth factor receptor-

mutated lung adenocarcinoma: A phase 2 randomized clinical trial. *JAMA Oncol* (2019) 5(11):e192553. doi: 10.1001/jamaoncol.2019.2553

22. van Houwelingen HC, Arends Lr Fau - Stijnen T, Stijnen T. Advanced methods in meta-analysis: Multivariate approach and meta-regression. *Stat Med* (2002) 21 (4):589–624. doi: 10.1002/sim.1040

23. Higgins JP, Thompson SG. Quantifying heterogeneity in a meta-analysis. *Stat Med* (2002) 21:1539–58. doi: 10.1002/sim.1186

24. Clarke N, Wiechno P, Alekseev B, Sala N, Jones R, Kocak I, et al. Olaparib combined with abiraterone in patients with metastatic castration-resistant prostate cancer: A randomised, double-blind, placebo-controlled, phase 2 trial. *Lancet Oncol* (2018) 19(7):975–86. doi: 10.1016/S1470-2045(18)30365-6

25. Clarke NW, Armstrong AJ, Thiery-Vuillemin A, Oya M, Shore N, Loredo E, et al. Abiraterone and olaparib for metastatic castration-resistant prostate cancer. *NEJM Evidence* (2022) 1(9). doi: 10.1056/EVIDoa2200043

26. Spritzer CE, Fau AP, Fau VE, Fau TJ, Fau MK, Fau FA, et al. Bone marrow biopsy: RNA isolation with expression profiling in men with metastatic castration-resistant prostate cancer–factors affecting diagnostic success. *Radiology* (2013) 269 (3):816–23. doi: 10.1148/radiol.13121782

27. Jimenez RE, Atwell TD, Sicotte H, Eckloff B, Wang L, Barman P, et al. A prospective correlation of tissue histopathology with nucleic acid yield in metastatic castration-resistant prostate cancer biopsy specimens. *Mayo Clin Proc Innov Qual Outcomes* (2019) 3(1):14–22. doi: 10.1016/j.mayocpiqo.2018.12.005

28. Zheng G, Lin MT, Lokhandwala PM, Beierl K, Netto GJ, Gocke CD, et al. Clinical mutational profiling of bone metastases of lung and colon carcinoma and Malignant melanoma using next-generation sequencing. *Cancer Cytopathol* (2016) 124 (10):744–53. doi: 10.1002/cncy.21743

29. Chowdhury S, Mainwaring P, Zhang L, Mundle S, Pollozi E, Gray A, et al. Systematic review and meta-analysis of correlation of progression-free survival-2 and overall survival in solid tumors. *Front Oncol* (2020) 10:1349. doi: 10.3389/fonc.2020.01349

30. Ledermann JA. PARP inhibitors in ovarian cancer. *Ann Oncol* (2016) 27(Suppl 1):i40–i4. doi: 10.1093/annonc/mdw094

31. Ryan CJ, Smith MR, Fong L, Rosenberg JE, Kantoff P, Raynaud F, et al. Phase I clinical trial of the CYP17 inhibitor abiraterone acetate demonstrating clinical activity in patients with castration-resistant prostate cancer who received prior ketoconazole therapy. *J Clin Oncol* (2010) 28(9):1481–8. doi: 10.1200/JCO.2009.24.1281

32. Wang C, Li J. Haematologic toxicities with PARP inhibitors in cancer patients: An up-to-date meta-analysis of 29 randomized controlled trials. *J Clin Pharm Ther* (2021) 46(3):571–84. doi: 10.1111/jcpt.13349

33. Wu J, Chen WK, Zhang W, Zhang JS, Liu JH, Jiang YM, et al. Network meta-analysis of the efficacy and adverse effects of several treatments for advanced/metastatic prostate cancer. *Oncotarget* (2017) 8(35):59709–19. doi: 10.18632/oncotarget.19810

34. Farrés J, Martín-Caballero J Fau - Martínez C, Martínez C Fau - Lozano JJ, Lozano Jj Fau - Llacuna L, Llacuna L Fau - Ampurdanés C, Ampurdanés C Fau - Ruiz-Herguido C, et al. Parp-2 is required to maintain hematopoiesis following sublethal γ-irradiation in mice. *Blood* (2013) 122(1):44–54. doi: 10.1182/blood-2012-12-472845

35. Takenaka M FT, Bomoto Y, Murase S. Ep993 macrocytosis associated with olaparib. *Int J Of Gynecological Cancer* (2019) 29(Suppl4):A524. doi: 10.1136/ijgc-2019-ESGO.1037

frontiers | Frontiers in Oncology

TYPE Case Report
PUBLISHED 10 October 2023
DOI 10.3389/fonc.2023.1221027

OPEN ACCESS

EDITED BY
Philippe E. Spiess,
Moffitt Cancer Center, United States

REVIEWED BY
Kun Pang,
Xuzhou Central Hospital, China
Kehua Jiang,
Guizhou Provincial People's Hospital, China
Yongbao Wei,
Fujian Provincial Hospital, China

*CORRESPONDENCE
Hongying Zhang
hy_zhang@scu.edu.cn;
hy_zh@263.net

†These authors have contributed equally to this work

RECEIVED 07 June 2023
ACCEPTED 18 September 2023
PUBLISHED 10 October 2023

CITATION
Cui J, Peng R, Zhang Y, Lu Y, He X, Chen M and Zhang H (2023) Case Report: Primary low-grade dedifferentiated liposarcoma of the urinary bladder with molecular confirmation. *Front. Oncol.* 13:1221027. doi: 10.3389/fonc.2023.1221027

Case Report: Primary low-grade dedifferentiated liposarcoma of the urinary bladder with molecular confirmation

Jian Cui†, Ran Peng†, Yahan Zhang, Yang Lu, Xin He, Min Chen and Hongying Zhang*

Department of Pathology, West China Hospital, Sichuan University, Chengdu, China

Liposarcomas originating in the urinary bladder are extremely rare. Only six cases of bladder liposarcoma have been reported, and all have been described as myxoid liposarcomas. Notably, none of the patients underwent molecular testing. Here, we report a dedifferentiated liposarcoma (DDL) that occurred in the urinary bladder, primarily in a 69-year-old Chinese woman, with infrequent low-grade dedifferentiation. Computed tomography (CT) revealed an ill-defined solid mass in the anterior bladder wall. The patient underwent a partial bladder resection. Histologically, the tumor cells with mild-to-moderate nuclear atypia were arranged in fascicular and storiform patterns, mimicking a low-grade fibroblastic tumor. In addition, scattered small foci of typical lipoma-like well-differentiated components were identified. Immunohistochemically, the tumor tested positivity for MDM2, CDK4, and p16. Fluorescence *in situ* hybridization revealed *MDM2* gene amplification in the neoplastic cells. Whole-exome sequencing showed that this tumor also harbored *CDK4*, *TSPAN31*, and *JUN* amplification. At the latest follow-up (85 months after surgery), the patient was alive, with no evidence of disease. To the best of our knowledge, this is the first example of a molecularly confirmed primary bladder liposarcoma and the first case of DDL at this site.

KEYWORDS

atypical lipomatous tumor/well-differentiated liposarcoma, dedifferentiated liposarcoma, urinary bladder, 12q13-15 amplification, MDM2 amplification, JUN amplification, whole exome sequencing

1 Introduction

Liposarcoma is one of the most common soft tissue sarcomas (STSs) among adults, accounting for approximately 15%–20% of all STSs (1). According to the latest World Health Organization (WHO) classification of soft tissue and bone tumors, liposarcoma is divided into four principal subtypes: atypical lipomatous tumor/well-differentiated liposarcoma/dedifferentiated liposarcoma (ALT/WDL/DDL), myxoid liposarcoma (ML),

pleomorphic liposarcoma (PL), and myxoid pleomorphic liposarcoma (MPL). ALT/WDL/DDL has the highest incidence (>50%) and harbors specific genetic features—12q13-15 amplification, including *MDM2*, *CDK4*, *FRS2*, and *CPM*. In particular, *MDM2* is amplified in almost all cases of ALT/WDL/DDL, and detection of *MDM2* amplification by fluorescence *in situ* hybridization (FISH) has been recognized as the gold standard for the diagnosis of this tumor (2). The term "ALT" has been introduced to emphasize superficial soft tissue masses (2). WDL often occurs in central anatomic sites, such as the retroperitoneum and mediastinum, where tumors are more likely to be removed incompletely and are associated with frequent recurrence (2). DDL accounts for 18%–20% of liposarcomas and arises mostly in the retroperitoneum (3). Accounting for 20%–30% of liposarcomas, ML typically occurs in the extremities and is characterized by *FUS/EWSR1::DDIT3* fusion. PL represents less than 5% of liposarcomas and often arises in the extremities and trunk with complex chromosomal alterations. MPL, an emerging new subtype, is extremely rare and shows a predilection for the mediastinum in young patients.

Bladder sarcomas account for <5% of all bladder tumors (4). Primary liposarcoma arising from the urinary bladder is extremely rare, with only six cases reported in the English literature (5–10), all of which have been described as ML. Most importantly, all reported cases lacked genetic confirmation. Here, we report the first case of primary DDL of the urinary bladder, in which the dedifferentiated area exhibited a low-grade fibromatosis-like appearance. Notably, genetic alterations were identified using various methods in this case.

2 Methods

2.1 Immunohistochemistry

The specimens were formalin-fixed paraffin-embedded (FFPE) and cut into 4-μm sections for examination. Standard immunohistochemical staining was performed using the EnVision Plus detection system (DAKO, Carpinteria, CA, USA) with positive and negative controls. Information on the antibodies is presented in Supplementary Table 1.

2.2 Fluorescence *in situ* hybridization

The Vysis LSI *MDM2* Spectrum Orange Probe (Abbott Molecular, Des Plaines, IL, USA), GSP *CDK4* Gene Amplification Probe and *FRS2* Probe (Anbiping, Guangzhou, China) were used for *MDM2*, *CDK4*, and *FRS2* amplification. *ALK* rearrangement was performed using the Vysis LSI *ALK* Dual Color Break Apart Rearrangement Probe (Abbott Molecular, Des Plaines, IL, USA). FISH tests were performed according to an established protocol (11).

The sections were scored by two investigators and ≥100 cells were counted. Amplification was defined as an average *MDM2*/CEP12 ratio, *FRS2*/CEP12 ratio, and *CDK4*/CSP12 ratio ≥2.0, while a ratio <2.0 was considered non-amplified (11, 12). Positivity for *ALK* rearrangement was considered when ≥15% of nuclei displayed split signals or when single red signals were observed.

2.3 Detection of *CTNNB1* mutation

The primers for *CTNNB1* gene mutation polymerase chain reaction (PCR) detection were *CTNNB1*-F: 5'TCCAATC TACTAATGCTAATACTGTTTCGTA3' and *CTNNB1*-R: 5' TCCAATCTACTAATGCTAATACTGTTTCGTA3'. Sanger sequencing was performed by BGI Genomics Co., Ltd. (Shenzhen, China).

2.4 Whole-exome sequencing

WES was performed by Novogene Technology Co., Ltd. (Beijing, China) on FFPE tissues to explore possible molecular abnormalities.

3 Case presentation

A 69-year-old female was admitted to our hospital with a one-month history of recurrent gross hematuria, accompanied by slight urgency and pain during urination. The patient had no history of trauma or infection. Physical examination revealed an approximately 5 cm × 4 cm palpable fixed smooth mass in the hypogastrium with no tenderness or rebound tenderness. Urine cytology revealed an increased number of leukocytes with no heterotypic cells or red blood cells. Computed tomography showed an ill-defined solid mass in the anterior wall of the bladder (Figure 1). During cystoscopy, the mucous membrane of the bladder wall appeared smooth with no evidence of novel organisms on the surface. Additionally, a bulge was identified at the bladder dome with a normal overlying urothelial mucosa. The biopsy indicated "chronic inflammation of the mucosa and lamina propria fibrous hyperplasia." Subsequently, the patient underwent transurethral partial resection of the bladder tumor (TUR-BT). Despite no visible abnormalities in the bladder mucosa, a mass deep in the muscle layer was identified in the bladder dome during TUR-BT. Regrettably, the biopsy after TUR-BT still exhibited no signs of the tumor. After evaluation and communication with the patient, who expressed a strong desire to preserve the bladder, median laparotomy and bladder exploration were performed. During this surgery, a mass was identified adhering to the apex of the bladder, pubic symphysis, and peritoneum and was completely resected together with part of the bladder and peritoneum.

Macroscopic examination revealed a partially excised bladder measuring 7 cm × 7 cm × 5 cm. The overlying urothelium is rough. Thickening of the bladder wall was almost completely replaced by gray-white woven lesions, which showed diffuse infiltrative growth into perivesical soft tissues. On the cut surface, a gray-white and tough mass resembled the scar tissue.

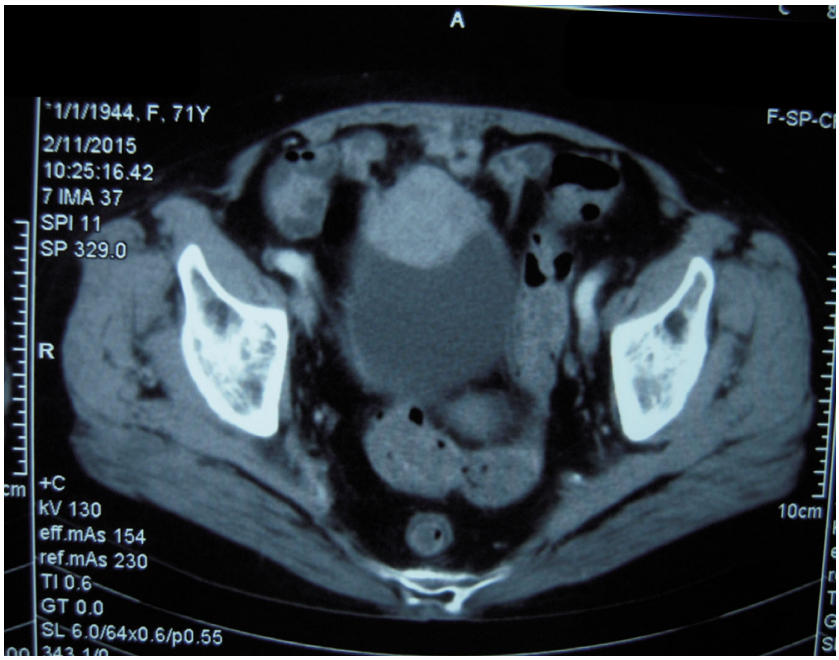

FIGURE 1
Abdominal computed tomography showed an irregular mass on the anterior wall of the bladder, which involved all layers of the bladder.

Microscopically, the urothelium and lamina propria of the bladder showed no abnormalities (Figure 2A). The muscle layer of the bladder and peripheral adipose tissue contained spindle cells, which were arranged in a fascicular growth pattern with mild to moderate atypia and hyperchromatic nuclei, mimicking low-grade fibroblastic tumors (Figure 2B). Pump spindle and scattered inflammatory cells were observed in the superficial layer of the muscularis propria (Figure 2C). Additionally, in the deep layers of the muscularis propria and serosa, slender spindle cells arranged in a fascicular growth pattern were separated by abundant eosinophilic collagen (Figure 2D). Bizarre and hyperchromatic stromal cells were observed in these areas (Figure 2E). Notably, small foci of typical lipoma-like WDL components were identified within the background of the spindle cell tumor using extensive sampling (Figure 2F). The surgical cautery margin was negative and the peritoneal tissue was normal. This lesion was classified morphologically as grade 2 using the Fédération Nationale des Centers de Lutte Contre le Cancer (FNCLCC) grading system, and the postoperative staging was T1N0M0 according to the TNM staging of soft tissues tumors.

Immunohistochemically, the neoplastic cells were positive for MDM2 (Figure 3A), CDK4 (Figure 3B), P16 (Figure 3C), smooth muscle actin (SMA), and focal positivity for muscle-specific antigen (MSA). The MIB-1 index value was 5%. Tests for Desmin, ALK-1, p63, CK7, PCK, S-100, CD34, EMA, and β-catenin were negative. FISH revealed *MDM2* and *CDK4* amplification in the spindle cells and adipocytes of the tumor (Figure 3D), whereas negative results was observed in the adipose components surrounding the bladder wall. There was no evidence of *FRS2* amplification, *ALK* rearrangement, or *CTNNB1* mutation. Further WES showed *TSPAN31* and *JUN* amplifications.

These findings were consistent with the ultimate diagnosis of low-grade fibromatosis-like DDL arising from the urinary bladder. The patient did not receive any adjuvant therapy other than close follow-up for surveillance. The surveillance plan involved regular physical examination with imaging (chest and abdomen CT scan) and urine tests 1 month after the operation, every 3–6 months for 3 years, and then annually. During an 85-month follow-up period, the patient was alive with no evidence of disease recurrence.

4 Discussion

This study describes a case of primary liposarcoma arising from the urinary bladder. Bladder mesenchymal tumors are rare, representing 1%–5% of all primary urinary bladder tumors, and leiomyomas and leiomyosarcomas are the most common benign and malignant mesenchymal tumors of the bladder, accounting for approximately 0.43% and 1% of all bladder tumors, respectively (13, 14). Although liposarcoma is one of the most common soft tissue sarcomas, it rarely occurs in the bladder. Only six cases of bladder liposarcoma have been reported in the English literature (5–10). The clinicopathological features of all published cases are summarized in Table 1.

All previously reported bladder liposarcomas were ML and round cell liposarcomas (high-grade ML). However, all published bladder ML studies lack genetic confirmation of the *FUS/EWSR1::DDIT3* fusion gene. In addition, ML occurs predominantly in the deep soft tissues of the extremities (especially the thigh) and rarely occurs in other sites, including the retroperitoneum. Previous studies proposed that there was no existence of true primary retroperitoneal ML, and these "retroperitoneal ML" were proven

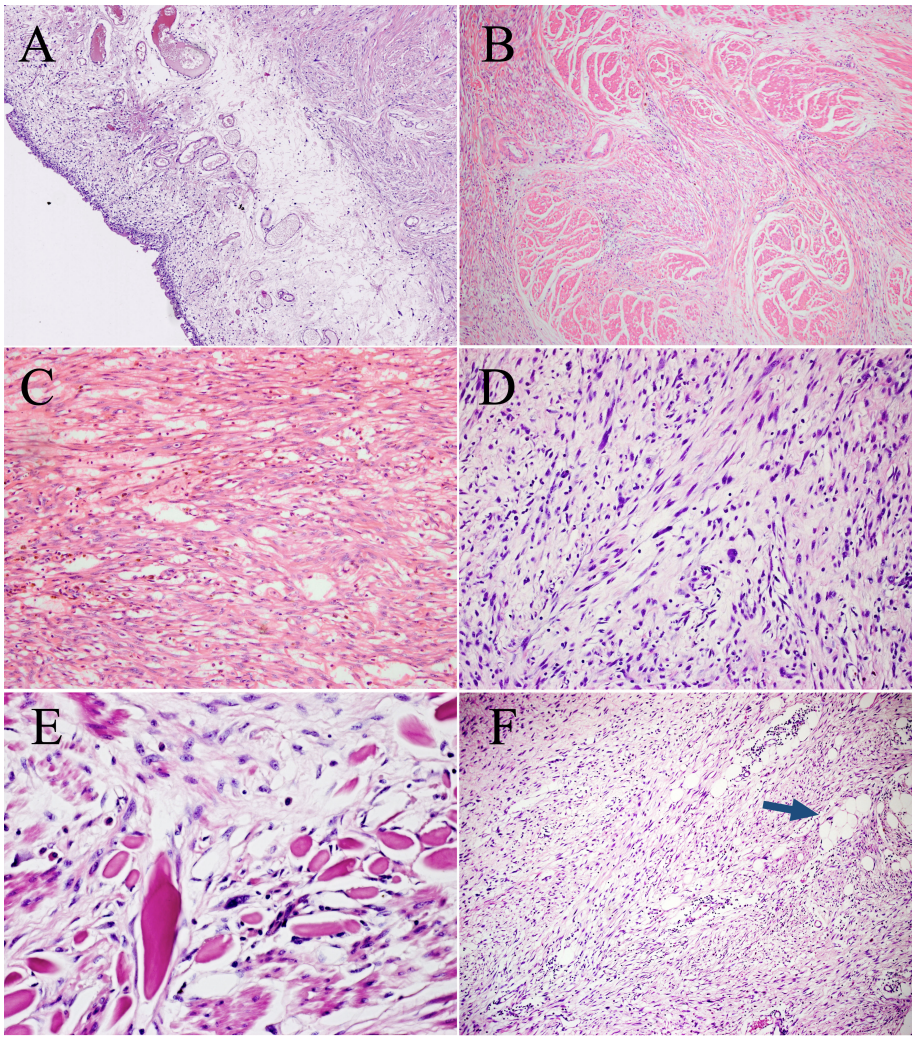

FIGURE 2
Microscopic features of the surgical resection sample. **(A)** The urothelium and lamina propria of the bladder show no abnormalities (H&E, ×100). **(B)** Bladder muscles were infiltrated to varying degrees by spindle cells. (H&E, ×100). **(C)** Pump spindle cells were mixed with a predominantly plasmacytic infiltrate (H&E, ×200). **(D)** The elongated spindle cells are arranged in a fascicular pattern (H&E, ×200). **(E)** Hyperchromatic tumor cells are observed within the background of spindle cells (H&E, ×400). **(F)** A few lipoma-like WDL components are identified (blue arrow, H&E, ×100).

as metastasis or DDL with myxoid-like changes (15, 16). Only 2.3% (5/214) of liposarcomas in the retroperitoneum were identified as primary ML by the detection of *DDIT3* arrangement in a large series study (17). Owing to the rarity of primary retroperitoneal ML, molecular genetic validation and examinations to exclude metastasis are required to confirm the primary retroperitoneal origin. Thus, it is possible that some of these reported bladder liposarcomas are not real primary ML. Some cases could be explained by the presence of myxoid-like stroma in sarcomas such as DDL, MPL, and undifferentiated sarcomas. Therefore, further studies with a larger series are needed to reveal whether there are unique features of liposarcomas occurring in the urinary bladder.

Notably, the current case exhibited peculiar low-grade fibroblastic tumor-like morphological features. DDL has a wide morphological spectrum, and most dedifferentiated areas exhibit an intermediate- to high-grade histological morphology, resembling undifferentiated pleomorphic sarcoma or myxofibrosarcoma. DDLs with low-grade differentiation have increasingly been recognized in recent years, and these dedifferentiated areas are histologically similar to low-grade myofibroblastic sarcoma, fibromatosis, or inflammatory myofibroblastic tumors (IMT) (18). Besides, this present lesion exhibited "pure" low-grade morphology. There are a limited number of cases of DDL entirely composed of low-grade dedifferentiated components, as low-grade and high-grade dedifferentiated areas commonly coexist.

The genetic results of this case, especially the amplification of genes in the 12q13-15 region, strongly supported the final diagnosis of DDL. However, all previously reported cases of bladder liposarcoma have lacked genetic confirmation. The current case is the first liposarcoma in the urinary bladder that was validated by molecular methods. Additionally, the results were negative for *FRS2* amplification. *FRS2* is located close to *MDM2* within the 12q13-15 region and is amplified in >90% of ALT/WDL/DDL and low-grade

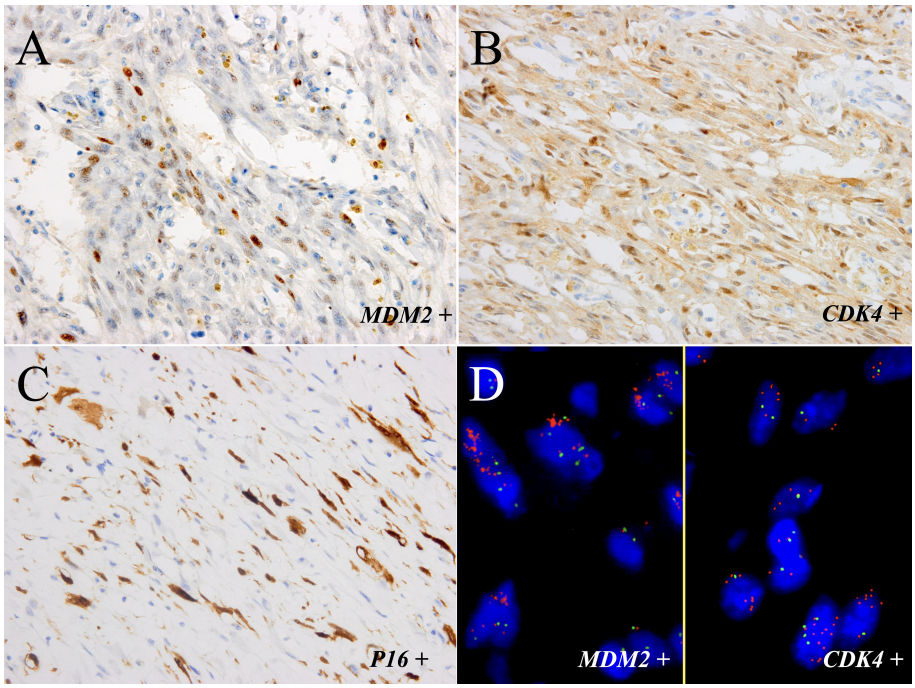

FIGURE 3
The tumor components of the sample were positive for MDM2 **(A)** and CDK4 **(B)** and focal positivity for P16 **(C)** (immunostaining, ×400). **(D)** FISH showed amplification of *MDM2* and *CDK4* in most neoplastic cells (left part: *MDM2*; right part: *CDK4;* red signals represent *MDM2* and *CDK4*, respectively. Green signals represent chromosome 12 centromeres (magnification: ×1000).

osteosarcoma cases (19, 20). Jing et al. (19) summarized 146 consecutive cases of ALT/WDL/DDL and identified 10 cases of *MDM2*(+)/*FRS2*(−) ALT/WDL/DDL (6.8%; including seven ALT/WDLs and three DDLs). All three previously reported *MDM2*(+)/*FRS2*(−) DDLs were in peripheral sites, and their dedifferentiation components included two homologous pleomorphic liposarcoma-like and one intermediate-grade fibrosarcoma-like. The present case represents the first case of *MDM2*(+)/*FRS2*(−) DDL located in a central site with a low-grade dedifferentiated area. Furthermore, amplification of the *JUN* gene was identified in this lesion. Outside of 12q13-15, amplification of 1p32 (including *JUN*) and 6q23 (including *ASK1*)

TABLE 1 Clinicopathological features of primary liposarcoma of the bladder in published English-language literatures.

Case No.	References (Published time)	Age/ Sex	Subtype	Size (cm)	Symptoms/ Preoperative Duration	IHC	Treatment	Outcome/ Follow-up duration	Genetic result
1	Rosi et al. (1983) (5)	36/M	Myxoid	2.5	Hematuria/NA	NA	Partial cystectomy	ANED/30 months	ND
2	Widdison et al. (1989) (6)	57/F	Myxoid	3.5	Hematuria/1 year	NA	Partial cystectomy	ANED/3 months	ND
3	Kunze et al. (1994) (7)	76/M	Round cell	15.0	NA	NA	NA	NA	ND
4	Biernat et al. (1996) (8)	36/F	Myxoid	NA	NA	NA	NA	NA	ND
5	Delport et al. (2021) (9)	57/F	Myxoid/round cell	6.9	Macrohematuria/ 30 years	NA	Incomplete TURBT	ANED/24 month	ND
6	Chudal et al. (2021) (10)	26/F	Myxoid	21.7	Abdominal mass/1 month	NA	Surgery and chemotherapy	NA	ND
7	Current case	68/F	Dedifferentiated	3.0	Hematuria/1 month	MDM2 (+), CDK4 (+), P16 (+)	Partial cystectomy	ANED/85 months	*MDM2, CDK4, TSPAN31*, and *JUN* amplified

F, Female; M, Male; NA, not available; ND, not done;+ positive; -, negative; ANED, alive, no evidence of disease; DOD, dead of disease; IHC, Immunohistochemistry; TURBT, transurethral resection of bladder tumor.

was observed in both ALT/WDL and DDL but was more correlated with undifferentiated histology (21–23). The detection of *JUN* amplification in this tumor could further assist in the diagnosis of the DDL subtype.

The overlapping clinical and histological features between this case and several spindle cell lesions resulted in diagnostic dilemmas (24). Misdiagnosis can easily occur, particularly when well-differentiated components are obscured. Differential diagnoses in this case included secondary DDL, cellular ALT/WDL, bladder sarcomatoid carcinoma (SC), and other more common bladder mesenchymal tumors, such as IMT, desmoid-type fibromatosis (DF), and rhabdomyosarcoma (RMS).

Owing to the rarity of bladder liposarcoma, the possibility of secondary DDL should first be excluded. However, the patient did not have a history of liposarcoma, and imaging examinations did not reveal any evidence of a tumor other than the bladder. More importantly, the distinction of *MDM2* amplification between mass and adipose tissue outside the bladder wall suggested that the tumor originated from the bladder.

Cellular ALT/WDL and DDL share overlapping histological features and common genetic alterations. However, cellular ALT/WDL is partly composed of adipocytic proliferation and contains atypical adipocytes or lipoblasts, whereas dedifferentiated areas of DDL are usually non-lipogenic. The overwhelming rate of fibroblastic tumor-like histology and hyperchromatic stromal cells with moderate atypia in this case was favorable for the diagnosis of DDL. The survival of DDL was shorter than that of cellular ALT/WDL in a study by Evans et al. (25). Although there were no signs of recurrence or metastasis in the current case, regular close follow-up is necessary.

SC would be indistinguishable from liposarcoma when SC with a heterologous liposarcoma component. However, only three cases of bladder SC with a liposarcomatous component have been reported (26–28). It should be noted that no carcinomatous component was identified, whereas a lipoma-like WDL component was found by wide sampling in our case. Combined with the negativity for epithelial markers and the amplification of several genes in 12q13-15 in this case, the diagnosis of DDL was more appropriate.

IMT, DF, and RMS appear to be the most common tumor types in the urinary bladder. Moreover, the dedifferentiated area in this case exhibited peculiar low-grade fibroblastic tumor-like morphological features mimicking IMT and DF. However, the identification of a typical lipoma-like WDL component, along with the absence of *ALK* rearrangement and the negativity of β-catenin and *CTNNB1* mutations, did not support the diagnosis of IMT and DF, respectively (29, 30). RMS mainly occurs in children and adolescents, is characterized by small primary round cells, and usually exhibits a high rate of mitotic activity, which differs from the demonstration in this case. Most importantly, detection of *MDM2* gene amplification by FISH in this lesion further confirmed the correct diagnosis of DDL.

Imaging, cystoscopy, and histopathological diagnosis with cystoscopy biopsy and TUR-BT were performed in this patient to comprehensively evaluate and opt for the optimum treatment. However, cystoscopy and TUR-BT biopsies were both too shallow to reach the muscle layer of the bladder where the tumor was located. The patient ultimately underwent partial bladder resection rather than a cystectomy. This consideration was made in view of the patient's desire to retain the bladder and the identification that the tumor was confined to the bladder during surgery, and the surrounding tissue was removed as much as possible to achieve a negative margin. Although the patient did not undergo postoperative chemoradiotherapy due to personal choice, close and regular follow-up ensured that any tumor progression could be managed promptly. Notably, both *MDM2* and *CDK4* were amplified in this tumor, which could provide an opportunity for the patient to benefit from targeted therapy. *CDK4* inhibitors, such as palbociclib, have recently been approved for clinical treatment of *CDK4*+ liposarcoma (31). *MDM2* is the most important driver gene of ALT/WDL/DDL, and although it is still being tested in clinical trials, it holds promise as an effective treatment option, especially for patients with disease recurrence or tumor metastasis (32).

Notably, this case had a favorable prognosis, and no recurrence or metastasis was observed 85 months after surgery. Extensive surgical resection with negative margins may be the main reason (33). Additionally, although malignant, DDL generally has a relatively better prognosis than most sarcomas, and the lesion is morphologically low-grade. Studies have indicated that low-grade DDL has longer survival times than high-grade DDL (34). Several studies have consistently demonstrated that increased *CDK4* amplification is strongly correlated with poor outcomes, and *CDK4* amplification levels are significantly higher in high-grade DDL than in low-grade DDL (23, 35). Despite the need for more studies based on large series for validation, the *MDM2*(+)/*FRS2*(−) genotype in this case has been reported to be associated with indolent clinical behavior (19, 20). Nevertheless, the current case harbored *JUN* amplification, which has been reported to be related to shorter recurrence-free survival time and poor prognosis in ALT/WDL/DDL (23). However, in that previous study, the comparison between amplification and non-amplification groups did not rule out the effect of subtype while *JUN* amplification has been known to be associated with DDL, which represents the subtype with a poorer outcome. The relationship between *JUN* amplification and liposarcoma prognosis requires further study. Notably, anatomical location is the most important prognostic factor for liposarcoma, and retroperitoneal liposarcomas generally exhibit the worst clinical behavior (2). This implies that bladder DDL have a poor prognosis. Although this case has shown a good prognosis during the follow-up period, it has been reported that almost all retroperitoneal DDLs recur locally if the follow-up duration is longer than 10 years (2). Therefore, the follow-up time in this specific case may have been insufficient. More cases and further extensive research are required to reveal the prognosis of bladder liposarcoma.

In conclusion, we report an exceedingly rare case of primary low-grade fibroblastic tumor-like DDL occurring in the urinary bladder, which should be the first genetically confirmed example using various methods. Additional cases and further studies are needed to explore the clinicopathological features of bladder liposarcomas. For cases arising from rare sites, careful histological inspection and rational application of molecular detection can be valuable for making a correct diagnosis.

Data availability statement

The original contributions presented in the study are included in the article/Supplementary Materials. Further inquiries can be directed to the corresponding author.

Ethics statement

The studies involving humans were approved by the Ethics Committee for Research in Human Beings of West China Hospital of Sichuan University. The studies were conducted in accordance with the local legislation and institutional requirements. The participants provided their written informed consent to participate in this study. Written informed consent was obtained from the individual(s) for the publication of any potentially identifiable images or data included in this article. Written informed consent was obtained from the participant/patient(s) for the publication of this case report. Written informed consent was obtained from the participant/patient(s) for the publication of this case report.

Author contributions

JC and RP analyzed the data and prepared the manuscript. YZ collected the clinicopathological data of the patient. YL and MC helped with molecular experiments. XH helped histopathology review. HZ was responsible for the diagnosis, study design and the manuscript revision. All authors contributed to the article and approved the submitted version.

Funding

This work was supported by the National Natural Science Foundation of China (No. 81972520).

Conflict of interest

The authors declare that the research was conducted in the absence of any commercial or financial relationships that could be construed as a potential conflict of interest.

Publisher's note

Supplementary material

The Supplementary Material for this article can be found online at: https://www.frontiersin.org/articles/10.3389/fonc.2023.1221027/full#supplementary-material

References

1. Lee A, Thway K, Huang PH, Jones RL. Clinical and molecular spectrum of liposarcoma. *J Clin Oncol* (2018) 36:151–9. doi: 10.1200/JCO.2017.74.9598

2. Antonescu CR, Blay J-Y, Bovee JVMG, Bridge JA, Cunha IW, Dei Tos AP, et al. *World Health Organization classifcation of tumours of soft tissue and bone. 5th ed*. Lyon: IARC Press (2020).

3. Coindre JM, Pedeutour F, Aurias A. Well-differentiated and dedifferentiated liposarcomas. *Virchows Arch* (2010) 456:167–79. doi: 10.1007/s00428-009-0815-x

4. Spiess PE, Kassouf W, Steinberg JR, Tuziak T, Hernandez M, Tibbs RF, et al. Review of the m.d. Anderson experience in the treatment of bladder sarcoma. *Urol Oncol* (2007) 25:38–45. doi: 10.1016/j.urolonc.2006.02.003

5. Rosi P, Selli C, Carini M, Rosi MF. Myxoid liposarcoma of the bladder. *J Urol* (1983) 130:560–1. doi: 10.1016/s0022-5347(17)51304-x

6. Widdison AD, Feneley RC. Liposarcoma of the bladder. *Br J Urol* (1989) 64:655–6. doi: 10.1111/j.1464-410x.1989.tb05336.x

7. Kunze E, Theuring F, Kruger G. Primary mesenchymal tumors of the urinary bladder. A histological and immunohistochemical study of 30 cases. *Pathol Res Pract* (1994) 190:311–32. doi: 10.1016/S0344-0338(11)80404-8

8. Biernat W, Salska Z, Biernat S. Myxoid liposarcoma of the urinary bladder. *Pol J Pathol* (1996) 47:41–3.

9. Delport JE, Makamba K. Early radical cystectomy with negative margins in a 57-year-old female with myxoid/round cell liposarcoma of the bladder suggests prolonged overall survival. *Afr J Urol* (2021) 27:52. doi: 10.1186/s12301-021-00152-y

10. Chudal S, Poudyal S, Chapagain S, Luitel BR, Chalise PR, Sharma UK. Myxoid liposarcoma of bladder: a rare case. *Int J Surg Case Rep* (2021) 79:116–8. doi: 10.1016/j.ijscr.2020.12.088

11. Zhang H, Erickson-Johnson M, Wang X, Oliveira JL, Nascimento AG, Sim FH, et al. Molecular testing for lipomatous tumors: critical analysis and test recommendations based on the analysis of 405 extremity-based tumors. *Am J Surg Pathol* (2010) 34:1304–11. doi: 10.1097/PAS.0b013e3181e92d0b

12. Peng R, Li N, Lan T, Chen H, Du T, He X, et al. Liposarcoma in children and young adults: a clinicopathologic and molecular study of 23 cases in one of the largest institutions of China. *Virchows Arch* (2021) 479:537–49. doi: 10.1007/s00428-021-03076-8

13. Cornella JL, Larson TR, Lee RA, Magrina JF, Kammerer-Doak D. Leiomyoma of the female urethra and bladder: report of twenty-three patients and review of the literature. *Am J Obstet Gynecol* (1997) 176:1278–85. doi: 10.1016/s0002-9378(97)70346-6

14. Rodriguez D, Preston MA, Barrisford GW, Olumi AF, Feldman AS. Clinical features of leiomyosarcoma of the urinary bladder: analysis of 183 cases. *Urol Oncol* (2014) 32:958–65. doi: 10.1016/j.urolonc.2014.01.025

15. de Vreeze RS, de Jong D, Tielen IH, Ruijter HJ, Nederlof PM, Haas RL, et al. Primary retroperitoneal myxoid/round cell liposarcoma is a nonexisting disease: an immunohistochemical and molecular biological analysis. *Mod Pathol* (2009) 22:223–31. doi: 10.1038/modpathol.2008.164

16. Alaggio R, Coffin CM, Weiss SW, Bridge JA, Issakov J, Oliveira AM, et al. Liposarcomas in young patients: a study of 82 cases occurring in patients younger than 22 years of age. *Am J Surg Pathol* (2009) 33:645–58. doi: 10.1097/PAS.0b013e3181963c9c

17. Setsu N, Miyake M, Wakai S, Nakatani F, Kobayashi E, Chuman H, et al. Primary retroperitoneal myxoid liposarcomas. *Am J Surg Pathol* (2016) 40:1286–90. doi: 10.1097/PAS.0000000000000657

18. Henricks WH, Chu YC, Goldblum JR, Weiss SW. Dedifferentiated liposarcoma: a clinicopathological analysis of 155 cases with a proposal for an expanded definition of dedifferentiation. *Am J Surg Pathol* (1997) 21:271–81. doi: 10.1097/00000478-199703000-00002

19. Jing W, Lan T, Chen H, Zhang Z, Chen M, Peng R, et al. Amplification of frs2 in atypical lipomatous tumour/well-differentiated liposarcoma and de-differentiated liposarcoma: a clinicopathological and genetic study of 146 cases. *Histopathology* (2018) 72:1145–55. doi: 10.1111/his.13473

20. He X, Pang Z, Zhang X, Lan T, Chen H, Chen M, et al. Consistent amplification of frs2 and mdm2 in low-grade osteosarcoma: a genetic study of 22 cases with clinicopathologic analysis. *Am J Surg Pathol* (2018) 42:1143–55. doi: 10.1097/PAS.0000000000001125

21. Mariani O, Brennetot C, Coindre JM, Gruel N, Ganem C, Delattre O, et al. Jun oncogene amplification and overexpression block adipocytic differentiation in highly aggressive sarcomas. *Cancer Cell* (2007) 11:361–74. doi: 10.1016/j.ccr.2007.02.007

22. Snyder EL, Sandstrom DJ, Law K, Fiore C, Sicinska E, Brito J, et al. C-jun amplification and overexpression are oncogenic in liposarcoma but not always sufficient to inhibit the adipocytic differentiation programme. *J Pathol* (2009) 218:292–300. doi: 10.1002/path.2564

23. Saada-Bouzid E, Burel-Vandenbos F, Ranchere-Vince D, Birtwisle-Peyrottes I, Chetaille B, Bouvier C, et al. Prognostic value of hmga2, cdk4, and jun amplification in well-differentiated and dedifferentiated liposarcomas. *Mod Pathol* (2015) 28:1404–14. doi: 10.1038/modpathol.2015.96

24. Shanks JH, Iczkowski KA. Spindle cell lesions of the bladder and urinary tract. *Histopathology* (2009) 55:491–504. doi: 10.1111/j.1365-2559.2009.03354.x

25. Evans HL. Atypical lipomatous tumor, its variants, and its combined forms: a study of 61 cases, with a minimum follow-up of 10 years. *Am J Surg Pathol* (2007) 31:1–14. doi: 10.1097/01.pas.0000213406.95440.7a

26. Bloxham CA, Bennett MK, Robinson MC. Bladder carcinosarcomas: three cases with diverse histogenesis. *Histopathology* (1990) 16:63–7. doi: 10.1111/j.1365-2559.1990.tb01062.x

27. Baschinsky DY, Chen JH, Vadmal MS, Lucas JG, Bahnson RR, Niemann TH. Carcinosarcoma of the urinary bladder–an aggressive tumor with diverse histogenesis. A clinicopathologic study of 4 cases and review of the literature. *Arch Pathol Lab Med* (2000) 124:1172–8. doi: 10.5858/2000-124-1172-COTUBA

28. Yasui M, Morikawa T, Nakagawa T, Miyakawa J, Maeda D, Homma Y, et al. Urinary bladder carcinoma with divergent differentiation featuring small cell carcinoma, sarcomatoid carcinoma, and liposarcomatous component. *Pathol Res Pract* (2016) 212:833–7. doi: 10.1016/j.prp.2016.04.014

29. Cessna MH, Zhou H, Sanger WG, Perkins SL, Tripp S, Pickering D, et al. Expression of ALK1 and p80 in inflammatory myofibroblastic tumor and its mesenchymal mimics: a study of 135 cases. *Mod Pathol* (2002) 15:931–8. doi: 10.1097/01.MP.0000026615.04130.1F

30. Le Guellec S, Soubeyran I, Rochaix P, Filleron T, Neuville A, Hostein I, et al. CTNNB1 mutation analysis is a useful tool for the diagnosis of desmoid tumors: a study of 260 desmoid tumors and 191 potential morphologic mimics. *Mod Pathol* (2012) 25:1551–8. doi: 10.1038/modpathol.2012.115

31. Dickson MA, Schwartz GK, Keohan ML, D'Angelo SP, Gounder MM, Chi P, et al. Progression-free survival among patients with well-differentiated or dedifferentiated liposarcoma treated with CDK4 inhibitor palbociclib: A phase 2 clinical trial. *JAMA Oncol* (2016) 2:937–40. doi: 10.1001/jamaoncol.2016.0264

32. Bill KL, Garnett J, Meaux I, Ma X, Creighton CJ, Bolshakov S, et al. SAR405838: A novel and potent inhibitor of the MDM2: p53 axis for the treatment of dedifferentiated liposarcoma. *Clin Cancer Res* (2016) 22:1150–60. doi: 10.1158/1078-0432.CCR-15-1522

33. Bonvalot S, Miceli R, Berselli M, Causeret S, Colombo C, Mariani L, et al. Aggressive surgery in retroperitoneal soft tissue sarcoma carried out at high-volume centers is safe and is associated with improved local control. *Ann Surg Oncol* (2010) 17:1507–14. doi: 10.1245/s10434-010-1057-5

34. Dantey K, Schoedel K, Yergiyev O, Bartlett D, Rao U. Correlation of histological grade of dedifferentiation with clinical outcome in 55 patients with dedifferentiated liposarcomas. *Hum Pathol* (2017) 66:86–92. doi: 10.1016/j.humpath.2017.02.015

35. Lee SE, Kim YJ, Kwon MJ, Choi DI, Lee J, Cho J, et al. High level of CDK4 amplification is a poor prognostic factor in well-differentiated and dedifferentiated liposarcoma. *Histopathology* (2014) 29:127–38. doi: 10.14670/HH-29.127

frontiers | Frontiers in Oncology

TYPE Systematic Review
PUBLISHED 09 November 2023
DOI 10.3389/fonc.2023.1236167

OPEN ACCESS

EDITED BY
Hailiang Zhang,
Fudan University, China

REVIEWED BY
Sentai Ding,
Shandong Provincial Hospital, China
Emmanuel Asante-Asamani,
Clarkson University, United States

*CORRESPONDENCE
Yunlin Feng
fengyunlin@med.uestc.edu.cn
Yu Mao
toil112@163.com
Yige Bao
baoyige@hotmail.com

†These authors have contributed equally to this work and share first authorship

RECEIVED 09 August 2023
ACCEPTED 25 October 2023
PUBLISHED 09 November 2023

CITATION
Ren S, Wang H, Yang B, Zheng Y, Ou Y, Bao Y, Mao Y and Feng Y (2023) Prognostic value of preoperative albumin-to-alkaline phosphatase ratio in patients with surgically treated urological cancer: a systematic review and meta-analysis. *Front. Oncol.* 13:1236167. doi: 10.3389/fonc.2023.1236167

Prognostic value of preoperative albumin-to-alkaline phosphatase ratio in patients with surgically treated urological cancer: a systematic review and meta-analysis

Shangqing Ren[1†], Han Wang[2†], Bo Yang[3], Yang Zheng[1,4], Yong Ou[1,4], Yige Bao[5*], Yu Mao[3*] and Yunlin Feng[6*]

[1]Robotic Minimally Invasive Surgery, Sichuan Academy of Medical Sciences and Sichuan Provincial People's Hospital, Chengdu, China, [2]Department of Gastroenterology, Sichuan Academy of Medical Sciences & Sichuan Provincial People's Hospital, Chengdu, China, [3]Department of Pediatric Surgery, Sichuan Academy of Medical Sciences & Sichuan Provincial People's Hospital, Chengdu, China, [4]School of Medicine, University of Electronic Science and Technology of China, Chengdu, China, [5]Department of Urology, Institute of Urology, West China Hospital, Sichuan University, Chengdu, China, [6]Department of Nephrology, Sichuan Provincial People's Hospital, University of Electronic Science and Technology of China, Chengdu, China

Objective: A novel albumin-to-alkaline phosphatase ratio (AAPR) is associated with the prognosis of several cancers. In the present study, we evaluate the prognostic significance of perioperative AAPR in urological cancers.

Method: Relevant studies were searched comprehensively from CNKI, PubMed, Embase and Web of Science up to March 2023. The pooled hazard ratio (HR) and 95% confidence interval (CI) were extracted from each study to evaluate the prognostic value of perioperative AAPR in patients with surgically treated urological cancers.

Results: A total of 8 studies consisting of 3,271 patients were included in the final results. A low AAPR was significantly associated with a worse OS (HR=2.21; P<0.001), CSS (HR=2.61; P<0.001) and RFS/DFS (HR=2.87; P=0.001). Stratified by disease, a low AAPR was also associated with worse OS in renal cell carcinoma (HR=2.01; P<0.001), bladder cancer (HR=3.37; P<0.001) and upper tract urothelial carcinoma (HR=1.59; P=0.002).

Conclusion: In conclusion, low AAPR could serve as an unfavorable factor in patients with surgically treated urological cancers. Stratified by tumor type, the low AAPR was also associated with inferior survival. While more prospective and large-scale studies are warranted to validate our findings.

KEYWORDS

albumin-to-alkaline phosphatase ratio, urological cancer, prognostic value, meta-analysis, surgical

Introduction

Urological cancers, mainly consisting of renal cell carcinoma (RCC), bladder cancer (BC), and prostate cancer (PCa), represent an increased global burden on human healthcare (1). RCC accounts for approximately 2%-3% of all malignancies (1). PCa is one of the common cancers in men, ranking the second most common cancer in 2020 worldwide (2). BC is also one of the most common malignancies, with an estimated 570,000 new cases and 210,000 deaths in 2020 worldwide (2).

Although the development of novel therapeutics such as immunotherapy and molecular target drugs has greatly improved clinical outcomes of patients with urological cancers (3–5), the cornerstone of treatment for localized for urological cancers has always been surgical resection (1). The management of urological cancer still face the dilemma of low objective response rate, local recurrence, and distant metastases. Therefore, identifying the prognostic factors of patients would be of great value to patients' risk stratification, treatment selection, and long-term outcomes prediction.

TNM stage, tumor grade, and histology are commonly used prognostic factors, yet bear the risk of missing information associated with patient-related factors. Increasing evidence has suggested that host nutrition status plays an important role in cancer development and progression (6–8), such as controlling nutritional status (CONUT) score and prognostic nutrition index (PNI) which have been found relevant to the prognosis of urological cancers (9, 10). Albumin-to-alkaline phosphatase ratio (AAPR) is another novel serum biomarker of nutritional status that has been demonstrated to be associated with the prognosis of several cancers, including lung cancer, hepatocellular carcinoma, and urological cancers (11–14); however, its role in urological cancers has only been reported in sporadic reports. There is a lack of evidence-based conclusion on the value of AAPR in urological cancer.

Therefore, we conducted this systematic review and meta-analysis to summarize all relevant studies and evaluate the prognostic significance of preoperative AAPR in patients with surgically treated urological cancers, in the hope of clarifying the value of AAPR in this field and provide evidence-based information for future studies.

Materials and methods

Search strategy

The study was carried out according to the Preferred Reporting Items for Systematic Reviews and Meta-Analyses (PRISMA) Statement (15). Relevant studies were searched comprehensively from CNKI, PubMed, Embase, and Web of Science up to 2023 March 08. The study search was conducted independently by two authors (SQR and HW) using search terms relevant to AAPR and urological cancers. The detailed search strategies are shown in Supplementary Table 1. References of eligible studies were also manually screened to avoid any omission.

Study screening

Studies eventually included in the systematic review must meet the following criteria (1): population-based studies; (2) reported patients with surgically treated urological cancers; (3) had AAPR with accurate definition and calculation based on accepted formula; (4) evaluated the prognostic value of preoperative AAPR; (5) reported analyzable data such as hazard ratio (HR) and 95% confidence interval (CI).

Studies were excluded if they met any of the following criterion: (1) did not report AAPR; (2) did not report sufficient data for meta-analysis; (3): review and conference abstracts. For reports of the same cohort, the study with the largest and latest data was included.

The study screening was conducted independently by two authors (SQR and HW). Any discrepancy was resolved by a third author (YLF).

Studied outcomes

The primary outcome of this systematic review is patient survival which might be reported in different modes, including overall survival (OS), cancer-specific survival (CSS), disease-free survival (DFS), and recurrence-free survival (RFS).

Data extraction and quality assessment

Two authors (SQR and YLF) extracted the following information from eligible studies independently based on the predefined items: the surname of the first author, publication year, participant, study design, disease, interventions, number and ages of patients, the cut-off value of AAPR, and duration of follow-up. The quality of studies was assessed by the Newcastle-Ottawa Quality Assessment Scale (NOS) which includes three main aspects, namely selection, comparability, and exposure/outcome. The total NOS scores ranges from 0 to 9, and a score of 7 or higher is deemed to be high quality (16).

Statistical analysis

All statistical analyses were performed with STATA (version 12, StataCorp, College Station, TX, USA). Pooled HRs and 95%CIs were extracted from each study to evaluate the prognostic value of AAPR in patients with urological cancers. The Cochran's Q test and the Higgins' I^2 statistic were used to evaluate the heterogeneity across studies (17). If the $I^2 \geq 50\%$ or $P<0.10$, the random-effect model was used, otherwise the fixed-effect model was applied. The sensitivity analyses were performed to identify the stability of the final results by omitting each study in sequence. The publication bias was tested by Egger's test and Begg's test. If publication bias was detected, the trim and fill method was conducted to estimate the missing studies and recalculate the pooled HRs (18). A two-sided P-value of <0.05 was considered significant.

Results

A total of 89 records were identified through the electronic database search. After removing the 27 duplicated records, the remaining 62 records were screened. 19 studies were reviewed in full-text after screening based on titles and abstracts. Finally, 8 studies consisting of 3,271 patients were included in the meta-analysis (11, 13, 19–24). The detailed flow diagram was illustrated in Figure 1.

Clinical characteristics of the included studies

All eight studies were retrospective cohort studies and had been published within the past 5 years. These studies reported a variety of urological cancers, including 4 for non-metastatic renal cell carcinoma (RCC) treated with nephrectomy (13, 19, 22, 23), 2 studies for BC treated with radical cystectomy (11, 24), 1 for upper tract urothelial carcinoma (UTUC) treated with radical nephroureterectomy (21), and 1 study involved prostate cancer treated with radical prostatectomy (20). The sample size of the studies ranged from 127 to 803. The cut-off value of APRP in each study is not uniform, ranging from 0.37 to 0.64. 6 studies had reported the overall survival (OS) (11, 19, 21–24), 6 studies had reported the cancer-specific survival (CSS) (11, 13, 21–24), and 5 studies reported disease-free survival (DFS)/recurrence-free survival (RFS) (11, 13, 20, 21, 24). All studies were regarded as high quality with NOS scores higher than 7. The basic characteristic of included studies were summarized in Table 1.

Survival outcomes

In the six studies that had reported the OS, low AAPR was significantly associated with worse OS compared with high AAPR (HR=2.21, 95% CI 1.60-3.05, P<0.001; I^2 = 49.7%, P=0.077; Figure 2A). In the six studies that had reported the CSS, low AAPR was also significantly associated with worse CSS compared with high AAPR (HR=2.61, 95% CI 1.80-3.76, P<0.001; I^2 = 47.7%, P=0.089; Figure 2B). In the five studies that had reported the DFS/RFS, low AAPR again was associated with worse DFS/RFS compared with high AAPR (HR=2.87, 95% CI 1.57-5.25, P=0.001; I^2 = 84.4%, P<0.001; Figure 2C).

Sensitivity analysis

The sensitivity analysis for OS and CSS by removing each study in sequence to reflect the impact of any individual study on the overall effect indicated that removing any single study did not dramatically change the trend of our results (Figure 3), indicating the robustness of the results.

Publication bias

Only the publication bias for OS and CSS were evaluated due to the small number of enrolled studies. A conflicting result according to the Egger's test (OS: P=0.038; CSS: P=0.026) and Begg's test (OS: P=0.060; CSS: P=0.260). Therefore, we conducted the trim and fill

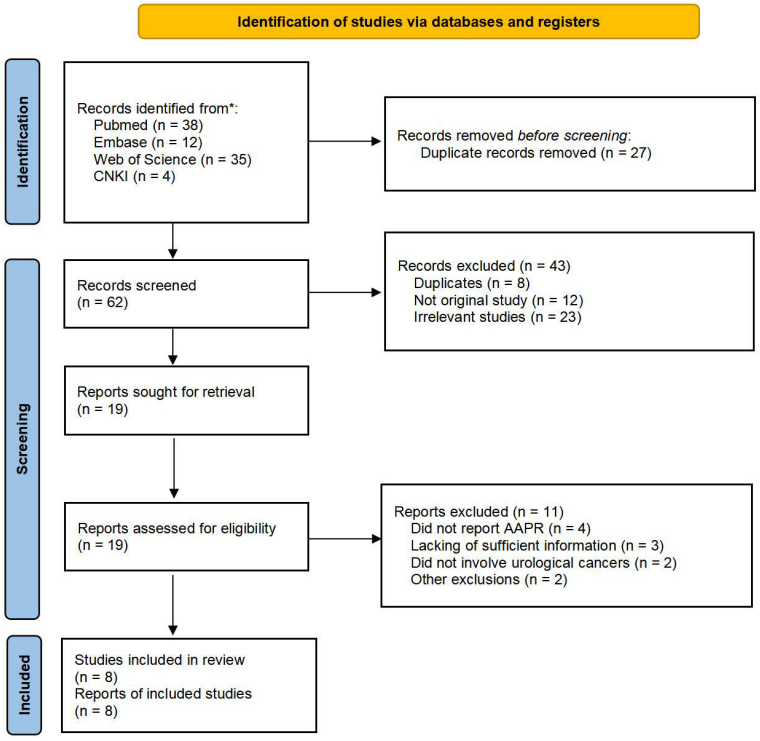

FIGURE 1
PRISMA flow diagram of the study.

TABLE 1 Basic characteristics of included studies.

Study/ Year	Study period/ Location	Disease	Treatment	Number of patients	Age (years)†	Cut off of AAPR	Reported outcomes	Follow-up (months)*	NOS score
Tan 2018 (21)	2003 to 2016/ China	UTUC	RUN	692	65.8 ± 11.4	0.58	OS, CSS, DFS	42 (20–75)	8
Xia 2019 (22)	January 2004 to July 2014/China	Non-metastatic RCC	Nephrectomy	803	61.0 ± 12.9	0.39	OS, CSS	50.0 (30.4-83.0)	8
Hu 2020 (23)	January 2010 to December 2013/ China	Non-metastatic RCC	Nephrectomy	648	54.84 ± 12.64	0.5	OS, CSS	84	8
Zhao 2020 (24)	2007 to 2015/ China	Bladder cancer	Radical cystectomy	174	Not reported	Trichotomous	OS, CSS, RFS	Median (range): 30 (1–125)	7
Li 2021 (11)	January 2012 to December 2017/ China	Bladder cancer	Radical cystectomy	199	64.0 ± 8.7	Trichotomous 0.37 0.59	OS, CSS, RFS	Mean 24	7
Chen 2021 (19)	January 2012 to January 2015/ China	Non-metastatic RCC	Nephrectomy	127	56.24 ± 10.13	0.4	OS	Not reported	7
Zhang 2021 (20)	May 2012 to October 2015 China	Prostate cancer	Radical prostatectomy	137	56.4 ± 20.71	Trichotomous 0.50 0.64	biochemical recurrence- free survival	55	7
Won 2022 (13)	June 1994 to December 2018/ Korea	Non-metastatic RCC	Nephrectomy	491	Median (range): 56.2 (18-83)	0.41	CSS, RFS	Median (range): 63 (4-272)	8

*The values are median (IQR) unless specified.
†The values are mean ± SD unless specified.
CSS, Cancer-specific survival; DFS, Disease-free survival; IQR, Interquartile range; NOS, Newcastle-Ottawa Quality Assessment Scale; OS, Overall survival; RCC, Renal cell carcinoma; RFS, Recurrence-free survival; RUN, Radical nephroureterectomy; SD, Standard deviation; UTUC, Upper tract urothelial carcinoma.

method to identify the effect of publication bias, finding that 3 studies were potentially missing in OS and CSS using the random-effect model (Figure 4). This approach resulted in a similar result, the pooled HRs for OS and CSS were 1.73 (95%CI 1.23-2.43, P=0.002) and 1.96 (95%CI 1.33-2.89, P=0.001), respectively.

Subgroup analysis

Subgroup analysis stratified by disease, number of patients and cut-off value of AAPR were conducted and indicated that disease and cut-off value of AAPR might be the source of heterogeneity of OS, but not for the CSS. In the subgroup analysis of disease, low AAPR predicts poor OS and CSS in RCC, BC, and UTUC. And in the subgroup with different sample sizes, low AAPR was also associated with the worse OS and CSS. As for cut-off value, low AAPR was an unfavorable factor in both subgroups. The detailed information was summarized in Table 2.

Discussion

The present study evaluated the association between AAPR and survival outcomes of urological cancers. The findings indicated that low AAPR was associated with poor survival outcomes of urological cancers. When stratified by diseases, low AAPR also predicted worse OS and CSS in RCC, BC, and UTUC. The cut-off values of AAPR and sample sizes in each individual study varied greatly. Corresponding subgroup analysis found these factors did not significantly affect the final results.

Urological cancers account for a relatively large proportion of all solid tumors, in which local recurrence or metastasis are highly likely to occur. For example, about three-fourths of high-risk bladder cancer will recur, progress, or die within 10 years after initial diagnosis (25). Besides, nearly 30% of RCC patients will develop local or distant recurrence after surgical resection (26). The prognosis of metastatic prostate cancer is also poor, with an approximate 5-year survival rate of 30% (27). Therefore, exploring prognostic factors of urological cancers has important role in the management of this population.

The association between nutrition and malignancy has been widely explored in the past decades. Sarcopenia, the degenerative and systemic loss of skeletal muscle mass, indicates patient frailty and unfavorable prognosis in urological cancer patients (28). The prognostic nutritional index (PNI), reflecting immune and nutritional status based on the serum lymphocyte count and albumin level, is associated with prognosis of RCC (10). AAPR, a novel nutritional index, was firstly introduced and observed to be associated with the prognosis in hepatocellular carcinoma (29). Hu et al. investigated patients with surgically treated non-metastatic

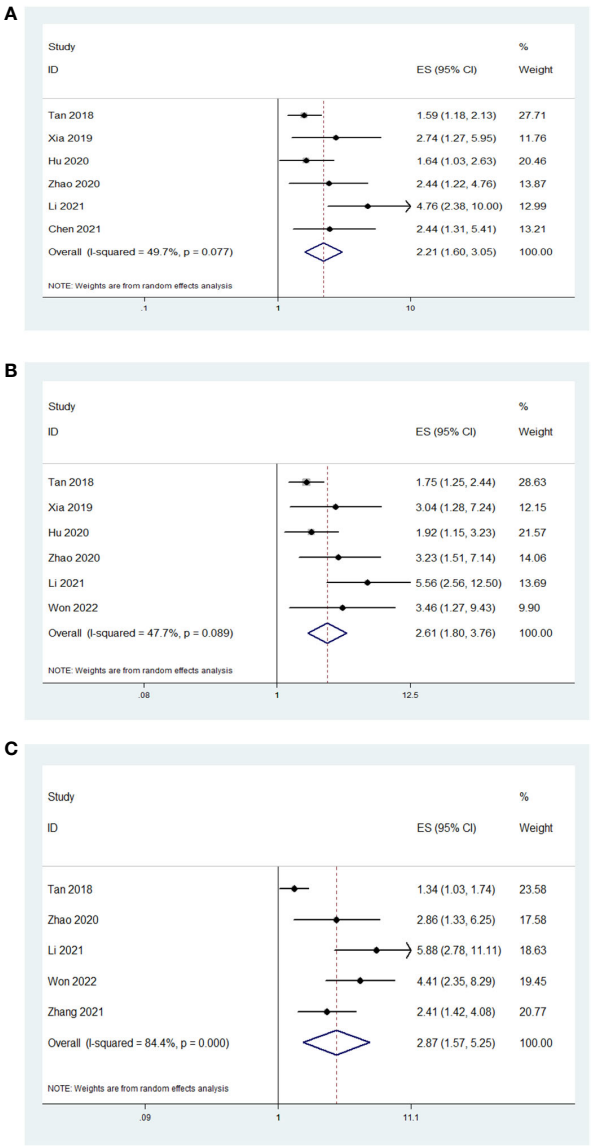

FIGURE 2
The association between AAPR and studied survival outcomes in patients with surgically treated urological cancers. Low AAPR was significantly associated with worse OS **(A)**, CSS **(B)** and DFS/RFS **(C)** compared with high AAPR.

renal cell carcinoma and found that low AAPR was an unfavorable prognostic factor. They also found that AAPR improved the predictive value of well-established models (23). Won et al. validated the prognostic value of AAPR in patients with RCC treated with nephrectomy using propensity score matching analysis (13). Yoshino et al. demonstrated that baseline AAPR was significantly associated with OS in patients with mRCC receiving nivolumab monotherapy (30). Furthermore, AAPR could predict survival outcomes in UTUC and bladder cancer patients treated with surgery (11, 21). As for prostate cancer, Zhang et al. revealed that AAPR was associated with biochemical recurrence-free survival (20). Based on the above-mentioned evidence, high AAPR could be served as an unfavorable factor in cancer patients. However, for the other urological cancers such as testicular and penile cancer, there is no relevant report about the association between perioperative AAPR and patients' prognosis. And more large-scale studies are required to verify our findings.

AAPR is a ready to use index in clinical practice. It is calculated based on the albumin and ALP values, which are convenient, easily obtained and commonly tested before treatment. AAPR could predict the prognosis of patients, which could be used for risk stratification. It could provide physicians with useful information and guide the treatment, adjuvant therapy, and follow-up for patients. While, the optimal cut-off value of AAPR remains unclear, which is need further exploration. The potential mechanisms for the prognostic value of AAPR might be explained by the functions of albumin and alkaline phosphatase (ALP). Albumin is a stable and abundant serum protein, reflecting the nutritional status. It also represents systemic inflammatory response, as inflammation that could influence the synthesis of albumin (31). Albumin also can stabilize cell proliferation and growth, as well as exert antioxidants agents against carcinogens (32). Evidence has found that albumin could predict prognosis in various malignancies such as RCC and bladder cancer (33, 34). ALP is a hydrolytic enzyme, found primarily in the bile duct, liver, kidney, bone, and several other organs. ALP can be affected by liver function damage from chronic wasting diseases and the cancer-related inflammatory microenvironment (35). The level of ALP level increases under certain pathological conditions, such as hepatocellular carcinoma, kidney, and bone diseases (21). ALP could also act as a potential indicator of oxidative stress and

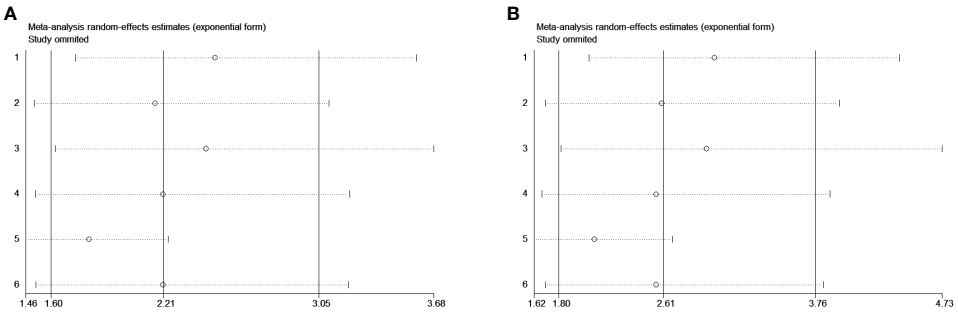

FIGURE 3
Sensitivity analysis for the studied outcomes. Removing any single study did not dramatically change the trend of our results in OS **(A)** and CSS **(B)**.

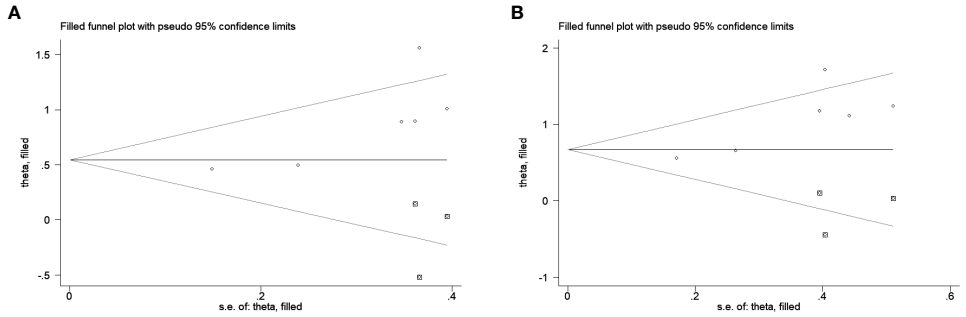

FIGURE 4
The trim and fill method to estimate publication bias for the survival outcomes. Three studies were potentially missing in OS **(A)** and CSS **(B)** using the random-effect model.

promotes high mutagenic metabolic activities, resulting in more aggressive carcinogenesis (36, 37). ALP has been reported to be associated with prognosis of gastric cancer, RCC, and hepatocellular carcinoma (38–40). Therefore, low AAPR may indicate low albumin and high ALP levels, suggesting weak nutrition and abnormal immune response in patients and finally facilitating the tumor invasion and metastasis.

Our study had limitations. First, only 8 studies consisting of 3,271 patients were included and the number of studies for each cancer is also limited, which may limit the power of final results. Second, all studies were retrospective studies with the potential inherent bias, which might account for the observed heterogeneities. Third, there are several factors unavailable including age and stage at subgroup analyses, precluding from additional investigations.

Conclusion

In conclusion, low AAPR could serve as an unfavorable factor for the survival outcomes in patients with surgically treated urological cancers. Stratified by tumor type, the low AAPR was also associated with worse survival. More prospective and large-scale studies are warranted to validate our findings.

TABLE 2 Subgroup analyses of studied outcomes.

Outcome	Variable		Number of studies	HR (95% CI)	I^2	P value of heterogeneity
OS	All		6	2.21 (1.60-3.05)	49.7%	0.077
	Disease	RCC	3	2.01 (1.42-2.84)	0	0.439
		BC	2	3.37 (1.75-6.50)	43.1%	0.185
		UTUC	1	1.59 (1.19-2.13)	–	–
	Cut-off	Dichotomous	4	1.75 (1.40-2.19)	0	0.447
		Trichotomous	2	3.37 (1.75-6.50)	43.1%	0.185
	Sample size	<200	3	3.03 (1.97-4.66)	0	0.427
		>200	3	1.68 (1.33-2.13)	11.8%	0.322
CSS	All		6	2.61 (1.80-3.76)	49.7%	0.077
	Disease	RCC	3	2.34 (1.56-3.51)	0	0.474
		BC	2	4.21 (2.42-7.33)	0	0.336
		UTUC	1	1.75 (1.25-2.44)	–	–
	Cut-off	Dichotomous	4	1.97 (1.52-2.55)	0	0.443
		Trichotomous	2	4.21 (2.42-7.33)	0	0.336
	Sample size	<200	2	4.21 (2.42-7.33)	0	0.336
		>200	4	1.97 (1.52-2.55)	0	0.443

BC, bladder cancer; CI, confidence interval; CSS, Cancer-specific survival; HR, hazards ratio; OS, overall survival; RCC, Renal cell carcinoma; UTUC, Upper tract urothelial carcinoma.

Data availability statement

The original contributions presented in the study are included in the article/Supplementary Material. Further inquiries can be directed to the corresponding authors.

Author contributions

SR and YF: Study conception and design, acquisition of data, analysis and interpretation of data and drafting of paper. SR, HW and YM: Acquisition of data, analysis and interpretation of data. YB, SR, and YF: Acquisition of data, drafting of paper and critical revision. YZ, YO, SR, and BY: Study conception and design, drafting of paper and critical revision. All authors contributed to the article and approved the submitted version.

Funding

The author(s) declare financial support was received for the research, authorship, and/or publication of this article. This study is supported by 2022YFS0135, 2023YFS0173, 2023YFSY0027 and SCR2023-210.

Conflict of interest

The authors declare that the research was conducted in the absence of any commercial or financial relationships that could be construed as a potential conflict of interest.

Publisher's note

Supplementary material

The Supplementary Material for this article can be found online at: https://www.frontiersin.org/articles/10.3389/fonc.2023.1236167/full#supplementary-material

References

1. Dy GW, Gore JL, Forouzanfar MH, Naghavi M, Fitzmaurice C. Global burden of urologic cancers, 1990-2013. *Eur Urol* (2017) 71(3):437–46. doi: 10.1016/j.eururo.2016.10.008

2. Sung H, Ferlay J, Siegel RL, Laversanne M, Soerjomataram I, Jemal A, et al. Global cancer statistics 2020: globocan estimates of incidence and mortality worldwide for 36 cancers in 185 countries. *CA: Cancer J Clin* (2021) 71(3):209–49. doi: 10.3322/caac.21660

3. Fitzgerald KN, Lee CH. Personalizing first-line management of metastatic renal cell carcinoma: leveraging current and novel therapeutic options. *J Natl Compr Cancer Network JNCCN* (2022) 20(13). doi: 10.6004/jnccn.2022.7003

4. Audisio M, Tucci M, Di Stefano RF, Parlagreco E, Ungaro A, Turco F, et al. New emerging targets in advanced urothelial carcinoma: is it the primetime for personalized medicine? *Crit Rev oncology/hematology* (2022) 174:103682. doi: 10.1016/j.critrevonc.2022.103682

5. Yamada Y, Beltran H. The treatment landscape of metastatic prostate cancer. *Cancer Lett* (2021) 519:20–9. doi: 10.1016/j.canlet.2021.06.010

6. Pena NF, Mauricio SF, Rodrigues AMS, Carmo AS, Coury NC, Correia M, et al. Association between standardized phase angle, nutrition status, and clinical outcomes in surgical cancer patients. *Nutr Clin Pract Off Publ Am Soc Parenteral Enteral Nutr* (2019) 34(3):381–6. doi: 10.1002/ncp.10110

7. Bossi P, Delrio P, Mascheroni A, Zanetti M. The spectrum of malnutrition/cachexia/sarcopenia in oncology according to different cancer types and settings: A narrative review. *Nutrients* (2021) 13(6):1980. doi: 10.3390/nu13061980

8. Bullock AF, Greenley SL, McKenzie GAG, Paton LW, Johnson MJ. Relationship between markers of malnutrition and clinical outcomes in older adults with cancer: systematic review, narrative synthesis and meta-analysis. *Eur J Clin Nutr* (2020) 74(11):1519–35. doi: 10.1038/s41430-020-0629-0

9. Niu X, Zhu Z, Bao J. Prognostic significance of pretreatment controlling nutritional status score in urological cancers: A systematic review and meta-analysis. *Cancer Cell Int* (2021) 21(1):126. doi: 10.1186/s12935-021-01813-2

10. Shim SR, Kim SI, Kim SJ, Cho DS. Prognostic nutritional index as a prognostic factor for renal cell carcinoma: A systematic review and meta-analysis. *PloS One* (2022) 17(8):e0271821. doi: 10.1371/journal.pone.0271821

11. Li S, Lu S, Liu X, Chen X. Association between the pretreatment albumin-to-alkaline phosphatase ratio and clinical outcomes in patients with bladder cancer treated with radical cystectomy: A retrospective cohort study. *Front Oncol* (2021) 11:664392. doi: 10.3389/fonc.2021.664392

12. Sandfeld-Paulsen B, Aggerholm-Pedersen N, Winther-Larsen A. Pretreatment albumin-to-alkaline phosphatase ratio is a prognostic marker in lung cancer patients: A registry-based study of 7077 lung cancer patients. *Cancers* (2021) 13(23):6133. doi: 10.3390/cancers13236133

13. Won I, Shim SR, Kim SI, Kim SJ, Cho DS. Albumin-to-alkaline phosphatase ratio as a novel prognostic factor in patients undergoing nephrectomy for non-metastatic renal cell carcinoma: propensity score matching analysis. *Clin genitourinary Cancer* (2022) 20(3):e253–e62. doi: 10.1016/j.clgc.2022.01.012

14. Zhang X, Xin Y, Chen Y, Zhou X. Prognostic effect of albumin-to-alkaline phosphatase ratio on patients with hepatocellular carcinoma: A systematic review and meta-analysis. *Sci Rep* (2023) 13(1):1808. doi: 10.1038/s41598-023-28889-2

15. Moher D, Liberati A, Tetzlaff J, Altman DG. Preferred reporting items for systematic reviews and meta-analyses: the prisma statement. *PloS Med* (2009) 6(7):e1000097. doi: 10.1371/journal.pmed.1000097

16. Margulis AV, Pladevall M, Riera-Guardia N, Varas-Lorenzo C, Hazell L, Berkman ND, et al. Quality assessment of observational studies in a drug-safety systematic review, comparison of two tools: the newcastle-ottawa scale and the rti item bank. *Clin Epidemiol* (2014) 6:359–68. doi: 10.2147/CLEP.S66677

17. Higgins JP, Thompson SG, Deeks JJ, Altman DG. Measuring inconsistency in meta-analyses. *BMJ (Clinical Res ed)* (2003) 327(7414):557–60. doi: 10.1136/bmj.327.7414.557

18. Duval S, Tweedie R. Trim and fill: A simple funnel-plot-based method of testing and adjusting for publication bias in meta-analysis. *Biometrics* (2000) 56(2):455–63. doi: 10.1111/j.0006-341x.2000.00455.x

19. Chen F, Chen Y, Zou Y, Wang Y, Wu X, Pu Y, et al. Evaluation value of preoperative prognostic nutritional index and albumin /alkaline phosphatase ratio in prognosis of patients with renal cancer. *J Regional Anat Operative Surg* (2021) 30(11):965–70. doi: 10.11659/jjssx.03E021127

20. Zhang Z, Zhou Q, Zhang J, Pu J, Ou Y. Predictive value of preoperative albumin-to-alkaline phosphatase ratio on biochemical recurrence after radical prostatectomy. *J Dalian Med University* (2021) 43(05):413–8. doi: 10.11724/jdmu.2021.05.06

21. Tan P, Xie N, Ai J, Xu H, Xu H, Liu L, et al. The prognostic significance of albumin-to-alkaline phosphatase ratio in upper tract urothelial carcinoma. *Sci Rep* (2018) 8(1):12311. doi: 10.1038/s41598-018-29833-5

22. Xia A, Chen Y, Chen J, Pan Y, Bao L, Gao X. Prognostic value of the albumin-to-alkaline phosphatase ratio on urologic outcomes in patients with non-metastatic renal cell carcinoma following curative nephrectomy. *J Cancer* (2019) 10(22):5494–503. doi: 10.7150/jca.34029

23. Hu X, Yang ZQ, Dou WC, Shao YX, Wang YH, Lia T, et al. Validation of the prognostic value of preoperative albumin-to-alkaline phosphatase ratio in patients with

surgically treated non-metastatic renal cell carcinoma. *OncoTargets Ther* (2020) 13:8287–97. doi: 10.2147/ott.S264217

24. Zhao M, Zhang M, Wang Y, Yang X, Teng X, Chu G, et al. Prognostic value of preoperative albumin-to-alkaline phosphatase ratio in patients with muscle-invasive bladder cancer after radical cystectomy. *OncoTargets Ther* (2020) 13:13265–74. doi: 10.2147/ott.S285098

25. Chamie K, Litwin MS, Bassett JC, Daskivich TJ, Lai J, Hanley JM, et al. Recurrence of high-risk bladder cancer: A population-based analysis. *Cancer* (2013) 119(17):3219–27. doi: 10.1002/cncr.28147

26. Jamil ML, Keeley J, Sood A, Dalela D, Arora S, Peabody JO, et al. Long-term risk of recurrence in surgically treated renal cell carcinoma: A *post hoc* analysis of the eastern cooperative oncology group-american college of radiology imaging network E2805 trial cohort. *Eur Urol* (2020) 77(2):277–81. doi: 10.1016/j.eururo.2019.10.028

27. Siegel RL, Miller KD, Wagle NS, Jemal A. Cancer statistics, 2023. *CA: Cancer J Clin* (2023) 73(1):17–48. doi: 10.3322/caac.21763

28. Fukushima H, Koga F. Impact of sarcopenia in the management of urological cancer patients. *Expert Rev Anticancer Ther* (2017) 17(5):455–66. doi: 10.1080/14737140.2017.1301209

29. Chan AW, Chan SL, Mo FK, Wong GL, Wong VW, Cheung YS, et al. Albumin-to-alkaline phosphatase ratio: A novel prognostic index for hepatocellular carcinoma. *Dis Markers* (2015) 2015:564057. doi: 10.1155/2015/564057

30. Yoshino M, Ishihara H, Ishiyama Y, Tachibana H, Toki D, Yamashita K, et al. Albumin-to-alkaline phosphatase ratio as a novel prognostic marker of nivolumab monotherapy for previously treated metastatic renal cell carcinoma. *In Vivo (Athens Greece)* (2021) 35(5):2855–62. doi: 10.21873/invivo.12573

31. Arroyo V, García-Martinez R, Salvatella X. Human serum albumin, systemic inflammation, and cirrhosis. *J Hepatol* (2014) 61(2):396–407. doi: 10.1016/j.jhep.2014.04.012

32. Nojiri S, Joh T. Albumin suppresses human hepatocellular carcinoma proliferation and the cell cycle. *Int J Mol Sci* (2014) 15(3):5163–74. doi: 10.3390/ijms15035163

33. Zhou X, Fu G, Zu X, Xu Z, Li HT, D'Souza A, et al. Albumin levels predict prognosis in advanced renal cell carcinoma treated with tyrosine kinase inhibitors: A systematic review and meta-analysis. *Urologic Oncol* (2022) 40(1):12.e3–.e22. doi: 10.1016/j.urolonc.2021.08.001

34. Li J, Cheng Y, Liu G, Ji Z. The association of pretreatment serum albumin with outcomes in bladder cancer: A meta-analysis. *OncoTargets Ther* (2018) 11:3449–59. doi: 10.2147/ott.S162066

35. Xiong JP, Long JY, Xu WY, Bian J, Huang HC, Bai Y, et al. Albumin-to-alkaline phosphatase ratio: A novel prognostic index of overall survival in cholangiocarcinoma patients after surgery. *World J gastrointestinal Oncol* (2019) 11(1):39–47. doi: 10.4251/wjgo.v11.i1.39

36. López-Posadas R, González R, Ballester I, Martínez-Moya P, Romero-Calvo I, Suárez MD, et al. Tissue-nonspecific alkaline phosphatase is activated in enterocytes by oxidative stress *via* changes in glycosylation. *Inflammatory bowel Dis* (2011) 17(2):543–56. doi: 10.1002/ibd.21381

37. Mantovani A, Allavena P, Sica A, Balkwill F. Cancer-related inflammation. *Nature* (2008) 454(7203):436–44. doi: 10.1038/nature07205

38. Wu YJ, Wang Y, Qin R, Cao ZY, Zhao HZ, Du XH, et al. Serum alkaline phosphatase predicts poor disease-free survival in patients receiving radical gastrectomy. *Med Sci monitor Int Med J Exp Clin Res* (2018) 24:9073–80. doi: 10.12659/msm.910480

39. Lee SE, Byun SS, Han JH, Han BK, Hong SK. Prognostic significance of common preoperative laboratory variables in clear cell renal cell carcinoma. *BJU Int* (2006) 98 (6):1228–32. doi: 10.1111/j.1464-410X.2006.06437.x

40. Wu SJ, Lin YX, Ye H, Xiong XZ, Li FY, Cheng NS. Prognostic value of alkaline phosphatase, gamma-glutamyl transpeptidase and lactate dehydrogenase in hepatocellular carcinoma patients treated with liver resection. *Int J Surg (London England)* (2016) 36(Pt A):143–51. doi: 10.1016/j.ijsu.2016.10.033

frontiers | Frontiers in Oncology

TYPE Original Research
PUBLISHED 27 November 2023
DOI 10.3389/fonc.2023.1243118

OPEN ACCESS

EDITED BY
Hailiang Zhang,
Fudan University, China

REVIEWED BY
Shengxi Chen,
Arizona State University, United States
Murat Akand,
University Hospitals Leuven, Belgium

*CORRESPONDENCE
Shuo Wang
wangshuoarea@pku.org.cn
Peng Du
dupeng9000@126.com

†These authors have contributed equally to this work and share first authorship

RECEIVED 28 June 2023
ACCEPTED 30 October 2023
PUBLISHED 27 November 2023

CITATION
Wang S, Ji Y, Liu Y, Du P, Ma J, Yang X, Yu Z and Yang Y (2023) The values of HER-2 expression in the non-muscle-invasive bladder cancer: a retrospective clinical study. *Front. Oncol.* 13:1243118. doi: 10.3389/fonc.2023.1243118

The values of HER-2 expression in the non-muscle-invasive bladder cancer: a retrospective clinical study

Shuo Wang[1*†], Yongpeng Ji[1†], Yiqiang Liu[2†], Peng Du[1*], Jinchao Ma[1], Xiao Yang[1], Ziyi Yu[1] and Yong Yang[1]

[1]Key Laboratory of Carcinogenesis and Translational Research (Ministry of Education), Urological Department, Peking University Cancer Hospital & Institute, Beijing, China, [2]Key Laboratory of Carcinogenesis and Translational Research (Ministry of Education), Department of Pathology, Peking University Cancer Hospital & Institute, Beijing, China

Purpose: The purpose of this research is to evaluate the association between HER-2 expression and clinicopathological features in patients with non-muscle-invasive bladder cancer (NMIBC).

Methods: Between 2019 and 2022, 204 patients treated with Transurethral resection of the bladder tumor (TURBT) were included in this study. Data of pathologic T (pT) stage, grades of the tumor, age, sex, tumor size and number of the tumors were collected and compared according to the expression level of the human epidermal growth factor 2 (HER-2). ROC curve analysis was performed to assess the discriminative ability of HER-2 expression for tumors grades and pT stage. Multivariable logistic regression analysis were used to evaluate the association between HER-2 expression and tumor grades and pT stage.

Results: Patients were divided into low grade (110, 53.9%) and high grade groups (94, 46.1%) according to the tumor grade. Pathologic stage consisted of pTa in 166 (81.4%) and pT1 in 38 (18.6%). HER-2 expression was semi quantitatively scored to 0 in 44 (21.6%), 1 in 58 (28.4%), 2 in 91 (44.6%), and 3 in 11 (5.4%) cases. HER-2 expression was significantly associated with tumor stages and histological grades, but not with sex, tumor size or number of tumors. The AUC for combination of HER-2 expression with tumor stages and histological grades was 0.652 ($p < 0.003$) and 0.727 ($p < 0.001$), respectively.

Conclusion: This study demonstrated that HER-2 expression is associated with tumor stages and histological grades in NMIBC. It has diagnostic value for cystoscopic biopsy.

KEYWORDS

non-muscle-invasive bladder cancer, human epidermal growth factor receptor 2 (HER-2), antibody-drug conjugate, ROC curve analyses, IHC

Introduction

Urinary carcinoma of bladder (UCB) is the ninth of the most common cancer in the world (1), Muscle-invasive bladder cancer (MIBC) and non-muscle-invasive bladder cancer (NMIBC) have completely different treatment strategies. NMIBC account for 70–75%, while the remaining 25–30% are MIBC (2). The tumor recurrence of NMIBC varies from 30% to 80%, furthermore, in 10% to 20% of patients the disease will progress to MIBC (3). However, high risk NMIBC in particular remains a challenging tumor to treat. High recurrence rates in NMIBC means patients are exposed to frequent hospital visits. Transurethral resection of the bladder tumor (TURBT) is the main procedure for treatment and diagnosis of UCB. Bacillus Calmette Guerin (BCG) still remains the gold standard for adjuvant treatment of high risk NMIBC patients (3, 4). BCG therapy is challenging in terms of its ineffectiveness and adverse effects. 35% patients who were tumor free at 2 years had recurrent tumors during the 2 to 11 years follow up (5). Surgical removal of the bladder should be considered in case of BCG unresponsive tumors or in NMIBC with the highest risk of progression. 15% of patients who discontinue treatment after first course of BCG treatment, 35% of them are known to have difficulty in continuing treatment due to side effects of bacterial or chemical cystitis, hematuria, and systemic febrile events (6).

The human epidermal growth factor receptor 2 (HER-2) expression has been extensively investigated as a target therapy and is known to be a prognostic and therapeutic marker in breast cancer. overexpression of HER-2 in 17% to 76% of cases has been reported in UCB, and there is a possible association between HER-2 overexpression with early recurrence, high grade disease, and worse prognosis (7–9).Before the development of antibody-drug conjugate (ADC), human epidermal growth factor receptor-2 (HER-2) received attention as a therapeutic target but was shown to be ineffective. Therefore, the predictive value of HER-2 status in bladder cancer remains controversial (10). Moreover, there are only a few studies of HER-2 status in NMIBC (11–13). Promising results in targeted therapy comes from novel ADC agents, ADCs bind to tumor associated antigens, triggering endocytosis, internalization, and release of the cytotoxic payload in target tumor cells after lysosomal degradation. There is an opportunity to develop an intravesical therapeutic agent for this identified target antigen by mediating ADCs, for example, RC48 using to develop a HER-2-targeting ADC for the treatment of mUCB (14). Meanwhile, here have been several advancements in UCB treatment (15, 16). To determine the prognostic values of HER-2 expression in bladder cancer, we recently analyzed the association between HER-2 expression and clinicopathological features in patients with non-muscle-invasive bladder cancer (NMIBC).

Materials and methods

Patients' characteristics

This retrospective study was approved by the Institutional Review Board of Peking University Cancer Hospital and Institute according to the principles of the Declaration of Helsinki. The requirement for informed consent was waived due to the retrospective nature of the study. In this study, we retrospectively analyzed clinical pathological data from 204 patients treated with TURBT at the Department of Urology of the Peking University Cancer Hospital between 2019 and 2022 who were initially diagnosed with NMIBC. They were diagnosed as pTa or pT1 papillary urothelial tumors based on primary TURBT, according to the 7th edition American Joint Committee on Cancer TNM system. The exclusion criteria were diagnosis of muscle invasive carcinoma of the bladder (≥pT2),the presence of carcinoma *in situ* (CIS),remaining tumor after initial resection, metastatic disease, concomitant diagnosis of another cancer. All patients did not receive treatment before TURBT and had no history of chemotherapy or radiotherapy. All patients had an immediate (within 8 hours) post-operation single intravesical treatment with pirarubicin (THP).

Immunohistochemistry

Formalin-fixed, paraffin-embedded tumor samples from specimens of 204 TURBT patients were collected. All specimens were examined in the pathology department of Peking University Cancer Hospital. Confirmation of T stage, tumor grade, and HER-2 expression were assessed by a single pathologist, and conducted a re-examined. The scoring was first semi quantitatively analyzed and grouped into 4 categories as follows: 0, no staining; 1+, faint/barely partial membrane staining less than 50% of tumor area; 2+, variable weak to moderate complete membrane staining in ≥ 50% of tumor area; 3+, strong complete membrane staining in all tumor area (Figure 1).

Statistical analysis

Descriptive statistics were used to summarize patient characteristics, categorical variables were presented as numbers and percentages, and continuous variables were presented as the mean and standard deviation. The chi-square or Fisher exact test was used to evaluate the statistical significance of the associations between clinicopathologic parameters. ROC curve analyses were performed to assess the discriminative ability of the HER-2 combined with tumor grade. The cutoff points for markers were defined by a criterion based on Youden's index defined as YI(C) = max c [Se(C) + SP(C)-1] and corresponding specificity–sensitivity levels were provided. The binary logistic regression model (multivariate analysis) was used to evaluate the association between clinicopathological characteristics and HER-2 expression. A p value of < 0.05 (two-tailed) was used to establish statistical significance. All statistical analyses were conducted using SPSS v. 19.0 (SPSS Inc., Chicago, IL, USA).

Results

The clinicopathological characteristics of the 204 patients with NMIBC are summarized in Table 1. The patients included 161 men (78.9%) and 43 women (21.1%). The mean age of the patients was

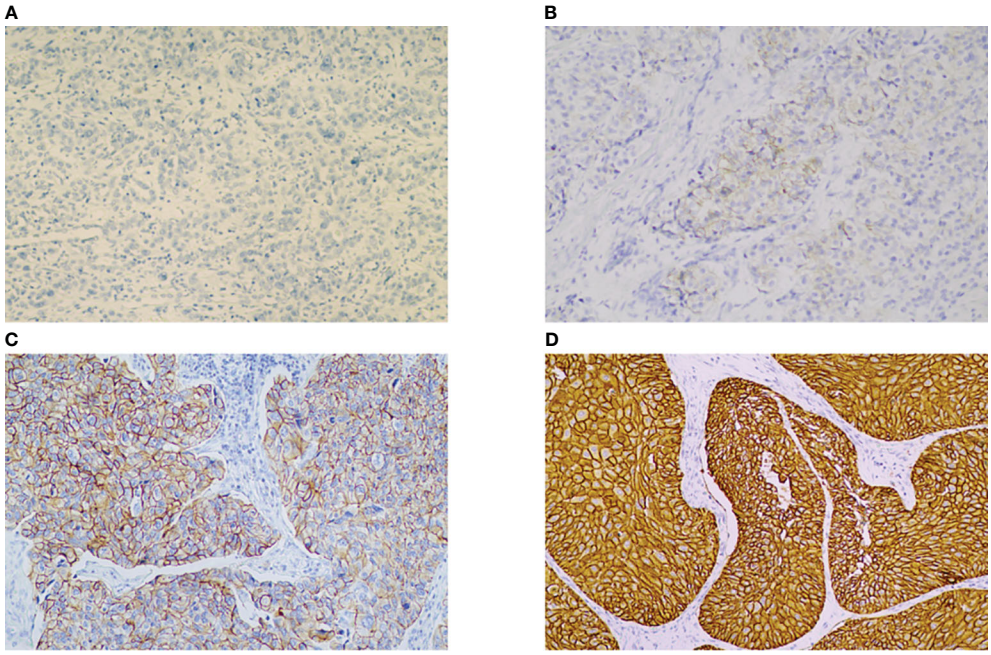

FIGURE 1
IHC for HER-2 showing 0, no staining **(A)**, 1+, faint/barely partial membrane staining less than 50% of tumor area. **(B)**, 2+, variable weak-to-moderate complete membrane staining in ≥ 50% of tumor area **(C)**, 3+ moderate to strong complete membrane staining in all tumor area. **(D)** (magnification × 200). HER-2: human epidermal growth factor receptor-2.

TABLE 1 Clinicopathological characteristics of 204 patients with NMIBC.

Characteristics	No. (%) of cases
Sex	
Male	161 (78.9)
Female	43 (21.1)
Age (mean, range, yrs)	61.6 (30-88) ± 11.1
Male	61.5 (30-88) ± 11.0
Female	62.1 (34-88) ± 11.6
pT stage	
Ta	166 (81.4)
T1	38 (18.6)
Tumor grade	
Low grade	110 (53.9)
High grade	94 (46.1)
HER2 protein expression (IHC)	
0	44 (21.6)
1+	58 (28.4)
2+	91 (44.6)
3+	11 (5.4)
Number of tumors	
Single	138 (67.6)
2-7	54 (26.5)
≥8	12 (5.9)
Tumor size	
< 3 cm	190 (93.1)
≥ 3 cm	14 (6.9)

TABLE 1 Continued

NMIBC, non-muscle invasive bladder cancer; HER-2, human epidermal growth factor receptor-2.

61.6 yr (range 30-88 yr). Among them, the mean age of male patients was 61.5 yr (range 30-88 yr),and the mean age of female patients was 62.1 yr (range 34-88 yr). The number of patients with tumors smaller than 3cm is 190(93.1%).3 cm or more sized tumor was found in 14 (6.9%). Patients with one tumor bladder was found in 138 cases (67.6%), and 2 or more of multifocality was found in 66 cases (32.4%). Patients were divided into low grade (110, 53.9%) and high grade groups (94, 46.1%) according to the tumor grade. Pathologic stage consisted of pTa in 166 (81.4%) and pT1 in 38 (18.6%).HER-2 expression was semi quantitatively scored to 0 in 44 (21.6%), 1 in 58 (28.4%), 2 in 91 (44.6%), and 3 in 11 (5.4%) cases.

Pathologic stage was significantly associated with HER-2 (P = 0.020), tumor grade (P < 0.001), Gross tumor appearance was evaluated. The proportion of patients with low grade was higher in the tumors< 3 cm group than in the tumors≥ 3 cm group (P = 0.011), but not with HER-2 (P = 0.402) or pathologic stage (P = 0.089). The proportion of patients with low grade was higher in

single tumor group than in the 2-7 tumors group and higher in the ≥8 tumors group than in the 2-7 tumors group (P = 0.006).And the proportion of patients with pTa tumors was higher in single tumor group than in the 2-7 tumors group and higher in the ≥8 tumors group than in the 2-7 tumors group (P = 0.021) (Table 2, 3).

In the low grade group the HER-2 expression has a similar proportion in 0,1+ and 2+, but there was no 3+. However, there was a high proportion of 2+and3+ HER-2 expression in high grade group (Figure 2). We classified patients and assessed clinical usefulness of HER-2 expression + tumor grade, and HER-2 expression + pathologic stage. The results revealed that HER2-positive could distinguish patients with high grade from low grade (AUC = 0.743,p < 0.001) with a sensitivity of 91.5% and a specificity of 67.3%, with a threshold value of 0.5; and HER2-positive could distinguish patients with pT1 tumors from pTa tumors (AUC = 0.652, p = 0.003) with a sensitivity of 92.1% and a specificity of 75.3%, with a threshold value of 0.5 (Figure 3, Table 4). There was a prognostic difference between HER 2 non expression and HER2 expression. We chose HER-2 0 and HER expression as different groups. Multivariable logistic regression models were used to evaluate the association between HER-2 and clinical characteristics. We found that HER-2 was only related to tumor grade (Table 5).

Discussion

HER-2 is a member of the epidermal growth factor receptor family having tyrosine kinase activity. The role of HER-2 is known in breast cancer and gastric cancer because it is a prognostic factor and a classic therapeutic target when over expressed (17). Bladder cancer is characterized by the presence of two different subtypes: NMIBC and MIBC. MIBC has a poor outcome with common progression to metastasis, while NMIBC shows frequent recurrences.

The prognostic values of HER-2 expression in bladder cancer have remained unclear due to inconsistent results. Most of the studies of HER-2 expression in bladder cancer have been performed on MIBC and show varying expression ranging between 9% and 81% (18). Potential reason for this variation is the fact that studies used bladder cancer samples with a varying degree of tumor stages and histological grades. Nevertheless, there have been presented HER-2 over expression was significantly associated with poor clinicopathological factors including lymph node metastasis and poor prognosis in bladder cancer (8, 19, 20). MIBC with a luminal molecular subtype have been shown to have a significantly higher rate of HER-2 alterations than those of the basal subtype. There were higher HER-2 2/3+ expression (46%) in MIBC and high grade NMIBC (21).

However, reports of HER-2 status in NMIBC are limited. A few studies have shown HER-2 protein over expression and gene amplification in 4–12% and 3–8% of NMIBC (11–13), respectively. Although predicting such behavior is clinically important as recurrence and invasion bear a significant risk of metastasis and impaired survival. The European Association of Urology (EAU) implemented EORTC risk tables in its guidelines for predicting tumor recurrence and progression (3).

Several challenges in pathologic stage have hindered its adoption in clinical guidelines for NMIBC. Chen et al. (22) showed that HER-2

TABLE 2 Comparison of clinicopathologic parameters according to the HER-2 expression.

Parameters Total (n = 204)	HER2 IHC				P value
	0	1+	2+	3+	
Tumor grade					
ow	36	38	36	0	< 0.001
High	8	20	55	11	
pT stage					
Ta	41	50	68	7	0.020
T1	3	8	23	4	
Sex					
Male	38	44	71	8	0.554
Female	6	14	20	3	
Tumor size					
< 3 cm	42	55	84	9	0.402
≥ 3 cm	2	3	7	2	
Number of tumors					
Single	36	40	58	4	0.119
2-7	7	15	26	6	
≥8	1	3	7	1	

NMIBC, non-muscle invasive bladder cancer. HER-2, human epidermal growth factor receptor-2.

10.3389/fonc.2023.1243118

TABLE 3 Comparison of clinicopathologic parameters according to the tumor grades or pT stage.

Parameters Total (n = 204)	Tumor grade		P value	pT stage		P value
	Low grade	High grade		Ta	T1	
Tumor grade						
Low	NA	NA	NA	106	4	< 0.001
High	NA	NA	NA	60	34	
Sex						
Male	81	80	0.045	130	31	0.656
Female	29	14		36	7	
Tumor size						
< 3 cm	107	83	0.011	157	33	0.089
≥ 3 cm	3	11		9	5	
Number of tumors						
Single	85	53	0.006	116	22	0.021
2-7	20	34		38	16	
≥8	5	7		12	0	

NMIBC, non-muscle invasive bladder cancer; pT stage, pathologic T stage; NA, Not Applicable.

amplification could distinguish a subset of NMIBC patients with a high risk of disease progression. But Olsson et al. (13) reported HER-2 expression could not predict patient prognosis in a larger study that included 285 patients. Because the detection of concurrent CIS increases the risk of recurrence and progression of Ta and T1 tumors (3). We only select patients with Ta and T1 and exclude patients with CIS. In the present study, we found the expression of HER-2 was significantly different in pathological groups, low and high grade NMIBC, and pathologic stage, but not in tumor size or number of tumors. As we know, the pathologic stage assessed by the severity of invasion depth is one of the most important prognostic predictors of NMIBC (23).

These findings could explain that HER-2 over expression has been found to correlate with the incidence of recurrence and progression in NMIBC. In our study, HER-2 expression was demonstrated to be a reliable independent factor associated with non-muscle-invasive tumor grade. It can be used to predict the prognosis of tumor in cystoscopic biopsy.

The guidelines for NMIBC remain controversial; and conservative management may allow tumor to progress to muscle invasion, which requires cystectomy. There have been attempts to translate over expression of HER-2 in UCB into therapeutic modalities. As widely known, the therapy is currently used

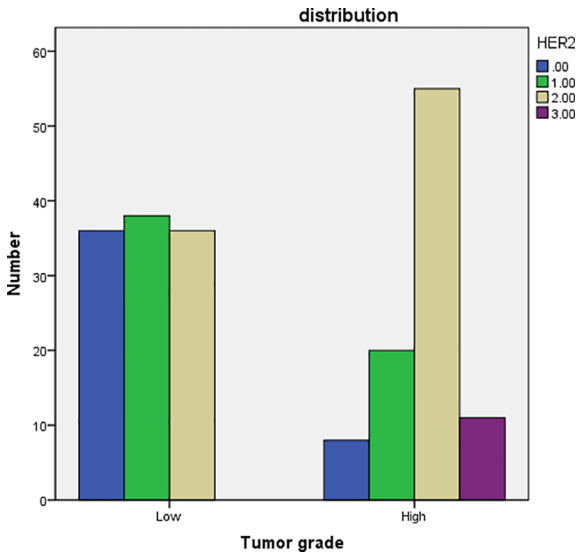

FIGURE 2
the bar chart of comparison of tumor grade with HER-2 IHC. HER-2: human epidermal growth factor receptor-2.

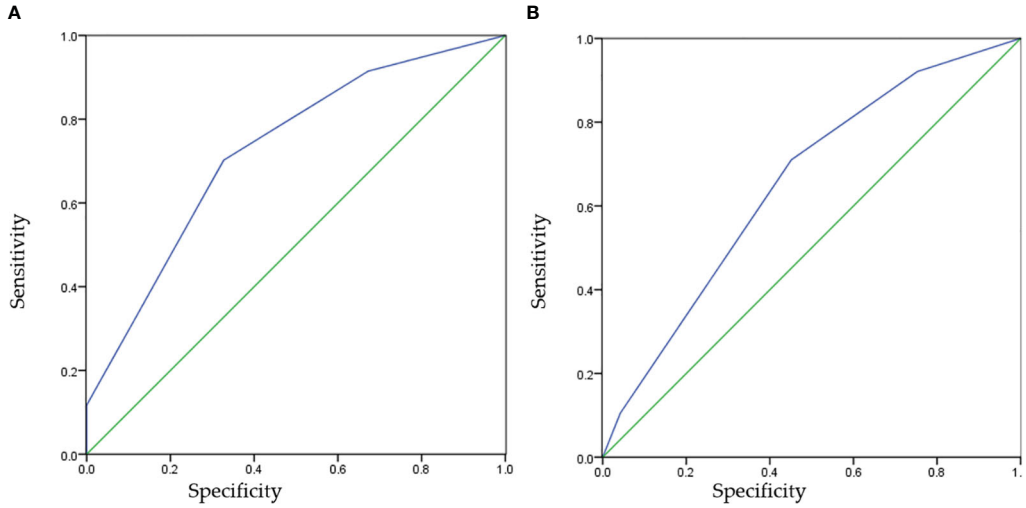

FIGURE 3
The receiver operating characteristic curves of HER-2 IHC for predicting tumor grades or pT stage. HER-2, human epidermal growth factor receptor-2. **(A)** Specificity=False Positive Rate, **(B)** Sensitivity=True Positive Rate.

TABLE 4 Cut-off, AUC, sensitivity and specificity values of HER-2 for pT stage and tumor grades.

Variables	AUC	Cut-off	Sensitivity	Specificity	95% CI	P values
tumor grade	0.727	0.5	91.5%	67.3%	0.658-0.796	< 0.001
pT stage	0.652	0.5	92.1%	75.3%	0.560-0.744	0.003

HER-2, human epidermal growth factor 2; pT stage, pathologic T stage.

TABLE 5 multivariable analyses of HER-2 expression for predicting tumor grades, pT stage.

	HER-2 (-) vs HER-2 (+)		
	OR	95% CI	P value
Tumor grade			
Low	1.00	1.848-11.774	0.001
High	4.665		
Pathologic stage			
Ta	1	0.419-6.500	0.473
T1	1.651		
Sex			
Female	1	0.134-0.960	0.141
Male	0.358		
Tumor size			
< 3 cm	1	0.175-4.935	0.931
≥ 3 cm	0.929		
Number of tumors			
Single	1		
2-7	0.275	0.032-2.346	0.238
≥8	0.513	0.053-4.952	

HER-2(-) was defined as HER-2 0 expression; HER-2 (+) was defined as HER-2 1+, 2+ or 3+.

worldwide for treating breast and gastric cancers (24, 25). However, the results have not been as promising as in breast cancer (10). The recent emergence of novel ADCs has renewed the interest in HER-2 targeted therapies for UCB. They effectively kill tumor cells with minimal systemic side effects. ADCs bind to tumor associated antigens, triggering endocytosis, internalization, and release of the cytotoxic payload in target tumor cells after lysosomal degradation (26).RC48-ADC is a novel humanized anti-HER-2 antibody, impairing the formation of the microtubule network of target cells. However, reports on RC48-ADC in HER-2 2+ or HER-2 3+ UCB patients suggest that only a moderate level of protein expression is sufficient to induce a response. In patients with advanced urothelial carcinoma, Sheng et al. (14) reported the RC48-ADC is a promising efficacy with a manageable safety profile. One of the main challenges in treating solid tumors with ADCs is the heterogeneous expression of the target antigen (Ag) in primary tumor tissues. Cleavable linkers and hydrophobic payloads have been proposed as a possible solution, mainly because of their hypothetical capital role played in the so-called "bystander killing effect", recently demonstrating promising clinical efficacy and preclinical activity even in HER-2 low tumors (27).

Although BCG is considered a very effective treatment for high risk NMIBC, consensus exists that not every patient with superficial bladder cancer should be treated with BCG due to its increased risk of toxicity (28). Meanwhile, urologists often have to treat patients not based on guidelines because of the chronic shortage of BCG and BCG failure remaining largely unknown (29). ADCs are promising

intravesical drugs that directly exert cytotoxic effects on tumor cells by targeting specific tumor antigens, with reduced systemic adverse effects. As previously mentioned, the expression of HER2 was significantly different in pathological groups and pathologic stage.

Conclusion

In summary, this study demonstrated that HER2 expression are associated with tumor stages and histological grades in NMIBC. It has diagnostic value for cystoscopic biopsy. and therapeutic strategies of HER2 expression could be considered for the management of NMIBC that tolerates BCG.

Data availability statement

The original contributions presented in the study are included in the article/supplementary material. Further inquiries can be directed to the corresponding authors.

Ethics statement

The studies involving humans were approved by Institutional Review Board of Peking University Cancer Hospital. The studies were conducted in accordance with the local legislation and institutional requirements. The human samples used in this study were acquired from primarily isolated as part of your previous study for which ethical approval was obtained. Written informed consent for participation was not required from the participants or the participants' legal guardians/next of kin in accordance with the national legislation and institutional requirements.

Author contributions

SW and PD designed the study. SW, YJ and YL made the same contribution in this study as the first coauthor. SW and PD made the same contribution in this study as the cor-corresponding authors. SW, YJ, YL, JM, XY, ZY, PD and YY performed the study and analyzed the data. PD, SW, YJ and YL wrote the manuscript draft and revised the manuscript. All authors have read and agreed to the published version of the manuscript.

Funding

The author(s) declare financial support was received for the research, authorship, and/or publication of this article. Science foundation of Peking University Cancer Hospital. 2021-7. Capital's Funds for Health Improvement and Research. 2022-1G-1021.

Conflict of interest

The authors declare that the research was conducted in the absence of any commercial or financial relationships that could be construed as a potential conflict of interest.

Publisher's note

References

1. Siegel RL, Miller KD, Jemal A. Cancer statistics,2019. *CA Cancer J Clin* (2019) 69:7–34. doi: 10.3322/caac.21551

2. Ploeg M, Aben KK, Kiemeney LA. The present and future burden of urinary bladder cancer in the world. *World J Urol* (2009) 27:289–93. doi: 10.1007/s00345-009-0383-3

3. Witjes JA, Bruins HM, Cathomas R, Compérat EM, Dominguez Escrigs JL, et al. European association of urology. *EAU guidelines non-muscle-invasive urothelial carcinoma bladder* (2020).

4. Jones JS, Larchian WA. *Chapter 81.Campbell-Walsh Urology,12th* .pp.2343.

5. Kodera A, Mohammed M, Lim P. The management of bacillus calmette-guérin (BCG) failure in high-risk non-muscle invasive bladder cancer: A review article. *Cureus* (2023) 15(6). doi: 10.7759/cureus.40962

6. Witjes JA, Palou J, Soloway M, Lamm D, Kamat AM, Brausi M, et al. Current Clinical Practice Gaps in the Treatment of Intermediate and High-Risk non Muscle-Invasive Bladder Cancer (NMIBC) With Emphasis on the Use of Bacillus Calmette–Gué rin (BCG): Results of an International Individual Patient Data Survey (IPDS). *BJU Int* (2013) 112:742–50. doi: 10.1111/bju.12012

7. Lae M, Couturier J, Oudard S, Radvanyi F, Beuzeboc P, Vieillefond A. Assessing HER2 gene amplification as a potential target for therapy in invasive urothelial bladder cancer with a standardized methodology: results in 1005 patients. *Ann Oncol* (2010) 21:815–9. doi: 10.1093/annonc/mdp488

8. Latif Z, Watters AD, Dunn I, Grigor K, Underwood MA, Bartlett JMS. HER2/ neu gene amplification and protein overexpression in G3 pT2 transitional cell carcinoma of the bladder: a role for anti-HER2 therapy? *Eur J Cancer* (2004) 40:56–63. doi: 10.1016/j.ejca.2003.08.027

9. Matsubara H, Yamada Y, Naruse K, Nakamura K, Aoki S, Taki T, et al. Potential for HER-2/neu molecular targeted therapy for invasive bladder carcinoma: comparative study of immunohistochemistry and fluorescent in *situ* hybridization. *Oncol Rep* (2008) 19:57–63. doi: 10.3892/or.19.1.57

10. Dreicer R. The future of drug development in urothelial cancer. *J Clin Oncol* (2012) 30:473–5. doi: 10.1200/JCO.2011.39.5566

11. Lim SD, Cho YM, Choi GS, Park HK, Paick SH, Kim WY, et al. Clinical significance of substaging and HER2 expression in papillary non-muscle invasive urothelial cancers of the urinary bladder. *J Korean Med Sci* (2015) 30:1068–77. doi: 10.3346/jkms.2015.30.8.1068

12. Kruger S, Lange I, Kausch I, Feller AC. Protein expression and gene copy number analysis of topoisomerase 2alpha, HER2 and P53 in minimally invasive urothelial carcinoma of the urinary bladder–a multitissue array study with prognostic implications. *Anticancer Res* (2005) 25:263–71.

13. Olsson H, Fyhr IM, Hultman P, Jahnson S. HER2 status in primary stage T1 urothelial cell carcinoma of the urinary bladder. *Scand J Urol Nephrol* (2012) 46:102–7. doi: 10.3109/00365599.2011.637955

14. Sheng X, Yan X, Guo J. Open-label, multicenter, phase II study of RC48-ADC, a HER2-targeting antibody-drug conjugate, in patients with locally advanced or metastatic urothelial carcinoma. *Clin Cancer Res* (2021) 27(1):43–51. doi: 10.1158/1078-0432.CCR-20-2488

15. Balar AV, Castellano D, O'Donnell PH, Grivas P, Vuky J, Powles T, et al. First-line pembrolizumab in cisplatin-ineligible patients with locally advanced and unresectable or metastatic urothelial cancer: A multicentre, single-arm, phase 2 study. *Lancet Oncol* (2017) 18:1483–92. doi: 10.1016/S1470-2045(17)30616-2

16. Balar AV, Galsky MD, Rosenberg JE, Powles T, Petrylak DP, Bellmunt J, et al. Atezolizumab as first-line treatment in cisplatin-Ineligible patients with locally advanced and metastatic urothelial carcinoma: a single-arm, multicentre, phase 2 trial. *Lancet* (2017) 389:67–76. doi: 10.1016/S0140-6736(16)32455-2

17. Harris L, Fritsche H, Mennel R, Norton L, Ravdin P, Taube S, et al. American society of clinical oncology 2007 update of recommendations for the use of tumor markers in breast cancer. *J Clin Oncol* (2007) 25:5287–312. doi: 10.1200/JCO.2007.14.2364

18. Grivas PD, Day M, Hussain M. Urothelial carcinomas: a focus on human epidermal receptors signaling. *Am J Transl Res* (2011) 3:362–73.

19. Latif Z, Watters AD, Dunn I, Grigor K, Underwood MA, Bartlett JMS. HER2/neu gene amplification and protein overexpression in G3 pT2 transitional cell carcinoma of the bladder: a role for anti-HER2 therapy? *Eur J Cancer* (2004) 40:56–63.

20. Nedjadi T, Al-Maghrabi J, Assidi M, Dallol A, Al-Kattabi H, Chaudhary A, et al. Prognostic value of HER2 status in bladder transitional cell carcinoma revealed by both IHC and BDISH techniques. *BMC Cancer* (2016) 16:653.

21. Ding W, Tong S, Gou Y, Sun C, Wang H, Chen Z, et al. Human epidermal growth factor receptor 2: a significant indicator for predicting progression in non-muscle-invasive bladder cancer especially in high-risk groups. *World J Urol* (2015) 33:1951–7. doi: 10.1007/s00345-015-1557-9

22. Kiss B, Wyatt AW, Douglas J, Skuginna V, Mo F, Anderson S, et al. Her2 alterations in muscle-invasive bladder cancer: patient selection beyond protein expression for targeted therapy. *Sci Rep* (2017) 7:42713. doi: 10.1038/srep42713

23. Chen PC, Yu HJ, Chang YH, Pan C-C. Her2 amplification distinguishes a subset of Moustakas et al. 11 non-muscle-invasive bladder cancers with a high risk of progression. *J Clin Pathol* (2013) 66:113–9. doi: 10.1136/jclinpath-2012-200944

24. Brimo F, Wu C, Zeizafoun N, Tanguay S, Aprikian A, Mansure JJ, et al. Prognostic factors in T1 bladder urothelial carcinoma: the value of recording millimetric depth of invasion, diameter of invasive carcinoma, and muscularis mucosa invasion. *Hum Pathol* (2013) 44:95–102. doi: 10.1016/j.humpath.2012.04.020

25. Wolff AC, Hammond MEH, Hicks DG, Dowsett M, McShane LM, Allison KH, et al. American society of clinical oncology; college of American pathologists. Recommendations for human epidermal growth factor receptor 2 testing in breast cancer: American society of clinical oncology/college of American pathologists clinical practice guideline update. *Arch Pathol Lab Med* (2014) 138:241–56. doi: 10.5858/arpa.2013-0953-SA

26. Kunz PL, Mojtahed A, Fisher GA, Ford JM, Chang DT, Balise RR, et al. HER2 expression in gastric and gastroesophageal junction adenocarcinoma in a US population: clinicopathologic analysis with proposed approach to HER2 assessment. *Appl Immunohistochem Mol Morphol* (2012) 20:13–24.

27. Skidmore L, Sakamuri S, Knudsen NA, Hewet AG, Milutinovic S, Barkho W, et al. ARX788, a Site-specific anti-HER2 Antibody-Drug Conjugate, Demonstrates potent and selective activity in HER2-low and T-DM1-resistant breast and gastric cancers. *Mol Cancer Ther* (2020) 19(9):1833–43. doi: 10.1158/1535-7163.MCT-19-1004

28. Kowalski M, Guindon J, Brazas L, Moore C, Entwistle J, Cizeau J, et al. A Phase II Study of Oportuzumab Monatox: An Immunotoxin therapy for patients with noninvasive urothelial carcinoma in situ previously treated with Bacillus Calmette–Guérin. *J Urol* (2012) 188:1712–8. doi: 10.1016/j.juro.2012.07.020

29. Nikas CV, Smith AB. Goldilocks and the BCG: bacillus calmette–guérin dose reduction in the age of shortage. *Eur Urol* (2020) 78:699–700. doi: 10.1016/j.eururo.2020.05.021

frontiers | Frontiers in Oncology

TYPE Original Research
PUBLISHED 29 February 2024
DOI 10.3389/fonc.2023.1229227

OPEN ACCESS

EDITED BY
Wen-Hao Xu,
Fudan University, China

REVIEWED BY
Tiezheng Qi,
Central South University, China
Wei Chen,
The University of Texas Health Science Center at San Antonio, United States
Weinian Shou,
Indiana University, United States

*CORRESPONDENCE
Yaling Tao
taoyaling@ucas.ac.cn
Ting Cai
caiting@ucas.ac.cn
Qian Chen
chenqian@ucas.ac.cn

RECEIVED 26 May 2023
ACCEPTED 22 November 2023
PUBLISHED 29 February 2024

CITATION
Tao Y, Yu X, Cong H, Li J, Zhu J, Ding H, Chen Q and Cai T (2024) Identification of *FLRT2* as a key prognostic gene through a comprehensive analysis of TMB and IRGPs in BLCA patients.
Front. Oncol. 13:1229227.
doi: 10.3389/fonc.2023.1229227

Identification of *FLRT2* as a key prognostic gene through a comprehensive analysis of TMB and IRGPs in BLCA patients

Yaling Tao[1,2*], Xiaoling Yu[2], Huaiwei Cong[2], Jinpeng Li[1,2], Junqi Zhu[3], Huaxin Ding[4], Qian Chen[2,3,5*] and Ting Cai[1,2*]

[1]Research Institute, Ningbo No.2 Hospital, Ningbo, China, [2]Ningbo Institute of Life and Health Industry, University of Chinese Academy of Sciences, Ningbo, China, [3]Department of Research and Development, Thorgene Co., Ltd., Beijing, China, [4]Department of Pathology, Ningbo Clinical Pathology Diagnosis Center, Ningbo, China, [5]Research Institute, Ningbo Hangzhou Bay Hospital, Ningbo, China

Introduction: The tumor immune environment and immune-related genes are instrumental in the development, progression, and prognosis of bladder cancer (BLCA). This study sought to pinpoint key immune-related genes influencing BLCA prognosis and decipher their mechanisms of action.

Methods and results: We analyzed differentially expressed genes (DEGs) between high- and low- tumor mutational burden (TMB) groups. Subsequently, we constructed a reliable prognostic model based on immune-related gene pairs (IRGPs) and analyzed DEGs between high- and low-risk groups. A total of 22 shared DEGs were identified across differential TMB and IRGPs-derived risk groups in BLCA patients. Through univariate Cox and multivariate Cox analyses, we highlighted five genes - *FLRT2, NTRK2, CYTL1, ZNF683, PRSS41* - significantly correlated with BLCA patient prognosis. Notably, the *FLRT2* gene emerged as an independent prognostic factor for BLCA, impacting patient prognosis via modulation of macrophage infiltration in immune microenvironment. Further investigation spotlighted methylation sites - cg25120290, cg02305242, and cg01832662 - as key regulators of *FLRT2* expression.

Discussion: These findings identified pivotal prognostic genes in BLCA and illuminated the intricate mechanisms dictating patient prognosis. This study not only presents a novel prognostic marker but also carves out potential avenues for immunotherapy and targeted therapeutic strategies in BLCA. By demystifying the profound impact of immune-related genes and the tumor immune environment, this study augments the comprehension and prognostic management of bladder cancer.

KEYWORDS

bladder cancer, prognosis, TMB, IRGPs, FLRT2, methylation

1 Introduction

Bladder cancer (BLCA), a globally acknowledged prevalent malignancy (1), had an estimated incidence of 81,180 and was responsible for 17,100 deaths in the United States in 2022 (2, 3). The majority of patients (i.e., 70%–75%) are diagnosed as having non-muscle-invasive bladder cancer (NMIBC) at onset, while approximately 20%–25% of patients are diagnosed as having muscle-invasive bladder cancer (MIBC) (4). The patients with NMIBC often experience high recurrence (50%–70%) and progression (10%–30%) rates (5). Advanced and metastatic BLCA, an invariably fatal disease, exhibits 5-year overall survival and progression-free survival rates of less than 15% (6, 7). Despite advancements in BLCA treatment through immunotherapy, targeted therapies, and neoadjuvant chemoimmunotherapy, high mortality and recurrence rates persist (8, 9). Hence, the critical need for new, efficient prognosis targets.

In recent years, gene expression profiling techniques, including gene microarrays and RNA sequencing, have become widely used in the search for biomarkers associated with BLCA prognosis (10–12). However, a major limitation of this approach is its inability to account for correlations between genes. Interestingly, the tumor mutational burden (TMB), which reflects the total load of neoantigens, displays a robust correlation with immunotherapy responsiveness (13–15). Additionally, immune-related genes, pivotal in modulating the immune system, have been deemed crucial in the development and progression of cancer (16, 17). Contemporary research is increasingly focusing on immune-related gene pairs (IRGPs) studies to identify prognostic biomarkers for patients (18, 19).

In this study, we conducted a combination analysis of TMB and IRGPs to identify prognostic genes in BLCA. We examined differentially expressed genes (DEGs) in high- and low-TMB groups, constructed a risk model using IRGPs, and then performed an analysis of the DEGs between the high- and low-risk groups. The common DEGs between the different TMB and risk groups were subsequently isolated. Through this process, we identified a key gene, fibronectin leucine-rich transmembrane protein 2 (*FLRT2*) and clarified its prognostic significance in BLCA.

FLRT2, a member of the FLRT family of proteins, contains 10 leucine-rich repeat (LRR) domains and a transmembrane domain (20). Flintoff KA et al. discovered that *FLRT2* interacted with fibronectin through either repulsion or adhesion, behaving as an adhesion molecule, suggesting a potential connection between *FLRT2* and cancer metastasis (21). Recent studies have shown that *FLRT2* expression correlates negatively with the long-term survival of colorectal cancer patients and that *FLRT2* facilitates the aggressiveness of colorectal cancer (22). However, the role of *FLRT2* in BLCA remains unexplored. In this study, we clarified the identification process of *FLRT2* and the impact of this gene on BLCA prognosis, thereby augmenting the understanding of its role in disease progression and its potential as a therapeutic target in BLCA.

2 Materials and methods

2.1 Sample data collection and processing

Publicly available data were utilized for this comprehensive analysis. The data of transcriptome cohorts and clinical features were obtained from The Cancer Genome Atlas (TCGA-BLCA, n = 433, https://portal.gdc.cancer.gov/) and the Gene Expression Omnibus (GSE31684, n = 93, https://www.ncbi.nlm.nih.gov/geo/). A list of 1,776 immune genes and their functional classification was retrieved from ImmPort (https://www.immport.org/shared/home), which was accessed on 25 November 2020. Ensembl ID conversion and extraction of the relevant clinical data were performed using Strawberry Perl (5.30.11). Other data processing was conducted using R (version 3.6.1; The R Foundation for Statistical Computing, Vienna, Austria).

2.2 Simple nucleotide variation data analysis and visualization

The BLCA simple nucleotide variation (SNV) data from TCGA, which is referred to as the "masked somatic mutation" subtype, were processed using VarScan software. The R package "maftools" [16] was employed to analyze and visualize the somatic variants in mutation annotation format (MAF). The germline DNA variants were removed, and the remaining mutation cases were used to determine the TMB using the R package "maftools".

2.3 Copy number variation data processing

The BLCA copy number variation (CNV) data, referred to as the "masked copy number segment" type, were downloaded from the TCGA database. The data processing was conducted with Strawberry Perl (5.30.11), and visualization was performed using the R package "RCircos".

2.4 Construction of a prognostic IRGP risk model based on the TCGA cohort

For sample-specific pairwise comparisons, two immune-related genes were paired, and if the first immune-related gene exhibited higher levels of expression than the second, the two genes were combined into one immune-related gene pair (IRGP) and assigned a score of 1; otherwise, the score was set to 0. Utilizing the initial candidate IRGPs, the prognostic model was constructed by univariate and multivariate Cox proportional risk regression. Finally, 62 gene pairs were used to define the final model. The optimal cutoff value for the IRGP index, which was analyzed by receiver operating characteristic (ROC) curves for 5-year overall survival (OS), enabled the division of patients into high-risk and

low-risk groups. Kaplan–Meier (K–M) survival curves were employed to compare the differences in OS between the high- and low-risk groups, and log-rank tests were applied.

2.5 Acquisition of differentially expressed genes

The DEG analysis was conducted with R package "limma" and visualized with R package "pheatmap" in this study. The gene filtering condition was set to a false-discovery rate (FDR) < 0.05.

2.6 Functional enrichment analysis

Gene ontology (GO) function and Kyoto Encyclopedia of Genes and Genomes (KEGG) pathway enrichment were performed using the R packages "clusterProfiler", "org.Hs.eg.db", and "enrichplot". Visualization was achieved with R package "ggplot2". The gene set enrichment analysis (GSEA) was carried out by gsea-3.0.jar and Strawberry Perl (5.30.11). Significant enrichment criteria were set as a p-value < 0.05 and a FDR < 0.05.

2.7 Infiltration of 22 types of immune cells in BLCA

To calculate the infiltration level of 22 types of immune cells, cell type identification by estimating relative subsets of RNA transcripts (CIBERSORT) was used to evaluate and predict the enrichment of the immune cells. The R packages "CIBERSORT" and "Leukocyte signature matrix" were used to analyze the percentage of 22 immune cells' infiltration in each sample. The p-values less than 0.05 were considered significant.

2.8 TIMER and GEPIA database analysis

The expression of the key gene *FLRT2* and overall survival were analyzed using GEPIA (Gene Expression Profiling Interactive Analysis; http://gepia2.cancer-pku.cn/). The relationship between the CNV level of *FLRT2* and immune cell infiltration was evaluated using TIMER (Tumor IMmune Estimation Resource; https://cistrome.shinyapps.io/timer/).

2.9 RNA isolation and real-time polymerase chain reaction

Tumor samples of six BLCA patients were obtained from Ningbo Clinical Pathology Diagnosis Center, Ningbo, China. The BLCA patients were divided into long-survival and short-survival patient groups by varying survival durations (long survival: overall survival > 5 years; short survival: overall survival < 2 years). The total RNA of tumor samples was extracted using RNeasy FFPE Kit (QIAGEN, 73504) according to the standard protocol. RNA concentration was measured by a NanoDrop™ 2000 Spectrophotometer (Thermo Fisher Scientific, Waltham MA, USA) by calculating from the optical density at 260 nm (OD_{260}). Then the RNA was reverse transcribed to cDNA with the PrimeScript™ RT Reagent Kit (Perfect Real Time) (Takara RR037A) following the manufacturer's instructions. Then RT-PCR was performed with a SLAN-96S real-time PCR thermal cycler, using a SYBR™ Green mixture (Takara RR820A) for relative mRNA quantification. Glyceraldehyde 3-phosphate dehydrogenase (GAPDH) was used as the loading control. Each qPCR reaction was conducted in triplicate. The following primers were used: GAPDH forward—5′-GATTCCACCCATGGCAAATTC-3′; GAPDH reverse—5′-CTGGAAGATGGTGATGGGATT-3′; *FLRT2* forward—5′-TGTGCCTGTTGGGCTTCCT-3′; and *FLRT2* reverse—5′-CGGCGATACCCTTGTTGGT-3′. The thermal cycling was conducted with the following parameters: 10 s at 60°C, 10 s at 95°C, 10 s at 95°C and 45 s at 58°C for 40 cycles, and 2 min at 60°C. The $2^{-\Delta\Delta Ct}$ method was used to estimate the relative mRNA expression of the target genes.

2.10 Immunohistochemistry

The antibody against *FLRT2* was purchased from Invitrogen (anti-*FLRT2* antibody, PA5–32122). Immunohistochemistry (IHC) of six BLCA tumor samples was performed according to the manufacturer's instructions. Four 5-μm sections were cut from each case. After dewaxing, slides were boiled with 1 mM EDTA pH 8.0 followed by 15 min at a sub-boiling temperature. The slides were washed with phosphate-buffered saline three times for 5 min each. The slides were subsequently quenched in 3% hydrogen peroxide for 15 min, and then blocked with 10% goat serum for 10 min. The slides were incubated overnight at 4°C with the primary antibody diluent (1: 2,000). The slides were then incubated with a biotinylated secondary antibody, per the manufacturer's recommendation, for 30 min. Antibody binding was visualized with 3,3′-diaminobenzidine (DAB; ZLI-9018, OriGene).

2.11 Gene methylation and sites methylation correlation statistics with gene expression

The BLCA gene methylation data were downloaded from the TCGA database. Gene methylation was statistically performed using the R package "limma", and site methylation was analyzed using Strawberry Perl. For the gene methylation difference analysis, the Wilcoxon test was used for data validation. Heatmaps and correlation charts were generated in R.

2.12 Statistical analysis

All statistical analyses and graphics were performed using R software (version 3.6.1). The data analysis was conducted using a Student's t-test or the Wilcoxon rank-sum test. Least absolute shrinkage and selection operator (lasso) Cox regression analysis

with 10-fold cross-validation was carried out using the R package "glmnet". The statistical significance was set as a p-value < 0.05.

3 Results

3.1 The workflow design of the current study

The workflow design of this study is presented in Figure 1. A total of 412 BLCA patients were included in this study for analysis. We obtained SNV data from the TCGA database, calculated tumor mutational burden (TMB) values, and further divided the patients into high- and low-TMB groups. The transcriptome sequencing data from the TCGA database and a list of immune-related genes from the ImmPort website were utilized to analyze BLCA IRGPs. A total of 62 IRGPs were identified through univariate and multivariate Cox analysis, which allowed the construction of a prognostic model for BLCA patients (Table S1). Based on the risk score calculated by this model, patients were divided into high- and low-risk groups. The common DEGs between the high- and low-risk groups and the high- and low-TMB groups that affected the prognosis of BLCA patients were analyzed. Finally, *FLRT2*, a new key gene affecting BLCA prognosis, was identified, and its mechanism of action on patient prognosis was further investigated.

3.2 The landscape of somatic mutations in BLCA patients

The somatic mutation data of BLCA were downloaded from the TCGA database. The variant classification of somatic mutations included missense mutations, nonsense mutations, splice sites, frameshift deletions, frameshift insertions, in-frame deletions, non-

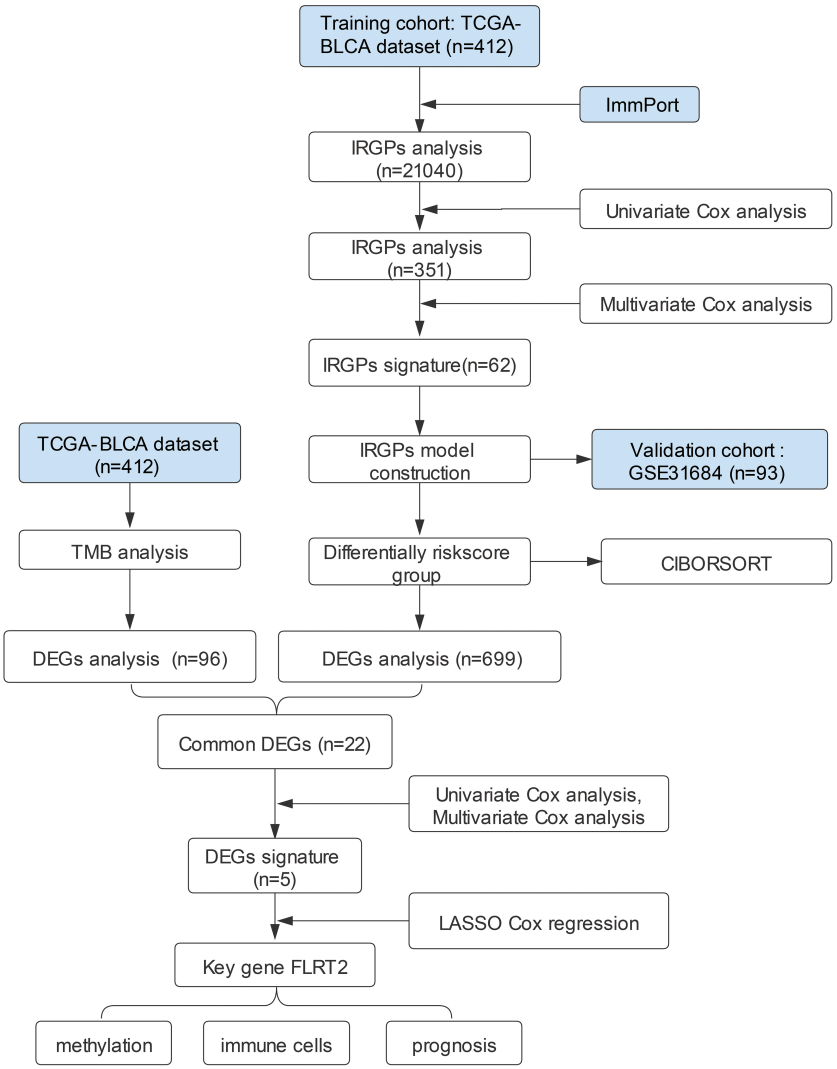

FIGURE 1
The workflow design of the current study. TCGA, the Cancer Genome Atlas; BLCA, bladder urothelial carcinoma; GEO, Gene Expression Omnibus; IRGPs, immune-related gene pairs; DEGs, differentially expressed genes; TMB, tumor mutational burden; CIBORSORT, cell-type identification by estimating relative subsets of RNA transcripts; LASSO, least absolute shrinkage and selection operator.

10.3389/fonc.2023.1229227

stop mutations, translation initiation sites, and in-frame insertions. The proportion of missense mutations was the highest. The number of single nucleotide polymorphisms (SNPs) was more than deletions (DELs) and insertions (INSs). The SNV type with C > T was the most common (Figure 2A). The frequency of variants for each sample was also calculated and displayed. The detailed mutation information for the 30 genes with the highest mutation frequency for all the sample (n = 412) is shown in Figure 2B. The mutation frequency of *TP53*, *TTN*, *KMT2D*, *KDM6A*, *ARID1A*, *MUC16*, and *PIK3CA* was above 20%. The co-occurrence and mutually exclusive associations across the top 20 mutated genes are exhibited in Figure 2C. The CNVs of BLCA patients were mainly located on chromosomes 4, 6, and 15 (Figure 2D). These results indicated the presence of a somatic mutation profile in BLCA, which may affect the prognosis of BLCA patients by influencing the tumor immune microenvironment and the sensitivity of tumor therapy.

3.3 The role of TMB in prognosis of BLCA patients

To explore the impact of TMB on the prognosis of BLCA patients, we calculated the TMB value for each sample, and then categorized the samples into high- and low-TMB groups based on the median TMB value. The TMB values for each sample are presented in Figure 3A. The figure shows statistically significant differences between the high- and low-TMB groups (p < 0.001). The Kaplan–Meier analysis indicated a significant correlation between TMB and prognosis (p = 0.006), revealing that BLCA patients in the high-TMB group had a more favorable prognosis than those in the low-TMB group (Figure 3B). To investigate whether or not TMB affects BLCA prognosis by modulating the immune microenvironment, we analyzed differences in infiltrated immune cells between the high- and low-TMB groups. The results indicated significant differences in the proportions of memory B cells, CD8 T cells, resting memory CD4 T cells, activated memory CD4 T cells, regulatory T cells (Tregs), M1 macrophages, resting mast cells, and neutrophils between the two groups (Figures S1A, S1B). To find the key immune genes that affect prognosis, we first identified 101 DEGs between the high- and low-TMB groups (Figure S2A). The heatmap displaying the top 40 DEGs is presented in Figure 3C. The gene ontology (GO) enrichment analysis showed that these DEGs were primarily related to the regulation of blood pressure (Figure 3D). On comparing the 101 DEGs with the ImmPort database, we identified 17 of these DEGs as being immune-related genes (Figure 3E). To assess their impact on patient prognosis, we performed univariate Cox analysis for these 17 immune DEGs. As a result, *GLP1R*, *KIR2DL4*, and *SSTR5* were found to be significantly associated with the prognosis of BLCA patients (Table S2). However, the subsequent multivariate Cox analysis did not show a statistically significance between the expression of these three genes and overall survival (OS) (Figure 3F). These findings suggest that these TMB-derived immune-related DEGs have a role in shaping the immune landscape; however, their effects on the prognosis of BLCA patients might be multifaceted.

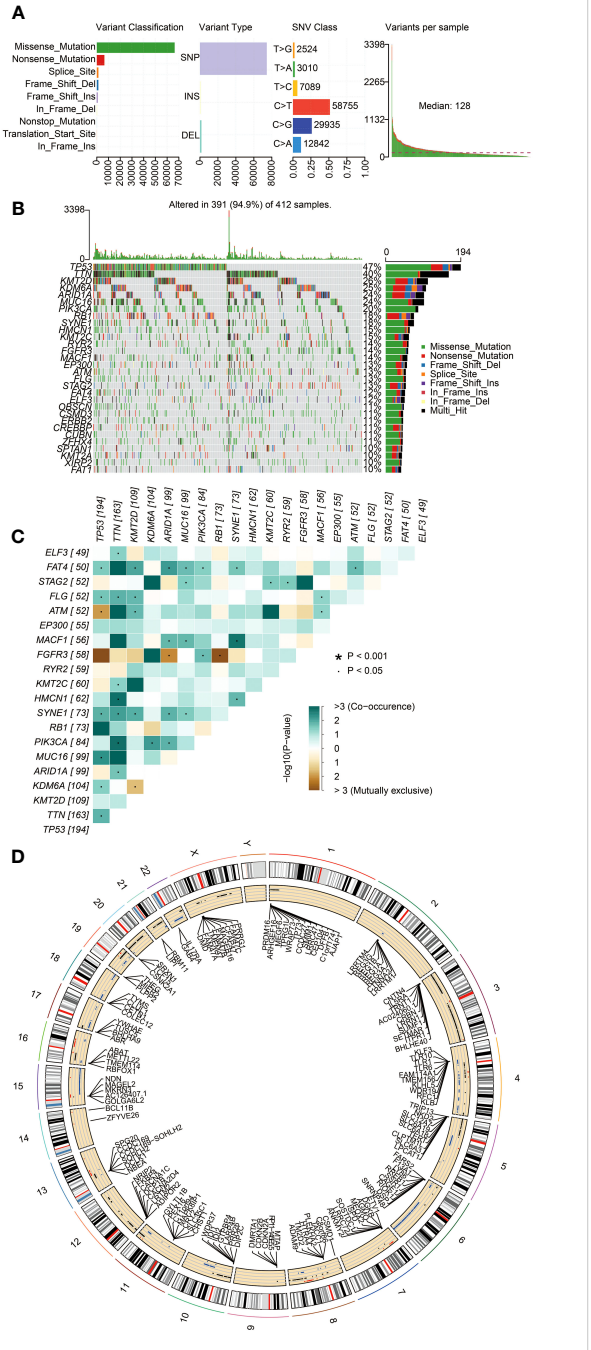

FIGURE 2
The landscape of somatic mutations in BLCA patients. **(A)** The diagram in order (from left to right): frequency of variant classification; frequency of variant types; frequency of SNV classes; and the level of gene variants in each sample. **(B)** Waterfall plot displaying the top 30 mutated genes in BLCA. The left panel shows different mutation types in each sample of BLCA. The right panel presents the genes ordered by their mutation frequencies. **(C)** The co-occurrence and mutually exclusive correlation with mutated genes. The solid black bullet (•) denotes a p-value < 0.05. The asterisk (*) denotes a p-value < 0.001. **(D)** Circos plot showing genes with copy number variation (CNV). The outer circle indicates the differential chromosomes, and the inner circle displays the genes with CNV. The red dot denotes increased CNV. The blue dot denotes decreased CNV.

10.3389/fonc.2023.1229227

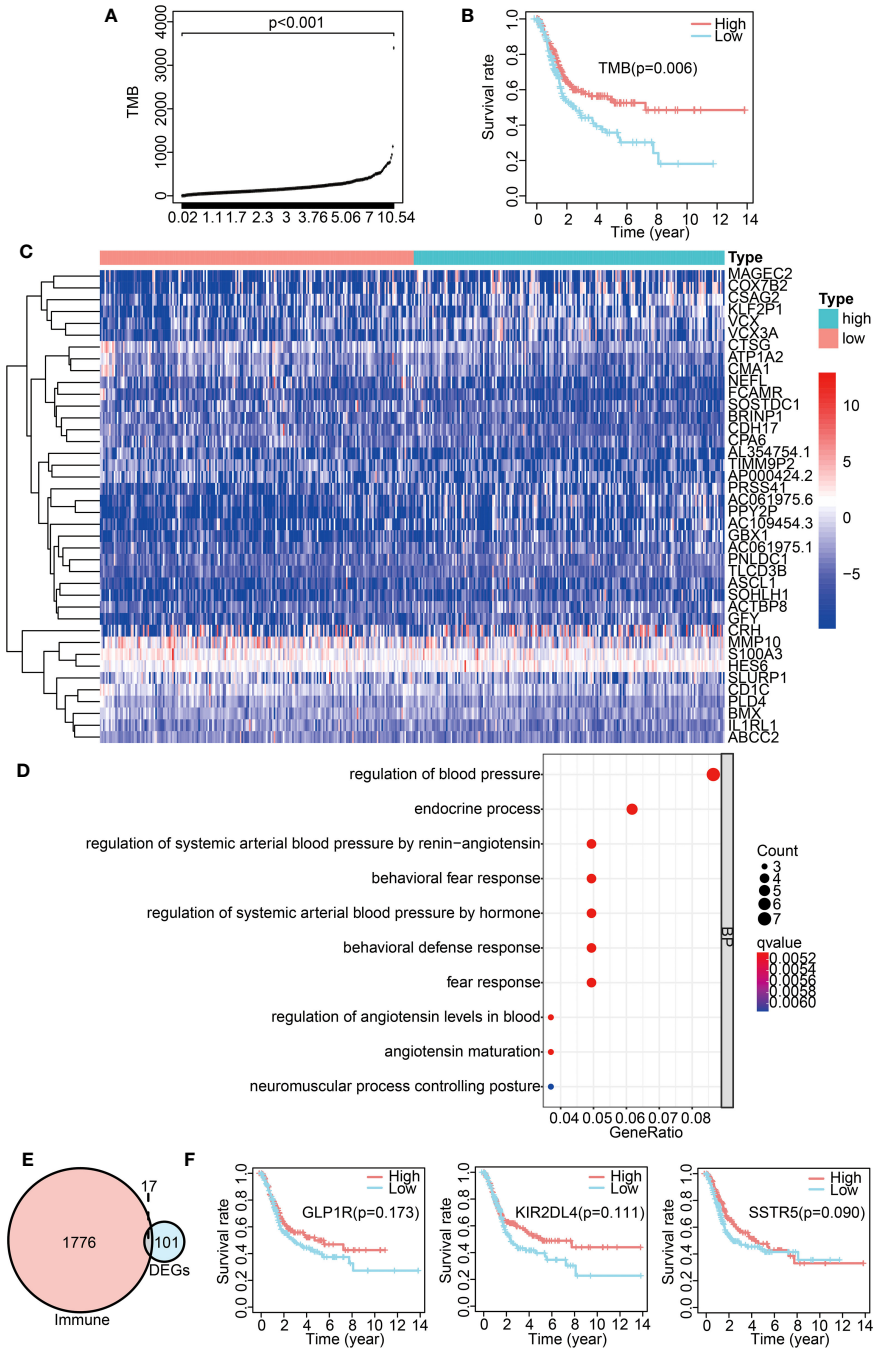

FIGURE 3
Analysis of TMB-derived DEGs and their correlation with BLCA prognosis. **(A)** TMB value in each sample. **(B)** Survival analysis between high- and low-TMB groups by Kaplan–Meier survival curves. **(C)** Heatmap exhibiting the top 40 DEGs between the high- and low-TMB groups. **(D)** GO enrichment analysis of DEGs. **(E)** Venn diagram of immune-related DEGs between the high- and low-TMB groups. **(F)** Kaplan–Meier curves displaying an association of *GLP1R*, *KIR2DL4*, and *SSTR5* expression with overall survival.

3.4 Construction of a prognostic risk model with IRGPs for BLCA patients

While the association analysis between TMB-derived immune genes and BLCA prognosis failed to identify a clear target, we shifted our focus on constructing a prognostic risk model based on IRGPs. For this, TCGA transcriptome data were designated as a training cohort, while the GEO transcriptome data were used for validation. From the ImmPort database, we extracted 1,713 immune-related genes. The IRGPs were constructed from these genes. To ensure the robustness of the risk model, only IRGPs with a median absolute deviation (MAD) more than 0.5 were retained. This filtration resulted in a comprehensive list of 21,040 IRGPs. With subsequent univariate and multivariate Cox regression analysis on the IRGPs within the TCGA cohort, 62 IRGPs were retained and used for constructing a prognostic risk model. A

majority of these IRGPs were associated with pathways such as BCR signaling, cytokine receptors, antimicrobials, and cytokine-related molecules (Table S1).

We then classified the patients into high- and low-risk groups based on the optimal risk model threshold (−1.176). Impressively, the AUC value of the ROC curve was 0.903, thus displaying a high accuracy and sensitivity for the model (Figure 4A). The Kaplan–Meier curve showed a significantly improved overall survival in the low-risk group (Figure 4B, left; $p < 0.001$), a finding consistent with the validation cohort GSE31684 (Figure 4B, right; $p = 0.011$). Subsequently, univariate and multivariate Cox proportional risk analyses were performed on the TCGA cohort. The results positioned the risk score of the prognosis model as an independent prognostic factor, with a high-risk score associated with a poor prognosis (Figure 4C). The validation set produced analogous results (Figure 4D).

We further sought to uncover any potential ties between the risk score and the immune landscape. With the CIBERSORT algorithm we estimated the relative proportions of 22 distinct immune cells for each patient in the high- and low-risk groups in the TCGA dataset.

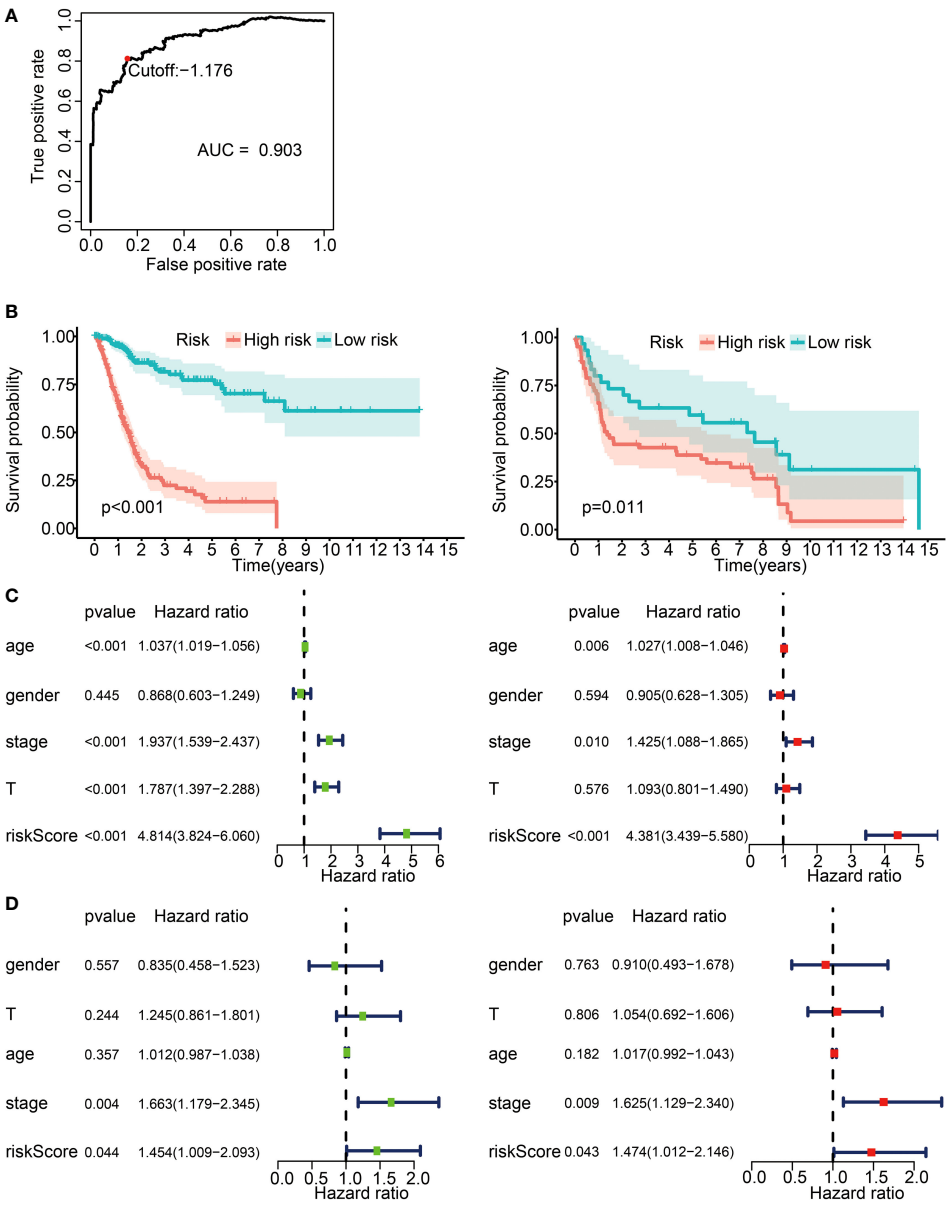

FIGURE 4
Prognostic risk model construction with 62 IRGPs for BLCA patients. **(A)** ROC curve for the IRGP risk model in the TCGA cohort. A risk score of −1.176 was used as a threshold for the IRGPs risk model to classify patients into high- and low-risk groups. ROC, receiver operating characteristic; AUC, area under curve. **(B)** Survival analysis of patients in the high- and low-risk groups with Kaplan–Meier survival curves. Left panel: the TCGA cohort. Right panel: the GSE31684 cohort. **(C)** Forest plot for univariate and multivariate Cox analysis in the TCGA cohort. Stage, clinical staging; T, T status of TNM staging; riskScore, risk score calculated from the prognostic risk model. Left: univariate Cox analysis. Right: multivariate Cox analysis. **(D)** Forest plot for univariate and multivariate Cox analysis in the GSE31684 cohort. Left panel: univariate Cox analysis. Right panel: multivariate Cox analysis.

The radar plots illustrate the disparities in various immune cells between the two groups (Figure S3A). We found that the infiltration levels of M0 macrophages, M2 macrophages, neutrophils, activated mast cells, and resting memory CD4 T cells were higher in the high-risk group ($p < 0.05$), while the infiltration levels of regulatory T cells (Treg), CD8 T cells, T follicular helper cells, plasma cells, and activated memory CD4 T cells were lower in the high-risk group (Figure S3B; $p < 0.05$).

Overall, these findings endorsed the reliability and sensitivity of our constructed risk model, firmly positioning the risk score as an independent prognostic factor for BLCA patients. Meanwhile, the results highlighted differences in the infiltration levels for several immune cells between the risk groups.

3.5 Common DEG analysis across differential TMB/IRGPs-derived risk groups

To identify the critical immune-related genes that may influence prognosis, we investigated the DEGs in the high- and low-risk groups. The DEG landscape was illustrated in a volcano plot (Figure S2B), while the top 40 DEGs were comprehensively portrayed in a heatmap (Figure 5A). The GO terms included three distinct domains: biological processes (BPs), molecular functions (MFs), and cellular components (CCs). The first 10 enrichment terms across each category are displayed in Figure 5B. We found that these DEGs were involved in the BPs such as extracellular matrix and structure formation, collagen production, and receptor ligand activity.

A significant difference was observed in the prognosis analysis between both high- and low-TMB groups and the high- and low-risk groups. To delve into the relationship between these groups, we investigated common DEGs across the high- and low-TMB groups and the high- and low-risk groups. The Venn diagram displaying the overlap of the DEGs is presented in Figure 5C. A total of 22 common DEGs were identified from this analysis. The results indicated that *FLRT2*, *NTRK2*, *CYTL1*, *ZNF683*, and *PRSS41* genes were significantly associated with prognosis using univariate Cox analysis (Table 1). Furthermore, we formulated a multivariate Cox model and conducted a Kaplan–Meier survival curve analysis, which confirmed the significant associations of *FLRT2* ($p = 0.002$), *NTRK2* ($p = 0.04$), *CYTL1* ($p = 0.045$), *ZNF683* ($p = 0.004$), and *PRSS41* ($p = 0.025$) genes with overall survival in BLCA patients (Figure 5D). Notably, patients exhibiting low expression levels of the *FLRT2*, *NTRK2*, and *CYTL1* genes had improved survival rates, while higher expression levels of *ZNF683* and *PRSS41* were associated with superior survival outcomes. In conclusion, our integrative analysis of TMB and IRGPs led to the identification of five key genes with significant prognostic relevance.

3.6 Prognostic significance and functional analysis of *FLRT2*

To identify the key genes among *FLRT2*, *NTRK2*, *CYTL1*, *ZNF683*, and *PRSS41*, we performed lasso regression analysis. Each gene was identified as an independent variable with a coefficient trajectory (Figure 6A, left). We then performed 10-fold cross-validation to assess the accuracy of this risk model and obtained confidence intervals under each log(λ) value (Figure 6A, right). This analysis brought the key gene *FLRT2* into focus. We conducted a Spearman correlation analysis based on GEPIA, examining the correlation of *FLRT2* with the other genes. The results revealed that *FLRT2* had a significant positive correlation with *NTRK2*, *CYTL1*, and *ZNF683* genes, while no association with *PRSS41* was found (Figure 6B). *PRSS41* expression was observed to significantly correlate with *ZNF683* expression (Figure S4). GSEA enrichment analysis was then performed to explore significantly enriched signaling pathways related to *FLRT2*. The top five significantly enriched signaling pathways are presented in Figure 6C. The GSEA enrichment scores of GO and KEGG analysis manifested that *FLRT2* was important with mitochondrial and peroxisome function in BLCA patients.

Subsequently, a comprehensive analysis was undertaken on the *FLRT2* gene. BLCA patients were categorized into high- and low-expression groups based on *FLRT2* expression levels. Survival analysis about OS and disease-free survival (DFS) rates were performed using GEPIA. The patients in the low *FLRT2* expression group presented an improved OS rate (Figure 6D, top; $p = 0.04$) and DFS rate (Figure 6D, bottom; $p = 1e\text{-}05$). To substantiate the prognostic significance of *FLRT2* in BLCA patients, we assessed its expression levels in tumor samples from six BLCA patients with varying survival durations through RT-PCR and immunohistochemical (IHC) analysis. Our analysis revealed that the mRNA expression levels of *FLRT2* were significantly higher in the short-survival patient group (overall survival < 2 years) than in those in long-survival patient group (overall survival > 5 years) ($p = 0.0002$; Figure 6E). Similarly, IHC analysis of paraffin-embedded tumor samples from the short-survival patient group demonstrated increased levels of *FLRT2* gene expression (Figure 6F), corroborating the RT-PCR results. These observations collectively indicated that elevated expression of *FLRT2* was associated with a poorer survival prognosis in BLCA patients. We then performed a multivariate Cox regression analysis and the results identified the *FLRT2* gene as a high-risk factor and an independent prognostic marker for BLCA patients [hazard ratio (HR) 1.78, 95% CI 1.36 to 2.3; $p < 0.001$] (Figure 6G).

Furthermore, to ascertain whether gene expression and CNVs of the *FLRT2* gene influence immune cell infiltration, we investigated the relationship between *FLRT2* and immune cell infiltration. Using a Spearman analysis of TIMER, we found that *FLRT2* expression was statistically significant correlated with tumor purity, B cells, $CD8^+$ T cells, $CD4^+$ T cells, macrophages, neutrophils, and dendritic cells (Figure 6H; $p < 0.05$). Further analysis disclosed that CNV amplification of the *FLRT2* gene was significantly associated with B-cell infiltration and CNV deletion of *FLRT2* was significantly correlated with $CD4^+$ T cell and neutrophil infiltration (Figure 6I; $p < 0.05$). The relationship between CNV levels of *NTRK2*, *CYTL1*, *ZNF683*, and *PRSS41* and immune cell infiltration are depicted in Figure S5. We also explored the impact of immune cells on overall survival, and the results are displayed in Figures 6J, S6. Notably, only macrophage infiltration level was

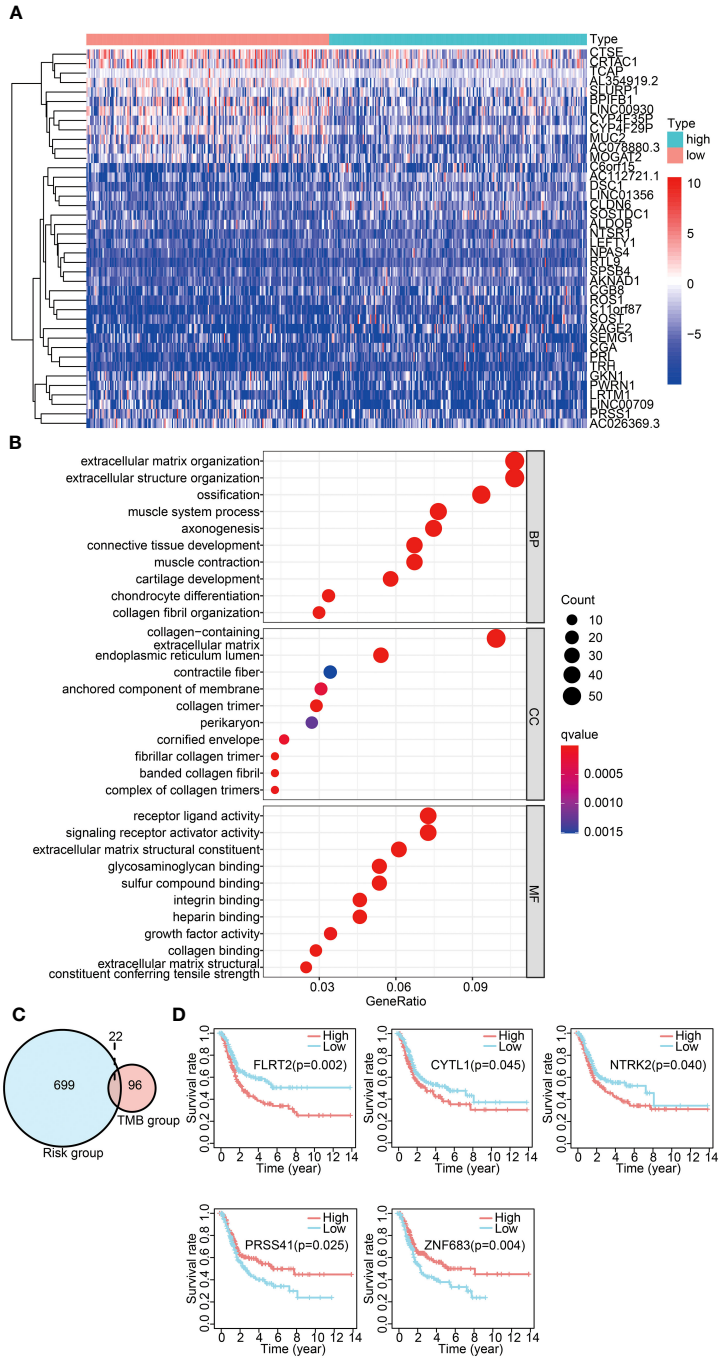

FIGURE 5
Common DEG analysis across differential TMB/IRGPs-derived risk groups. **(A)** Heatmap displaying the top 40 DEGs between the high- and low-risk groups. **(B)** GO analysis of DEGs in three categories (BPs, MFs, and CCs). BPs, biological processes; MFs, molecular functions; CCs, cellular components. **(C)** Venn diagram of common DEGs between different TMB groups and different IRGP-derived risk groups. **(D)** Survival analysis of five significantly related genes with Kaplan–Meier survival curves.

found to be significantly associated with overall survival in BLCA patients (p = 0.002), with high levels of macrophage infiltration correlating with a poor prognosis.

In summary, the results suggested that *FLRT2* was a high-risk and an independent prognostic factor in BLCA patients. *FLRT2* expression appeared to modulate the expression of other genes, including *NTRK2*, *CYTL1*, *ZNF683*, and *PRSS41* either directly or indirectly. Additionally, we found that *FLRT2* gene expression may affect the overall survival of BLCA patients by regulating the levels of macrophage infiltration.

3.7 The methylation landscape of *FLRT2*

To delve into the potential mechanisms impacting *FLRT2* expression, we considered the role of methylation, as it had been

TABLE 1 *FLRT2*, *NTRK2*, *CYTL1*, *ZNF683*, and *PRSS41* genes were significantly associated with prognosis as determined by univariate Cox analysis.

Gene	HR	HR.95L	HR.95H	*p*-value
NTRK2	1.0509	1.0167	1.0862	0.0032
FLRT2	0.7742	0.6152	0.9741	0.0290
ZNF683	1.0136	1.0026	1.0247	0.0146
CYTL1	0.9227	0.8517	0.9997	0.0491
PRSS41	1.3954	1.2026	1.6190	1.1156e-05

reported to modulate *FLRT2* expression. We analyzed the methylation levels in the TCGA-BLCA cohort, finding a slight increase in methylation in BLCA patients compared with the control cohort (0.41 vs 0.37; p = 0.002) (Figure 7A). Subsequently, we explored the correlation between *FLRT2* methylation and expression level, but no statistically significant relationship was uncovered (Figure S7). We further examined the site-specific methylation of *FLRT2* in the tumor cohort. Compared with the control cohort, the sites of cg25120290 and cg02305242 displayed hypermethylation, whereas the site cg01832662 was hypomethylated in the tumor group (Figure 7B). An analysis of the relationship between the differential methylation status at sites cg25120290, cg02305242, and cg01832662 and the *FLRT2* gene expression revealed that methylation at sites cg25120290 (cor = −0.257; p = 7.254e-08) and cg02305242 (cor = −0.225; p = 2.754e-06) was negatively correlated with *FLRT2* expression. Conversely, methylation at site cg01832662 was positively correlated with *FLRT2* expression (cor = 0.407; p = 1.79e-18)

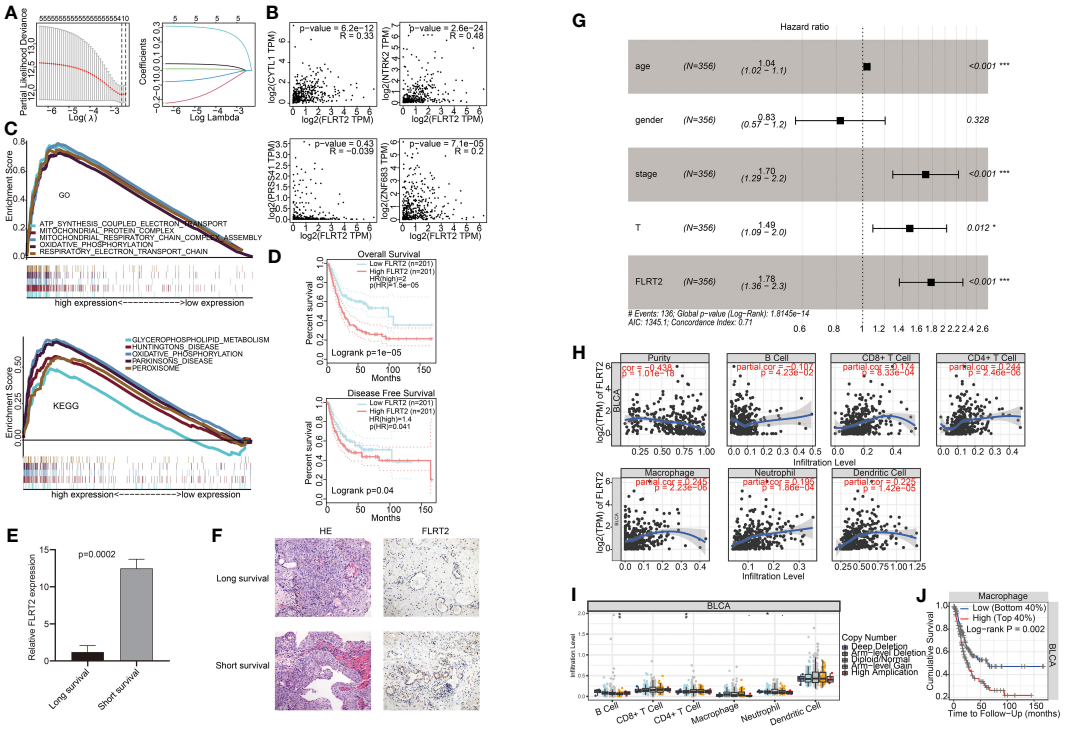

FIGURE 6
Correlation of *FLRT2* expression with BLCA prognosis and immune cell infiltration. **(A)** Lasso regression analysis of *FLRT2*, *NTRK2*, *CYTL1*, *ZNF683*, and *PRSS41*. Left panel: 10-fold cross-validation result identifying optimal values of the penalty parameter λ; right panel: lasso coefficient profiles of the five significantly related genes. **(B)** Spearman correlation analysis between the expression level of *FLRT2* and *NTRK2*, *CYTL1*, *ZNF683*, and *PRSS41* using GEPIA. **(C)** Top 5 significantly different pathways of the GO (top panel) and KEGG (bottom panel) enrichment analysis as displayed in GSEA enrichment score plots. GSEA, gene set enrichment analysis; GO, Gene Ontology; KEGG, Kyoto Encyclopedia of Genes and Genomes. **(D)** Survival analysis of *FLRT2* expression with OS and DFS using GEPIA. Top panel: correlation of *FLRT2* expression with OS; bottom panel: correlation of *FLRT2* expression with DFS. **(E)** The mRNA expression levels of *FLRT2* gene in the long-survival and short-survival patient group as determined by RT-PCR. Long survival, overall survival > 5 years; short survival, overall survival < 2 years. **(F)** Representative HE (200×) and IHC (200×) images of tumor samples from the long-survival and short-survival patient group. Long survival, overall survival > 5 years; short survival, overall survival < 2 years. **(G)** Multivariate Cox regression analysis of the prognostic factors in the TCGA cohort. ***p < 0.001; **p < 0.01; p < 0.05. **(H)** TIMER Spearman correlation analysis between *FLRT2* expression and immune cell infiltration levels. **(I)** Differences in infiltration levels of immune cells with different CNVs of the *FLRT2* gene using TIMER. ***p < 0.001; **p < 0.01; *p < 0.05; •p < 0.1. **(J)** Kaplan–Meier plots displaying the impact of macrophage infiltration levels on BLCA prognosis.

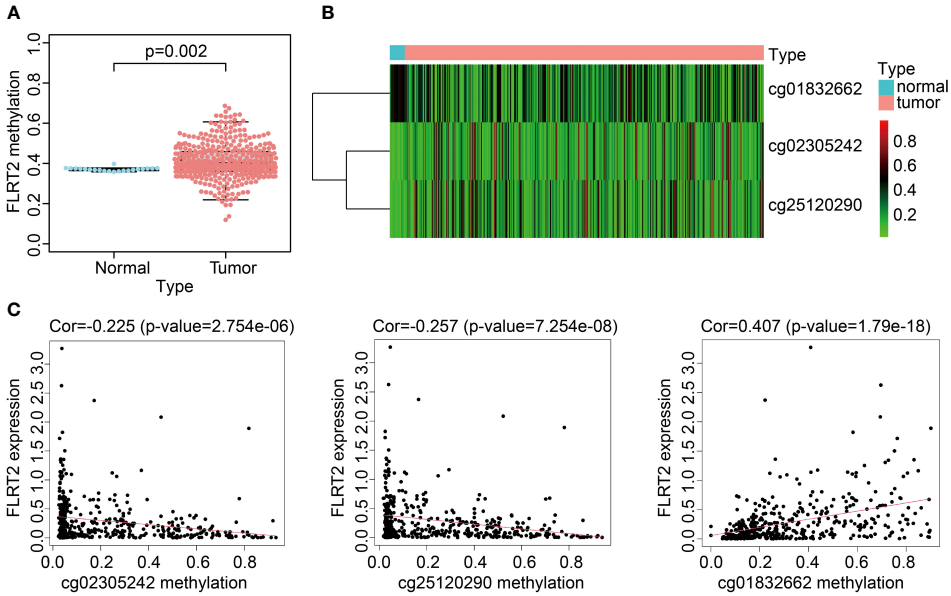

FIGURE 7
FLRT2 methylation landscape. **(A)** Scatterplot showing *FLRT2* differential methylation between the normal and tumor groups. **(B)** Heatmap exhibiting site-specific methylation differences in the tumor and normal groups. **(C)** Correlation analysis between site-specific methylation and *FLRT2* gene expression.

(Figure 7C). In conclusion, the combination of hypermethylation at sites cg25120290 and cg02305242 and hypomethylation at site cg01832662 resulted in diminished *FLRT2* gene expression, resulting in a favorable prognosis for BLCA patients.

4 Discussion

Bladder cancer (BLCA) is a prevalent malignant tumor in the urinary system (1). The mortality and incidence rates of bladder cancer are increasing in countries, such as the United States and China (2, 3). Despite advancements in immunotherapy, the prognosis for BLCA remains poor, and recurrence is common (23–27). Therefore, identification of relevant prognostic predictors is crucial for improving disease management, treatment approaches, and prognosis. In this study, we constructed a prognostic risk model with high accuracy using IRGPs. We then analyzed TMB and IRGPs, and identified a key prognosis gene, *FLRT2*, in BLCA patients.

Previous studies have shown that TMB is an effective biomarker for predicting responses to immunotherapy, with a higher TMB correlating with improved outcomes in BLCA patients (28, 29). Consistent with these findings, we also observed that patients with a high TMB had an improved overall survival. However, no association between TMB-derived immune-related DEGs and BLCA prognosis was found in this study. Therefore, we analyzed the IRGPs in bladder cancer patients. The constructed prognostic risk model using IRGPs exhibited an AUC value of 0.903, thus indicating high accuracy and sensitivity. The model-derived risk score was further verified as an independent prognostic factor for BLCA patients using multivariate Cox regression analysis. Additionally, the validation cohort (GSE31684) was analyzed and the results were consistent with this finding. Thus, this study succeeded in constructing a highly accurate prognostic model for BLCA patients, and the risk score derived from this model offered a reliable approach to predicting BLCA patient prognosis. A previous study identified two 5-methylcytosine (5mC) clusters, including 5mC cluster 1 and cluster 2, in BLCA (30). This finding provided an avenue for constructing robust models using 5mc subtypes. On this basis, we will evaluate the effectiveness of our model for different molecular types of BLCA, and construct innovative models in future research.

According to this risk prediction model, BLCA patients were categorized into high- and low-risk groups, and we investigated the DEGs between these two groups in combination with the DEGs in the the high- and low-TMB groups. Through Cox regression analysis we identified five genes associated with prognosis, including *FLRT2*, *NTRK2*, *CYTL1*, *ZNF683*, and *PRSS41*. Among them, *NTRK2* was identified as an oncogene in 1982 by Mariano Barbacid and colleagues (31). *CYTL1* mediates proangiogenic functions attributed to endothelial progenitor cells (such as ECFC) *in vivo* and may be a candidate to support angiogenesis and tissue regeneration in ischemic pathology (32). *ZNF683* is a transcription factor that mediates the transcriptional program in various innate and adaptive immune tissue-resident lymphocyte T-cell types, such as tissue-resident memory T (Trm), natural killer (trNK), and natural killer T (NKT) cells (33, 34). In addition, *PRSS41* is a kind of serine protease. *FLRT2* has been shown to participate in cell–cell adhesion, cell migration, and axon guidance. These five genes have important functions in the process of cancer development, angiogenesis, and immune cell regulation. Using lasso regression analysis, *FLRT2* was identified as the most crucial gene. Its expression was found to be significantly correlated with the other four genes directly or indirectly.

Cai et al. (35) and Hu et al. (36) revealed the critical significance of BCAT2 and Siglec15 in the tumor microenvironment of BLCA patients. In this study, we identified a novel prognostic gene and clarified its functional mechanisms in BLCA patients. A significant association was observed between lower levels of *FLRT2* expression and improved survival outcomes in BLCA patients. Through multivariable Cox analysis, *FLRT2* emerged as an independent prognostic factor for BLCA patients. Furthermore, a positive correlation was found between *FLRT2* expression and macrophage cell infiltration. Additionally, lower levels of macrophage infiltration correlated with improved BLCA patient survival. These findings revealed that *FLRT2* had a potential impact on BLCA prognosis by modulating macrophage cell infiltration. Notably, hypermethylation at sites cg25120290 and cg02305242, combined with hypomethylation at site cg01832662 were associated with reduced levels of expression of *FLRT2*. To conclude, we suggested that methylation at these sites led to reduced *FLRT2* expression, influencing macrophage infiltration levels, and, ultimately, improving survival outcomes in BLCA patients.

However, this study has certain limitations. The functional analysis of *FLRT2* was confined to the TCGA-BLCA cohort, without further external validation. To address this limitation, the implementation of molecular biological experiments should be performed for confirming the prognostic significance and function mechanism of the *FLRT2* gene in BLCA patients.

5 Conclusions

In this study, we identified *FLRT2* as a novel predictor indicative of poor prognosis in BLCA patients through a comprehensive analysis of TMB and IRGPs. We also revealed that *FLRT2* might influence patient prognosis by modulating macrophage cell infiltration. Notably, hypermethylation at sites cg25120290 and cg02305242, combined with hypomethylation at site cg01832662 correlated with decreased levels of *FLRT2* expression. We inferred that these methylation patterns led to decreased levels of *FLRT2* expression, which potentially contributed to a reduced level of macrophage infiltration, thereby prolonging survival rates in BLCA patients. The identification of *FLRT2* as a predictive biomarker for poor prognosis provides a promising avenue for refining clinical prognosis management and tailoring therapeutic strategies for BLCA patients.

Data availability statement

The original contributions presented in the study are included in the article/Supplementary Material. Further inquiries can be directed to the corresponding author.

Ethics statement

The studies involving humans were approved by Ethics Committee of Ningbo No.2 Hospital. The studies were conducted in accordance with the local legislation and institutional requirements. The participants provided their written informed consent to participate in this study.

Author contributions

Conceptualization, YT; investigation and formal analysis, YT and XY; data curation and validation, HC and JL; methodology, YT and QC; visualization, YT and JZ; resources, TC and HD; supervision, TC and QC; funding acquisition, YT, JL, QC and TC; writing – original draft, YT; writing – review & editing, YT, TC and QC.

Funding

The author(s) declare financial support was received for the research, authorship, and/or publication of this article. This research was funded by National Natural Science Foundation of China (62106248), Medical Scientific Research Foundation of Zhejiang Province, China (2021KY302), Ningbo Natural Science Foundation, China (2021J325), the Key Program of Ningbo Natural Science Foundation, China (2023J002), and Research Foundation of Ningbo Institute of Life and Health Industry, University of Chinese Academy of Sciences, China (2020YJY0207).

Acknowledgments

We thank all the staff, researchers, and the involved patients who supported The Cancer Genome Atlas and Gene Expression Omnibus Research Network.

Conflict of interest

Authors JZ and QC were employed by the company Thorgene Co., Ltd.

The remaining authors declare that the research was conducted in the absence of any commercial or financial relationships that could be construed as a potential conflict of interest.

Publisher's note

Supplementary material

The Supplementary Material for this article can be found online at: https://www.frontiersin.org/articles/10.3389/fonc.2023.1229227/full#supplementary-material

References

1. Richters A, Aben KK, Kiemeney LA. The global burden of urinary bladder cancer: an update. *World J Urol* (2020) 38:1895–904. doi: 10.1007/s00345-019-02984-4

2. Siegel R, Miller K, Fuchs H. Cancer statistics, 2022. *CA Cancer J Clin* (2022) 72:7–33. doi: 10.3322/caac.21708

3. Xia C, Dong X, Li H, Cao M, Sun D, He S, et al. Cancer statistics in China and United States, 2022: profiles, trends, and determinants. *Chin Med J* (2022) 135(05):584–90. doi: 10.1097/CM9.0000000000002108

4. Wu Y, Zheng Q, Li Y, Wang G, Gao S, Zhang X, et al. Metformin targets a yap1-tead4 complex *via* ampkα to regulate ccne1/2 in bladder cancer cells. *J Exp Clin Cancer Res* (2019) 38(1):1–16. doi: 10.1186/s13046-019-1346-1

5. Cambier S, Sylvester RJ, Collette L, Gontero P, Brausi MA, Van Andel G, et al. Eortc nomograms and risk groups for predicting recurrence, progression, and disease-specific and overall survival in non–muscle-invasive stage ta–T1 urothelial bladder cancer patients treated with 1–3 years of maintenance bacillus calmette-guérin. *Eur Urol* (2016) 69(1):60–9. doi: 10.1016/j.eururo.2015.06.045

6. von der Maase H, Hansen S, Roberts J, Dogliotti L, Oliver T, Moore M, et al. Gemcitabine and cisplatin versus methotrexate, vinblastine, doxorubicin, and cisplatin in advanced or metastatic bladder cancer: results of a large, randomized, multinational, multicenter, phase iii study. *J Clin Oncol* (2000) 18(17):3068–77. doi: 10.1200/JCO.2000.18.17.3068

7. von der Maase H, Sengelov L, Roberts JT, Ricci S, Dogliotti L, Oliver T, et al. Long-term survival results of a randomized trial comparing gemcitabine plus cisplatin, with methotrexate, vinblastine, doxorubicin, plus cisplatin in patients with bladder cancer. *J Clin Oncol* (2005) 23(21):4602–8. doi: 10.1200/JCO.2005.07.757

8. Kamat AM, Hahn NM, Efstathiou JA, Lerner SP, Malmström P-U, Choi W, et al. Bladder cancer. *Lancet* (2016) 388(10061):2796–810. doi: 10.1016/S0140-6736(16)30512-8

9. Hu J, Chen J, Ou Z, Chen H, Liu Z, Chen M, et al. Neoadjuvant immunotherapy, chemotherapy, and combination therapy in muscle-invasive bladder cancer: A multi-center real-world retrospective study. *Cell Rep Med* (2022) 3(11):100785. doi: 10.1016/j.xcrm.2022.100785

10. Lelo A, Prip F, Harris BT, Solomon D, Berry DL, Chaldekas K, et al. Stag2 is a biomarker for prediction of recurrence and progression in papillary non–muscle-invasive bladder cancer. *Clin Cancer Res* (2018) 24(17):4145–53. doi: 10.1158/1078-0432.CCR-17-3244

11. George B, Datar RH, Wu L, Cai J, Patten N, Beil SJ, et al. P53 gene and protein status: the role of P53 alterations in predicting outcome in patients with bladder cancer. *J Clin Oncol* (2007) 25(34):5352–8. doi: 10.1200/JCO.2006.10.4125

12. Cao R, Yuan L, Ma B, Wang G, Qiu W, Tian Y. An emt-related gene signature for the prognosis of human bladder cancer. *J Cell Mol Med* (2020) 24(1):605–17. doi: 10.1111/jcmm.14767

13. Dong Z-Y, Zhong W-Z, Zhang X-C, Su J, Xie Z, Liu S-Y, et al. Potential predictive value of tp53 and kras mutation status for response to pd-1 blockade immunotherapy in lung adenocarcinoma. *Clin Cancer Res* (2017) 23(12):3012–24. doi: 10.1158/1078-0432.CCR-16-2554

14. Rizvi NA, Hellmann MD, Snyder A, Kvistborg P, Makarov V, Havel JJ, et al. Mutational landscape determines sensitivity to pd-1 blockade in non–small cell lung cancer. *Science* (2015) 348(6230):124–8. doi: 10.1126/science.aaa1348

15. Chan TA, Wolchok JD, Snyder A. Genetic basis for clinical response to ctla-4 blockade in melanoma. *New Engl J Med* (2014) 371(23):2189–99. doi: 10.1056/NEJMoa1406498

16. Gentles AJ, Newman AM, Liu CL, Bratman SV, Feng W, Kim D, et al. The prognostic landscape of genes and infiltrating immune cells across human cancers. *Nat Med* (2015) 21(8):938–45. doi: 10.1038/nm.3909

17. Chen Y, Li Z-Y, Zhou G-Q, Sun Y. An immune-related gene prognostic index for head and neck squamous cell carcinomairgpi as an immune-related prognostic biomarker in hnscc. *Clin Cancer Res* (2021) 27(1):330–41. doi: 10.1158/1078-0432.CCR-20-2166

18. Wu J, Zhao Y, Zhang J, Wu Q, Wang W. Development and validation of an immune-related gene pairs signature in colorectal cancer. *Oncoimmunology* (2019) 8 (7):e1596715. doi: 10.1080/2162402X.2019.1596715

19. Xue Y-N, Xue Y-N, Wang Z-C, Mo Y-Z, Wang P-Y, Tan W-Q. A novel signature of 23 immunity-related gene pairs is prognostic of cutaneous melanoma. *Front Immunol* (2020) 11:576914. doi: 10.3389/fimmu.2020.576914

20. Lacy SE, Bönnemann CG, Buzney EA, Kunkel LM. Identification of flrt1, flrt2, and flrt3: A novel family of transmembrane leucine-rich repeat proteins. *Genomics* (1999) 62(3):417–26. doi: 10.1006/geno.1999.6033

21. Flintoff K, Arudchelvan Y, Gong SG. Flrt2 interacts with fibronectin in the atdc5 chondroprogenitor cells. *J Cell Physiol* (2014) 229(10):1538–47. doi: 10.1002/jcp.24597

22. Ando T, Tai-Nagara I, Sugiura Y, Kusumoto D, Okabayashi K, Kido Y, et al. Tumor-specific interendothelial adhesion mediated by FLRT2 facilitates cancer aggressiveness. *J Clin Invest* (2022) 135(5):584–90. doi: 10.1172/JCI153626

23. Teoh JY-C, Kamat AM, Black PC, Grivas P, Shariat SF, Babjuk M. Recurrence mechanisms of non-muscle-invasive bladder cancer—a clinical perspective. *Nat Rev Urol* (2022) 19(5):280–94. doi: 10.1038/s41585-022-00578-1

24. van Hoogstraten LM, Vrieling A, van der Heijden AG, Kogevinas M, Richters A, Kiemeney LA. Global trends in the epidemiology of bladder cancer: challenges for public health and clinical practice. *Nat Rev Clin Oncol* (2023) 20(5):287–304. doi: 10.1038/s41571-023-00744-3

25. Vlaming M, Kiemeney LA, van der Heijden AG. Survival after radical cystectomy: progressive versus *de novo* muscle invasive bladder cancer. *Cancer Treat Res Commun* (2020) 25:100264. doi: 10.1016/j.ctarc.2020.100264

26. Martini A, Sfakianos JP, Renström-Koskela L, Mortezavi A, Falagario UG, Egevad L, et al. The natural history of untreated muscle-invasive bladder cancer. *BJU Int* (2020) 125(2):270–5. doi: 10.1111/bju.14872

27. Felsenstein KM, Theodorescu D. Precision medicine for urothelial bladder cancer: update on tumour genomics and immunotherapy. *Nat Rev Urol* (2018) 15 (2):92–111. doi: 10.1038/nrurol.2017.179

28. Necchi A, Anichini A, Raggi D, Briganti A, Massa S, Lucianò R, et al. Pembrolizumab as neoadjuvant therapy before radical cystectomy in patients with muscle-invasive urothelial bladder carcinoma (Pure-01): an open-label, single-arm, phase ii study. *J Clin Oncol* (2018) 36(34):3353–60. doi: 10.1200/JCO.18.01148

29. Chan TA, Yarchoan M, Jaffee E, Swanton C, Quezada SA, Stenzinger A, et al. Development of tumor mutation burden as an immunotherapy biomarker: utility for the oncology clinic. *Ann Oncol* (2019) 30(1):44–56. doi: 10.1093/annonc/mdy495

30. Hu J, Othmane B, Yu A, Li H, Cai Z, Chen X, et al. 5mc regulator-mediated molecular subtypes depict the hallmarks of the tumor microenvironment and guide precision medicine in bladder cancer. *BMC Med* (2021) 19(1):1–20. doi: 10.1186/s12916-021-02163-6

31. Pulciani S, Santos E, Lauver AV, Long LK, Aaronson SA, Barbacid M. Oncogenes in solid human tumours. *Nature* (1982) 300(5892):539–42. doi: 10.1038/300539a0

32. Schneller D, Hofer-Warbinek R, Sturtzel C, Lipnik K, Gencelli B, Seltenhammer M, et al. Cytokine-like 1 is a novel proangiogenic factor secreted by and mediating functions of endothelial progenitor cells. *Circ Res* (2019) 124(2):243–55. doi: 10.1161/CIRCRESAHA.118.313645

33. Marquardt N, Kekäläinen E, Chen P, Lourda M, Wilson JN, Scharenberg M, et al. Unique transcriptional and protein-expression signature in human lung tissue-resident nk cells. *Nat Commun* (2019) 10(1):3841. doi: 10.1038/s41467-019-11632-9

34. Post M, Cuapio A, Osl M, Lehmann D, Resch U, Davies DM, et al. The transcription factor znf683/hobit regulates human nk-cell development. *Front Immunol* (2017) 8:535. doi: 10.3389/fimmu.2017.00535

35. Cai Z, Chen J, Yu Z, Li H, Liu Z, Deng D, et al. Bcat2 shapes a noninflamed tumor microenvironment and induces resistance to anti-pd-1/pd-L1 immunotherapy by negatively regulating proinflammatory chemokines and anticancer immunity. *Adv Sci* (2023) 10(8):2207155. doi: 10.1002/advs.202207155

36. Hu J, Yu A, Othmane B, Qiu D, Li H, Li C, et al. Siglec15 shapes a non-inflamed tumor microenvironment and predicts the molecular subtype in bladder cancer. *Theranostics* (2021) 11(7):3089. doi: 10.7150/thno.53649

Frontiers in Oncology

Advances knowledge of carcinogenesis and tumor progression for better treatment and management

The third most-cited oncology journal, which highlights research in carcinogenesis and tumor progression, bridging the gap between basic research and applications to imrpove diagnosis, therapeutics and management strategies.

Discover the latest Research Topics

See more →

Frontiers

Avenue du Tribunal-Fédéral 34
1005 Lausanne, Switzerland
frontiersin.org

Contact us

+41 (0)21 510 17 00
frontiersin.org/about/contact